

# MECHANICAL LOADING AND BONE

EDITED BY: Jonathan H. Tobias

PUBLISHED IN: Frontiers in Endocrinology



# frontiers

## **Frontiers Copyright Statement**

© Copyright 2007-2016 Frontiers Media SA. All rights reserved.

All content included on this site, such as text, graphics, logos, button icons, images, video/audio clips, downloads, data compilations and software, is the property of or is licensed to Frontiers Media SA ("Frontiers") or its licensees and/or subcontractors. The copyright in the text of individual articles is the property of their respective authors, subject to a license granted to Frontiers.

The compilation of articles constituting this e-book, wherever published, as well as the compilation of all other content on this site, is the exclusive property of Frontiers. For the conditions for downloading and copying of e-books from Frontiers' website, please see the Terms for Website Use. If purchasing Frontiers e-books from other websites or sources, the conditions of the website concerned apply.

Images and graphics not forming part of user-contributed materials may not be downloaded or copied without permission.

Individual articles may be downloaded and reproduced in accordance with the principles of the CC-BY licence subject to any copyright or other notices. They may not be re-sold as an e-book.

As author or other contributor you grant a CC-BY licence to others to reproduce your articles, including any graphics and third-party materials supplied by you, in accordance with the Conditions for Website Use and subject to any copyright notices which you include in connection with your articles and materials.

All copyright, and all rights therein, are protected by national and international copyright laws.

The above represents a summary only. For the full conditions see the Conditions for Authors and the Conditions for Website Use.

**ISSN 1664-8714**

**ISBN 978-2-88919-751-4**

**DOI 10.3389/978-2-88919-751-4**

## **About Frontiers**

Frontiers is more than just an open-access publisher of scholarly articles: it is a pioneering approach to the world of academia, radically improving the way scholarly research is managed. The grand vision of Frontiers is a world where all people have an equal opportunity to seek, share and generate knowledge. Frontiers provides immediate and permanent online open access to all its publications, but this alone is not enough to realize our grand goals.

## **Frontiers Journal Series**

The Frontiers Journal Series is a multi-tier and interdisciplinary set of open-access, online journals, promising a paradigm shift from the current review, selection and dissemination processes in academic publishing. All Frontiers journals are driven by researchers for researchers; therefore, they constitute a service to the scholarly community. At the same time, the Frontiers Journal Series operates on a revolutionary invention, the tiered publishing system, initially addressing specific communities of scholars, and gradually climbing up to broader public understanding, thus serving the interests of the lay society, too.

## **Dedication to quality**

Each Frontiers article is a landmark of the highest quality, thanks to genuinely collaborative interactions between authors and review editors, who include some of the world's best academicians. Research must be certified by peers before entering a stream of knowledge that may eventually reach the public - and shape society; therefore, Frontiers only applies the most rigorous and unbiased reviews.

Frontiers revolutionizes research publishing by freely delivering the most outstanding research, evaluated with no bias from both the academic and social point of view.

By applying the most advanced information technologies, Frontiers is catapulting scholarly publishing into a new generation.

## **What are Frontiers Research Topics?**

Frontiers Research Topics are very popular trademarks of the Frontiers Journals Series: they are collections of at least ten articles, all centered on a particular subject. With their unique mix of varied contributions from Original Research to Review Articles, Frontiers Research Topics unify the most influential researchers, the latest key findings and historical advances in a hot research area! Find out more on how to host your own Frontiers Research Topic or contribute to one as an author by contacting the Frontiers Editorial Office: [researchtopics@frontiersin.org](mailto:researchtopics@frontiersin.org)

# MECHANICAL LOADING AND BONE

Topic Editor:

**Jonathan H. Tobias**, University of Bristol, United Kingdom

This research topic is focused on recent advances in our understanding of effects of mechanical loading on the skeleton, and research methods used in addressing these. Though it is well established that mechanical loading provides an essential stimulus for skeletal growth and maintenance, there have been major advances recently in terms of our understanding of the molecular pathways involved, which are thought to provide novel drug targets for treating osteoporosis. The articles included in this topic encompass the full spectrum of laboratory and clinical research, and range from review articles, editorials, hypothesis papers and original research articles. Together, they demonstrate how mechanical loading underpins many aspects of bone biology, including the pathogenesis and treatment of osteoporosis and other clinical disorders associated with skeletal fragility.

**Citation:** Tobias, J. H., ed. (2016). Mechanical Loading and Bone. Lausanne: Frontiers Media.  
doi: 10.3389/978-2-88919-751-4

# Table of Contents

- 05 Editorial: Mechanical Loading and Bone**  
Jonathan H. Tobias
- 07 Alterations in the synthesis of IL-1 $\beta$ , TNF- $\alpha$ , IL-6, and their downstream targets RANKL and OPG by mouse calvarial osteoblasts in vitro: inhibition of bone resorption by cyclic mechanical strain**  
Salvador García-López, Rosina Villanueva and Murray C. Meikle
- 14 Physical activity and bone: may the force be with you**  
Jonathan H. Tobias, Virginia Gould, Luke Brunton, Kevin Deere, Joern Rittweger, Matthijs Lipperts and Bernd Grimm
- 19 Objectively measured physical activity predicts hip and spine bone mineral content in children and adolescents ages 5–15 years: Iowa bone development study**  
Kathleen F. Janz, Elena M. Letuchy, Shelby L. Francis, Kristen M. Metcalf, Trudy L. Burns and Steven M. Levy
- 26 The contribution of experimental in vivo models to understanding the mechanisms of adaptation to mechanical loading in bone**  
Lee B. Meakin, Joanna S. Price and Lance E. Lanyon
- 39 A new method to investigate how mechanical loading of osteocytes controls osteoblasts**  
Marisol Vazquez, Bronwen A. J. Evans, Daniela Riccardi, Sam L. Evans, Jim R. Ralphs, Christopher Mark Dillingham and Deborah J. Mason
- 57 Mechanical regulation of bone regeneration: theories, models, and experiments**  
Duncan Colin Betts and Ralph Müller
- 71 The effect of altering the mechanical loading environment on the expression of bone regenerating molecules in cases of distraction osteogenesis**  
Mohammad M. Alzahrani, Emad A. Anam, Asim M. Makhdum, Isabelle Villemure and Reggie Charles Hamdy
- 82 New insights into Wnt-Lrp5/6- $\beta$ -catenin signaling in mechanotransduction**  
Kyung Shin Kang and Alexander G. Robling
- 87 Improvement of skeletal fragility by teriparatide in adult osteoporosis patients: a novel mechanostat-based hypothesis for bone quality**  
Toshihiro Sugiyama, Tetsuya Torio, Tsuyoshi Sato, Masahito Matsumoto, Yoon Taek Kim and Hiromi Oda

**90      *Ethnic differences in bone health***

Ayse Zengin, Ann Prentice and Kate Anna Ward

**96      *Romosozumab and blosozumab: alternative drugs of mechanical strain-related stimulus toward a cure for osteoporosis***

Toshihiro Sugiyama, Tetsuya Torio, Tsuyoshi Miyajima, Yoon Taek Kim  
and Hiromi Oda



# Editorial: Mechanical Loading and Bone

Jonathan H. Tobias\*

Musculoskeletal Research Unit, School of Clinical Sciences, University of Bristol, Bristol, UK

**Keywords:** mechanical loading, skeleton, accelerometry, osteoblast, osteoporosis

## The Editorial on the Research Topic

### Mechanical Loading and Bone

## INTRODUCTION

This Research Topic comprises 11 interesting and topical articles describing a mixture of clinical and laboratory approaches to how mechanical loading influences the skeleton. Of the five clinical papers, those by Tobias et al. and Janz et al. address important methodological issues concerning the use of accelerometers to record physical activity in a way that is relevant to mechanical loading of bone. Two separate papers by Toshihiro Sugiyama et al. discuss how understanding of skeletal responses to mechanical loading can help interpret the mechanism of action of bone anabolic drugs. The paper by Zengin et al. illustrates how understanding of mechanical loading responses can be used to interpret ethnic differences in skeletal structure. Of the six laboratory papers, those by Meakin et al. and Vazquez et al. focus on methodological approaches to study mechanical loading *in vivo* and *in vitro*, respectively. Four of the papers explore the mechanisms involved in mediating different aspects of mechanical loading responses of bone. García-López et al. report their findings concerning the mechanisms involved in the inhibition of bone resorption by cyclical mechanical strain *in vitro*; Kang and Robling review the role of the Wnt pathway in mechanotransduction; Alzahrani et al. review the mechanisms involved in distraction osteogenesis; and Betts and Müller review theories and models of mechanical regulation of bone regeneration after bone injury.

## OPEN ACCESS

### Edited and reviewed by:

Derek LeRoith,  
Icahn School of Medicine at  
Mount Sinai, USA

### \*Correspondence:

Jonathan H. Tobias  
jon.tobias@bristol.ac.uk

### Specialty section:

This article was submitted to Bone Research, a section of the journal *Frontiers in Endocrinology*

**Received:** 12 November 2015

**Accepted:** 23 November 2015

**Published:** 14 December 2015

### Citation:

Tobias JH (2015) Editorial: Mechanical Loading and Bone. *Front. Endocrinol.* 6:184.  
doi: 10.3389/fendo.2015.00184

## CLINICAL PAPERS

The papers by Tobias and Janz represent contrasting approaches to study the relationships between physical activity and bone measures based on accelerometry. While the former addresses the role of physical activity in preserving bone in older people, and the latter examines its role in bone accrual in childhood. Moreover, these papers utilize distinct approaches to extract relevant information about mechanical loading from accelerometry data. Janz et al. use conventional counts per minute thresholds but apply a relatively high threshold denoting vigorous PA on the basis that such activity is more likely to be osteogenic, as borne out by their results. By contrast, Tobias et al. extracted the number of counts beyond specific g thresholds on the basis that these are more directly related to ground reaction forces.

The remaining three clinical papers illustrate how understanding of mechanical loading responses can be used to explain findings from epidemiological to interventional studies of the skeleton. In their hypothesis article on teriparatide effects on bone, Toshihiro Sugiyama et al. suggest that the reason why gains in bone at the outer surface are limited is because simultaneous gains at the inner surface act to limit strain at the outer surface. In a further hypothesis article, the same authors, Sugiyama et al. suggest that the anti-sclerostin inhibitors blosozumab and romosozumab are particularly effective at simulating bone formation as a consequence of their ability to overcome negative

feedback of the mechanostat by interfering with this process due to its dependence on sclerostin. In their review of ethnic differences in bone health, Ayse Zengin et al. conclude that differences in fracture rate between ethnic groups cannot adequately be explained by differences in areal bone mineral density, suggesting the need to describe these based on more detailed measures of bone structure. Differences in the latter may in turn reflect ethnic differences in muscle mass and force, or alternatively how the skeleton responds to mechanical loading by these factors.

## LABORATORY PAPERS

The papers by Meakin et al. and Vazquez et al. describe contrasting methodological approaches to studying the mechanisms that mediate mechanical loading responses. Meakin et al. describe how use of *in vivo* studies based on a range of animal models has contributed to our understanding of the type of strain stimulus to which the skeleton is most responsive. Vazquez focuses on *in vitro* models of mechanical strain responses, describing a novel 3D osteocyte–osteoblast co-culture system.

The remaining four laboratory papers describe different aspects of the mechanisms involved in mechanical loading responses. García-López et al. report that cyclical strain of osteoblast monolayers reduces expression of the bone resorptive cytokine RANKL, but surprisingly other cytokines that might be expected to mediate this response show a paradoxical increase in expression. The review by Kang and Robling focuses on the role of Wnt signaling in mediating osteogenic responses to mechanical strain and suggests that while LRP5 is known to be involved, the

closely related receptor LRP6 may also play a hitherto unrecognized role.

In their review article, Alzahrani et al. discuss how characterization of the molecular pathways involved in mediating responses to mechanical loading can be used to select improved protocols for distraction osteogenesis, a surgical technique used to treat bony deformities via limb lengthening. Finally, in their paper, Betts and Müller review the different experimental studies, models, and theories that explain how mechanical stimuli are sensed and incorporated during bone regeneration as part of the healing process after bone injury.

## CONCLUSION

Together, the 11 papers published in this Research Topic provide a good illustration of how mechanical loading underpins many facets of bone biology, including the pathogenesis and treatment of osteoporosis and other clinical disorders associated with skeletal fragility.

**Conflict of Interest Statement:** The author declares that the research was conducted in the absence of any commercial or financial relationships that could be construed as a potential conflict of interest.

Copyright © 2015 Tobias. This is an open-access article distributed under the terms of the Creative Commons Attribution License (CC BY). The use, distribution or reproduction in other forums is permitted, provided the original author(s) or licensor are credited and that the original publication in this journal is cited, in accordance with accepted academic practice. No use, distribution or reproduction is permitted which does not comply with these terms.



# Alterations in the synthesis of IL-1 $\beta$ , TNF- $\alpha$ , IL-6, and their downstream targets RANKL and OPG by mouse calvarial osteoblasts *in vitro*: inhibition of bone resorption by cyclic mechanical strain

Salvador García-López<sup>1,2,3</sup>, Rosina Villanueva<sup>1</sup> and Murray C. Meikle<sup>4\*</sup>

<sup>1</sup> Health Science Department/Cell Biology and Immunology Laboratory, Universidad Autónoma Metropolitana-Xochimilco, Mexico City, Mexico

<sup>2</sup> Orthodontic Department, General Hospital "Dr. Manuel Gea González," Universidad Nacional Autónoma de México, Mexico City, Mexico

<sup>3</sup> Orthodontic Department, Universidad Intercontinental, Mexico City, Mexico

<sup>4</sup> Faculty of Dentistry, National University of Singapore, Singapore

## Edited by:

Jonathan H. Tobias, University of Bristol, UK

## Reviewed by:

Jonathan H. Tobias, University of Bristol, UK

Jennifer Tickner, University of Western Australia, Australia

## \*Correspondence:

Murray C. Meikle, Faculty of Dentistry, National University of Singapore, 11 Lower Kent Ridge Road, 119083 Singapore

e-mail: murray.meikle@cantab.net

Mechanical strain is an important determinant of bone mass and architecture, and the aim of this investigation was to further understand the role of the cell–cell signaling molecules, IL-1 $\beta$ , TNF- $\alpha$ , and IL-6 in the mechanobiology of bone. Mouse calvarial osteoblasts in monolayer culture were subjected to a cyclic out-of-plane deformation of 0.69% for 6 s, every 90 s for 2–48 h, and the levels of each cytokine plus their downstream targets RANKL and OPG measured in culture supernatants by ELISAs. Mouse osteoblasts constitutively synthesized IL-1 $\beta$ , TNF- $\alpha$ , and IL-6, the production of which was significantly up-regulated in all three by cyclic mechanical strain. RANKL and OPG were also constitutively synthesized; mechanical deformation however, resulted in a down-regulation of RANKL and an up-regulation OPG synthesis. We next tested whether the immunoreactive RANKL and OPG were biologically active in an isolated osteoclast resorption pit assay – this showed that culture supernatants from mechanically deformed cells significantly inhibited osteoclast-mediated resorptive activity across the 48 h time-course. These findings are counterintuitive, because IL-1 $\beta$ , TNF- $\alpha$ , and IL-6 have well-established reputations as bone resorptive agents. Nevertheless, they are pleiotropic molecules with multiple biological activities, underlining the complexity of the biological response of osteoblasts to mechanical deformation, and the need to understand cell–cell signaling in terms of cytokine networks. It is also important to recognize that osteoblasts cultured *in vitro* are deprived of the mechanical stimuli to which they are exposed *in vivo* – in other words, the cells are in a physiological default state that in the intact skeleton leads to decreased bone strains below the critical threshold required to maintain normal bone structure.

**Keywords:** mouse osteoblasts, mechanical deformation, pleiotropic cytokines, RANKL, OPG

## INTRODUCTION

Mechanical stimuli play an important role in the growth, structure, and maintenance of skeletal tissues. It has been estimated that environmental factors such as physical activity and nutrition account for 20–40% of individual variation in bone mass, the remaining 60–80% being determined by genetic factors (1, 2). Mechanical stimuli may be growth-generated as in embryonic tissues with differential growth rates (3), the result of functional movement as in synovial joints (4, 5), the consequence of physical activity (6), or by the activation of orthodontic appliances. In contrast, prolonged bed rest or weightlessness leads to bone loss and osteopenia (7, 8).

In the adult skeleton, during normal physiological turnover there is a balance between the amount of bone resorbed by osteoclasts and that formed by osteoblasts to maintain a constant bone mass (9). Bone resorption and bone formation are therefore said to be coupled, a process of renewing the skeleton

while maintaining its structural integrity, embodied in the A-R-F (activation-resorption-formation) sequence of the bone remodeling cycle. Bone remodeling is orchestrated by cells of the osteoblast lineage and involves a complex network of cell–cell signaling mediated by systemic osteotropic hormones, locally produced cytokines, growth factors, and the mechanical environment of the cells (10–13). One of the most significant developments in connective tissue biology during the 1980s was the finding that cytokines such as interleukin-1 (IL-1), tumor necrosis factor (TNF), and IL-6, originally identified as immunoregulatory molecules, could also act as regulators of pathophysiological resorption (14–17) and were produced by many different cell types including osteoblasts (18).

Another key advance was the observation that osteoclast formation and function *in vitro* was dependent upon the presence of stromal cells/osteoblasts, which suggested that soluble factor(s) were involved in osteoblast–osteoclast signaling (19). This led to

the discovery of OPG (osteoprotegerin) and RANKL (receptor activator of nuclear factor κB ligand), two cytokines synthesized by osteoblasts (20–24), and constituents of a ligand–receptor system known as the RANK/RANKL/OPG triad that directly regulates the final steps of the bone resorptive cascade. RANKL which exists in both membrane-bound and soluble forms stimulates the differentiation and function of osteoclasts, an effect mediated by RANK, a member of the TNF receptor family expressed primarily on cells of the monocyte/macrophage lineage, including osteoclasts and their precursor cells (25). OPG is a secreted protein that inhibits osteoclastogenesis by acting as a decoy receptor, binding to and neutralizing both cell-bound and soluble(s) RANKL.

Following the initial mechanotransduction event at the cell membrane, mechanical stimuli appear to influence bone remodeling by their ability to regulate the synthesis and/or action of cytokines. Since remodeling occurs at distinct sites throughout the skeleton, osteoblast cytokines are ideally placed to regulate or modify the action of other cell types in bone, although the interactions are complex and poorly understood. Using mouse calvarial osteoblasts as our model, the aim of this study was to determine the effect of cyclic mechanical strain on the synthesis and biological activity of the pleiotropic cytokines IL-1 $\beta$ , TNF- $\alpha$ , IL-6, and their downstream targets RANKL and OPG.

## MATERIALS AND METHODS

### PREPARATION OF MOUSE OSTEOBLASTS

Calvarial osteoblasts were prepared and characterized by a modification of the method previously described by Heath et al. (26). Neonatal mouse calvaria from BALB/C mice were dissected free from adherent soft tissue, washed in Ca<sup>2+</sup> and Mg<sup>2+</sup>free Tyrode's solution (10 min) and sequentially digested with 1 mg/ml trypsin (for 20 and 40 min). Cells from these digests were discarded; the bones were washed in phosphate buffered saline (PBS) and cut into pieces for a third trypsin digest (20 min). The cells released from this digest were washed in PBS, centrifuged at 1000 rpm for 5 min and the pelleted cells resuspended in 1:1 F12/Dulbecco's modification of Eagle's medium (DMEM) supplemented with 20% fetal calf serum (GIBCO, Invitrogen, Carlsbad, CA, USA), 100 units/ml penicillin, and 100  $\mu$ g/ml streptomycin, then seeded into 75-cm flasks and grown to confluence at 37°C in a humidified atmosphere of 5% CO<sub>2</sub>/95% air. The cells were identified as osteoblasts by morphological criteria and the fact that more than 95% stained strongly for alkaline phosphatase (ALP).

### APPLICATION OF MECHANICAL DEFORMATION TO MOUSE OSTEOBLASTS

After the cells had reached confluence (20–25 days), adherent cells were detached with trypsin-EDTA (0.25%; Sigma), resuspended in F12/DMEM with 10% fetal calf serum (Gibco), 100 units/ml penicillin and 100  $\mu$ g/ml streptomycin and plated at an initial cell density of 10<sup>6</sup> cells/dish into 35 mm Petriperm dishes (*In vitro* Systems & Services GmbH, Germany) with flexible bases. Vacuum pressure was used to displace the substrate – maximal deflection 2 mm, according to the method of Banes et al. (27) and a cyclic strain applied to the cells for 6 s (0.166 Hz), every 90 s for 2–48 h as

described previously (28). The maximal strain applied to the cells was calculated according to the formula:

$$Arc = \frac{1}{2} \sqrt{d^2 + 16b^2} + \frac{d^2}{8b} \ln \left( 4b + \frac{\sqrt{d^2 + 16b^2}}{d} \right)$$

$d$  = diameter (33 mm);  $b$  = maximum deflection (2 mm); Arc = 33.23 mm

$$\text{max strain} = \frac{Arc - d}{d} 100 = 0.69\%.$$

Each dish contained 4 ml of F12/DMEM medium; 500  $\mu$ l was sampled at each time point and 500  $\mu$ l fresh medium added. Because the deformation is out-of-plane, the level of strain experienced by the cells will be greatest at the center and least at the perimeter of the substrate and roughly half that programmed into the computer. The overall level of deformation is therefore comparable with strain levels recorded at the surface of diaphyseal bone *in vivo* (1–3  $\times$  10<sup>6</sup> microstrain) depending on location following dynamic loading (29, 30).

### CULTURE MEDIA PROTEOMICS

Media samples were supplemented with 1 mg/ml protease inhibitor cocktail (Sigma-Aldrich P1860, St. Louis, MO, USA), stored at −70°C and assayed 2 days later for IL-1 $\beta$ , TNF- $\alpha$ , IL-6, OPG, and soluble sRANKL protein by enzyme-linked immunosorbent assays (ELISAs; R & D Systems, Minneapolis, MN, USA). Absorbance was measured at 450 nm according to the manufacturer's instructions.

### OSTEOCLAST RESORPTION PIT ASSAY

The osteoclast resorption assay is based on the ability of isolated osteoclasts to resorb cortical bone, dentine, or ivory slices *in vitro* (31). Ivory was chosen as the substrate being free of vascular channels and pre-existing resorbing surfaces and osteoclasts produce resorption pits in its smooth surface greatly facilitating quantification. Ivory slices (250  $\mu$ m in thickness) were cut with a Micro Slice 2 machine (Metals Research, Cambridge, England) at low speed from a 1 cm diameter rod. Osteoclasts were obtained from the femurs of 2–3-day-old BALB/C mice and allowed to settle on the slices for 20 min at 37°C as described previously (32). The substrate was then washed free of non-adherent cells, and the slices incubated for 24 h in a humidified atmosphere of 5% CO<sub>2</sub>/95% air at 37°C in 500  $\mu$ l of conditioned medium plus 500  $\mu$ l of fresh DMEM supplemented with 5% fetal calf serum, 100 units/ml penicillin, and 100  $\mu$ g/ml streptomycin in 1.5 cm multiwall plates. At the completion of the culture period the cells were removed, the ivory slices stained with trypan blue and resorption quantified by measuring the surface area of the resorption lacunae by image analysis (Stereoscopy Microscope model SKD/SKO/KTD, Arhe, Holland). A single experiment consisted of eight ivory slices bearing the cells from one mouse, with four slices for each control and test variable.

### STATISTICAL ANALYSIS

Data are expressed as mean ± standard error of the mean (SEM). Differences between control and experimental cultures were determined by the Student's *t*-test (two tailed) using GraphPad Prism

4 software (GraphPad Software Inc., San Diego, CA, USA) and the level of significance set at  $P < 0.05$ .

## RESULTS

### EFFECTS OF CYCLIC MECHANICAL STRAIN ON CYTOKINE PRODUCTION

Mouse calvarial osteoblasts in monolayer culture constitutively synthesized IL-1 $\beta$ , TNF- $\alpha$ , and IL-6 over the 48 h time-course of the experiments; for IL-1 $\beta$  and TNF- $\alpha$  the levels were  $10^3$  pg/ml and for IL-6,  $2-3 \times 10^3$  pg/ml (Figure 1). Cyclic tensile strain significantly up-regulated IL-1 $\beta$  and TNF- $\alpha$  synthesis two- to threefold from 2 to 24 h, returning to control levels by 48 h (Figure 1). In the case of IL-6 the increments were smaller (one- to twofold), but of greater magnitude ( $4-8 \times 10^3$  pg/ml), and were sustained over the entire 48 h time-course (Figure 2).

### EFFECTS OF CYCLIC STRAIN ON sRANKL AND OPG

Cultured mouse osteoblasts constitutively synthesized sRANKL and OPG. From 2 to 24 h there was a significant reduction in the level of sRANKL of approximately one- to twofold in mechanically deformed cultures; from 24 to 48 h, however, immunoreactive sRANKL returned to control levels (Figure 3). In contrast, OPG levels were not significantly different over the first 24 h, but from

24 to 48 h had increased by approximately 50% in culture media from mechanically deformed cells (Figure 3).

### INHIBITION OF OSTEOCLAST RESORPTION

In view of the well-established ability of IL-1 $\beta$ , TNF- $\alpha$ , and IL-6 to stimulate bone resorption *in vitro*, and the importance of OPG and RANKL in regulating the terminal pathway of the bone resorptive cascade, we next tested the biological activity of the RANKL/OPG ratio in the culture media using an isolated osteoclast resorption pit assay. Figure 4 shows the contrary to expectation there was a significant inhibition of osteoclast resorption by culture media from mechanically strained cultures over the entire 2–48 h time scale.

## DISCUSSION

Rubin et al. (33) have shown that tensile mechanical strain (2% at 10 cycles/min) applied to mouse bone marrow stromal cells *in vitro*, decreased RANKL mRNA levels by 60%. Kusumi et al. (34) have similarly reported a decrease in RANKL mRNA expression and sRANKL release from human osteoblasts following 7% cyclic tensile strain; they also found that mechanical strain increased OPG synthesis. The present study builds on these findings, providing evidence for an upstream mechanism, and shows that contrary to what one might have expected, mechanical stress up-regulated the synthesis of IL-1 $\beta$ , TNF- $\alpha$ , and IL-6, three cytokines known to be potent stimulators of bone resorption *in vitro* (14–17).

IL-1 $\beta$ , TNF- $\alpha$ , and IL-6 have also been shown to stimulate osteoclast differentiation and bone resorption in a synergistic manner (35), and perhaps unexpectedly, to increase the production of both RANKL and OPG in the human osteosarcoma cell line MG-63 (36–38), although the dominant outcome was a net increase in RANKL activity (39, 40). We were therefore surprised to find that while intermittent tensile strain up-regulated IL-1 $\beta$ , TNF- $\alpha$ , and IL-6 synthesis, OPG production increased and sRANKL decreased, and when tested in an osteoclast resorption assay, culture supernatants from mechanically deformed cells were found

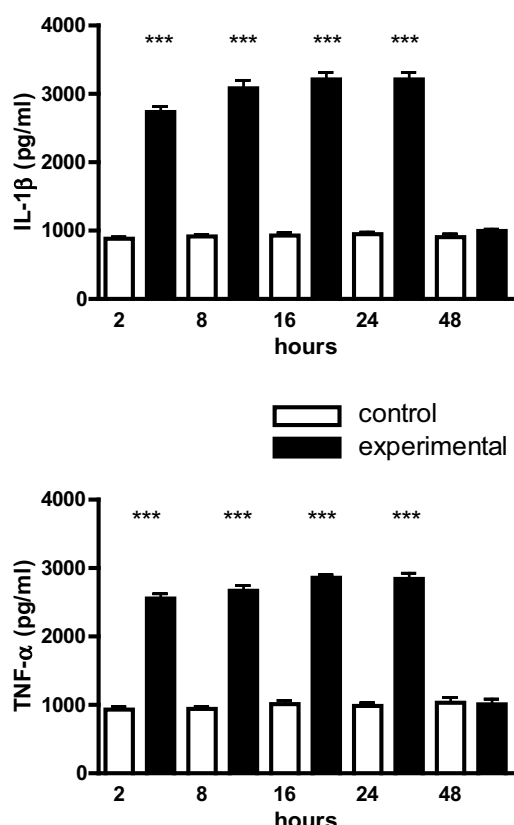


**FIGURE 1 | IL-1 $\beta$  and TNF- $\alpha$  production by mouse calvarial osteoblasts.**

Osteoblasts in monolayer culture were subjected to a cyclic tensile strain (6 s every 90 s) for 2–48 h and the culture media assayed for IL-1 $\beta$  and TNF- $\alpha$  by ELISAs. Results are expressed as mean  $\pm$  SEM for 10 cultures.

\*\*\*Experimental significantly greater than control.  $P < 0.001$ .

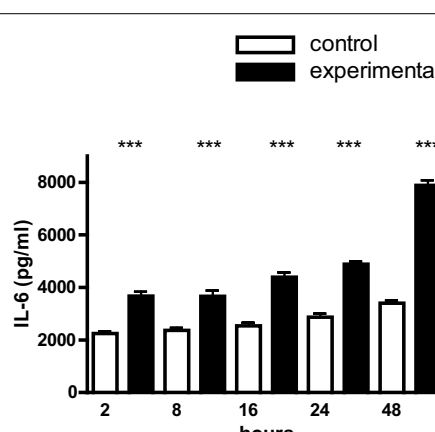


**FIGURE 2 | IL-6 production by mouse calvarial osteoblasts.**

Osteoblasts in monolayer culture were subjected to a cyclic tensile strain (6 s every 90 s) for 2–48 h and the culture media assayed for IL-6 by an ELISA. Results are mean  $\pm$  SEM for 10 cultures. \*\*\*Experimental significantly greater than control.  $P < 0.001$ .

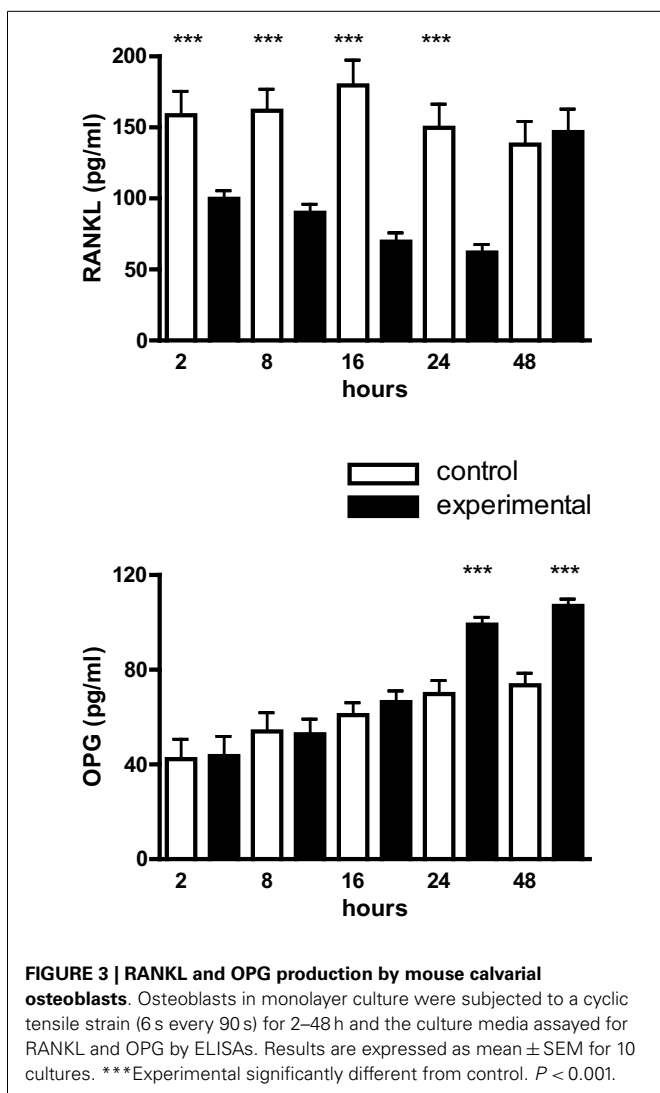


**FIGURE 3 | RANKL and OPG production by mouse calvarial osteoblasts.** Osteoblasts in monolayer culture were subjected to a cyclic tensile strain (6 s every 90 s) for 2–48 h and the culture media assayed for RANKL and OPG by ELISAs. Results are expressed as mean  $\pm$  SEM for 10 cultures. \*\*\*Experimental significantly different from control.  $P < 0.001$ .

to be inhibitory. This highlights the importance of bioassays. The bone literature contains a good deal of information about gene expression in normal and transformed cell lines, rather less about whether the expressed genes of interest are translated into protein, and if they are, whether the proteins are biologically active – in other words, real functional molecules.

We have previously shown that cyclic mechanical strain in the same model system inhibits IL-10 and stimulates IL-12 production by mouse calvarial osteoblasts (28), two cytokines with the ability to inhibit bone resorption. IL-10 selectively blocks osteoclastogenesis by inhibiting the differentiation of osteoclast progenitors into preosteoclasts (41, 42), while IL-12 inhibits RANKL-induced osteoclast formation in mouse bone marrow cell cultures, an effect mediated by IFN- $\gamma$  (43, 44). IL-10 also suppresses osteoblast differentiation in mouse bone marrow cultures by inhibition of TGF- $\beta$ 1 production (45, 46).

These data underline the complexity of the biological response of osteoblasts to mechanical deformation and the potential disadvantage of investigating a relatively small number of cytokines at

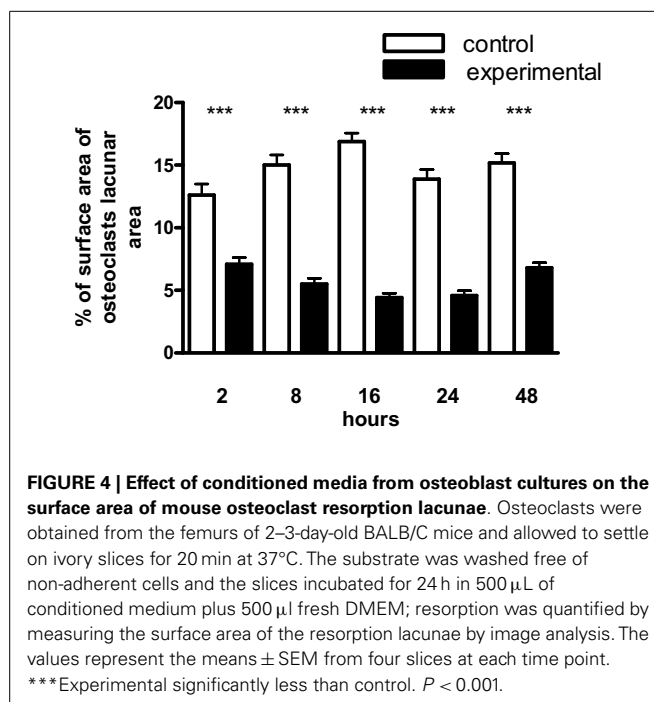


**FIGURE 4 | Effect of conditioned media from osteoblast cultures on the surface area of mouse osteoclast resorption lacunae.** Osteoclasts were obtained from the femurs of 2–3-day-old BALB/C mice and allowed to settle on ivory slices for 20 min at 37°C. The substrate was washed free of non-adherent cells and the slices incubated for 24 h in 500  $\mu$ L of conditioned medium plus 500  $\mu$ L fresh DMEM; resorption was quantified by measuring the surface area of the resorption lacunae by image analysis. The values represent the means  $\pm$  SEM from four slices at each time point. \*\*\*Experimental significantly less than control.  $P < 0.001$ .

any one time. The fusion of real-time RT-PCR with microarray technology, which enables a large panel of genes to be screened at the same time under identical experimental conditions using relatively small quantities of RNA, provides an opportunity to significantly expand our knowledge of the number of mechanoresponsive genes expressed by bone cells. This has been used recently for periodontal ligament cells in an attempt to understand cell–cell signaling in terms of cytokine networks, and how these regulate complex biological processes such as tooth movement (47, 48). The downside is that more genomic data increases the difficulty of establishing a coherent sequence of events at the protein level.

This brings us to the significance of the present findings in the context of intact bone. Mechanical strain is an important determinant of bone mass and architecture, and the introduction of *in vivo* models in which carefully controlled external loads could be applied to bone, led to important advances in understanding the strain-dependent adaptation of bone to altered function (49–51). These showed that increased bone strains above a certain critical threshold resulted in bone formation, while reductions in strain magnitude resulted in bone loss and osteopenia. In the jaws, for example, masticatory hypofunction resulting from reduced occlusal loading leads to a reduction in alveolar bone mass and bone mineral density (52–55). Stress-shielding and disuse atrophy resulting from the implantation of rigid metallic devices into bone, is also a well-recognized complication of total hip arthroplasty and fracture fixation in orthopedic surgery (56–58).

To describe this tissue-level regulatory negative-feedback mechanism and add some clarity to the relationship between form and function in bone, the principle of a “mechanostat” for regulating bone mass was revived by Frost (59); the basic idea being that for each bone in the skeleton, there is a functional or mechanically adapted state within the boundaries of which normal bone

mass is maintained. Osteoblasts cultured *in vitro* are deprived of the mechanical stimuli to which they would normally be exposed *in vivo* – in other words, the cells are in a physiological default state that in the intact skeleton leads to a decrease in bone strains below the critical threshold required for the maintenance of normal osseous architecture. The result is a localized negative skeletal balance or osteopenia and the reason why *in vitro* models are ideal for investigating bone resorption – the osteopenia is not permanent, however, and can be reversed by the restoration of normal functional loading.

The use of neonatal mouse calvaria as a source of primary cells of the osteoblast lineage as an alternative to transformed cell lines in bone biology is well-established. However, phenotypic differences exist between individual bones of the skeleton depending on their anatomical location, and calvarial and limb bones do not demonstrate the same responses to mechanical loading. Rawlinson et al. (60) recorded normal functional strains as low as 30 microstrain ( $\mu\text{e}$ ) on rat parietal bone and found that unlike tibial osteoblasts (derived from lateral plate mesoderm), calvarial osteoblasts (of neural crest cell origin) did not show the same early responses to dynamic mechanical strain. Direct strain measurements in a human volunteer further showed that in the skull, the highest strains recorded (200  $\mu\text{e}$ ) were 10-fold lower than for the tibia (61), levels that in the rest of the skeleton would lead to profound bone loss.

Differences between neural crest and mesodermal bone in the concentration of growth factors (62, 63), heterogeneity of the enzymes produced by their osteoclasts (64, 65), patterns of expression of bone morphogenetic proteins (66) and the abundance of several matrix proteins, notably collagen in calvarial bone (67) have been reported. However, none provide an adequate answer to the question: what makes calvarial bone resistant to levels of mechanical strain that in the rest of the skeleton would lead to profound bone loss? It cannot be because calvarial bone is derived

from the neural crest – the bones of the jaws are also of neural crest cell origin and do not show the same resistance to reduced mechanical loading. The well-characterized primary human calvarial and femoral osteoblasts now available from commercial sources provides an opportunity to further investigate these aspects of the mechanobiology of bone, but whether *in vitro* models are able to provide the answer remains to be seen.

In conclusion, the findings of this investigation are counterintuitive because IL-1 $\beta$ , TNF- $\alpha$ , and IL-6 have well-established reputations as bone resorptive agents. Nevertheless, they are pleiotropic molecules with multiple biological activities in addition to the stimulation of resorption, underlining the complexity of the biological response of osteoblasts to mechanical deformation, and the need to understand cell–cell signaling in terms of cytokine networks. It is also important to recognize that osteoblasts cultured *in vitro* are in a physiological default state that in the skeleton leads to decreased bone strains and osteopenia; this suggests that the application of mechanical strain to osteoblasts *in vitro* results in an osteogenic stimulus by restoring the metabolic activity of the cells to levels approaching that produced by functional osteoblasts *in vivo*.

## ACKNOWLEDGMENTS

We are grateful to Dr. Martyn Sheriff, King's College London Dental Institute at Guy's, King's College and St. Thomas's Hospitals, University of London for the formula used to calculate the maximal percentage base distortion of the Petriperm dishes. To Dr. Anthony Tumber, Research Scientist at Structural Genomics Consortium, University of Oxford for advice on osteoclast culture techniques and the resorption pit assay. To Ing. Patricia Castillo Ocampo, Scan Electronic Microscopy Unit–Universidad Autónoma Metropolitana Unidad Iztapalapa, Mexico City. This study has been supported by a grant from PROMEP-CA-S.E.P. and Universidad Autónoma Metropolitana Mexico City.

## REFERENCES

- Krall EA, Dawson-Hughes B. Heritable and lifestyle determinants of bone mineral density. *J Bone Miner Res* (1993) **8**:1–9. doi:10.1002/jbm.5650080102
- Välimäki MJ, Karkkainen M, Lamberg-Allardt C, Laitinen K, Alhava E, Heikkilä J, et al. Exercise, smoking and calcium intake during adolescence and early childhood as determinants of peak bone mass. Cardiovascular Risk in Young Finns Study Group. *BMJ* (1994) **309**: 230–5. doi:10.1136/bmj.309.6949.230
- Henderson JH, Carter DR. Mechanical induction in limb morphogenesis: the role of growth-generated strains and pressures. *Bone* (2002) **31**:645–53. doi:10.1016/S8756-3282(02)00911-0
- Murray PDF, Smiles M. Factors in the evocation of adventitious (secondary) cartilage in the chick embryo. *Aust J Zool* (1965) **13**:351–81. doi:10.1071/ZO9650351
- Meikle MC. In vivo transplantation of the mandibular joint of the rat; an autoradiographic investigation into cellular changes at the condyle. *Arch Oral Biol* (1973) **18**:1011–20. doi:10.1016/0003-9969(73)90183-0
- Nilsson BE, Westlin NE. Bone density in athletes. *Clin Orthop Relat Res* (1971) **77**:179–82.
- Donaldson CL, Hulley SB, Vogel JM, Hattner RS, Bayers JH, McMillan DE. Effect of prolonged bed rest on bone mineral. *Metabolism* (1970) **19**:1071–84. doi:10.1016/0026-0495(70)90032-6
- Jee WSS, Wronski TJ, Morey TJ, Kimmel DB. Effects of space flight on trabecular bone in rats. *Am J Physiol* (1983) **244**:R310–4.
- Frost HM. *Bone Remodeling Dynamics*. Springfield, IL: Charles C. Thomas (1963).
- Skerry TM, Bitensky L, Chayen J, Lanyon LE. Early strain-related changes in enzyme activity in osteocytes following bone loading *in vivo*. *J Bone Miner Res* (1989) **4**:783–8. doi:10.1002/jbmr.5650040519
- Lanyon LE. Using functional loading to influence bone mass and architecture: objectives, mechanisms and relationship with estrogen of the mechanically adaptive process in bone. *Bone* (1996) **18**:37S–43S. doi:10.1016/8756-3282(95)00378-9
- Roodman GD. Advances in bone biology: the osteoclast. *Endocr Rev* (1996) **17**:308–22. doi:10.1210/edrv-17-4-308
- Manolagas SC. Birth and death of bone cells; basic regulatory mechanisms and implications for the pathogenesis and treatment of osteoporosis. *Endocr Rev* (2000) **21**:115–37. doi:10.1210/er.21.2.115
- Gowen M, Wood DD, Ihrie EJ, McGuire MKB, Russell RGG. An interleukin 1-like factor stimulates bone resorption *in vitro*. *Nature* (1983) **306**:378–80. doi:10.1038/306378a0
- Heath JK, Saklatvala J, Meikle MC, Atkinson SJ, Reynolds JJ. Pig interleukin 1 (catabolin) is a potent stimulator of bone resorption *in vitro*. *Calcif Tissue Int* (1985) **37**:95–7. doi:10.1007/BF02557686
- Bertolini DR, Nedwin GE, Birmingham TS, Smith DD, Mundy GR. Stimulation of bone resorption and inhibition of bone formation *in vitro* by human tumor necrosis factors. *Nature* (1986) **319**:518–518. doi:10.1038/319516a0
- Ishimi Y, Miyaura C, Jin CH, Akatsu T, Abe E, Nakamura Y, et al. IL-6 is produced by osteoblasts and induces bone resorption. *J Immunol* (1990) **145**:3297–303.
- Gowen M. Interleukin-1 and tumor necrosis factor. In: Gowen M, editor. *Cytokines and Bone Metabolism*. Boca Raton, FL: CRC Press (1992). p. 71–91.

19. Takahashi N, Yamana H, Yoshiki S, Roodman GD, Mundy GR, Jones SJ, et al. Osteoclast-like cell formation and its regulation by osteotropic hormones in mouse bone marrow cultures. *Endocrinology* (1998) **122**:1373–82. doi:10.1210/endo-122-4-1373
20. Simonet WS, Lacey DL, Dunstan CR, Kelley M, Chang MS, Lüthy R, et al. Osteoprotegerin: a novel secreted protein involved in the regulation of bone density. *Cell* (1997) **89**:309–19. doi:10.1016/S0092-8674(00)80209-3
21. Tsuda E, Goto M, Mochizuki S, Yano K, Kobayashi F, Morinaga T, et al. Isolation of a novel cytokine from human fibroblasts that specifically inhibits osteoclastogenesis. *Biochem Biophys Res Commun* (1997) **234**:137–42. doi:10.1006/bbrc.1997.6603
22. Lacey DL, Timms E, Tan HL, Kelley MJ, Dunstan CR, Burgess T, et al. Osteoprotegerin ligand is a cytokine that regulates osteoclast differentiation and activation. *Cell* (1998) **93**:165–76. doi:10.1016/S0092-8674(00)81569-X
23. Yasuda H, Shima N, Nakagawa N, Yamaguchi K, Kinoshita M, Mochizuki S, et al. Osteoclast differentiation factor is a ligand for osteoprotegerin/osteoclastogenesis-inhibitory factor and is identical to TRANCE/RANKL. *Proc Natl Acad Sci U S A* (1998) **95**:3597–602. doi:10.1073/pnas.95.7.3597
24. Tsukii K, Shima N, Mochizuki S, Yamaguchi K, Kinoshita M, Yano K, et al. Osteoclast differentiation factor mediates an essential signal for bone resorption induced by 1α,25-dihydroxyvitamin D<sub>3</sub>, prostaglandin E<sub>2</sub>, or parathyroid hormone in the microenvironment of bone. *Biochem Biophys Res Commun* (1998) **246**:337–41. doi:10.1006/bbrc.1998.8610
25. Nakagawa N, Kinoshita M, Yamaguchi K, Shima N, Yasuda H, Yano K, et al. RANK is the essential signaling receptor for osteoclast differentiation factor in osteoclastogenesis. *Biochem Biophys Res Commun* (1998) **253**:395–400. doi:10.1006/bbrc.1998.9788
26. Heath JK, Atkinson SJ, Meikle MC, Reynolds JJ. Mouse osteoblasts synthesize collagenase in response to bone resorbing agents. *Biochim Biophys Acta* (1984) **802**:151–4. doi:10.1016/0304-4165(84)90046-1
27. Banes AJ, Gilbert J, Taylor D, Monbureau O. A new vacuum-operated stress-providing instrument that applies static or variable tension or compression to cells in vitro. *J Cell Sci* (1985) **75**:35–42.
28. García-López S, Meikle MC, Villanueva RE, Montaño L, Massó F, Ramírez-Amador V, et al. Mechanical deformation inhibits IL-10 and stimulates IL-12 production by mouse calvarial osteoblasts in vitro. *Arch Oral Biol* (2005) **50**:449–52. doi:10.1016/j.anchoralbio.2004.09.001
29. Rubin CT, Lanyon LE. Regulation of bone formation by applied dynamic loads. *J Bone Joint Surg* (1984) **66A**:397–402.
30. Hsieh Y-F, Robling AG, Ambrosius WT, Burr DB, Turner CH. Mechanical loading of diaphyseal bone in vivo: the strain threshold for an osteogenic response varies with location. *J Bone Miner Res* (2001) **16**:2291–7. doi:10.1359/jbmr.2001.16.12.2291
31. Boyde A, Ali NN, Jones SJ. Resorption of dentine by isolated osteoclasts in vitro. *Br Dent J* (1984) **156**:216–20. doi:10.1038/sj.bdj.4805313
32. Tumber A, Papaioannou J, Breckon JJW, Meikle MC, Reynolds JJ, Hill PA. The effects of serine proteinase inhibitors on bone resorption in vitro. *J Endocrinol* (2003) **178**:437–47. doi:10.1677/joe.0.1780437
33. Rubin J, Murphy T, Nanes MS, Fan X. Mechanical strain inhibits expression of osteoclast differentiation factor by murine stromal cells. *Am J Physiol Cell Physiol* (2000) **278**:C1126–32.
34. Kusumi A, Sakaki H, Kusumi T, Oda M, Narita K, Nakagawa H, et al. Regulation of synthesis of osteoprotegerin and soluble receptor activator of nuclear factor-κB ligand in normal human osteoblasts via the p38 mitogen-activated protein kinase pathway by the application of cyclic tensile strain. *J Bone Miner Metab* (2005) **23**:373–81. doi:10.1007/s00774-005-0615-6
35. Ragab AA, Nalepka JL, Bi Y, Greenfield EM. Cytokines synergistically induce osteoclast differentiation: support by immortalized or normal calvarial cells. *Am J Physiol Cell Physiol* (2004) **283**:C679–87. doi:10.1152/ajpcell.00421.2001
36. Brändström H, Jonsson KB, Vidal O, Ljunghall S, Ohlsson C, Ljunghall Ö. Tumor necrosis factor-α and -β upregulates the levels of osteoprotegerin mRNA in human osteosarcoma MG-63 cells. *Biochem Biophys Res Commun* (1998) **248**:454–7. doi:10.1006/bbrc.1998.8993
37. Vidal ON, Sjögren K, Eriksson B, Ljunghall Ö, Ohlsson C. Osteoprotegerin mRNA is increased by interleukin-1α in the human osteosarcoma cell line MG-63 and in human osteoblast-like cells. *Biochem Biophys Res Commun* (1998) **248**:696–700. doi:10.1006/bbrc.1998.9035
38. Pantouli E, Boehm MM, Koka S. Inflammatory cytokines activate p38 MAPK to induce osteoprotegerin synthesis by MG-63 cells. *Biochem Biophys Res Commun* (2005) **329**:224–9. doi:10.1016/j.bbrc.2005.01.122
39. Kwan Tat S, Padrines M, Théoleyre S, Heymann D, Fortun Y. IL-6, RANKL, TNF-alpha/IL-1: interactions in bone resorption pathophysiology. *Cytokine Growth Factor Rev* (2004) **15**:49–60. doi:10.1016/j.cytofr.2003.10.005
40. Théoleyre S, Wittrant Y, Kwan Tat S, Fortun Y, Redini F, Heymann D. The molecular triad OPG/RANK/RANKL: involvement in the orchestration of pathophysiological bone remodeling. *Cytokine Growth Factor Rev* (2004) **15**:457–75. doi:10.1016/j.cytofr.2004.06.004
41. Xu LX, Kukita T, Kukita A, Otsuka T, Niho Y, Iijima T. Interleukin-10 selectively inhibits osteoclastogenesis by inhibiting differentiation of osteoclast progenitors into preosteoclast-like cells in rat bone marrow culture system. *J Cell Physiol* (1995) **165**:624–9. doi:10.1002/jcp.1041650321
42. Owens JM, Gallagher AC, Chambers TJ. IL-10 modulates formation of osteoclasts in murine hemopoietic cultures. *J Immunol* (1996) **157**:936–40.
43. Horwood NJ, Elliot J, Martin TJ, Gillespie MT. IL-12 alone and in synergy with IL-18 inhibits osteoclast formation in vitro. *J Immunol* (2001) **166**:4915–21.
44. Nagata N, Kitaura H, Yoshida N, Nakayama K. Inhibition of RANKL-induced osteoclast formation in mouse bone marrow cultures by IL-12: involvement of IFN-γ possibly induced from non-T cell populations. *Bone* (2003) **33**:721–32. doi:10.1016/S8756-3282(03)00213-8
45. Van Vlasseler P, Borremans B, Van Den Heuvel R, Van Gorp U, de Waal Malefyt R. Interleukin-10 inhibits the osteogenic activity of mouse bone marrow. *Blood* (1993) **82**:2361–70.
46. Van Vlasseler P, Borremans B, Van Gorp U, Dasch JR, de Waal Malefyt R. Interleukin-10 inhibits transforming growth factor-β (TGF-β) synthesis required for osteogenic commitment of mouse bone marrow cells. *J Cell Biol* (1994) **124**:569–72. doi:10.1083/jcb.124.4.569
47. Wescott DC, Pinkerton MN, Gaffey BJ, Beggs KT, Milne TJ, Meikle MC. Osteogenic gene expression by human periodontal ligament cells under cyclic tension. *J Dent Res* (2007) **86**:1212–6. doi:10.1177/154405910708601214
48. Pinkerton MN, Wescott DC, Gaffey BJ, Beggs KT, Milne TJ, Meikle MC. Cultured human periodontal ligament cells constitutively express multiple osteotropic cytokines and growth factors, several of which are responsive to mechanical deformation. *J Periodontal Res* (2008) **43**:343–51. doi:10.1111/j.1600-0765.2007.01040.x
49. Hert J, Lisková M, Landa J. Reaction of bone to mechanical stimuli. Part 1. Continuous and intermittent loading of tibia in rabbit. *Folia Morphol* (1971) **19**:290–300.
50. Lisková M, Hert J. Reaction of bone to mechanical stimuli. Part 2. Periosteal and endosteal reaction of tibial diaphysis in rabbit to intermittent loading. *Folia Morphol (Praha)* (1971) **19**:301–17.
51. Lanyon LE. Functional strain as a determinant for bone remodeling. *Calcif Tissue Int* (1984) **36**:S56–61. doi:10.1007/BF02406134
52. Bresin A, Kiliaridis S, Strid KG. Effect of masticatory function on the internal bone structure in the mandible of the growing rat. *Eur J Oral Sci* (1999) **107**:35–44. doi:10.1046/j.0909-8836.1999.eos107107.x
53. Mavropoulos A, Kiliaridis S, Bresin A, Amman P. Effect of different masticatory functional and mechanical demands on the structural adaptation of the mandibular alveolar bone in young growing rats. *Bone* (2004) **35**:191–7. doi:10.1016/j.bone.2004.03.020
54. Kunii R, Yamaguchi M, Aoki Y, Watanabe A, Kasai K. Effects of experimental occlusal hypofunction and its recovery on mandibular bone mineral density in rats. *Eur J Orthod* (2008) **30**:52–6. doi:10.1093/ejo/cjm057
55. Vinoth JK, Patel KJ, Lih W-S, Seow Y-S, Cao T, Meikle MC. Appliance-induced osteopenia of dentoalveolar bone in the rat: effect of reduced bone strains on serum bone markers and the multifunctional hormone

- leptin. *Eur J Oral Sci* (2013). doi: 10.1111/eos.12091. [Epub ahead of print].
56. Huiskes R, Weinans H, van Rietbergen B. The relationship between stress shielding and bone resorption around total hip stems and the effects of flexible materials. *Clin Orthop Relat Res* (1992) **274**:124–34.
57. Glassman AH, Bobyn JD, Tanzer M. New femoral designs: do they influence stress shielding? *Clin Orthop Relat Res* (2006) **453**:64–74. doi:10.1097/01.blo.0000246541. 41951.20
58. Uthhoff HK, Poitras P, Backman DS. Internal plate fixation of fractures: short history and recent developments. *J Orthop Sci* (2006) **11**:118–126. doi:10.1007/s00776-005-0984-7
59. Frost HM. Bone ‘mass’ and the ‘mechanostat’: a proposal. *Anat Rec* (1987) **219**:1–9. doi:10.1002/ar.1092190104
60. Rawlinson SCF, Mosley JR, Suswillo Pitsillides AA, Lanyon LE. Calvarial and limb bone cells in organ and monolayer culture do not show the same early responses to dynamic mechanical strain. *J Bone Miner Res* (1995) **10**:1225–32. doi: 10.1002/jbm.5650100813
61. Hillam RA, Jackson M, Goodship AE, Skerry TM. Comparison of physiological strains in the human skull and tibia. *Bone* (1996) **19**:686. doi:10.1016/S8756-3282(97)84305-0 (Abstract),
62. Finkelman RD, Eason AL, Rakjian DR, Tutundzyan Y, Hardesty RA. Elevated IGF-II and TGF-beta concentrations in human calvarial bone: potential mechanism for increased graft survival and resistance to osteoporosis. *Plast Reconstr Surg* (1994) **93**:732–8. doi:10.1097/00006534-199404000-00012
63. Kasperk C, Wegerdal J, Strong D, Farley J, Wangerin K, Gropp H, et al. Human bone cell phenotypes differ depending on their skeletal site of origin. *J Clin Endocrinol Metab* (1995) **80**:2511–7. doi:10.1210/jc.80.8.2511
64. Hill PA, Murphy G, Docherty AJP, Hembry RM, Millican TA, Reynolds JJ, et al. The effects of selective inhibitors of matrix metalloproteinases (MMPs) on bone resorption and the identification of MMPs and TIMP-1 in isolated osteoclasts. *J Cell Sci* (1994) **107**:3055–64.
65. Everts V, Korper W, Jansen DC, Steinfort J, Lammerse I, Heera S, et al. Functional heterogeneity of osteoclasts: matrix metalloproteinases participate in osteoclastic resorption of calvarial bone but not in resorption of long bones. *FASEB J* (1999) **13**:1219–30.
66. Sutapreysri S, Kootongkaew S, Phongdara A, Leggat U. Expression of bone morphogenetic proteins in normal human intramembranous and endochondral bones. *Int J Oral Maxillofac Surg* (2006) **35**:444–52. doi:10.1016/j.ijom.2006.01.021
67. van den Bos T, Speijer D, Bank RA, Bromme D, Everts V. Differences in matrix composition between calvaria and long bone in mice suggest differences in biomechanical properties and resorption. Special emphasis on collagen. *Bone* (2008) **43**:459–68. doi:10.1016/j.bone.2008.05.009
- conducted in the absence of any commercial or financial relationships that could be construed as a potential conflict of interest.
- Received: 07 August 2013; accepted: 11 October 2013; published online: 28 October 2013.*
- Citation: García-López S, Villanueva R and Meikle MC (2013) Alterations in the synthesis of IL-1 $\beta$ , TNF- $\alpha$ , IL-6, and their downstream targets RANKL and OPG by mouse calvarial osteoblasts in vitro: inhibition of bone resorption by cyclic mechanical strain. Front. Endocrinol. 4:160. doi: 10.3389/fendo.2013.00160*
- This article was submitted to Bone Research, a section of the journal *Frontiers in Endocrinology*.
- Copyright © 2013 García-López, Vil- lanueva and Meikle. This is an open-access article distributed under the terms of the Creative Commons Attribution License (CC BY). The use, distribution or reproduction in other forums is permitted, provided the original author(s) or licensor are credited and that the original publication in this journal is cited, in accordance with accepted academic practice. No use, distribution or reproduction is permitted which does not comply with these terms.



# Physical activity and bone: may the force be with you

**Jonathan H. Tobias<sup>1\*</sup>, Virginia Gould<sup>1</sup>, Luke Brunton<sup>1</sup>, Kevin Deere<sup>1</sup>, Joern Rittweger<sup>2</sup>, Matthijs Lippert<sup>3</sup> and Bernd Grimm<sup>3</sup>**

<sup>1</sup> Musculoskeletal Research Unit, University of Bristol School of Clinical Sciences, Avon Orthopaedic Centre, Southmead Hospital, Bristol, UK

<sup>2</sup> German Aerospace Center, Institute of Aerospace Medicine, Cologne, Germany

<sup>3</sup> Atrium Medical Centre, AHORSE Foundation, Heerlen, Netherlands

**Edited by:**

Mark Stuart Cooper, University of Birmingham, UK

**Reviewed by:**

Mark Stuart Cooper, University of Birmingham, UK

Nicola Jane Crabtree, Birmingham Children's Hospital NHS Foundation Trust, UK

**\*Correspondence:**

Jonathan H. Tobias, Musculoskeletal Research Unit, University of Bristol School of Clinical Sciences, Avon Orthopaedic Centre, Southmead Hospital, Southmead Road, Bristol BS10 5NB, UK  
e-mail: jon.tobias@bristol.ac.uk

Physical activity (PA) is thought to play an important role in preventing bone loss and osteoporosis in older people. However, the type of activity that is most effective in this regard remains unclear. Objectively measured PA using accelerometers is an accurate method for studying relationships between PA and bone and other outcomes. We recently used this approach in the Avon Longitudinal Study of Parents and Children (ALSPAC) to examine relationships between levels of vertical impacts associated with PA and hip bone mineral density (BMD). Interestingly, vertical impacts >4g, though rare, largely accounted for the relationship between habitual levels of PA and BMD in adolescents. However, in a subsequent pilot study where we used the same method to record PA levels in older people, no >4g impacts were observed. Therefore, to the extent that vertical impacts need to exceed a certain threshold in order to be bone protective, such a threshold is likely to be considerably lower in older people as compared with adolescents. Further studies aimed at identifying such a threshold in older people are planned, to provide a basis for selecting exercise regimes in older people which are most likely to be bone protective.

**Keywords:** impact loading, bone, physical activity, BMD, exercise

## INTRODUCTION

Physical Activity (PA) declines markedly in older people; less than 30% of 65- to 74-year-olds and less than 15% of adults >75 report any moderate-intensity PA lasting >10 min in the previous 4 weeks (1). As well as increasing physical frailty and co-morbidities, psychological, social, and economic factors contribute to this decrease. For example, the OPAL study, which used a socio-ecological approach to identify psycho-social and socio-environmental influences on PA as assessed by accelerometry (2), found relationships with the nature and frequency of outings (3), neighborhood social deprivation (4), lack of intrinsic motivation, and lack of an activity companion (5). Higher levels of PA benefit a wide range of physiological systems in older people, including cardiovascular, respiratory, metabolic, neurological and neuromuscular, and cognitive function<sup>1</sup>, and improve life expectancy (6). The WHO recommends that those above age 65 partake in a minimum of 150 min of moderate-intensity aerobic PA per week (e.g., brisk walking), or 75 min of vigorous-intensity PA (e.g., jogging)<sup>2</sup>.

## PA AND OLDER PEOPLE'S BONE HEALTH

Hip fracture is a major cause of morbidity and mortality in older people, leading to loss of independence, and a huge economic burden through both direct medical costs and social sequelae (7). It is thought that age related declines in the intensity and quantity of PA contribute to this increase in risk of osteoporotic fracture, and that promotion of PA in older people helps to maintain bone

mass: epidemiological studies report that risk of hip fracture is reduced in older adults who remain more physically active (8); walking for leisure is associated with reduced hip fracture risk (9–11). Therefore, although increased PA in the elderly leads to greater exposure to falls risk, it would seem that any tendency for this to increase fracture risk is outweighed by other benefits and that the net effect is a reduction in fracture risk. As well as benefits in terms of bone mass as described below, PA may also reduce the risk of falls through specific muscle-strengthening and balance-training activities, which preserve muscle strength, delaying sarcopenia, and maintaining neuromuscular function necessary to keep balance and react to a fall.

In terms of effects on bone mass, PA may stimulate bone formation and thus improve bone mineral density (BMD), which is strongly related to hip fracture risk (12), through exposing the skeleton to mechanical strain (defined as deformation of bone per unit length in response to loading). An important physiological link exists between exercise and bone, as demonstrated by findings from animal studies over 30 years ago that the skeleton is exquisitely responsive to mechanical strain; bone loss caused by immobilization was prevented by only four loading cycles per day (13). Though related to fracture risk, there is little evidence that walking interventions improve BMD, as judged by findings of a recent meta-analysis (14). In contrast, protocols that combined jogging, walking, and stair climbing consistently improve hip BMD in older people (15). Interventions to increase aerobic activities, high impact exercises, “odd-impact” exercise loading, and resistance training (designed to increase bone loading through increased muscle strength) also improve hip BMD in this group (15–19). However, the optimum type of activity for improving

<sup>1</sup><http://www.health.gov/paguidelines/report/pdf/committeereport.pdf>

<sup>2</sup>[http://whqlibdoc.who.int/publications/2010/9789241599979\\_eng.pdf](http://whqlibdoc.who.int/publications/2010/9789241599979_eng.pdf)

BMD remains unknown, and it is unclear whether a specific strain needs to be exceeded. Moreover, other aspects of impacts may also be important, such as movement frequency. In addition, specific activities may affect BMD at certain sites in preference to others, which may be important if improved BMD is to translate into reduced fracture risk which is the primary goal, in light of evidence that hip fracture risk is related to thinning of a specific portion of the femoral neck (20).

### MEASUREMENT OF PA ACCORDING TO LEVEL OF IMPACT LOAD

Observational studies may be useful for estimating relationships between PA and bone outcomes, providing the PA measure in question is related to strain. PA questionnaires have been used to record participation in different sporting activities graded according to vertical impact loads (21). Pedometers were used in a cross sectional study of 105 individuals aged 49–64 years, with a dose-response relationship observed in females between cumulative loading as calculated from a combination of number of steps, walking speed, and weight, and hip BMD (22). Lower limb impact during weight bearing reflects their ground reaction force which is the product of mass times acceleration, and so depending on placement accelerometers can provide objective measures of exposure to different levels of impact load. To detect vertical movement of the center of mass, accelerometers need to be attached to the trunk, for example held in a belt laterally just below the waist, despite the fact that some dampening through the skin will occur particularly in obese individuals (other placements such as the ankle are less accurate as movements can occur independently of the center of mass). Using an Actigraph device in this way in adolescents from the Avon Longitudinal Study of Parents and Children (ALSPAC), vigorous PA (based on a threshold of 6200 cpm, equivalent to jogging) was positively related to cortical bone mass, but no independent relationship was seen for moderate PA after adjusting for vigorous PA (23).

Although these findings suggest that the Actigraph differentiates between PA exposure and bone outcomes according to impact level, earlier versions of this device were primarily designed to measure general body movement, and externally calibrated to energy consumption to be associated with obesity-related outcomes (24). They were limited in detecting brief high impact events with high osteogenic potential due to a narrow dynamic range (original devices had an upper range of 2.13g), filtering out of high frequency motion, and summation of records into epochs of typically 30–60 s. Moreover, rather than a true representation of “event” frequency, the counts per minute (cpm) output of the Actigraph integrates movement frequency with level of acceleration, making it difficult to relate the output to specific impacts or activities.

Newer generations of digital accelerometers [e.g., Actigraph GT3X-BT, Gulf Coast Data Concepts (GCDC) X16-1c] have wider dynamic ranges (8 and 16g, respectively), high sampling frequencies (>100 Hz), and the raw signal can be accessed without filtering or summation into epochs. Previous studies using a research prototype developed by Newtest suggest that the ability to derive impact loads from the raw signal, ideally suited for studying PA effects on the skeleton, can yield important insights. The Newtest prototype recorded the number of counts within

33 pre-specified acceleration bands, and distinguished exposure to high impact loads associated with osteogenic activities like running and jumping (25). In a prospective study of PA exposure in 64 premenopausal women using this device, a positive relationship was only observed between hip BMD and counts >3.9g (seen during running) (25). Similarly, after analyzing cross sectional relationships between exposure to different g-forces and bone development in ALSPAC 17-year-olds, hip BMD was most strongly related to counts >4g, in spite of their rarity, whereas no association was seen for lower impact loads after adjusting for exposure to higher impacts (26). This 4g threshold represents a higher impact than the 6200 cpm threshold for vigorous PA as used in our previous Actigraph study (23), but is entirely consistent with current understanding of skeletal physiology (27).

Subsequent analysis of pQCT-based measures performed at the mid-tibia suggested high impacts improve BMD of the lower limb through a combination of increased cortical thickness and periosteal circumference, with the latter effect strongest in boys (28). In future studies, we hope to repeat these measures to establish whether exposure to high impacts during childhood and adolescence has persisting effects on subsequent peak bone mass. Evidence that past history of sporting activity in childhood and adolescence is positively associated with cortical bone mass in young adult men is consistent with the suggestion that the positive influence of high impact activity on bone which we observed has a persisting effect (29).

Interestingly, impacts >3.1g (seen during jogging and running) were also particularly related to lean mass (30), suggesting this approach may also be more accurate in analyzing relationships with lean mass, with potential application to the study of sarcopenia. In contrast, impacts within 1–3g (e.g., moderately brisk walking and jogging (25) were most strongly related to fat mass (30). The latter relationship was equivalent to that previously reported from the same cohort based on moderate and vigorous physical activity (MVPA) as measured by Actigraph (31), consistent with cross calibration studies showing reasonably high correlation between Actigraph (MVPA), and the sum of counts in g bands >1.1g measured by Newtest ( $r^2 = 0.41$ ). Hence, exposure to lower impacts may be helpful in evaluating effects of PA on other systems.

### PA IMPACTS IN OLDER PEOPLE

While assessment of PA according to impact level has provided novel insights in adolescents and premenopausal women, it is unclear whether these findings also apply to older individuals. Even in adolescents, impacts >4g, or even >3.1g are rare (e.g., median 39 impacts >3.1g/day) (30). These impacts are likely to be even rarer in older people, but we are not aware of any previous studies examining this question. Therefore, we performed two pilot studies to characterize habitual exposure to PA in older people according to level of impact.

### PILOT STUDY POST HIP/KNEE REPLACEMENT

We aimed to record habitual PA over 7 days in older people as part of a wider study of functional outcomes following hip/knee joint replacement surgery. We studied patients who were 3 months post joint replacement, by which time they had largely recovered from

the effects of surgery and returned to their pre-operative functional level. After obtaining written informed consent, a GCDC Series X250-2 tri-axial accelerometer was attached to an elasticated belt, and worn in a horizontal orientation just anterior to the ischial crest during waking hours (except when washing, swimming, or bathing). Vertical impacts were classified into five bands (0.5–1, 1–2, 2–3, 3–4, >4g), and the mean count calculated at each band for each individual. Results were subsequently expressed as number of counts per day.

All participants wore the monitors for the full 7 days (for a median of 106 h). Nineteen of 24 participants had usable data (median age 68.9). As a group, their level of function was relatively low as reflected by a median of 20 s for their 20 m walk time and 14 s for “get-up-and-go” test. Very few vertical impacts at the hip of 3g or higher were recorded in this study; 12 of the 19 participants achieved one or more impacts over 3g, with a maximum count of 8 impacts at this level over the 7 days (**Table 1**). Similarly, only 8 of

**Table 1 | Median and quartiles of the number of daily activity counts for each g band, and total activity counts, for 19 individuals 3 months post joint replacement.**

|                      | Median | 25th   | 75th    |
|----------------------|--------|--------|---------|
| 0.5–1g               | 512.86 | 373.71 | 1744.07 |
| 1–2g                 | 72.86  | 29.00  | 89.36   |
| 2–3g                 | 1.43   | 0.43   | 4.50    |
| 3–4g                 | 0.14   | 0.00   | 0.21    |
| >4g                  | 0.00   | 0.00   | 0.21    |
| Total activity count | 538.57 | 434.29 | 1827.79 |

the 19 achieved one or more impacts at the hip of 4g or greater, with a maximum of 4 impacts at this level recorded in the 7 days period. In order to investigate whether the most active individuals were also those achieving the highest vertical impacts, mean daily total counts against mean daily counts in the higher impact bands were plotted for each individual. The most active individuals, by total number of activity counts, were not necessarily those sustaining the highest vertical impacts (**Figures 1 and 2**).

### AEROBICS CLASS PILOT STUDY

Twenty participants were recruited from a group of older females regularly attending exercise classes at the University of Bristol Centre for Sports, Exercise and Health. Four study sessions, each with five participants, were held. Each participant was fitted with a tri-axial accelerometer as described above. Monitors were turned on just before the start of the session, and recordings matched to different activities within it. The study sessions consisted of a short exercise routine to music, similar to that carried out in the participants’ usual classes (**Table 2**). This was also extended by other activities (20 m walking normal pace, 20 m brisk walking, 20 cm step up and down with repeats, 30 cm step up and down with repeats). Data was analyzed as counts of vertical impacts for each activity, with impacts grouped in 0.3g bands (from 0–0.3 to >2.1g).

Participants were a mean of 67 years of age, and had a relatively good level of function as reflected by median of 14 s for 20 walk and 8 s for “get-up-and-go” test. For one participant, no data was recorded due to failure of the monitor. In another case, the monitor stopped working after the exercise class part of the session, but before the further individual activities. No vertical impacts higher than 2.1g were recorded in this study. One individual recorded 46

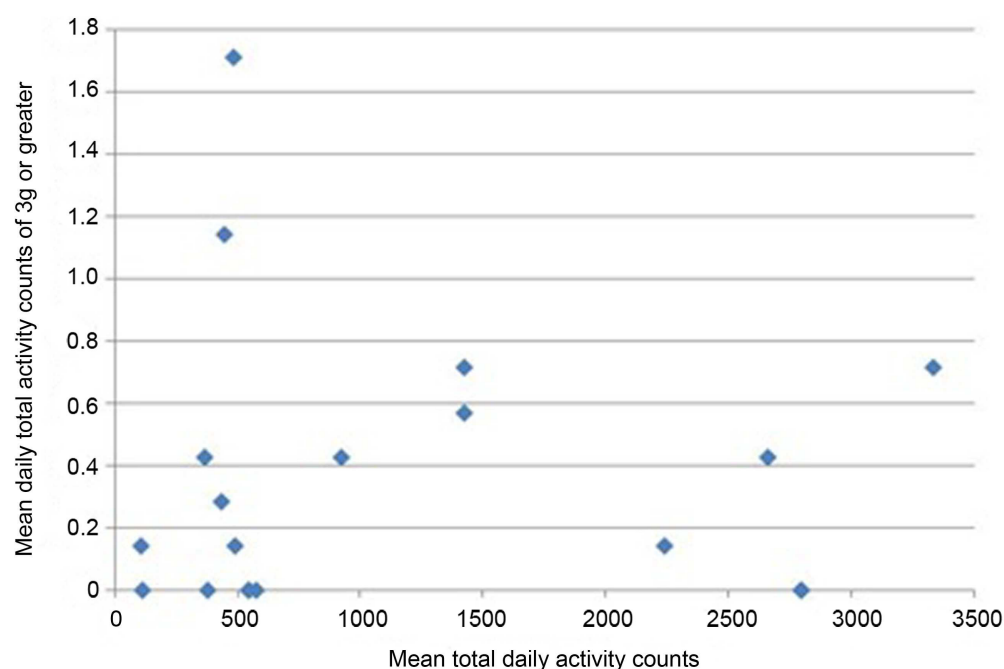


**FIGURE 1 | Mean daily total activity counts plotted against mean daily vertical impacts >3g for each individual.**

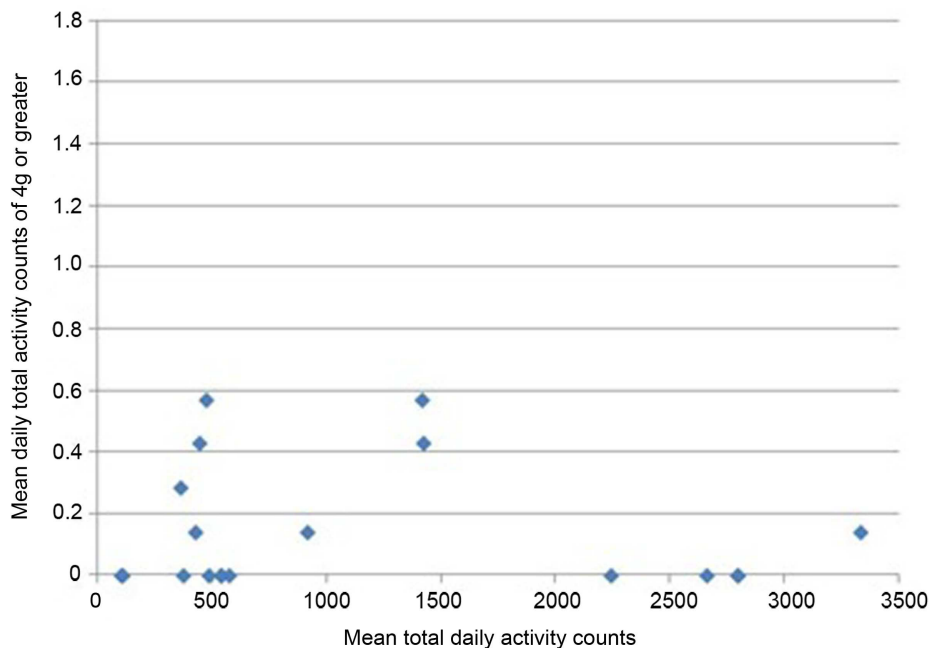


**FIGURE 2 |** Mean daily total activity counts plotted against mean daily vertical impacts >4g for each individual.

**Table 2 | Aerobics class activities.**

- 1 "Mambo" leading from the left leg (left leg step forward, right leg step in place, left leg step backward).
- 2 "Mambo" leading from the right leg.
- 3 "Easy walk" leading from the left leg (Left foot forward, right foot forward and wide, left foot back, right foot next to left).
- 4 "Easy walk" leading from the right leg.
- 5 "Double side-step" (left foot sideways, right on spot, left foot next to right, right foot sideways, left on spot, right foot next to left).
- 6 "Half Jack" (jump to five-pointed star with arms to shoulder height, jump to standing with arms down, and feet together).
- 7 "Hamstring Curl" (alternate sides step sideways, bring other foot up to rear).
- 8 "Knee Lift" (lifting knee on alternate sides).

counts of 1.8–2.1g over all activities, and another 25 counts. Seven of the 19 participants with impact data achieved no counts in the 1.8–2.1g band, and in one case the highest impact recorded was in the 0.9–1.2g band.

### FUTURE RESEARCH QUESTIONS

Taken together, these pilot studies suggest that not surprisingly, older individuals are exposed to considerably lower g-forces compared to adolescents and premenopausal women. For example, there was virtually a complete lack of higher impacts at the level suggested to be required for optimal bone development in adolescents. Due to the small size of the pilot studies presented here,

and the selective nature of their recruitment, our findings are not necessarily generalizable to the wider population; in the Vertical Impacts and Bone in the Elderly (VIBE) study, we are in the process of extending our studies to characterize vertical impacts in much larger population-based cohorts of older people. Assuming our findings are at least partly representative of the level of vertical forces to which older people are exposed, impacts within lower g ranges which we recorded may well exert some protective effect on the skeleton. Loss of these low impacts may represent an important contribution to the development of osteoporosis in later life. The skeleton of older individuals may be more sensitive to low impacts compared to children and younger adults for several reasons. For example, lower g-forces may be needed to preserve bone, as opposed to stimulate its acquisition during peak bone mass attainment. In children and adolescents, bone accrual is achieved by a process of bone modeling involving a combination of longitudinal growth and periosteal expansion; it may well be that these physiological processes are regulated by a different level of strain, compared to bone remodeling responsible for preservation of bone in the mature skeleton. Furthermore, a given level of impact will produce greater strains in older people, due to their reduced bone strength.

Therefore, although a dose–response relationship between impact level and BMD may still exist in older people, this is likely to be shifted to the left. Defining such relationships will be key to identifying the types of activity that are likely to be the most effective in preventing bone loss and osteoporosis in older individuals. An important caveat is that exposure to such forces must be safe and without risk of injury. If forces between 1.8 and 2.1g, in the upper range of that observed in older participants performing an aerobics class, are found to be bone protective, it

seems highly unlikely that these are sufficient to cause injury by themselves. However, performing such activities without supervision or appropriate training, or in the presence of co-morbidities affecting musculoskeletal or neurological function, may lead to a significant risk of falls and fractures. Therefore, having found which activities are likely to be bone protective, an important goal in their evaluation will be to ensure they can be delivered safely as well as effectively.

## REFERENCES

- Craig R. *Health Survey for England*. Leeds: NHS (2009).
- Davis MG, Fox KR, Hillsdon M, Sharp DJ, Coulson JC, Thompson JL. Objectively measured physical activity in a diverse sample of older urban UK adults. *Med Sci Sports Exerc* (2011) **43**:647–54. doi:10.1249/MSS.0b013e3181f36196
- Davis MG, Fox KR, Hillsdon M, Coulson JC, Sharp DJ, Stathi A, et al. Getting out and about in older adults: the nature of daily trips and their association with objectively assessed physical activity. *Int J Behav Nutr Phys Act* (2011) **8**:116. doi:10.1186/1479-5868-8-116
- Fox KR, Hillsdon M, Sharp D, Cooper AR, Coulson JC, Davis M, et al. Neighbourhood deprivation and physical activity in UK older adults. *Health Place* (2011) **17**:633–40. doi:10.1016/j.healthplace.2011.01.002
- Stathi A, Gilbert H, Fox KR, Coulson J, Davis M, Thompson JL. Determinants of neighborhood activity of adults age 70 and over: a mixed-methods study. *J Aging Phys Act* (2012) **20**:148–70.
- Lee IM, Shiroma EJ, Lobelo F, Puska P, Blair SN, Katzmarzyk PT. Effect of physical inactivity on major non-communicable diseases worldwide: an analysis of burden of disease and life expectancy. *Lancet* (2012) **380**:219–29. doi:10.1016/S0140-6736(12)61031-9
- Burge RT. The cost of osteoporotic fractures in the UK: projections for 2000–2020. *J Med Econ* (2001) **4**:51–62. doi:10.1159/000176049
- Moayyeri A. The association between physical activity and osteoporotic fractures: a review of the evidence and implications for future research. *Ann Epidemiol* (2008) **18**:827–35. doi:10.1016/j.annepidem.2008.08.007
- Feskanich D, Willett W, Colditz G. Walking and leisure-time activity and risk of hip fracture in postmenopausal women. *JAMA* (2002) **288**:2300–6. doi:10.1001/jama.288.18.2300
- Moayyeri A, Besson H, Luben RN, Wareham NJ, Khaw KT. The association between physical activity in different domains of life and risk of osteoporotic fractures. *Bone* (2010) **47**:693–700. doi:10.1016/j.bone.2010.06.023
- Cummings SR, Nevitt MC, Browner WS, Stone K, Fox K, Ensrud KE, et al. Group ftsOFR. 1995. Risk factors for hip fracture in white women. *N Engl J Med* (1995) **332**:767–73. doi:10.1056/NEJM199503233321202
- Cummings SR, Black DM, Nevitt MC, Browner W, Cauley J, Ensrud K, et al. Bone density at various sites for prediction of hip fractures. *Lancet* (1993) **341**:72–5. doi:10.1016/0140-6736(93)92555-8
- Rubin LT, Lanyon CE. Regulation of bone formation by applied dynamic loads. *J Bone Joint Surg.* (1984) **66A**:397–402.
- Martyn-St James M, Carroll S. Meta-analysis of walking for preservation of bone mineral density in postmenopausal women. *Bone* (2008) **43**:521–31. doi:10.1016/j.bone.2008.05.012
- Martyn-St James M, Carroll S. A meta-analysis of impact exercise on postmenopausal bone loss: the case for mixed loading exercise programmes. *Br J Sports Med* (2009) **43**:898–908. doi:10.1136/bjsm.2008.052704
- Bemben DA, Bemben MG. Dose-response effect of 40 weeks of resistance training on bone mineral density in older adults. *Osteoporos Int* (2011) **22**:179–86. doi:10.1007/s00198-010-1182-9
- Nikander R, Kannus P, Dastidar P, Hannula M, Harrison L, Cervinka T, et al. Targeted exercises against hip fragility. *Osteoporos Int* (2009) **20**:1321–8. doi:10.1007/s00198-008-0785-x
- Martyn-St James M, Carroll S. Effects of different impact exercise modalities on bone mineral density in premenopausal women: a meta-analysis. *J Bone Miner Metab* (2010) **28**:251–67. doi:10.1007/s00774-009-0139-6
- Marques EA, Wanderley F, Machado L, Sousa F, Viana JL, Moreira-Goncalves D, et al. Effects of resistance and aerobic exercise on physical function, bone mineral density, OPG and RANKL in older women. *Exp Gerontol* (2011) **46**(7):524–32. doi:10.1016/j.exger.2011.02.005
- Johannesdottir F, Poole KE, Reeve J, Siggeirsottir K, Aspelund T, Mogensen B, et al. Distribution of cortical bone in the femoral neck and hip fracture: a prospective case-control analysis of 143 incident hip fractures; the AGES-REYKJAVIK Study. *Bone* (2011) **48**:1268–76. doi:10.1016/j.bone.2011.03.776
- Lorentzon M, Mellstrom D, Ohlsson C. Association of amount of physical activity with cortical bone size and trabecular volumetric BMD in young adult men: the GOOD study. *J Bone Miner Res* (2005) **20**:1936–43. doi:10.1359/JBMR.050709
- Boyer KA, Kiratli BJ, Andriacchi TP, Beaupre GS. Maintaining femoral bone density in adults: how many steps per day are enough? *Osteoporos Int* (2011) **22**:2981–8. doi:10.1007/s00198-011-1538-9
- Sayers A, Mattocks C, Deere K, Ness A, Riddoch C, Tobias JH. Habitual levels of vigorous, but not moderate or light, physical activity is positively related to cortical bone mass in adolescents. *J Clin Endocrinol Metab* (2011) **96**:E793–802. doi:10.1210/jc.2010-2550
- Mattocks C, Leary S, Ness A, Deere K, Saunders J, Tilling K, et al. Calibration of an accelerometer during free-living activities in children. *Int J Pediatr Obes* (2007) **2**:218–26.
- Vainionpaa A, Korpelainen R, Vihrilala E, Rinta-Paavola A, Leppaluoto J, Jamsa T. Intensity of exercise is associated with bone density change in premenopausal women. *Osteoporos Int* (2006) **17**:455–63. doi:10.1007/s00198-005-0005-x
- Deere K, Sayers A, Rittweger J, Tobias JH. Habitual levels of high, but not moderate or low, impact activity are positively related to hip BMD and geometry: results from a population-based study of adolescents. *J Bone Miner Res* (2012) **27**:1887–95. doi:10.1002/jbmr.1631
- Sievanen H. Bone: impact loading—nature's way to strengthen bone. *Nat Rev Endocrinol* (2012) **8**:391–3. doi:10.1038/nrendo.2012.88
- Deere K, Sayers A, Rittweger J, Tobias JH. A cross-sectional study of the relationship between cortical bone and high-impact activity in young adult males and females. *J Clin Endocrinol Metab* (2012) **97**:3734–43. doi:10.1210/jc.2012-1752
- Nilsson M, Ohlsson C, Mellstrom D, Lorentzon M. Previous sport activity during childhood and adolescence is associated with increased cortical bone size in young adult men. *J Bone Miner Res* (2009) **24**:125–33. doi:10.1359/jbmr.080909
- Deere K, Sayers A, Davey Smith G, Rittweger J, Tobias JH. High impact activity is related to lean but not fat mass: findings from a population-based study in adolescents. *Int J Epidemiol* (2012) **41**:1124–31. doi:10.1093/ije/dys073
- Riddoch CJ, Leary SD, Ness AR, Blair SN, Deere K, Mattocks C, et al. Prospective associations between objective measures of physical activity and fat mass in 12–14 year old children: the Avon Longitudinal Study of Parents and Children (ALSPAC). *BMJ* (2009) **339**:b4544. doi:10.1136/bmj.b4544

**Conflict of Interest Statement:** The authors declare that the research was conducted in the absence of any commercial or financial relationships that could be construed as a potential conflict of interest.

Received: 06 January 2014; paper pending published: 22 January 2014; accepted: 13 February 2014; published online: 03 March 2014.

Citation: Tobias JH, Gould V, Brunton L, Deere K, Rittweger J, Lipperts M and Grimm B (2014) Physical activity and bone: may the force be with you. *Front. Endocrinol. 5*:20. doi: 10.3389/fendo.2014.00020

This article was submitted to Bone Research, a section of the journal *Frontiers in Endocrinology*.

Copyright © 2014 Tobias, Gould, Brunton, Deere, Rittweger, Lipperts and Grimm. This is an open-access article distributed under the terms of the Creative Commons Attribution License (CC BY). The use, distribution or reproduction in other forums is permitted, provided the original author(s) or licensor are credited and that the original publication in this journal is cited, in accordance with accepted academic practice. No use, distribution or reproduction is permitted which does not comply with these terms.



# Objectively measured physical activity predicts hip and spine bone mineral content in children and adolescents ages 5–15 years: Iowa bone development study

Kathleen F. Janz<sup>1,2\*</sup>, Elena M. Letuchy<sup>2</sup>, Shelby L. Francis<sup>1</sup>, Kristen M. Metcalf<sup>1</sup>, Trudy L. Burns<sup>2</sup> and Steven M. Levy<sup>3</sup>

<sup>1</sup> Department of Health and Human Physiology, University of Iowa, Iowa City, IA, USA

<sup>2</sup> Department of Epidemiology, University of Iowa, Iowa City, IA, USA

<sup>3</sup> Department of Preventive and Community Dentistry, University of Iowa, Iowa City, IA, USA

**Edited by:**

Jonathan H. Tobias, University of Bristol, UK

**Reviewed by:**

Katherine Brooke-Wavell,  
Loughborough University, UK  
Jonathan H. Tobias, University of Bristol, UK

**\*Correspondence:**

Kathleen F. Janz, Department of Health and Human Physiology, University of Iowa, 130 Field House, Iowa City, IA 52242, USA  
e-mail: kathleen-janz@uiowa.edu

This study examined the association between physical activity (PA) and bone mineral content (BMC; gram) from middle childhood to middle adolescence and compared the impact of vigorous-intensity PA (VPA) over moderate- to vigorous-intensity PA (MVPA). Participants from the Iowa bone development study were examined at ages 5, 8, 11, 13, and 15 years ( $n=369, 449, 452, 410$ , and 307, respectively). MVPA and VPA (minutes per day) were measured using ActiGraph accelerometers. Anthropometry was used to measure body size and somatic maturity. Spine BMC and hip BMC were measured via dual-energy x-ray absorptiometry. Sex-specific multi-level linear models were fit for spine BMC and hip BMC, adjusted for weight (kilogram), height (centimeter), linear age (year), non-linear age (year<sup>2</sup>), and maturity (pre peak height velocity vs. at/post peak height velocity). The interaction effects of PA  $\times$  maturity and PA  $\times$  age were tested. We also examined differences in spine BMC and hip BMC between the least (10th percentile) and most (90th percentile) active participants at each examination period. Results indicated that PA added to prediction of BMC throughout the 10-year follow-up, except MVPA, did not predict spine BMC in females. Maturity and age neither modify the PA effect for males nor females. At age 5, the males at the 90th percentile for VPA had 8.5% more hip BMC than males in the 10th percentile for VPA. At age 15, this difference was 2.0%. Females at age 5 in the 90th percentile for VPA had 6.1% more hip BMC than those in the 10th percentile for VPA. The age 15 difference was 1.8%. VPA was associated with BMC at weight-bearing skeletal sites from childhood to adolescence, and the effect was not modified by maturity or age. Our findings indicate the importance of early and sustained interventions that focus on VPA. Approaches focused on MVPA may be inadequate for optimal bone health, particularly for females.

**Keywords:** accelerometry, adolescence, childhood, dual-energy x-ray absorptiometry, exercise, mechanical loading, skeletal health

## INTRODUCTION

Skeletal fractures associated with osteoporosis have significant health consequences including chronic pain, loss of function, and loss of independence (1). The economic cost of osteoporotic fractures is also high and growing, e.g., by 2025 in the U.S., fractures are projected to cost of \$25.3 billion/year (2). Previous epidemiological studies have estimated that a 10% increase in peak bone mass may reduce osteoporotic fracture risk by 50% in post-menopausal women (3, 4). Because of this, prevention strategies during childhood and adolescence aimed at increasing peak bone mass are critical.

A promising method for preventing osteoporosis is participation in bone-strengthening physical activity (PA). The ability of PA to stimulate bone remodeling (osteogenic potential) is determined by the dynamic and odd nature of the load, magnitude of the load, rate at which the load is applied, and duration of

the loading session. In general, activities that produce ground reaction forces (GRF)  $>1\text{--}2$  times body weight or require significant muscle loading of the bones are more effective (5). Because of its importance in osteoporosis prevention (6), bone-strengthening PA has been included in the PA Guidelines for Americans, recommending that children and adolescents include these activities as part of their 60 min of daily PA on at least 3 days/week (7).

The beneficial effects of PA on bone health throughout the lifespan are evident (6). For example, a review of controlled trials of weight-bearing exercise and bone mineral content (BMC) in children and adolescents from 3 to 17 years (8) conducted by Hind and Burrows (9) found increases in BMC of 0.9–4.9% in prepubertal children, 1.1–5.5% in early pubertal children, and 0.3–1.9% in pubertal children. However, only one study examined spine BMC and hip BMC in children younger than age 7 and reported that

PA did not increase BMC (10). The paucity of studies examining young children's PA and BMC make it difficult to understand expected dose-response and therefore plan appropriate interventions. In addition, PA dose on BMC during intervention studies may not necessarily be generalizable to everyday physical activities that children and adolescents would voluntarily select. Therefore, the purpose of our study was to observationally and longitudinally examine the association between PA and BMC, including young children (age 5) and to compare the impact of vigorous-intensity PA (VPA) over moderate- to vigorous-intensity PA (MVPA) from ages 5 to 15.

## MATERIALS AND METHODS

### PARTICIPANTS

Participants were recruited for the Iowa bone development study between 1998 and 2001 from a cohort of families participating in the Iowa fluoride study. The Iowa bone development study is a longitudinal study of bone health during childhood, adolescence, and young adulthood. Additional information about the study design and demographic characteristics of the participants have been described elsewhere (9, 11–13). This report focuses on data collected at ages 5, 8, 11, 13, and 15 years ( $N = 369, 449, 452, 410$ , and 307, respectively). To be included in the analyses, participants were required to have at least two measurements with at least one of those measurements occurring after age 8. Approval for this study was obtained from the University of Iowa Institutional Review Board for human subjects. Parents provided written informed consent and participants provided assent.

### PHYSICAL ACTIVITY

Physical activity was measured via the ActiGraph activity monitor model 7164 at ages 5, 8, 11, and 13. Due to the unavailability of this ActiGraph model at the age 15 measurement, model GT1M was used. Previous research has shown a high correlation ( $r = 0.99$ ) in movement counts data between the two monitors (14). Movement counts (a proxy for acceleration magnitude) were collected in 1-min epochs for ages 5, 8, 11, and 13 years and 5-s epochs for age 15. The 5-s epochs at age 15 were later reintegrated to 1-min epochs to maintain consistency with the earlier measurements. Participants at ages 5 and 8 were asked to wear the monitor during all waking hours for four consecutive days, including one weekend day. Using the Spearman–Brown prophecy formula, this amount of wear time provided an 82% reliability coefficient (15). Older children have previously been shown to have less stable intra-class correlation coefficients in activity monitored PA compared to younger children, indicating the need for an additional day of monitoring (16). Therefore, at ages 11, 13, and 15, the participants were asked to wear the monitor for five consecutive days, including both weekend days. To be included in the analyses, participants were required to have at least three valid days of monitor wear for each measurement period. A day was considered valid if the monitor was worn for at least 8 h. To reduce seasonal effects, PA was only measured during the autumn months.

The PA variables of interest were time spent in MVPA (minutes per day) and time spent in VPA (minutes per day). After comparing five independently developed sets of cut points on a sample of 5–15 years old, Trost and colleagues recommended that researchers

use the Evenson cut points (17, 18) for children and adolescents. As specified by Evenson and colleagues, cut points were defined as  $\geq 2296$  counts/min for MVPA and  $\geq 4012$  counts/min for VPA. These cut points were evaluated using area-under-the-receiver operating characteristic (ROC-AUC) curve and have been shown to exhibit good classification accuracy separately (moderate ROC-AUC = 0.74; vigorous ROC-AUC = 0.84). When combined to MVPA, the cut points exhibited excellent classification accuracy (ROC-AUC = 0.90) (17).

### BONE MINERAL CONTENT

Bone mineral content (gram) of the lumbar spine and hip was determined using dual-energy x-ray absorptiometry (DXA) during clinical visits to the University of Iowa General Clinical Research Center by one of three trained technicians. Scans using Hologic QDR 2000 DXA (Hologic, Inc., Bedford, MA, USA) were conducted with software version 7.20B and pencil-beam mode at ages 5 and 8. When the participants were 11, 13, and 15, the Hologic QDR 4500 DXA (Delphi upgrade) with software version 12.3 and fan-beam mode was used. Software-specific global regions of interest (ROI) were used to designate the general boundaries of the spine and hip images. A review of the bone within the ROI box was confirmed by the operator and edited to ensure appropriate bone-edge detection. Quality control scans were performed daily using the Hologic spine phantom. To minimize operator-related variability, all measurements were conducted by one of three experienced technicians. The precision error for BMC measurements is low in our laboratory (coefficient of variation of  $<1\%$  for quality control scans performed daily using the Hologic phantom). Translational equations for 4500 DXA measures to 2000 DXA measures were used to adjust for the differences between the two DXA machines. A separate study was conducted where 60 children (32 boys and 28 girls) ages 9–12 were scanned on each machine in random order during one clinical visit. The actual observations were closely aligned around the translational equation regression line, and the coefficient of determination ( $R^2$ ) for the 4500 DXA regressed on the 2000 DXA data was 0.98 [unpublished observation, linear regression for spine BMC: intercept = 2.57 (SE = 0.4), slope = 0.92 (SE = 0.02); hip BMC: intercept = 1.04 (SE = 0.4), slope = 0.993 (SE = 0.002)].

### ANTHROPOOMETRY

At the DXA visits, research nurses measured height (centimeter) and weight (kilogram). Height was measured using a Harpenden stadiometer (Holtain, UK), and weight was measured using a Healthometer physician's scale (Continental, Bridgeview, IL, USA); both devices were routinely calibrated. Participants were measured while wearing indoor clothes, without shoes. At ages 11, 13, and 15 years, sitting height was also measured and used to estimate maturity offset [year from peak height velocity (PHV)] using predictive equations established by Mirwald and colleagues (19). These equations include age, sex, weight, height, sitting height, and leg length as predictors of years from PHV or somatic maturity. This method has been validated in white Canadian children and adolescents ( $R^2 = 0.91$ – $0.92$ , SEE = 0.49–0.50) (19). Somatic maturity was dichotomized as 0 (pre PHV, or premature) or 1 (at/post PHV, or mature).

## STATISTICAL ANALYSIS

Descriptive statistics (means, SD, medians, and interquartile range) were calculated for the anthropometric, PA, and BMC characteristics of the participants. Student's *t*-tests were used to examine sex differences. Sex-specific multi-level models (random- and fixed-effects) (SAS 9.2 MIXED procedure) were used to create BMC growth curves for individual participants (level 1) and to test the group effect of PA (level 2). This approach allowed us to include participants who missed measurement periods. In the multi-level models, the intercept and slope for age (at the time of the DXA scan) were specified as random effects and PROC MIXED estimated their variance–covariance parameters (20). Residual diagnostic plots were used to check the model assumptions and possible outliers. Time-varying predictors that changed over the multiple assessments included height (centimeter), weight (kilogram), linear age (year), non-linear age (year<sup>2</sup>) (to allow for non-linearity of growth), maturity (Pre PHV = 0; at/post PHV = 1), and either MVPA or VPA. Box–Cox transformations were used for MVPA and VPA variables due to skewed

distributions. We tested the interaction effects of PA × maturity and PA × age. The Akaike information criterion (AIC) determined the fit of the models. Lower AIC values describe better fits. The differences in BMC between the least (10th percentile) and most (90th percentile) active children were estimated as predicted values from growth models with typical trajectories of covariates' change over time.

## RESULTS

### PARTICIPANT CHARACTERISTICS

The participant characteristics are shown in Table 1. Males were significantly taller than females at ages 5, 8, 13, and 15 ( $p < 0.05$ ) and significantly heavier than females at ages 8 and 15 ( $p < 0.05$ ). Males participated in significantly more MVPA and VPA than females at every measurement period ( $p < 0.01$ ). For males, the mean number of minutes of MVPA and VPA/day increased until age 11, then decreased thereafter. For females, the highest mean number of minutes of MVPA/day occurred at age 5 and decreased thereafter, but VPA increased from age 5 to 8, then decreased

**Table 1 | Characteristics of the participants by sex and age.**

|                        | Age 5 years<br>(n = 172) | Age 8 years<br>(n = 215) | Age 11 years<br>(n = 217) | Age 13 years<br>(n = 205) | Age 15 years<br>(n = 158) |
|------------------------|--------------------------|--------------------------|---------------------------|---------------------------|---------------------------|
| <b>Males</b>           |                          |                          |                           |                           |                           |
| Age (years)            | 5.2 (0.4)                | 8.7 (0.6)                | 11.2 (0.3)                | 13.3 (0.4)                | 15.4 (0.3)                |
| Height (cm)            | 112.3 (5.8)*             | 134.7 (7.1)**            | 149.1 (7.6)               | 163.0 (9.5)**             | 175.2 (7.9)**             |
| Weight (kg)            | 20.5 (3.6)               | 33.7 (9.4)*              | 45.3 (13.1)               | 58.2 (16.2)               | 70.4 (16.2)**             |
| MVPA (min/day)         | 59.0 (23.7)**            | 64.2 (27.3)**            | 64.4 (28.5)**             | 50.5 (23.6)**             | 37.6 (19.4)**             |
| VPA (min/day)          | 12.9 (9.4)**             | 17.9 (13.7)**            | 22.2 (15.6)**             | 16.1 (11.8)**             | 10.4 (10.2)**             |
| Monitor wear/day (min) | 731.0 (44.1)             | 749.3 (42.4)             | 743.1 (45.2)              | 745.9 (55.9)              | 731.7 (74.6)              |
| Spine BMC (g)          | 16.1 (2.4)*              | 24.0 (3.9)**             | 30.1 (5.3)**              | 41.8 (11.0)**             | 60.1 (13.2)               |
| Hip BMC (g)            | 7.1 (1.5)                | 13.1 (2.9)**             | 19.2 (4.6)                | 27.6 (7.5)**              | 37.9 (8.6)**              |
|                        | Median (IR)              | Median (IR)              | Median (IR)               | Median (IR)               | Median (IR)               |
| MVPA (min/day)         | 56.3 (43.5, 74.5)        | 63.8 (44.8, 82.3)        | 60.2 (42.8, 84.4)         | 46.6 (33.4, 65.8)         | 34.8 (22.8, 51.8)         |
| VPA (min/day)          | 10.4 (6.8, 16.5)         | 14.0 (8.5, 22.8)         | 18.0 (10.8, 29.8)         | 13.5 (7.6, 22.3)          | 7.1 (3.3, 14.2)           |
| <b>Females</b>         | <b>(n = 197)</b>         | <b>(n = 234)</b>         | <b>(n = 235)</b>          | <b>(n = 205)</b>          | <b>(n = 149)</b>          |
| Age (years)            | 5.3 (0.4)                | 8.7 (0.6)                | 11.2 (0.3)                | 13.2 (0.4)                | 15.3 (0.3)                |
| Height (cm)            | 110.0 (5.4)              | 132.7 (6.7)              | 149.2 (7.5)               | 160.5 (6.6)               | 164.4 (6.4)               |
| Weight (kg)            | 20.0 (3.8)               | 31.8 (8.5)               | 44.5 (12.3)               | 55.5 (14.0)               | 61.6 (14.3)               |
| MVPA (min/day)         | 46.7 (19.9)              | 45.9 (20.6)              | 38.6 (18.5)               | 32.3 (18.0)               | 25.9 (16.6)               |
| VPA (min/day)          | 9.9 (7.9)                | 11.8 (8.8)               | 10.5 (8.3)                | 9.3 (9.2)                 | 6.8 (8.2)                 |
| Monitor wear/day (min) | 731.8 (43.7)             | 743.4 (43.3)             | 741.8 (48.6)              | 752.2 (63.4)              | 740.4 (74.2)              |
| Spine BMC (g)          | 15.5 (2.4)               | 22.9 (4.0)               | 32.0 (7.9)                | 47.3 (10.8)               | 57.7 (10.7)               |
| Hip BMC (g)            | 6.9 (1.3)                | 12.2 (2.6)               | 18.6 (4.5)                | 25.8 (5.3)                | 29.2 (5.7)                |
|                        | Median (IR)              | Median (IR)              | Median (IR)               | Median (IR)               | Median (IR)               |
| MVPA (min/day)         | 43.5 (31.8, 59.0)        | 43.3 (30.3, 58.5)        | 35.2 (25.8, 48.8)         | 31.0 (18.8, 41.8)         | 23.4 (13.3, 37.2)         |
| VPA (min/day)          | 7.8 (4.8, 13.8)          | 9.4 (5.5, 15.3)          | 8.4 (4.6, 13.8)           | 6.3 (3.3, 11.8)           | 4.2 (1.5, 9.5)            |

Values are presented as mean (SD) and when skewed medians (IR).

Untransformed MVPA and VPA minutes reported here; Box–Cox transformed values used in all inferential analyses.

MVPA, moderate and vigorous-intensity physical activity; VPA, vigorous-intensity physical activity; BMC, bone mineral content.

\* $p < 0.05$ , \*\* $p < 0.01$  Student's *t*-test of males vs. females.

thereafter. There were no statistically significant differences in the mean number of minutes the ActiGraph was worn/day between males and females. Males had significantly more spine BMC than females at ages 5 and 8 ( $p < 0.05$ ), but females had significantly more spine BMC than males at ages 11 and 13 ( $p < 0.05$ ). At age 15, there was no significant difference in spine BMC between males and females. Males had significantly more hip BMC than females at ages 8, 13, and 15 ( $p < 0.05$ ), but there were no significant differences in hip BMC between males and females at ages 5 and 11 ( $p > 0.05$ ).

### ASSOCIATIONS BETWEEN MVPA, VPA, AND BMC

Results for sex-specific multi-level models examining the effects of MVPA on BMC and VPA on BMC are shown in **Tables 2–5**. For males, both MVPA and VPA were significantly associated with spine BMC and hip BMC. The AIC were similar for both models (MVPA spine AIC = 5471.7, VPA spine AIC = 5474.0; MVPA hip AIC = 4382.1, VPA hip AIC = 4382.2). For females, MVPA predicted hip BMC but not spine BMC; however, VPA predicted both spine BMC and hip BMC. The model fit was significantly better for models with VPA than MVPA (MVPA spine AIC = 5495.8, VPA spine AIC = 5490.6; MVPA hip AIC = 3909.3, VPA hip AIC = 3902.3). While both maturity offset and age were statistically significant in all BMC models, PA  $\times$  maturity and PA  $\times$  age interaction effects were not significant. This was true for both PA intensity levels (MVPA and VPA). We therefore present models without interaction in **Tables 2–5**.

At each measurement age, values were predicted for spine BMC and hip BMC for the 90th percentile (high VPA) and the 10th percentile (low VPA) (**Figure 1**). In these comparisons, weight, height, and maturity were set as the average values specific to sex and measurement age. Differences in BMC were statistically significant between high VPA and low VPA ( $p < 0.05$ ) at all measurement ages. Greater percent differences in BMC were seen in younger participants with high vs. low VPA as compared to older participants because of both increase in BMC and decrease in VPA over study period. For example, at age 5 years (15 years), males at the 90th percentile of VPA had 8.5% (2.0%) more hip BMC than those at the 10th percentile. For females, the differences were 6.1 and 1.8%, at ages 5 and 15 years, respectively.

### DISCUSSION

This study examined the effect of PA on BMC from middle childhood to middle adolescence using two metabolic intensities, MVPA and VPA. Measurement of BMC at the spine and hip skeletal sites were chosen because they are clinically relevant for osteoporotic fractures. Spinal fractures can lead to chronic disabling pain (21), and ~20% of hip fracture patients require long-term nursing home care (6). The multi-level models, which we used fit each participant with an individual growth trajectory for spine BMC and hip BMC. This was important since the slope and intercept coefficients (level 1, not shown) varied across participants. This approach allowed us to identify the independent inter-group effects of PA on BMC while controlling for growth (age) and age-dependent covariates of height, weight, and maturity. With the exception of MVPA in the female spine BMC

**Table 2 | Fixed-effects of the multi-level models examining the association of MVPA with spine and hip BMC in males.**

| Effect                                    | $\beta$ estimate | SE   | p-Value |
|---|------------------|------|---------|
| <b>SPINE</b>                              |                  |      |         |
| Intercept                                 | -16.81           | 3.66 | <0.0001 |
| Age centered (years)                      | 1.89             | 0.16 | <0.0001 |
| Age centered squared (year <sup>2</sup> ) | 0.26             | 0.02 | <0.0001 |
| Height (cm)                               | 0.29             | 0.03 | <0.0001 |
| Weight (kg)                               | 0.04             | 0.02 | 0.0591  |
| Maturity (pre vs. at/post PHV)            | 8.52             | 0.56 | <0.0001 |
| MVPA (min/day)                            | 0.16             | 0.05 | 0.0020  |
| <b>HIP</b>                                |                  |      |         |
| Intercept                                 | -12.98           | 2.14 | <0.0001 |
| Age centered (years)                      | 1.34             | 0.10 | <0.0001 |
| Age centered squared (year <sup>2</sup> ) | 0.14             | 0.01 | <0.0001 |
| Height (cm)                               | 0.17             | 0.02 | <0.0001 |
| Weight (kg)                               | 0.11             | 0.01 | <0.0001 |
| Maturity (pre vs. at/post PHV)            | 3.91             | 0.30 | <0.0001 |
| MVPA (min/day)                            | 0.12             | 0.03 | <0.0001 |

Box-Cox transformed values for MVPA.

**Table 3 | Fixed-effects of the multi-level models examining the association of MVPA with spine and hip BMC in females.**

| Effect                                     | $\beta$ estimate | SE   | p-Value |
|--|------------------|------|---------|
| <b>SPINE</b>                               |                  |      |         |
| Intercept                                  | -6.11            | 3.35 | 0.0692  |
| Age centered (year)                        | 2.54             | 0.12 | <0.0001 |
| Age centered squared (years <sup>2</sup> ) | 0.30             | 0.01 | <0.0001 |
| Height (cm)                                | 0.20             | 0.03 | <0.0001 |
| Weight (kg)                                | 0.18             | 0.02 | <0.0001 |
| Maturity (pre vs. at/post PHV)             | 3.85             | 0.39 | <0.0001 |
| MVPA (min/day)                             | 0.06             | 0.05 | 0.2319  |
| <b>HIP</b>                                 |                  |      |         |
| Intercept                                  | -24.38           | 1.83 | <0.0001 |
| Age centered (years)                       | 0.42             | 0.06 | <0.0001 |
| Age centered squared (year <sup>2</sup> )  | 0.10             | 0.01 | <0.0001 |
| Height (cm)                                | 0.24             | 0.01 | <0.0001 |
| Weight (kg)                                | 0.13             | 0.01 | <0.0001 |
| Maturity (pre vs. at/post PHV)             | 1.78             | 0.16 | <0.0001 |
| MVPA (min/day)                             | 0.06             | 0.02 | 0.0072  |

Box-Cox transformed values for MVPA.

model, results showed that PA predicts BMC in males and females from ages 5 to 15 and the slope of the relationship between PA and BMC does not change across age groups or (somatic) maturity. The results also show that as PA decreases with aging, the effect size decreases. The percentage differences (~1–8%) that we report between high VPA participants (90th percentile) and low (10th percentile) are comparable to differences observed in targeted exercise interventions designed to increase BMC (10). For example, Gunter and colleagues reported that the 7- to 9-year-old children in their intervention group had 7.9% more BMC at

the spine and 8.4% more BMC at the hip than the control group after a 7-month jumping intervention (22). Meyer and colleagues reported that the 6–7 and 11–12-year olds in their intervention group had 4.7% more bone mineral density (BMD) at the spine and 5.4% more BMD at the hip than the control group after a 9-month multi-component intervention including daily physical education with at least 10 min of jumping or strength training (23). Finally, McKay and colleagues reported a 1.9% increase in spine areal BMD and 3.2% increase in hip areal BMD in their third and

fourth graders after participating in an 8-month jumping intervention twice/week during physical education classes. However, not all of the increases in areal BMD were significantly different from the increases seen in the control participants (24).

Similar reports from others (25–27), we found VPA to be a more consistent predictor of BMC than MVPA and, importantly, for the same duration of time, VPA would be expected to provide greater increases in BMC (when compared to MVPA). For females, the prediction slopes that we report would, on average, suggest that a 30-min/day increase in VPA would result in a 0.5-g increase in hip BMC (vs. 0.2 g for a similar increase in MVPA). For low active (10th percentile) 5-year-old females, this is an 8% increase in hip BMC associated with VPA (when compared to a 4% increase associated with MVPA). For males, increases of 0.7 and 0.5 g in hip BMC would be expected with a 30-min increase in VPA and MVPA, respectively. These values correspond to a 10% increase (VPA) vs. a 6% increase (MVPA) for 5-year-old low VPA males. Consistent with findings of Fuchs et al., MacKelvie et al., Heinonen et al., Stear et al., and Witzke and Snow, we also found greater increases in BMC at the hip when compared to the spine (28–32).

We have previously shown that the effect of PA at age 5 is sustained 3–6 years later (at age 8 and 11) but not at age 13 and 15 (33, 34). Our current report using a larger sample size and multi-level modeling, assesses acute effects of PA on BMC rather than sustained. The results suggest that what children and adolescents do in the present is associated with BMC. The lack of significance of the PA × maturity and PA × age interaction effects suggest that the BMC response to PA is consistent between 5 and 15 years of age. However, our data also show that the percent increases are greater when participants are more active. From a public health perspective, this finding is important since most young children are active and willing to engage in age-appropriate PA (when compared to adolescents) and therefore compliance with activity interventions is likely to be high. In addition, consistent with others (35–37), we have previously shown moderate tracking of activity behaviors in our cohort from ages 5 to 15 (38) suggesting that establishing a habit of bone-enhancing PA early in life is likely to continue through adolescence.

Limitations of our study include the use of a 1-min ActiGraph epoch, and a low minority, mostly white, convenience sample. It is possible that other, unmeasured factors could have contributed to differences in BMC, such as genetics or diet. Strengths of this report are the use of a longitudinal study design spanning 10 years, multi-level model to reduce confounding by growth and maturation, the clinically relevant outcomes of spine and hip BMC, and the use of an objective measure of PA. Although, we used a metabolic cut point to count minutes of PA, the ActiGraph accelerometer measures acceleration (meter per square second), which is proportional to the impact and muscular load forces acting on the skeletal system (22). Our placement of the ActiGraph at the waist provided a sensitive measure of weight-bearing PA but not swimming and cycling, activities thought to contribute little to bone loading. Recently, Deere and colleagues have shown positive associations between hip BMD and accelerometry-measured PA calibrated to mechanical load (gravitational force, g). Their findings indicated that only high impacts (>4.2 g) were

**Table 4 | Fixed-effects of the multi-level models examining the association of VPA with spine and hip BMC in males.**

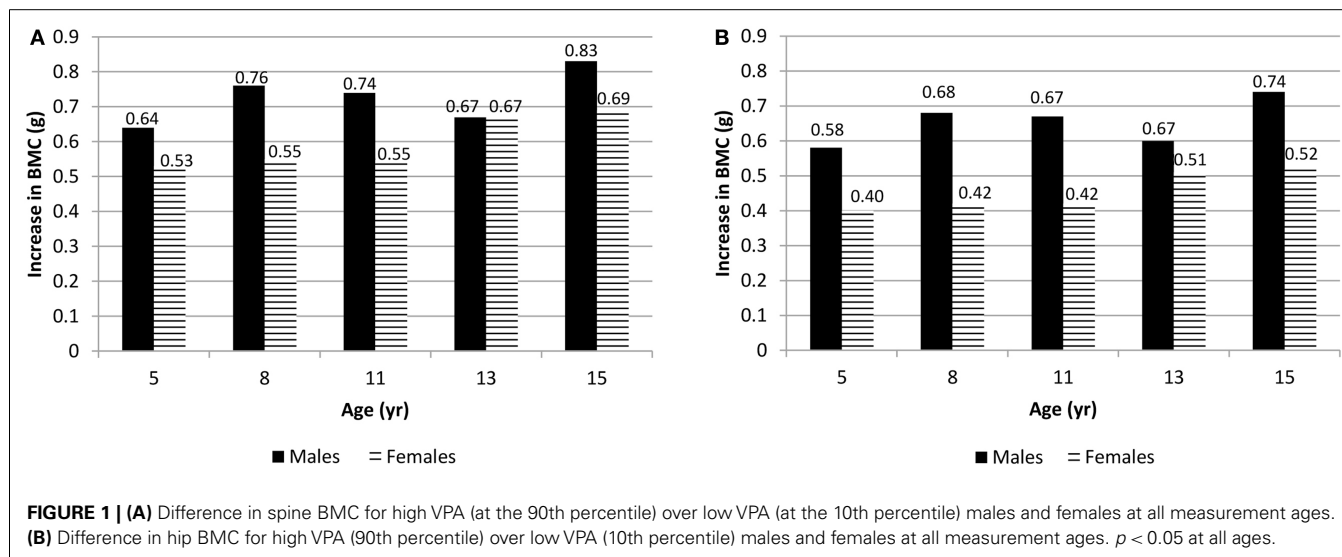
| Effect                                    | β estimate | SE   | p-Value |
|---|------------|------|---------|
| <b>SPINE</b>                              |            |      |         |
| Intercept                                 | −15.77     | 3.66 | <0.0001 |
| Age centered (years)                      | 1.88       | 0.16 | <0.0001 |
| Age centered squared (year <sup>2</sup> ) | 0.25       | 0.02 | <0.0001 |
| Height (cm)                               | 0.29       | 0.03 | <0.0001 |
| Weight (kg)                               | 0.04       | 0.02 | 0.0825  |
| Maturity (pre vs. at/post PHV)            | 8.59       | 0.56 | <0.0001 |
| VPA (min/day)                             | 0.25       | 0.10 | 0.0178  |
| <b>HIP</b>                                |            |      |         |
| Intercept                                 | −12.16     | 2.14 | <0.0001 |
| Age centered (years)                      | 1.34       | 0.10 | <0.0001 |
| Age centered squared (year <sup>2</sup> ) | 0.14       | 0.01 | <0.0001 |
| Height (cm)                               | 0.17       | 0.02 | <0.0001 |
| Weight (kg)                               | 0.11       | 0.01 | <0.0001 |
| Maturity (pre vs. at/post PHV)            | 3.96       | 0.30 | <0.0001 |
| VPA (min/day)                             | 0.23       | 0.06 | 0.0001  |

Box-Cox transformed values for VPA.

**Table 5 | Fixed-effects of the multi-level models examining the association of VPA with spine and hip BMC in females.**

| Effect                                    | β estimate | SE   | p-Value |
|---|------------|------|---------|
| <b>SPINE</b>                              |            |      |         |
| Intercept                                 | −6.30      | 3.34 | 0.0599  |
| Age centered (years)                      | 2.53       | 0.12 | <0.0001 |
| Age centered squared (year <sup>2</sup> ) | 0.30       | 0.01 | <0.0001 |
| Height (cm)                               | 0.20       | 0.03 | <0.0001 |
| Weight (kg)                               | 0.19       | 0.02 | <0.0001 |
| Maturity (pre vs. at/post PHV)            | 3.80       | 0.39 | <0.0001 |
| VPA (min/day)                             | 0.22       | 0.10 | 0.0223  |
| <b>HIP</b>                                |            |      |         |
| Intercept                                 | −24.30     | 1.83 | <0.0001 |
| Age centered (years)                      | 0.41       | 0.06 | <0.0001 |
| Age centered squared (year <sup>2</sup> ) | 0.10       | 0.01 | <0.0001 |
| Height (cm)                               | 0.24       | 0.01 | <0.0001 |
| Weight (kg)                               | 0.13       | 0.01 | <0.0001 |
| Maturity (pre vs. at/post PHV)            | 1.75       | 0.16 | <0.0001 |
| VPA (min/day)                             | 0.17       | 0.05 | 0.0004  |

Box-Cox transformed values for VPA.



associated with BMD. High impacts are, in general, associated with VPA.

In conclusion, we found that objectively measured VPA is associated with BMC at the spine and hip from childhood to adolescence. The magnitude of impact was greater when children were younger. Current public health approaches focusing on moderate PA, with an emphasis on reducing obesity, may be inadequate. Emphasizing VPA in young children, prior to the known decline in PA, may help to optimize peak BMC.

## ACKNOWLEDGMENTS

We are grateful to the parents, children, and staff of the Iowa bone development study. This work was supported by the National Institute for Dental and Craniofacial Research (R01-DE12101 and R01-DE09551) and the National Center for Research Resources (UL1 RR024979 and M01-RR00059).

## REFERENCES

- Magaziner J, Lydick E, Hawkes W, Fox KM, Zimmerman SI, Epstein RS, et al. Excess mortality attributable to hip fracture in white women aged 70 years and older. *Am J Public Health* (1997) **87**(10):1630–6. doi:10.2105/AJPH.87.10.1630
- Burge R, Dawson-Hughes B, Solomon DH, Wong JB, King A, Tosteson A. Incidence and economic burden of osteoporosis-related fractures in the United States, 2005–2025. *J Bone Miner Res* (2007) **22**(3):465–75. doi:10.1359/jbm.061113
- World Health Organization. Assessment of fracture risk and its application to screening for postmenopausal osteoporosis: report of a WHO study group. *World Health Organ Tech Rep Ser* (1994) **843**:1–129.
- Cummings SR, Browner W, Cummings S, Black D, Nevitt M, Browner W, et al. Bone density at various sites for prediction of hip fractures. *Lancet* (1993) **341**(8837):72–5. doi:10.1016/0140-6736(93)92555-8
- Baptista F, Janz KF. Habitual physical activity and bone growth and development in children and adolescents: a public health perspective. In: Preedy VR, editor. *Handbook of Growth and Growth Monitoring in Health and Disease*. New York: Springer (2012). p. 2395–411.
- US Department of Health and Human Services. *Bone Health and Osteoporosis: A Report of the Surgeon General*. University Press of the Pacific (2004).
- Secretary of Health and Human Services. Be active, healthy, and happy. In: Leavitt MO, editor. *2008 Physical Activity Guidelines for Americans*. Washington, DC: US Department of Health and Human Services (2008). p. 1–76
- Hind K, Burrows M. Weight-bearing exercise and bone mineral accrual in children and adolescents: a review of controlled trials. *Bone* (2007) **40**(1):14–27. doi:10.1016/j.bone.2006.07.006
- Janz KF, Levy SM, Burns TL, Torner JC, Willing MC, Warren JJ. Fatness, physical activity, and television viewing in children during the adiposity rebound period: the Iowa bone development study. *Prev Med* (2002) **35**(6):563–71. doi:10.1006/pmed.2002.1113
- Laing EM, Wilson AR, Modlesky CM, O'Connor PJ, Hall DB, Lewis RD. Initial years of recreational artistic gymnastics training improves lumbar spine bone mineral accrual in 4-to 8-year-old females. *J Bone Miner Res* (2005) **20**(3):509–19. doi:10.1359/JBMR.041127
- Janz KF, Burns TL, Torner JC, Levy SM, Paulos R, Willing MC, et al. Physical activity and bone measures in young children: the Iowa bone development study. *Pediatrics* (2001) **107**(6):1387–93. doi:10.1542/peds.107.6.1387
- Janz KF, Burns TL, Levy SM, Torner JC, Willing MC, Beck TJ, et al. Everyday activity predicts bone geometry in children: the Iowa bone development study. *Med Sci Sports Exerc* (2004) **36**(7):1124–31. doi:10.1249/01.MSS.0000132275.65378.9D
- Janz K. Physical activity and bone development during childhood and adolescence. Implications for the prevention of osteoporosis. *Minerva Pediatr* (2002) **54**(2):93–104.
- Kozey SL, Staudenmayer JW, Troiano RP, Freedson PS. Comparison of the ActiGraph 7164 and the ActiGraph GT1M during self-paced locomotion. *Med Sci Sports Exerc* (2010) **42**(5):971–6. doi:10.1249/MSS.0b013e3181c29e90
- Penpraze V, Reilly JJ, MacLean CM, Montgomery C, Kelly LA, Paton JY, et al. Monitoring of physical activity in young children: how much is enough? *Pediatr Exerc Sci* (2006) **18**:4.
- Janz KF, Witt J, Mahoney LT. The stability of children's physical activity as measured by accelerometry and self-report. *Med Sci Sports Exerc* (1995) **27**(9):1326–32. doi:10.1249/00005768-199509000-00014
- Evenson KR, Catellier DJ, Gill K, Ondrak KS, McMurray RG. Calibration of two objective measures of physical activity for children. *J Sports Sci* (2008) **26**(14):1557–65. doi:10.1080/02640410802334196
- Trost SG, Loprinzi PD, Moore R, Pfeiffer KA. Comparison of accelerometer cut points for predicting activity intensity in youth. *Med Sci Sports Exerc* (2011) **43**(7):1360–8. doi:10.1249/MSS.0b013e318206476e
- Mirwald RL, Baxter-Jones AD, Bailey DA, Beunen GP. An assessment of maturity from anthropometric measurements. *Med Sci Sports Exerc* (2002) **34**(4):689–94. doi:10.1097/00005768-200204000-00020
- Hauspie RC, Cameron N, Molinari L. *Methods in Human Growth Research*. Cambridge: Cambridge University Press (2004).
- NIH Consensus Development Panel on Osteoporosis Prevention, Diagnosis, and Therapy. Osteoporosis prevention, diagnosis, and therapy. *JAMA* (2001) **285**(6):785–95. doi:10.1001/jama.285.6.785

22. Gunter K, Baxter-Jones AD, Mirwald RL, Almstedt H, Fuller A, Durski S, et al. Jump starting skeletal health: a 4-year longitudinal study assessing the effects of jumping on skeletal development in pre and circum pubertal children. *Bone* (2008) **42**(4):710–8. doi:10.1016/j.bone.2008.01.002
23. Meyer U, Romann M, Zahner L, Schindler C, Puder JJ, Kraenzlin M, et al. Effect of a general school-based physical activity intervention on bone mineral content and density: a cluster-randomized controlled trial. *Bone* (2011) **48**(4):792–7. doi:10.1016/j.bone.2010.11.018
24. McKay HA, Petit MA, Schutz RW, Prior JC, Barr SI, Khan KM. Augmented trochanteric bone mineral density after modified physical education classes: a randomized school-based exercise intervention study in prepubescent and early pubescent children. *J Pediatr* (2000) **136**(2):156–62. doi:10.1016/S0027-3476(00)70095-3
25. Deere K, Sayers A, Rittweger J, Tobias JH. Habitual levels of high, but not moderate or low, impact activity are positively related to hip BMD and geometry: results from a population-based study of adolescents. *J Bone Miner Res* (2012) **27**(9):1887–95. doi:10.1002/jbmr.1631
26. Gracia-Marco L, Moreno LA, Ortega FB, León F, Sioen I, Kafatos A, et al. Levels of physical activity that predict optimal bone mass in adolescents: the HELENA study. *Am J Prev Med* (2011) **40**(6):599–607. doi:10.1016/j.amepre.2011.03.001
27. Sardinha LB, Baptista F, Ekelund U. Objectively measured physical activity and bone strength in 9-year-old boys and girls. *Pediatrics* (2008) **122**(3):e728–36. doi:10.1542/peds.2007-2573
28. Fuchs RK, Bauer JJ, Snow CM. Jumping improves hip and lumbar spine bone mass in prepubescent children: a randomized controlled trial. *J Bone Miner Res* (2001) **16**(1):148–56. doi:10.1359/jbmr.2001.16.1.148
29. MacKelvie KJ, Khan KM, Petit MA, Janssen PA, McKay HA. A school-based exercise intervention elicits substantial bone health benefits: a 2-year randomized controlled trial in girls. *Pediatrics* (2003) **112**(6):e447–52. doi:10.1542/peds.112.6.e447
30. Heinonen A, Sievänen H, Kannus P, Oja P, Pasanen M, Vuori I. High-impact exercise and bones of growing girls: a 9-month controlled trial. *Osteoporos Int* (2000) **11**(12):1010–7. doi:10.1007/s001980070021
31. Stear SJ, Prentice A, Jones SC, Cole TJ. Effect of a calcium and exercise intervention on the bone mineral status of 16–18-y-old adolescent girls. *Am J Clin Nutr* (2003) **77**(4):985–92.
32. Witzke KA, Snow CM. Effects of plyometric jump training on bone mass in adolescent girls. *Med Sci Sports Exerc* (2000) **32**(6):1051–7. doi:10.1097/00005768-200006000-00003
33. Janz KF, Kwon S, Letuchy EM, Eichenberger Gilmore JM, Burns TL, Torner JC, et al. Sustained effect of early physical activity on body fat mass in older children. *Am J Prev Med* (2009) **37**(1):35–40. doi:10.1016/j.amepre.2009.03.012
34. Francis SL, Letuchy EM, Levy SM, Janz KF. Sustained effects of physical activity on bone health: Iowa bone development study. *Bone* (2014) **63**:95–100. doi:10.1016/j.bone.2014.03.004
35. Janz KF, Dawson JD, Mahoney LT. Tracking physical fitness and physical activity from childhood to adolescence: the Muscatine study. *Med Sci Sports Exerc* (2000) **32**(7):1250–7. doi:10.1097/00005768-200007000-00011
36. Kelder SH, Perry CL, Klepp KI, Lytle LL. Longitudinal tracking of adolescent smoking, physical activity, and food choice behaviors. *Am J Public Health* (1994) **84**(7):1121–6. doi:10.2105/AJPH.84.7.1121
37. Telama R, Yang X, Laakso L, Viikari J. Physical activity in childhood and adolescence as predictor of physical activity in young adulthood. *Am J Prev Med* (1997) **13**(4):317–23.
38. Francis SL, Morrissey JL, Letuchy EM, Levy SM, Janz KF. Ten-year objective physical activity tracking: Iowa bone development study. *Med Sci Sports Exerc* (2013) **45**(8):1508–14. doi:10.1249/MSS.0b013e31828b2f3a

**Conflict of Interest Statement:** The authors declare that the research was conducted in the absence of any commercial or financial relationships that could be construed as a potential conflict of interest.

Received: 30 April 2014; accepted: 27 June 2014; published online: 15 July 2014.

Citation: Janz KF, Letuchy EM, Francis SL, Metcalf KM, Burns TL and Levy SM (2014) Objectively measured physical activity predicts hip and spine bone mineral content in children and adolescents ages 5–15 years: Iowa bone development study. *Front Endocrinol*. 5:112. doi: 10.3389/fendo.2014.00112

This article was submitted to Bone Research, a section of the journal *Frontiers in Endocrinology*.

Copyright © 2014 Janz, Letuchy, Francis, Metcalf, Burns and Levy. This is an open-access article distributed under the terms of the Creative Commons Attribution License (CC BY). The use, distribution or reproduction in other forums is permitted, provided the original author(s) or licensor are credited and that the original publication in this journal is cited, in accordance with accepted academic practice. No use, distribution or reproduction is permitted which does not comply with these terms.



# The contribution of experimental *in vivo* models to understanding the mechanisms of adaptation to mechanical loading in bone

Lee B. Meakin\*, Joanna S. Price and Lance E. Lanyon

School of Veterinary Sciences, University of Bristol, Bristol, UK

**Edited by:**

Jonathan H. Tobias, University of Bristol, UK

**Reviewed by:**

Mark H. Edwards, MRC Lifecourse Epidemiology Unit, UK

Niklas Rye Jørgensen, Glostrup University Hospital, Denmark

**\*Correspondence:**

Lee B. Meakin, School of Veterinary Sciences, University of Bristol, Langford House, Langford, Bristol BS40 5DU, UK  
e-mail: lee.meakin@bristol.ac.uk

Changing loading regimens by natural means such as exercise, with or without interference such as osteotomy, has provided useful information on the structure:function relationship in bone tissue. However, the greatest precision in defining those aspects of the overall strain environment that influence modeling and remodeling behavior has been achieved by relating quantified changes in bone architecture to quantified changes in bones' strain environment produced by direct, controlled artificial bone loading. Jiri Hert introduced the technique of artificial loading of bones *in vivo* with external devices in the 1960s using an electromechanical device to load rabbit tibiae through transfixing stainless steel pins. Quantifying natural bone strains during locomotion by attaching electrical resistance strain gages to bone surfaces was introduced by Lanyon, also in the 1960s. These studies in a variety of bones in a number of species demonstrated remarkable uniformity in the peak strains and maximum strain rates experienced. Experiments combining strain gage instrumentation with artificial loading in sheep, pigs, roosters, turkeys, rats, and mice has yielded significant insight into the control of strain-related adaptive (re)modeling. This diversity of approach has been largely superseded by non-invasive transcutaneous loading in rats and mice, which is now the model of choice for many studies. Together such studies have demonstrated that over the physiological strain range, bone's mechanically adaptive processes are responsive to dynamic but not static strains; the size and nature of the adaptive response controlling bone mass is linearly related to the peak loads encountered; the strain-related response is preferentially sensitive to high strain rates and unresponsive to static ones; is most responsive to unusual strain distributions; is maximized by remarkably few strain cycles, and that these are most effective when interrupted by short periods of rest between them.

**Keywords:** bone, mechanical loading, experimental models, mechanostat, mechanical strain

## INTRODUCTION

The effect of mechanical loading on bone has been studied since the nineteenth century. These studies have primarily utilized animal models of mechanical loading since bone adaptation is a highly complex process that is difficult to fully appreciate *in vitro* or *in silico*. The first aim of this review is to discuss the various models that have aided our understanding of this adaptive process. The second section will discuss the knowledge that has been gained from such *in vivo* studies, which have determined how to modify the mechanical strain stimulus to give a more osteogenic outcome. Finally, we will explore the effect of physiological context on bone's adaptive response to loading using the example of estrogen's role in the adaptive process and its contribution to post-menopausal osteoporosis.

## WOLFF'S LAW AND THE MECHANOSTAT

In 1892, the anatomist and orthopedic surgeon Julius Wolff postulated that bone adapted to its mechanical environment according to strict mathematical laws. This principle, now commonly known as Wolff's Law (1) was based on anatomical dissection studies

which demonstrated increased bone mass in areas predicted to be subject to high mechanical stresses and low bone mass where stresses were predicted to be low. Incorporating previous work by the anatomist Meyer and the Swiss engineer Culmann, Wolff further observed that trabeculae in the femoral head and neck were orientated to reduce bending stresses when the material was loaded. These observations allowed Wolff to state his "Law" as "*Every change in form or function of bone or of their function alone is followed by certain definite changes in their internal architecture, and equally definite alteration in their external conformation, in accordance with mathematical laws*" (2). Wolff's Law was expanded by Wilhelm Roux who suggested bone adaptation was the result of a "quantitative self-regulating mechanism" based in the tissue at the level of the cell (3).

Architectural bone changes such as those observed by Wolff were hypothesized to occur due to a dynamic adaptive process in response to changes in the mechanical stimulus derived from load-bearing. This theory was further developed by Harold Frost in 1960 whose thoughts form the basis of the current "mechanostat" theory of bone adaptation (4). Frost recognized that the most likely

loading-derived stimulus for bone cells would be the strains developed in the bone tissue as a result of loading. His mechanostat theory suggests a negative feedback system in which the input is local mechanical strain, engendered by functional mechanical loading, and the output is a structurally appropriate bone mass and architecture. Accordingly, in areas of bone experiencing mechanical strains higher than the strain set point, bone formation would occur to make a stiffer bone construct thus reducing strains and restoring set point strains. Conversely, if bones experienced strains lower than the set point, then bone resorption would occur, bone mass would decrease and, for the same loads, strains would again be restored to the level of the set point. This theory was extensively described in the Utah Paradigm of Skeletal Physiology (4). It is an important component of this theory that the mechanostat is a local phenomenon with local changes in strain adjusting local bone mass through local bone formation or resorption. However, it is also important to remember that the mechanostat operates within a wider physiological context and that its ability to establish and maintain structural competence may be substantially modified, or overwhelmed, by systemic circumstances (5, 6).

### EXTRINSIC MODELS OF MECHANICAL LOADING

What neither Wolff nor Frost was able to state was the specific components of bone cells' strain environment that act as the controlling stimulus for architectural modeling and remodeling. It is this question that has been addressed principally by animal experiments.

One of the simplest ways to increase the mechanical loads experienced by bones in the skeleton is to increase the level of exercise undertaken. A large variety of techniques have been described to achieve this in experimental animals, usually taking the form of forced exercise such as treadmill running (7–9), swimming (10–12), or jumping (13, 14). Other models have also been described in which animals (usually rats) wear increasingly weighted backpacks or have to press levers with increasing levels of resistance to get food rewards (15).

In these exercise models, the whole body is loaded through coordinated muscular contraction and ground reaction forces in

a manner that is an exaggeration or extension of that to which they are habituated. Such studies are useful since they require little in the way of specialized equipment and they mimic the natural challenge to skeletal strength that the mechanostat presumably evolved to address. However, while exercise may be the easiest therapy to prescribe in an attempt to regulate bone mass or adjust bone architecture, it involves a mixed stimulus of change in loading and physiological context that makes the results difficult to interpret.

As well as (presumably) altering local mechanical strain, exercise engenders a great many other physiological responses such as increasing tissue blood flow and oxygenation (16, 17), changing the endocrine environment (18), muscular contraction, and local release of potentially osteogenic factors from muscle (19), which could complicate interpretation of the intrinsic loading-related response of the bone alone. A further disadvantage with exercise models is that exercise is a whole body phenomenon, therefore comparison has to be made with controls whose total exercise experience (both during the exercise periods and the rest of the day) has to mimic the experimental subjects in every respect, except the modified exercise under study. Lastly, but by no means least, the changes in the strain environment of bone cells brought about by change in exercise can usually only be estimated mathematically with no means of experimental verification. Such verification had to await the introduction of the chronically implanted electrical resistance strain gage (20).

### QUANTIFYING THE MECHANICAL STRAIN STIMULUS

Although Gaynor Evans had attached electrical resistance strain gages to bone surfaces *in vivo* in the 1940s (21), these were only used for the assessment of bone strains in response to impact loading in anesthetized animals in short term experiments. Lanyon and co-workers were the first to chronically implant electrical resistance strain gages attached to the surfaces of bones of a variety of living animals, including humans (Figure 1), and analyze the various components of the strain stimulus during a variety of activities (20, 22–30). In the majority of weight bearing long bones, the peak mechanical strains were remarkably similar across different species and activities measuring approximately 2–3000  $\mu\epsilon$ .

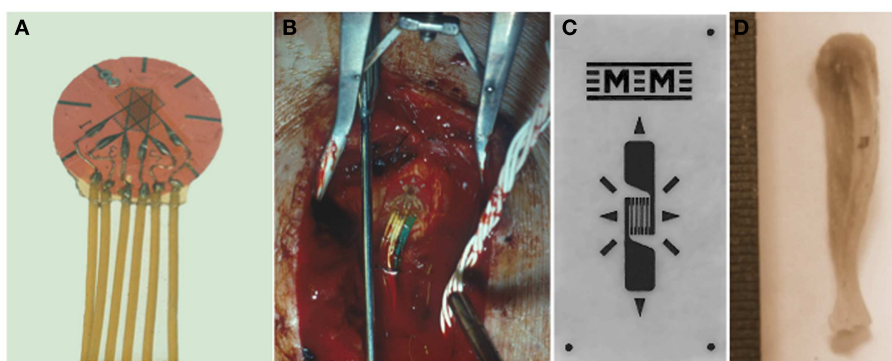


**FIGURE 1 | Quantifying the mechanical strain stimulus.** Rosette (**A**) or linear (**C**) electrical resistance strain gages are bonded to the surface of bones to measure the strain stimulus being engendered during a variety

of activities and also to match experimental groups with different bone stiffness. (**B**) A strain gage bonded to a human tibia and (**D**) to a mouse tibia.

( $2\text{--}3 \times 10^{-3}$ ). Peak compressive strains have subsequently been recorded from the horse third metacarpal bone during galloping where the recorded maximum strain magnitude reached  $5,000 \mu\epsilon$  ( $5 \times 10^{-3}$ ) (26).

This similarity in peak strains recorded from different bones from different species supported Frost's mechanostat theory of bone adaptation and suggested that the set point for peak functional strain was similar across species. Nevertheless, it is important to remember that this similarity in peak strains across different load-bearing bones in different animals does not imply a single target strain at every skeletal location. Since the highest physiologically induced strains are due to bending, the peak longitudinal strains around the bone's circumference will change from compression to tension and pass through the neutral axis. However, the cortical thickness is reasonably similar around the circumference of the bone. Additionally, significantly lower strains have also been recorded at other sites in load-bearing bones and on the surfaces of bones whose primary role may not be sustaining high loads. For example, low functional strains have been recorded on the skull during activities such as chewing, smiling, and even heading a ball ( $80\text{--}200 \mu\epsilon$ ). This suggests that different bones, and different sites on the same bone, have different local settings for the target strains that their mechanostat attempts to achieve (31).

Most of the early studies using bone-bonded strain gages were undertaken using rosette gages which respond to strain in three different directions and therefore allow the direction of the principal tensile, compressive, and shear strains to be calculated. These calculations confirmed the essence of Wolff's hypothesis in his trajectory theory that bone trabeculae tend to be aligned in the directions of principal tension and compression strains (22). In addition to measurement of strain magnitude and direction, electrical resistance gages allow recording of the rate of change of strain (the strain rate) experienced by the bone during loading and unloading. The highest strain rate so far recorded during natural activity was from the sunfish operculum (the bone covering the gills) during striking at prey. At  $-615 \times 10^8 \mu\epsilon$  this peak strain rate is over 10 times higher than anything so far recorded in terrestrial animals during locomotion (32). Despite the obvious advantage of using rosette strain gages they substantially complicate the experimental procedure due to their size and the extra number of channels that need to be monitored. Thus, particularly in studies on small animals such as rodents, it has been more usual to use single element gages (33, 34). These can only respond to strains in the direction in which they are aligned so cannot distinguish between changes in strain magnitude and changes in strain direction. When using single element gages it is important to ensure that the gage is aligned in the direction of interest and to realize that a reduction in strain reading may mean a change in direction as well as a reduction in strain magnitude.

Although used most widely, particularly *in vivo*, strain gages are not the only devices employed to measure mechanical strains on bone surfaces, particularly *ex vivo*. Other techniques include the use of digital image correlation. This method requires a speckle pattern to be applied to the surface of the bone of interest. Sequential images are then taken during loading to trace the movement of the speckle pattern. This allows the resulting strain to be calculated across different areas of the bone surface (35). Finite element

analysis is widely employed to calculate stresses (and thus strains) but this requires substantial assumptions to be made as to the load path within the bones and the material properties of the bone tissue, which are not homogeneous along the bone's length (36, 37). Despite these limitations, finite element analysis allows estimation of the strain pattern throughout a whole bone, something that is impossible with strain gages, which can only sample the strain from the surfaces to which they are attached. Thus finite element analysis can extend knowledge of the strain situation to the depths of the bone and to the bone trabecule where strain measurements using strain gages would be impossible (38–40). Using finite element analysis combined with *in vivo*  $\mu$ CT scanning, accurate prediction of sites of bone formation and resorption following the application of mechanical loading has been possible (39).

Whichever technique is used to measure loading-engendered mechanical strains, it is vital that strains and strain rates are normalized between experimental groups. The same loads applied to bones of different size, shape, or material properties will inevitably result in different strains. Therefore the loads, and load rates, must be adjusted so that the strain stimulus is the same in all bones in the same study. It is only by doing this that their adaptive responses can be directly compared.

## INVASIVE MODELS OF MECHANICAL LOADING

While the availability of chronically implanted bone-bonded strain gages provided the means to sample the strain environment experienced by bone cells, it was still necessary to find a suitable means to alter this environment in a controlled manner and assess the adaptive response. One means used to achieve this was to surgically remove a bone, or piece of bone, where paired bones exist, to alter the functional strains on the remaining bone. An example of this technique is the ulna osteotomy experiments performed by Goodship et al. (41). In this experiment, a portion of the pig ulna was removed, which increased the strains during ambulation in the remaining radius. This had the effect of causing an increase in radial bone formation. After 3 months, the strains in the radius had normalized back to those measured in the contralateral radius in the intact limb. An advantage of this model over the whole body exercise models is that there is a control limb with which to compare bone's adaptive response. However, osteotomy involves invasive surgery near to the site being investigated and thus it is only possible to monitor rather than control the various components of the strain stimulus.

The first successful attempts to control bones' mechanical loading in order to study their adaptive responses was established in the 1960s by Jiri Hert who applied different loading regimens from an external electromagnetically operated device to the tibia of rabbits through transfixing pins (Figure 2). By using this approach and assessing the adaptive response of the bone Hert and his co-workers were able to establish, amongst other findings, that adaptive bone (re)modeling occurred without the need for any central nervous connection (42–44). Hert's experiments, while groundbreaking, lacked knowledge of what the actual strains were that his device engendered. This capability was established by Lanyon and co-workers by combining the techniques of loading a bone *in vivo* through transfixing pins with that of chronically implanted strain gages. Although the first animal they used for this approach was the

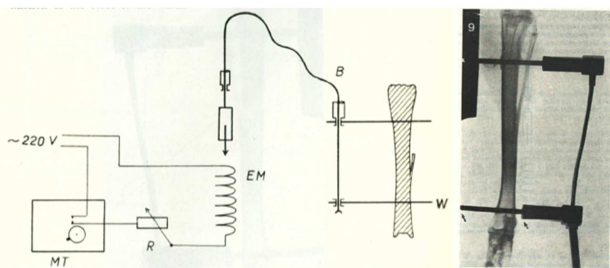


**FIGURE 2 | The invasive rabbit loading model.** Jiri Hert was the first to describe an artificial mechanical loading model in 1969. Loading was applied through surgically implanted pins in the lapine tibia. Using this approach and assessing the adaptive response of the bone Hert and his co-workers were able to establish, amongst other findings, that adaptive bone (re)modeling occurred without the need for any central nervous connection (42–44).

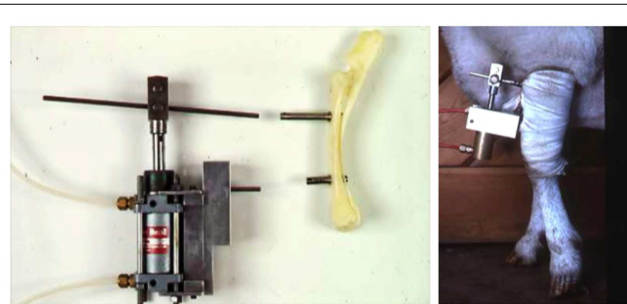


**FIGURE 3 | The invasive sheep loading model.** Lance Lanyon adapted Hert's original loading model to the sheep radius and combined the loading with strain measurements using implanted strain gages (45).

sheep (**Figure 3**) (45) their most productive large animal model was the avian (rooster and later turkey) ulna (**Figure 4**) (46–48). This was chosen since the ulna was large enough to receive transfixing pins at its ends and three rosette strain gages around the circumference of its midshaft. Furthermore, as domestic turkeys and roosters are flightless, functional isolation of the bone's natural loading did not greatly inconvenience their lifestyle.

The preparation used in the functionally isolated externally loadable avian ulna model involved performing a proximal and distal ulna osteotomy, placing metal caps over each end of the cut section of bone and securing them in place with metal pins placed through predrilled holes in the caps. This model has an advantage over the previous limb long bone models in that the section of bone being loaded is functionally isolated from the rest of the wing preventing any confounding strain stimulus derived from habitual activity. Using these models, several important observations were made documenting the effects of the different components of the strain stimulus on bone mass and architecture. These will be discussed in a later section of this review.

One of the disadvantages of the invasive loading models is that placing pins through the bone to be loaded invokes a local periosteal woven bone response (46, 48). This prevents the whole

bone from being analyzed. Furthermore, since the majority of trabecular bone resides at either end of the long bones, this cannot be analyzed since it is not loaded. To overcome these problems, Chambers et al. developed the rat tail vertebra loading model (49). This involves placing pins through tail vertebrae in the rat (later adapted for the mouse) adjacent to the vertebra of interest that will undergo mechanical loading. This means that any periosteal woven bone reaction is limited to bones on either side of the one being loaded thereby permitting full analysis of the bone of interest. Furthermore, the tail vertebrae contain abundant trabecular bone enabling study of trabecular bone's adaptive response to loading. For these reasons, the tail vertebra loading model is still in use today (50–52). However, there remains a concern that surgical placement of pins invokes not only the woven bone reaction in the region immediately surrounding the pin, but also a local inflammatory reaction, which could affect adjacent bones. Another concern is the relevance of bone adaptation in a bone that is not normally subject to such loads since it is likely that rodent tail vertebrae normally experience low strains during locomotion and other activities. A further disadvantage is that there must be a period, once the pins have been placed, to allow their integration into the bone prior to starting any loading studies.

### NON-INVASIVE MODELS OF MECHANICAL LOADING

The first of the non-invasive artificial loading models was described by Charles Turner et al. in 1991 (53) where he reported applying four-point bending to the rat tibia and observing the subsequent adaptive response. The loading arrangement consists of two contact points on the underside (the lateral aspect) of the limb and two on the upper medial side of the limb, which are inside those on the underside. A force is applied by downwards pressure from the upper contact points, which generates a bending of the tibia and causes a subsequent remodeling response. A sham loading arrangement where pressure is applied but no bending force generated can be created by placing the upper contact points directly opposite the lower ones. Although this model has advantages over the invasive models previously described, the contact points through which the loading is applied are quite close together and they apply their loads through the periosteum. Periosteal disturbance such as this is sufficient by itself to induce periosteal woven bone formation (54). This limited the region of analysis to the endosteal surface, which may behave inherently differently in response to strain from the periosteum.

To address some of the issues of the four-point bending model, Ted Gross' group developed a cantilever bending model in which the knee and the ankle of the mouse hindlimb were placed in specially designed cups and the ankle moved laterally in relation to the knee to generate a bending moment in the tibia/fibula (55). This eliminated the periosteal woven bone observed with the previous bending model allowing analysis of both periosteal and endosteal bone compartments. However, there was still the concern that this bending moment does not accurately recreate the axial loading generated during ambulation in people and animals. Furthermore, only the central diaphyseal region of the bone displays a response to loading meaning the metaphyseal region containing the majority of the trabecular bone is not loaded and therefore does not display an adaptive process.

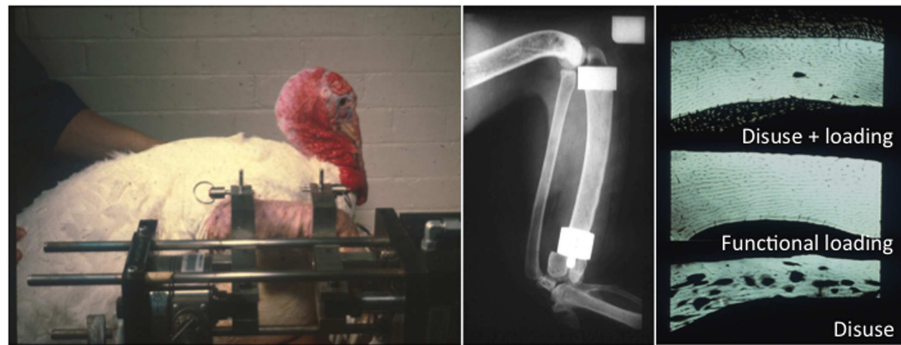


**FIGURE 4 | The functionally isolated invasive turkey loading model.** Lanyon and Rubin further applied the invasive loading model to the functionally isolated avian ulna, which had the advantage that the loaded bone is isolated from the confounding influence of background strain stimuli (46–48).

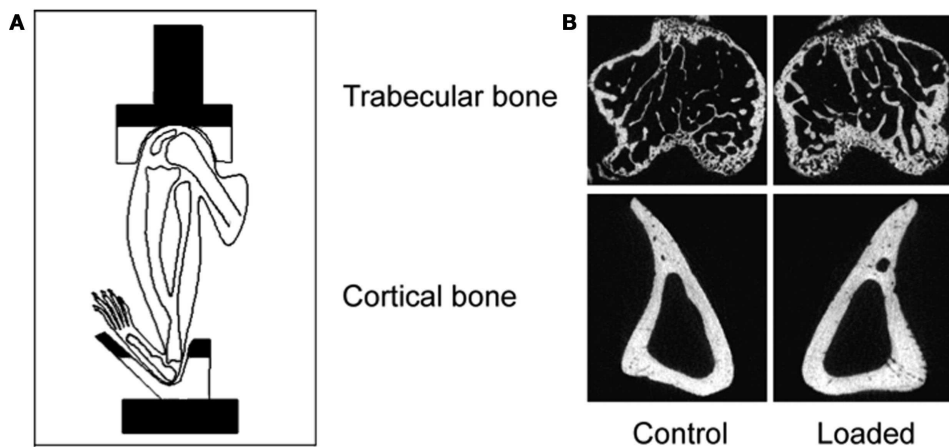


**FIGURE 5 | The non-invasive axial murine tibial loading model.** (A) De Souza et al. adapted the non-invasive rat (56) and ulna (33) axial loading models to the tibia enabling study of trabecular and cortical

compartments in a single loaded bone (34). (B) Representative  $\mu$ CT scans demonstrating trabecular and cortical bone formation within a single loaded bone (58).

A significant advance was made when Torrance et al. (56) established that physiologically relevant strains could be engendered in the ulna of rats when their forearm was loaded axially through the skin over the olecranon and flexed carpus. They used the ulna rather than the tibia because the loads necessary to engender sufficiently high strains in the tibia caused necrosis of the skin over the knee and ankle. This disadvantage did not occur when the tibia was loaded in mice and these have more recently become the species of choice for such experiments (5, 33, 34, 57).

The advantage of the non-invasive mouse tibial loading model is that precisely controlled loading regimens can be established in long bones in mice over a sufficient period of time to allow the adaptive response to be completed. Also no surgical invasion is required and the loading-related response throughout the whole bone can be studied. These substantial advantages were further increased when extended to the mouse fibula (57). The design of the mouse tibia/fibula loading model is relatively simple with custom-designed cups placed over the knee and tarsus (**Figure 5**). The uppermost cup is attached to the actuator arm of

a hydraulic or electromagnetic materials testing machine and the lower cup attached to a load cell so that the load applied to the bone can be accurately controlled. Axial compression causes strain due to compression and bending of the bone increasing the strain stimulus and inciting an adaptive response.

Due to the placement of the cups in the tibia/fibula axial loading model, the whole bone is loaded including the metaphyseal region so the adaptive response can be observed in both cortical and trabecular bone compartments (5). Additionally, the loaded tibia and fibula have no direct contact with the loading machine cups since the load is applied through the distal femur and the flexed tarsus. Since this arrangement allows the simultaneous loading of both the tibia and fibula, the adaptive response in both bones can then be differentially processed for different analytical techniques reducing the number of experimental animals required. Finally, there are regions of the tibia (37% site measured from the proximal end) where the loading response is maximal while other regions (75%) where no loading response is observed (5). Interestingly, maximal strains are estimated to be similar at

both regions however, down-regulation of osteocytic sclerostin, a necessary step in bone's response to mechanical loading (59), is more closely related to sites of bone formation than to maximum strain (36).

Because the axial loading models can be used in both the rat and mouse, it is possible to use genetically modified animals enabling the role of specific genes (and pathways) in bone's adaptive response to be determined (60–62). One of the disadvantages with the axial loading models is that the bone is stiffer when loaded in this direction, compared to being loaded in a non-physiological direction, so the loads required to engender an adaptive response are higher in the axial models than the bending models. A consequence of this may be premature closure of the growth plates when skeletally immature animals undergo axial loading of the ulna or tibia and fibula (63, 64).

## MODELS OF MECHANICAL UNLOADING

In addition to studying the effect of artificially increasing mechanical strain and observing how bone adapts to this change in strain, it is also important to determine how bone adapts to a decrease in the mechanical strain stimulus. As well as increasing our knowledge of both extremes of the mechanostat theory of bone (re)modeling, these models can also be used to simulate clinical conditions associated with low bone mass such as disuse osteoporosis and bone loss following space flight.

The ideal model would allow bone strains to be reduced to zero. However, even in animals experiencing weightlessness during space flight, muscle contractions will still generate strains on the bone surface. Nevertheless, multiple animal studies have been performed during space flight and the resultant bone resorption has been studied (65–68). However, for most experiments this is not a feasible option.

More practical alternative experimental models of mechanical unloading have been described in the literature, which include applying a cast to a limb, performing an Achilles tenotomy to unload the calcaneus, performing a tenotomy of the knee tendons to unload the tibia, and bandaging a limb to the abdomen (69–75).

A surrogate to recapitulate the conditions of weightlessness is the tail suspension model (76). Using this model, mice or rats have their hindlimbs suspended by their tail while they are free to move around "normally" on their forelimbs. This model eliminates ground reaction forces on the hindlimbs although again, muscular contractions will still produce some mechanical strain on the bones involved. Using this model, researchers have demonstrated marked reductions in bone mass and deterioration in bone architecture (77–79). An adaptation of the tail suspension model has been developed, which allows graded levels of mechanical unloading (80). To try and further recapitulate the effects of space flight, one group simultaneously irradiated the tibia of mice and then performed hindlimb suspension (81). Interestingly, the effect of mechanical unloading on bone mass combined with radiation was far more extensive than that of radiation alone. Although hindlimb suspension causes measurable bone loss in the tibia, several disadvantages are associated with this model. Firstly, special cages are required, which have pulley systems to allow the animals to move around the cages. Secondly, there is a redistribution of

blood to the cranial end of the animal with some systemic stress responses observed (82). Thirdly, this model causes bilateral bone loss losing the ability to compare one limb with its contralateral control and thus at least doubling the number of experimental animals required. Finally, in some countries, e.g., the UK, this model has been prohibited based on concerns for animal welfare since animals are unable to move freely.

A further two methods have been reported, which induce neurogenic paralysis of the hindlimb and therefore bone loss. This is achieved either by sciatic or tibial denervation or by the injection of botulinum toxin (83–86). These neurogenic paralysis methods have the advantage of reducing bone surface strains to around  $300 \mu\epsilon$  (one tenth of the normal peak strains) and the tibia can be subsequently reloaded using the axial tibial loading model to prevent bone loss (85, 86). Both approaches have their advantages and disadvantages. Sciatic neurectomy causes a permanent paralysis whereas botulinum toxin only lasts 1–2 weeks before some ambulation is regained. Sciatic neurectomy causes a more complete paralysis since botulinum toxin injection-induced paralysis, which affects the neuromuscular junction, relies on separate injections into each muscle group. Finally, botulinum toxin is more difficult to obtain due to its status as a prescription only medicine. In contrast, sciatic neurectomy requires minimal surgical instruments and the surgery is simple taking approximately 3–4 min per mouse in experienced hands.

A recent paper has reported the combined effects of hindlimb suspension and injection of botulism toxin (87). This showed that bone and muscle loss following hindlimb suspension and botulinum toxin injection were similar but when combined had additive effects. Interestingly, they also report bone and muscle loss in the contralateral (non-injected) hindlimb following botulinum toxin injections alone, suggesting systemic effects even though the injection primarily targets local muscle. An additional consideration is that inducing unilateral paralysis may increase load-bearing in the contralateral limb, although this does not appear to hold true for the botulinum toxin model.

## KNOWLEDGE GAINED FROM *IN VIVO* ANIMAL LOADING MODELS

### BONE RESPONDS TO DYNAMIC BUT NOT STATIC LOADS

Hert was the first to publish data suggesting that bone (re)modeling was not affected by static strains but rather by dynamic strain change (42). This inference was confirmed by one of the first studies published using the isolated avian ulna loading model. This study compared the effect of a continuous static load with that of the same magnitude of load applied dynamically for a single 100-s period per day in a trapezoidal waveform for an 8-week period (48). When the load was applied in a static manner, there was a 13% loss of bone due to endosteal expansion and an increase in cortical porosity. This level of bone loss was no different to that exhibited by the control group, which underwent osteotomy but no loading. However, the group in which the load was applied in a dynamic manner exhibited a 24% increase in bone mass due to periosteal bone formation. For this reason, the majority of studies using exogenously applied load apply a dynamic waveform of either triangular, sinusoidal, or trapezoidal shape (5, 34, 38, 88–90). However, to our knowledge, no studies have directly

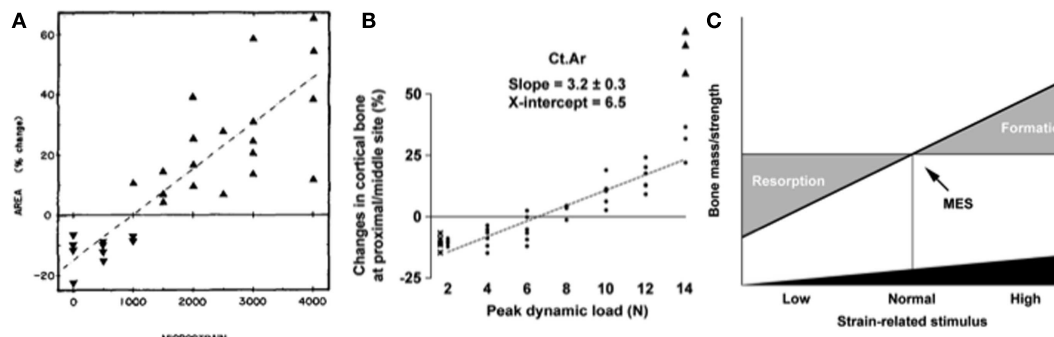


**FIGURE 6 |**The “lazy zone” is an artifact associated with background mechanical strain stimuli. Increasing mechanical strain is associated with a linear increase in bone mass in studies when background strains are eliminated in the isolated avian ulna [(A), (91)] and combined sciatic neurectomy and tibial loading models [(B), (86)]. This indicates there is no “lazy zone” in bone’s adaptation to loading [(C), (86)]. MES, minimum effective strain stimulus.

compared the relative effects of these different waveforms on bone formation.

#### LOADING-RELATED BONE FORMATION CORRELATES WITH PEAK STRAIN MAGNITUDE

The single most important component of the strain stimulus to engender an osteogenic response to mechanical loading is the peak strain magnitude. Multiple studies by our laboratory and others have demonstrated that by varying the peak strain magnitude, but keeping all other parameters the same, there is a dose:response relationship between the peak strains engendered and the amount of new bone formed (53, 61, 86, 88, 91). Several previous studies made the assumption that there was an adapted window or lazy zone in which bone mass and architecture would not change over a set range of strain stimuli. However, in the isolated turkey ulna where disuse and artificial loading are combined, there was no evidence of this window (91). A more recent study, stimulated by editors’ refusal to accept the veracity of this earlier finding, confirmed the absence of this lazy zone using the combined sciatic neurectomy and axial tibial loading model (Figure 6) (86). This is also supported by the graded mechanical unloading model of Ellman et al., which confirmed a linear relationship between percentage weight bearing and bone loss (80). It is important to realize that these experiments refer only to a single loading modality. In the natural situation where the osteoregulatory effects of all the normal loading modalities are added together this may constitute a spectrum of strain magnitudes that averaged within a particular window do indeed result in little or no adaptive response.

As previously discussed, the mechanostat is a local phenomenon (5, 6, 92). As such, mechanical loading will engender a range of peak strain magnitudes in different regions of the same bone (34, 36). Studies have repeatedly shown periosteal bone formation following mechanical loading to occur primarily in regions where strains are high and lower levels of bone formation, or even resorption, to occur where peak strains are lower (37, 51, 93, 94).

#### STRAIN-RELATED STIMULUS IS DETERMINED BY THE NOVELTY OF LOADING

In the avian ulna studies, substantial increases in bone mass occurred with artificially applied loads, despite these loads

engendering lower peak maximum strains and strain rates than those measured during normal wing flapping (46). Thus it is impossible to say that peak strain *per se* engendered the strain-related stimulus. It is instead likely that this substantial stimulus arises from the strains being engendered in a novel configuration. Similarly, in the tibial bending studies (53, 55), relatively low loads were required to induce adaptive new bone formation. Conversely in the axial loading models where the load is being applied more closely to the normal direction in which the bone is loaded, higher loads appear to be necessary to generate new bone formation, although since the bone is more resistant to load in this direction the strains may be similar in magnitude.

Nevertheless, a recent study used different enclosure designs to force growing female C57Bl/6J mice to use non-linear, diverse-orientation locomotor loading showed that, when compared to mice using primarily linear locomotion, those with diverse non-linear locomotion had increased humeral trabecular bone volume fraction and indices of cortical bone volume (95). This is despite no difference in overall activity levels between mice in the two different types of enclosure. These findings support a previous study that used transarticular external fixators in sheep to prevent calcaneal load-bearing, which resulted in bone loss (96). When disuse was interrupted by periods of steady walking on a treadmill, when the tarsus was mobilized, the strain stimulus from walking was unable to prevent bone loss suggesting either that the duration of the stimulus was insufficient [unlikely in view of the turkey ulna data (47)] or that the variety or novelty of the strain-related stimulus was not being provided. Another study demonstrated that fighting between male mice housed in groups was associated with an increase in measures of cortical and trabecular bone mass and architecture, which “masked” the effect of mechanical loading in these animals (97). When males were individually housed, and thus not involved in vigorous diverse activity, their response to mechanical loading was no different from that observed in group or individually housed female mice, which did not fight.

#### INCREASING STRAIN RATE DURING LOADING AND UNLOADING STIMULATES BONE FORMATION

The rate of change of strain magnitude, both when load is applied and released, is an important determinant of a strain

regimen's osteogenic potential. This was first suggested in an early study using an invasive loading model in sheep where (in the rather uncontrolled loading situation achievable with a pneumatic loading device) change in strain rate accounted for more of the variation in the amount of new bone formed in response to loading than peak strain magnitude (45). Interestingly, this effect of maximum strain rate was unaffected by whether this occurred during loading (compression) or unloading (tension). A later study using the much better controlled rat ulnar axial loading model demonstrated, using various strain rates but the same peak magnitude, number of loading cycles, etc. that increasing the strain rate by approximately fivefold (from  $-0.018$  to  $-0.100\text{ s}^{-1}$ ) increased the osteogenic bone formation response both in amount and extent (98). A further study by Turner et al. found similar results concluding that the amount of new bone formation was directly proportional to the rate of change in strain in bone tissue (99). However, one of the difficulties with interpretation of both of these studies is that to increase strain rates but keep all other parameters the same, a period of rest has to be inserted between each of the loading cycles. Although not appreciated at the time there is now evidence that such a rest period can itself enhance bone's adaptive response to artificial loading. Despite this reservation, the consensus from a number of studies is that the rate of change of strain is an important determinant of the stimulus for a bone formation response. This finding is consistent with the results from human studies; exercise regimens involving high levels of impact loading (squash, tennis, and triple jump) being far more effective than those that do not (swimming and cycling) in stimulating new bone and thus increasing bone mass (100–103). In an additional study by LaMothe et al. using the cantilever bending model, they increased the dwell time (the length of time the load was applied for) when the strain rate was increased ensuring the duration of each loading cycle and frequency of cycles was consistent between groups (104). Again they showed a significant increase in the bone formation response when strain rate was increased.

In the first study describing the non-invasive axial tibial loading model, there was actually a loss of trabecular bone volume fraction reported, which we now believe is due to their use of a relatively low strain rate of  $1,500\text{--}2,000\text{ }\mu\text{es}^{-1}$  during loading and unloading (34). Another more recent paper using a much higher number of cycles but with the same low strain rate reported in the first study also documented a loss of trabecular bone in the proximal tibia with loading (38). However, studies using an identical experimental protocol, but with a strain rate 10 times higher than that used in the first study, have consistently reported a robust increase in trabecular bone volume fraction, thickness, and even number (58, 61, 62, 86, 97, 105). To the authors' knowledge, no studies have directly compared the influence of strain rate on the relative responses of cortical and trabecular bone.

#### **NUMBER OF LOADING CYCLES REQUIRED TO MAXIMALLY STIMULATE BONE FORMATION IS SMALL**

Two important studies have compared the number of cycles of loading required to stimulate an osteogenic response and have shown it to be surprisingly small. Rubin and Lanyon first demonstrated in the isolated avian ulna that increasing the number of loading cycles in a given episode of mechanical loading from 36 to

as many as 1,800 did not generate any additional adaptive response (46). Perhaps as interesting, was their finding that only four loading cycles a day were sufficient to prevent the bone loss associated with disuse (zero cycles). Another study in rats trained to jump a 40 cm height showed little additional effect on increasing the number of jumps from 5 up to 40 per day (14).

Although relatively few cycles of loading are required to maximize the amount of new bone formed, there are a number of publications using *in vivo* mechanical loading where several thousand loading cycles are performed. For some this is a deliberate design to induce fatigue loading of bone and examine subsequent damage repair (106). However, for many studies, although a robust way of ensuring osteogenesis, this high number of cycles is likely to be unnecessary and may indeed have detrimental effects. These include an increase in the length of anesthesia time required for each episode of loading and also an increased likelihood of bone and soft tissue damage.

#### **INSERTING REST BETWEEN LOADING CYCLES INCREASES BONE FORMATION**

A study by Robling et al. demonstrated that partitioning 360 loading cycles into 4 bouts of 90 cycles or 6 bouts of 60 cycles per day enhanced the osteogenic response to loading (107). Robling went on to demonstrate that inserting a 14-s rest period between loading cycles optimized the bone formation response to loading (108). This was confirmed by LaMothe and Zernicke using the cantilever bending model which showed that when a 10 s rest period was inserted every 11 s in a 30 Hz 100 s loading protocol, the bone formation response increased by 72% despite a 100-fold decrease in the number of loading cycles (104). Additional studies by Gross' group, also using the cantilever bending model, observed that inserting a 10 or 15 s rest period between each loading cycle enhanced the osteogenic stimulus in both young and aged mice (109–111). Finally, a study by Charles Turner's group demonstrated that as the length of the loading study is increased, the percentage new bone formation response per week decreases suggesting the stimulus may become less potent over time. However, introducing a rest period of several weeks between bouts of mechanical loading can partially restore this decreased response to loading (112).

#### **MAXIMIZING THE STRAIN STIMULUS**

It is important when designing a loading protocol that all of the evidence reported in the previous section is taken into account. The method for applying mechanical load using the tibial loading model has already been extensively described (34, 113). The protocol in current use in our laboratory is as follows:

The tibia is held in place by a 0.5 N continuous static pre-load. Forty cycles of dynamic load are superimposed using a trapezoidal waveform with 10 s rest intervals between each cycle. The protocol for one cycle consists of loading to the target peak load, hold for 0.05 s at the peak load, and unloading back to the 0.5 N pre-load. Strain gaging data from our current materials testing machine (Bose ElectroForce 3100) indicate that a load of 15N is equivalent to  $2500\text{ }\mu\text{e}$  on the medial surface of the tibia at 37% of the length from the proximal end in a young adult 17-week old female C57Bl/6J mouse. The load rate we use in young adult

female mice is  $500\text{Ns}^{-1}$ , which equates to an average strain rate of  $30,000\ \mu\text{es}^{-1}$ . These values are within the normal physiological range recorded for this species (34). Using this protocol, we observe approximately a 20–30% increase in cortical bone area at the 37% site and approximately a 50–75% increase in trabecular BV/TV in the secondary spongiosa. While we do not believe that the same loading protocol should be recapitulated in all laboratories using the non-invasive axial tibial loading model, designing a protocol should be based on previous studies so that interpretation of novel or unexpected results is made more reliable.

## INFLUENCE OF PHYSIOLOGICAL CONTEXT ON THE MECHANOSTAT

As discussed earlier in this review, the mechanostat is primarily a local phenomenon in which bone responds to local changes in mechanical strain and adapts its local bone mass and architecture accordingly to adjust strains to restore the set point. However, it is well accepted that the functioning of the mechanostat can be influenced by systemic changes. For example, during the menopause in women there is a loss of bone mass sufficient to increase the incidence of fragility fractures (114, 115). The rapidity of this loss is unlikely to be accounted for by any sudden change in mechanical loading of the bone through decreased exercise, etc. Therefore, there must be some mechanism, which influences the mechanostat and impairs its function (116). The most likely candidate is decline in the levels of available estrogen and we have attributed at least part of this failure to altered function of its receptors; estrogen receptor (ER)  $\alpha$  and  $\beta$  (62, 90). Aspects of the changes that are likely to occur with the menopause have been recapitulated in animal models where loading can be artificially increased and therefore allowing interrogation of the link between the mechanostat and estrogen receptor signaling in more detail. The interventions used to investigate this mechanism will now be discussed.

## SURGICAL MODELING OF PATHOLOGY

A simple way to recreate the menopause and deplete endogenous estrogen in animals is by removal of the gonads i.e., an ovariectomy. The earliest study which investigated the effect of ovariectomy on the loading response was using the four-point bending model in rats (117). They concluded that the cortical response to loading was not affected by ovariectomy, although a concurrent loss of trabecular bone due to estrogen depletion was observed. As discussed earlier in this review, there are issues, which surround the use of bending models of loading, particularly in these circumstances where analysis of trabecular bone is key. However, more recently the lack of the effect of ovariectomy on the adaptive response has been confirmed using the axial tibial loading model (60). Chambers' group have also investigated the effect of combining ovariectomy with invasive mechanical loading of the rat tail vertebra, which contains predominantly trabecular bone (118). Unexpectedly, they found that the trabecular bone formation rate following loading was increased in ovariectomized compared to control animals. Interestingly, the enhancing effect of ovariectomy on the response to loading was not inhibited by the addition of pamidronate, a bisphosphonate, which inhibits bone resorption by inducing osteoclast apoptosis. This suggests that estrogen may have an inhibitory effect on

osteoblastic bone formation such that once removed by ovariectomy, loading-induced bone formation is increased. More recently, these findings have been confirmed using the non-invasive axial tibial loading model where it was also demonstrated that ovariectomy increases the loading-related gain in trabecular but not cortical bone (119).

## PHARMACOLOGIC INTERVENTIONS

In addition to investigating the effect of loss of estrogen following ovariectomy on the function of the mechanostat, studies have also been performed to examine the effect of estrogen supplementation by injecting rats daily with biologically active  $17\beta$ -estradiol (118). In agreement with the previously mentioned enhanced response to loading following ovariectomy, in trabecular bone, estrogen supplementation inhibited the response to loading. This was also unexpected since estradiol is well accepted to prevent the deleterious effects of ovariectomy on trabecular bone (120). Interestingly, estrogen also appears to have an inhibitory effect on cortical bone's response to mechanical loading (121), which is surprising given the lack of effect of ovariectomy on cortical bone's response to mechanical loading (60, 119). One of the complexities encountered when interpreting these studies are the relative effects of ER $\alpha$  and  $\beta$  activation. Newer drugs have been developed, which act as selective ER modulators (SERMs). One of these SERMs, tamoxifen, is used clinically as a breast cancer treatment and has been shown to be more potent than estradiol at preventing the ovariectomy-induced loss of trabecular bone (120). Perhaps more beneficially, it has been demonstrated that tamoxifen causes a synergistic increase in trabecular bone formation when combined with mechanical loading (119).

## GENETIC MANIPULATION

To further decipher the relative involvement of ER $\alpha$  and  $\beta$  in bone's response to mechanical loading, an alternative to the administration of selective pharmacologic agents is to create animals, usually mice, with genetic modifications and apply mechanical loading. As discussed previously, one vital undertaking prior to mechanical loading of genetically modified animals is to determine whether the intrinsic load:strain relationship in these animals has also been modified such that similar strain stimuli can be applied to mice with potentially different bone phenotypes. The first study to investigate the effect of ER deletion on bone's response to mechanical loading was by Lee et al. (90). Using the axial ulna loading model (33), they demonstrated that global deletion of ER $\alpha$  in mice significantly impaired cortical bone's adaptive response to mechanical loading. Later studies confirmed these findings using the axial tibial loading model (60, 62, 122). One of these studies subsequently investigated the effect of genetic modifications of the specific activation function regions of the ER $\alpha$  found that deletion of AF1, but not AF2, was responsible for the effect of ER $\alpha$  knockout on the cortical response to mechanical loading (60). This is interesting because estrogen's effect on bone mass is via AF2 and not AF1 (123) suggesting that in cortical bone, the effect of mechanical loading is via the ER $\alpha$  but independent of estrogen itself, potentially explaining why ER $\alpha$  deletion, but not depletion of estrogen, decreases bone's adaptive response to mechanical loading.

Other studies have investigated the role of ER $\beta$  using the non-invasive ulna and tibia loading models and found that global deletion of ER $\beta$  in mice enhances cortical bone's response to mechanical loading (62, 124). Taken together, these data suggest that ER $\alpha$  and  $\beta$  have opposing roles in bone's adaptation to loading. However, the story is more complex since global deletion of one ER can result in up regulation of circulating estrogen and other hormones confounding interpretation of these experiments (125–127). With the more recent advent of cell-type specific knockout mice being available (128–130), the cell-type specific role of ERs in the mechanostat is currently being further investigated. For example, deletion of ER $\alpha$  specifically from osteocytes has no effect on cortical bone's adaptation to loading (128).

Another level of complexity is added when the role of the ERs in trabecular bone's adaptation to loading is considered. In female mice, deletion of ER $\alpha$  does not affect the response to loading while in male mice ER $\alpha$  deletion increases the response to loading (62). In contrast deletion of ER $\beta$  enhances loading-related trabecular bone gain (62). However, interpretation of the effect of ER deletion on loading-related changes in trabecular bone is problematic since strain-matching between groups is not possible due to the limited means to measure loading-engendered strains in these compartments and because deletion of ER $\alpha$ , and ER $\beta$  in female but not male mice, increases trabecular bone mass (131).

Inevitably, it is to be expected that elucidation of the role of estrogen and the ERs is likely to be complex and to complete our understanding it is likely that a combined *in vivo* and *in vitro* approach will be required. However, the purpose of its discussion here was to illustrate the type of interventions that can be combined with mechanical loading studies to determine the mechanisms involved in the mechanostat in more detail.

## CONCLUSION

In this review, we have discussed the animal models of mechanical loading, which are available to dissect the mechanisms of the mechanostat and how they have been used to determine the components of the strain stimulus involved in bone's adaptive response to mechanical loading. The complex process of bone modeling and remodeling can only be fully observed in animals and humans. Nearly all the understanding we have of the bones' adaptive response to mechanical loading has been derived from experiments using animal models.

In summary, over the physiological strain range bones' mechanically adaptive processes are responsive to dynamic but not static strains; the size and nature of the adaptive response is linearly related to the peak strains engendered; it is preferentially sensitive to high strain rates and unresponsive to static ones; it is most responsive to unusual strain distributions; it is maximized by remarkably few strain cycles, and that these are most effective when interrupted by short periods of rest between them.

No studies have so far demonstrated any unique mechanically responsive pathway in bone cells, rather the mechanisms of the mechanostat appear to be those used by a wide variety of cells to also respond to endocrine, paracrine, and autocrine influences. How these complex influences combine to so precisely regulate bone architecture that in the vast majority of situations it is appropriate to each individual's changing loading history remains to be determined. When it is, much of the essential data contributing to

the solution will have been generated by animal experimentation of the type described here.

## REFERENCES

1. Wolff J. *The Law of Bone Transformation*. Berlin: Hirschwald (1892).
2. Cowin SC. Wolff's law of trabecular architecture at remodeling equilibrium. *J Biomech Eng* (1986) **108**(1):83–8. doi:10.1115/1.3138584
3. Roesler H. The history of some fundamental concepts in bone biomechanics. *J Biomech* (1987) **20**(11–12):1025–34. doi:10.1016/0021-9290(87)90020-0
4. Frost HM. *The Utah Paradigm of Skeletal Physiology, Vol. 1, Bone and Bones and Associated Problems*. Athens, Greece: ISMNI (2004).
5. Sugiyama T, Price JS, Lanyon LE. Functional adaptation to mechanical loading in both cortical and cancellous bone is controlled locally and is confined to the loaded bones. *Bone* (2010) **46**(2):314–21. doi:10.1016/j.bone.2009.08.054
6. Lanyon LE, Sugiyama T, Price JS. Regulation of bone mass: local control or systemic influence or both? *IBMS Bonekey* (2009) **6**(6):218–26. doi:10.1138/20090382
7. Woo SL, Kuei SC, Amiel D, Gomez MA, Hayes WC, White FC, et al. The effect of prolonged physical training on the properties of long bone: a study of Wolff's law. *J Bone Joint Surg Am* (1981) **63**(5):780–7.
8. Loitz BJ, Zernicke RF. Strenuous exercise-induced remodelling of mature bone: relationships between in vivo strains and bone mechanics. *J Exp Biol* (1992) **170**:1–18.
9. Yeh JK, Aloia JF, Chen MM, Tierney JM, Sprintz S. Influence of exercise on cancellous bone of the aged female rat. *J Bone Miner Res* (1993) **8**(9):1117–25. doi:10.1002/jbmr.5650080913
10. Bourrin S, Ghaemmaghami F, Vico L, Chappard D, Gharib C, Alexandre C. Effect of a five-week swimming program on rat bone: a histomorphometric study. *Calcif Tissue Int* (1992) **51**(2):137–42. doi:10.1007/BF00298502
11. Snyder A, Zierath JR, Hawley JA, Sleeper MD, Craig BW. The effects of exercise mode, swimming vs. running, upon bone growth in the rapidly growing female rat. *Mech Ageing Dev* (1992) **66**(1):59–69. doi:10.1016/0047-6374(92)90073-M
12. Martínez-Mota L, Ulloa R-E, Herrera-Pérez J, Chavira R, Fernández-Guasti A. Sex and age differences in the impact of the forced swimming test on the levels of steroid hormones. *Physiol Behav* (2011) **104**(5):900–5. doi:10.1016/j.physbeh.2011.05.027
13. Ju Y-I, Sone T, Ohnaru K, Choi H-J, Fukunaga M. Differential effects of jump versus running exercise on trabecular architecture during remobilization after suspension-induced osteopenia in growing rats. *J Appl Physiol* (2012) **112**(5):766–72. doi:10.1152/japplphysiol.01219.2011
14. Umemura Y, Ishiko T, Yamauchi T, Kurono M, Mashiko S. Five jumps per day increase bone mass and breaking force in rats. *J Bone Miner Res* (1997) **12**(9):1480–5. doi:10.1359/jbmr.1997.12.9.1480
15. Buhl KM, Jacobs CR, Turner RT, Evans GL, Farrell PA, Donahue HJ. Aged bone displays an increased responsiveness to low-intensity resistance exercise. *J Appl Physiol* (2001) **90**(4):1359–64.
16. Schefer V, Talam MI. Oxygen consumption in adult and AGED C57BL/6J mice during acute treadmill exercise of different intensity. *Exp Gerontol* (1996) **31**(3):387–92. doi:10.1016/0531-5565(95)02032-2
17. Albuqaini K, Eged M, Alahmar A, Wright DJ. Cardiopulmonary exercise testing and its application. *Heart* (2007) **93**(10):1285–92. doi:10.1136/hrt.2007.121558
18. Price JS, Sugiyama T, Galea GL, Meakin LB, Sunters A, Lanyon LE. Role of endocrine and paracrine factors in the adaptation of bone to mechanical loading. *Curr Osteoporos Rep* (2011) **9**(2):76–82. doi:10.1007/s11914-011-0050-7
19. Bonewald LF, Kiel DP, Clemens TL, Esser K, Orwoll ES, O'Keefe RJ, et al. Forum on bone and skeletal muscle interactions: summary of the proceedings of an ASBMR workshop. *J Bone Miner Res* (2013) **28**(9):1857–65. doi:10.1002/jbmr.1980
20. Lanyon LE, Smith RN. Measurements of bone strain in the walking animal. *Res Vet Sci* (1969) **10**(1):93–4.
21. Evans FG, Lissner HR, Pedersen HH. Deformation studies of the femur under dynamic vertical loading. *Anat Rec* (1948) **101**(2):225–41. doi:10.1002/ar.1091010208
22. Lanyon LE. Analysis of surface bone strain in the calcaneus of sheep during normal locomotion. Strain analysis of the calcaneus. *J Biomech* (1973) **6**(1):41–9. doi:10.1016/0021-9290(73)90036-5

23. Lanyon LE, Hampson WG, Goodship AE, Shah JS. Bone deformation recorded in vivo from strain gauges attached to the human tibial shaft. *Acta Orthop Scand* (1975) **46**(2):256–68. doi:10.3109/17453677508989216
24. Lanyon LE, Smith RN. Bone strain in the tibia during normal quadrupedal locomotion. *Acta Orthop Scand* (1970) **41**(3):238–48. doi:10.3109/17453677008991511
25. Lanyon LE. In vivo bone strain recorded from thoracic vertebrae of sheep. *J Biomech* (1972) **5**(3):277–81. doi:10.1016/0021-9290(72)90044-9
26. Rubin CT, Lanyon LE. Limb mechanics as a function of speed and gait: a study of functional strains in the radius and tibia of horse and dog. *J Exp Biol* (1982) **101**:187–211.
27. Lanyon LE. Strain in sheep lumbar vertebrae recorded during life. *Acta Orthop Scand* (1971) **42**(1):102–12. doi:10.3109/17453677108989030
28. Lanyon LE, Hartman W. Strain related electrical potentials recorded in vitro and in vivo. *Calcif Tissue Res* (1977) **22**(3):315–27. doi:10.1007/BF02010370
29. Lanyon LE. The measurement of bone strain “in vivo”. *Acta Orthop Belg* (1976) **42**(Suppl 1):98–108.
30. Clark EA, Goodship AE, Lanyon LE. Locomotor bone strain as the stimulus for bone’s mechanical adaptability. *J Physiol (Lond)* (1975) **245**(2):57.
31. Skerry TM. One mechanostat or many? Modifications of the site-specific response of bone to mechanical loading by nature and nurture. *J Musculoskeletal Neuronal Interact* (2006) **6**(2):122–7.
32. Lauder GV, Lanyon LE. Functional anatomy of feeding in the bluegill sunfish, *Lepomis macrochirus*: in vivo measurement of bone strain. *J Exp Biol* (1980) **80**:33–55.
33. Lee KC, Maxwell A, Lanyon LE. Validation of a technique for studying functional adaptation of the mouse ulna in response to mechanical loading. *Bone* (2002) **31**(3):407–12. doi:10.1016/S8756-3282(02)00842-6
34. De Souza RL, Matsuura M, Eckstein F, Rawlinson SC, Lanyon LE, Pitsillides AA. Non-invasive axial loading of mouse tibiae increases cortical bone formation and modifies trabecular organization: a new model to study cortical and cancellous compartments in a single loaded element. *Bone* (2005) **37**(6):810–8. doi:10.1016/j.bone.2005.07.022
35. Sztefek P, Vanleene M, Olsson R, Collinson R, Pitsillides AA, Shefelbine S. Using digital image correlation to determine bone surface strains during loading and after adaptation of the mouse tibia. *J Biomech* (2010) **43**(4):599–605. doi:10.1016/j.jbiomech.2009.10.042
36. Moustafa A, Sugiyama T, Prasad J, Zaman G, Gross TS, Lanyon LE, et al. Mechanical loading-related changes in osteocyte sclerostin expression in mice are more closely associated with the subsequent osteogenic response than the peak strains engendered. *Osteoporos Int* (2011) **23**(4):1225–34. doi:10.1007/s00198-011-1656-4
37. Gross TS, Edwards JL, McLeod KJ, Rubin CT. Strain gradients correlate with sites of periosteal bone formation. *J Bone Miner Res* (1997) **12**(6):982–8. doi:10.1359/jbmr.1997.12.6.982
38. Willie BM, Birkhold AI, Razi H, Thiele T, Aido M, Kruck B, et al. Diminished response to in vivo mechanical loading in trabecular and not cortical bone in adulthood of female C57Bl/6 mice coincides with a reduction in deformation to load. *Bone* (2013) **55**(2):335–46. doi:10.1016/j.bone.2013.04.023
39. Lambers FM, Kuhn G, Schulte FA, Koch K, Müller R. Longitudinal assessment of in vivo bone dynamics in a mouse tail model of postmenopausal osteoporosis. *Calcif Tissue Int* (2012) **90**(2):108–19. doi:10.1007/s00223-011-9553-6
40. Lambers FM, Stuker F, Weigt C, Kuhn G, Koch K, Schulte FA, et al. Longitudinal in vivo imaging of bone formation and resorption using fluorescence molecular tomography. *Bone* (2013) **52**(2):587–95. doi:10.1016/j.bone.2012.11.001
41. Goodship AE, Lanyon LE, MacFie H. Functional adaptation of bone to increased stress. An experimental study. *J Bone Joint Surg Am* (1979) **61**(4):539–46.
42. Hert J, Lisková M, Landa J. Reaction of bone to mechanical stimuli. 1. Continuous and intermittent loading of tibia in rabbit. *Folia Morphol (Praha)* (1971) **19**(3):290–300.
43. Lisková M, Hert J. Reaction of bone to mechanical stimuli. 2. Periosteal and endosteal reaction of tibial diaphysis in rabbit to intermittent loading. *Folia Morphol (Praha)* (1971) **19**(3):301–17.
44. Hert J, Sklenářská A, Lisková M. Reaction of bone to mechanical stimuli. 5. Effect of intermittent stress on the rabbit tibia after resection of the peripheral nerves. *Folia Morphol (Praha)* (1971) **19**(4):378–87.
45. O’Connor JA, Lanyon LE, MacFie H. The influence of strain rate on adaptive bone remodelling. *J Biomech* (1982) **15**(10):767–81. doi:10.1016/0021-9290(82)90092-6
46. Rubin CT, Lanyon LE. Regulation of bone formation by applied dynamic loads. *J Bone Joint Surg Am* (1984) **66**(3):397–402.
47. Lanyon LE. Functional strain as a determinant for bone remodeling. *Calcif Tissue Int* (1984) **36**(Suppl 1):S56–61. doi:10.1007/BF02406134
48. Lanyon LE, Rubin CT. Static vs dynamic loads as an influence on bone remodelling. *J Biomech* (1984) **17**(12):897–905. doi:10.1016/0021-9290(84)90003-4
49. Chambers TJ, Evans M, Gardner TN, Turner-Smith A, Chow JW. Induction of bone formation in rat tail vertebrae by mechanical loading. *Bone Miner* (1993) **20**(2):167–78. doi:10.1016/S0169-6009(98)80025-6
50. Webster DJ, Morley PL, van Lenthe GH, Müller R. A novel in vivo mouse model for mechanically stimulated bone adaptation – a combined experimental and computational validation study. *Comput Methods Biomed Engin* (2008) **11**(5):435–41. doi:10.1080/10255840802078014
51. Lambers FM, Schulte FA, Kuhn G, Webster DJ, Müller R. Mouse tail vertebrae adapt to cyclic mechanical loading by increasing bone formation rate and decreasing bone resorption rate as shown by time-lapsed in vivo imaging of dynamic bone morphometry. *Bone* (2011) **49**(6):1340–50. doi:10.1016/j.bone.2011.08.035
52. Lambers FM, Koch K, Kuhn G, Ruffoni D, Weigt C, Schulte FA, et al. Trabecular bone adapts to long-term cyclic loading by increasing stiffness and normalization of dynamic morphometric rates. *Bone* (2013) **55**(2):325–34. doi:10.1016/j.bone.2013.04.016
53. Turner CH, Akhter MP, Raab DM, Kimmel DB, Recker RR. A noninvasive, in vivo model for studying strain adaptive bone modeling. *Bone* (1991) **12**(2):73–9. doi:10.1016/8756-3282(91)90003-2
54. Turner CH, Forwood MR, Rho JY, Yoshikawa T. Mechanical loading thresholds for lamellar and woven bone formation. *J Bone Miner Res* (1994) **9**(1):87–97. doi:10.1002/jbmr.5650090113
55. Gross TS, Srinivasan S, Liu CC, Clemens TL, Bain SD. Noninvasive loading of the murine tibia: an in vivo model for the study of mechanotransduction. *J Bone Miner Res* (2002) **17**(3):493–501. doi:10.1359/jbmr.2002.17.3.493
56. Torrance AG, Mosley JR, Susillo RF, Lanyon LE. Noninvasive loading of the rat ulna in vivo induces a strain-related modeling response uncomplicated by trauma or periostal pressure. *Calcif Tissue Int* (1994) **54**(3):241–7. doi:10.1007/BF00301686
57. Moustafa A, Sugiyama T, Saxon LK, Zaman G, Sunters A, Armstrong VJ, et al. The mouse fibula as a suitable bone for the study of functional adaptation to mechanical loading. *Bone* (2009) **44**(5):930–5. doi:10.1016/j.bone.2008.12.026
58. Sugiyama T, Meakin LB, Galea GL, Jackson BF, Lanyon LE, Ebetino FH, et al. Risedronate does not reduce mechanical loading-related increases in cortical and trabecular bone mass in mice. *Bone* (2011) **49**(1):133–9. doi:10.1016/j.bone.2011.03.775
59. Tu X, Rhee Y, Condon KW, Bivi N, Allen MR, Dwyer D, et al. Sost downregulation and local Wnt signaling are required for the osteogenic response to mechanical loading. *Bone* (2012) **50**(1):209–17. doi:10.1016/j.bone.2011.10.025
60. Windahl S, Saxon L, Börjesson A, Lagerquist M, Frenkel B, Henning P, et al. Estrogen receptor- $\alpha$  is required for the osteogenic response to mechanical loading in a ligand-independent manner involving its activation function 1 but not 2. *J Bone Miner Res* (2012) **28**(2):291–301. doi:10.1002/jbmr.1754
61. Saxon LK, Jackson BF, Sugiyama T, Lanyon LE, Price JS. Analysis of multiple bone responses to graded strains above functional levels, and to disuse, in mice in vivo show that the human Lrp5 G171V High Bone Mass mutation increases the osteogenic response to loading but that lack of Lrp5 activity reduces it. *Bone* (2011) **49**(2):184–93. doi:10.1016/j.bone.2011.03.683
62. Saxon LK, Galea G, Meakin L, Price J, Lanyon LE. Estrogen receptors  $\alpha$  and  $\beta$  have different gender-dependent effects on the adaptive responses to load bearing in cancellous and cortical bone. *Endocrinology* (2012) **153**(5):2254–66. doi:10.1210/en.2011-1977
63. Mosley JR, Lanyon LE. Growth rate rather than gender determines the size of the adaptive response of the growing skeleton to mechanical strain. *Bone* (2002) **30**(1):314–9. doi:10.1016/S8756-3282(01)00626-3
64. Ohashi N, Robling AG, Burr DB, Turner CH. The effects of dynamic axial loading on the rat growth plate. *J Bone Miner Res* (2002) **17**(2):284–92. doi:10.1359/jbmr.2002.17.2.284

65. Földes I, Szilágyi T, Rapcsák M, Velkey V, Oganov VS. Changes of lumbar vertebrae after Cosmos-1887 space flight. *Physiologist* (1991) **34**(1 Suppl):S57–8.
66. Vico L, Novikov VE, Very JM, Alexandre C. Bone histomorphometric comparison of rat tibial metaphysis after 7-day tail suspension vs. 7-day spaceflight. *Aviat Space Environ Med* (1991) **62**(1):26–31.
67. Zérath E, Holy X, Malouvier A, Caillard JC, Noguès C. Rat and monkey bone study in the Biocosmos 2044 space experiment. *Physiologist* (1991) **34**(1 Suppl):S194–5.
68. Vico L, Alexandre C. Microgravity and bone adaptation at the tissue level. *J Bone Miner Res* (1992) **7**(Suppl 2):S445–7. doi:10.1002/jbmr.5650071415
69. Uhthoff HK, Jaworski ZF. Bone loss in response to long-term immobilisation. *J Bone Joint Surg Br* (1978) **60-B**(3):420–9.
70. Turner RT, Bell NH. The effects of immobilization on bone histomorphometry in rats. *J Bone Miner Res* (1986) **1**(5):399–407. doi:10.1002/jbmr.5650010504
71. Rubin CT, Pratt GW, Porter AL, Lanyon LE, Poss R. Ultrasonic measurement of immobilization-induced osteopenia: an experimental study in sheep. *Calcif Tissue Int* (1988) **42**(5):309–12. doi:10.1007/BF02556365
72. Weinreb M, Rodan GA, Thompson DD. Osteopenia in the immobilized rat hind limb is associated with increased bone resorption and decreased bone formation. *Bone* (1989) **10**(3):187–94. doi:10.1016/8756-3282(89)90052-5
73. Li XJ, Jee WS, Chow SY, Woodbury DM. Adaptation of cancellous bone to aging and immobilization in the rat: a single photon absorptiometry and histomorphometry study. *Anat Rec* (1990) **227**(1):12–24. doi:10.1002/ar.1092270103
74. Skerry TM, Lanyon LE. Immobilisation induced bone loss in the sheep is not modulated by calcitonin treatment. *Bone* (1993) **14**(3):511–6. doi:10.1016/8756-3282(93)90188-G
75. Thomas T, Vico L, Skerry TM, Caulin F, Lanyon LE, Alexandre C, et al. Architectural modifications and cellular response during disuse-related bone loss in calcaneus of the sheep. *J Appl Physiol* (1996) **80**(1):198–202.
76. Shaw SR, Zernicke RF, Vailas AC, DeLuna D, Thomason DB, Baldwin KM. Mechanical, morphological and biochemical adaptations of bone and muscle to hindlimb suspension and exercise. *J Biomech* (1987) **20**(3):225–34. doi:10.1016/0021-9290(87)90289-2
77. Sakai A, Nakamura T. Changes in trabecular bone turnover and bone marrow cell development in tail-suspended mice. *J Musculoskeletal Neuronal Interact* (2001) **1**(4):387–92.
78. Sakai A, Mori T, Sakuma-Zenke M, Takeda T, Nakai K, Katae Y, et al. Osteoclast development in immobilized bone is suppressed by parathyroidectomy in mice. *J Bone Miner Metab* (2005) **23**(1):8–14. doi:10.1007/s00774-004-0534-y
79. Aguirre JI, Plotkin LI, Stewart SA, Weinstein RS, Parfitt AM, Manolagas SC, et al. Osteocyte apoptosis is induced by weightlessness in mice and precedes osteoclast recruitment and bone loss. *J Bone Miner Res* (2006) **21**(4):605–15. doi:10.1359/jbmr.060107
80. Ellman R, Spatz J, Cloutier A, Palme R, Christiansen BA, Bouxsein ML. Partial reductions in mechanical loading yield proportional changes in bone density, bone architecture, and muscle mass. *J Bone Miner Res* (2013) **28**(4):875–85. doi:10.1002/jbmr.1814
81. Lloyd SA, Bandstra ER, Willey JS, Riffle SE, Tirado-Lee L, Nelson GA, et al. Effect of proton irradiation followed by hindlimb unloading on bone in mature mice: a model of long-duration spaceflight. *Bone* (2012) **51**(4):756–64. doi:10.1016/j.bone.2012.07.001
82. Can A, Dao DT, Terrillion CE, Piantadosi SC, Bhat S, Gould TD. The tail suspension test. *J Vis Exp* (2012) **59**:e3769. doi:10.3791/3769
83. Warner SE, Sanford DA, Becker BA, Bain SD, Srinivasan S, Gross TS. Botox induced muscle paralysis rapidly degrades bone. *Bone* (2006) **38**(2):257–64. doi:10.1016/j.bone.2005.08.009
84. Ausk BJ, Huber P, Poliachik SL, Bain SD, Srinivasan S, Gross TS. Cortical bone resorption following muscle paralysis is spatially heterogeneous. *Bone* (2012) **50**(1):14–22. doi:10.1016/j.bone.2011.08.028
85. De Souza RL, Pitsillides AA, Lanyon LE, Skerry TM, Chenu C. Sympathetic nervous system does not mediate the load-induced cortical new bone formation. *J Bone Miner Res* (2005) **20**(12):2159–68. doi:10.1359/JBMR.050812
86. Sugiyama T, Meakin LB, Browne WJ, Galea GL, Price JS, Lanyon LE. Bones' adaptive response to mechanical loading is essentially linear between the low strains associated with disuse and the high strains associated with the lamellar/woven bone transition. *J Bone Miner Res* (2012) **27**(8):1784–93. doi:10.1002/jbmr.1599
87. Warden SJ, Galley MR, Richard JS, George LA, Dirks RC, Guildenbecher EA, et al. Reduced gravitational loading does not account for the skeletal effect of botulinum toxin-induced muscle inhibition suggesting a direct effect of muscle on bone. *Bone* (2013) **54**(1):98–105. doi:10.1016/j.bone.2013.01.043
88. Brodt MD, Silva MJ. Aged mice have enhanced endocortical response and normal periosteal response compared with young-adult mice following 1 week of axial tibial compression. *J Bone Miner Res* (2010) **25**(9):2006–15. doi:10.1002/jbmr.96
89. Zaman G, Saxon LK, Sunter A, Hilton H, Underhill P, Williams D, et al. Loading-related regulation of gene expression in bone in the contexts of estrogen deficiency, lack of estrogen receptor alpha and disuse. *Bone* (2010) **46**(3):628–42. doi:10.1016/j.bone.2009.10.021
90. Lee K, Jessop H, Susillo R, Zaman G, Lanyon L. Endocrinology: bone adaptation requires oestrogen receptor-alpha. *Nature* (2003) **424**(6947):389. doi:10.1038/424389a
91. Rubin CT, Lanyon LE. Regulation of bone mass by mechanical strain magnitude. *Calcif Tissue Int* (1985) **37**(4):411–7. doi:10.1007/BF02553711
92. McKenzie JA, Silva MJ. Comparing histological, vascular and molecular responses associated with woven and lamellar bone formation induced by mechanical loading in the rat ulna. *Bone* (2011) **48**(2):250–8. doi:10.1016/j.bone.2010.09.005
93. Judex S, Gross TS, Zernicke RF. Strain gradients correlate with sites of exercise-induced bone-forming surfaces in the adult skeleton. *J Bone Miner Res* (1997) **12**(10):1737–45. doi:10.1359/jbmr.1997.12.10.1737
94. Kotha SP, Hsieh YF, Strigel RM, Müller R, Silva MJ. Experimental and finite element analysis of the rat ulnar loading model—correlations between strain and bone formation following fatigue loading. *J Biomech* (2004) **37**(4):541–8. doi:10.1016/j.jbiomech.2003.08.009
95. Wallace IJ, Kwaczala AT, Judex S, Demes B, Carlson KJ. Physical activity engendering loads from diverse directions augments the growing skeleton. *J Musculoskeletal Neuronal Interact* (2013) **13**(3):283–8.
96. Skerry TM, Lanyon LE. Interruption of disuse by short duration walking exercise does not prevent bone loss in the sheep calcaneus. *Bone* (1995) **16**(2):269–74. doi:10.1016/8756-3282(94)00039-3
97. Meakin LB, Sugiyama T, Galea GL, Browne WJ, Lanyon LE, Price JS. Male mice housed in groups engage in frequent fighting and show a lower response to additional bone loading than females or individually housed males that do not fight. *Bone* (2013) **54**(1):113–7. doi:10.1016/j.bone.2013.01.029
98. Mosley JR, Lanyon LE. Strain rate as a controlling influence on adaptive modeling in response to dynamic loading of the ulna in growing male rats. *Bone* (1998) **23**(4):313–8. doi:10.1016/S8756-3282(98)00113-6
99. Turner CH, Owani I, Takano Y. Mechanotransduction in bone: role of strain rate. *Am J Physiol* (1995) **269**(3 Pt 1):E438–42.
100. Taaffe DR, Robinson TL, Snow CM, Marcus R. High-impact exercise promotes bone gain in well-trained female athletes. *J Bone Miner Res* (1997) **12**(2):255–60. doi:10.1359/jbmr.1997.12.2.255
101. Jones HH, Priest JD, Hayes WC, Tichenor CC, Nagel DA. Humeral hypertrophy in response to exercise. *J Bone Joint Surg Am* (1977) **59**(2):204–8.
102. Deere K, Sayers A, Rittweger J, Tobias JH. Habitual levels of high, but not moderate or low, impact activity are positively related to hip BMD and geometry: results from a population-based study of adolescents. *J Bone Miner Res* (2012) **27**(9):1887–95. doi:10.1002/jbmr.1631
103. Bennell KL, Malcolm SA, Khan KM, Thomas SA, Reid SJ, Brukner PD, et al. Bone mass and bone turnover in power athletes, endurance athletes, and controls: a 12-month longitudinal study. *Bone* (1997) **20**(5):477–84. doi:10.1016/S8756-3282(97)00026-4
104. LaMothe JM, Zernicke RF. Rest insertion combined with high-frequency loading enhances osteogenesis. *J Appl Physiol* (2004) **96**(5):1788–93. doi:10.1152/japplphysiol.01145.2003
105. Meakin LB, Galea GL, Sugiyama T, Lanyon LE, Price JS. Age-related impairment of bones' adaptive response to loading in mice is associated with gender-related deficiencies in osteoblasts but no change in osteocytes. *J Bone Miner Res* (2014) **29**(8):1859–71. doi:10.1002/jbmr.2222
106. Kennedy OD, Herman BC, Laudier DM, Majeska RJ, Sun HB, Schaffler MB. Activation of resorption in fatigue-loaded bone involves both apoptosis and active pro-osteoclastogenic signaling by distinct osteocyte populations. *Bone* (2012) **50**(5):1115–22. doi:10.1016/j.bone.2012.01.025

107. Robling AG, Burr DB, Turner CH. Partitioning a daily mechanical stimulus into discrete loading bouts improves the osteogenic response to loading. *J Bone Miner Res* (2000) **15**(8):1596–602. doi:10.1359/jbmr.2000.15.8.1596
108. Robling AG, Burr DB, Turner CH. Recovery periods restore mechanosensitivity to dynamically loaded bone. *J Exp Biol* (2001) **204**(Pt 19):3389–99.
109. Srinivasan S, Ausk BJ, Poliachik SL, Warner SE, Richardson TS, Gross TS. Rest-inserted loading rapidly amplifies the response of bone to small increases in strain and load cycles. *J Appl Physiol* (2007) **102**(5):1945–52. doi:10.1152/japplphysiol.00507.2006
110. Srinivasan S, Agans SC, King KA, Moy NY, Poliachik SL, Gross TS. Enabling bone formation in the aged skeleton via rest-inserted mechanical loading. *Bone* (2003) **33**(6):946–55. doi:10.1016/j.bone.2003.07.009
111. Srinivasan S, Weimer DA, Agans SC, Bain SD, Gross TS. Low-magnitude mechanical loading becomes osteogenic when rest is inserted between each load cycle. *J Bone Miner Res* (2002) **17**(9):1613–20. doi:10.1359/jbmr.2002.17.9.1613
112. Saxon LK, Robling AG, Alam I, Turner CH. Mechanosensitivity of the rat skeleton decreases after a long period of loading, but is improved with time off. *Bone* (2005) **36**(3):454–64. doi:10.1016/j.bone.2004.12.001
113. de Souza RL, Saxon L. In vivo mechanical loading. *Methods Mol Biol* (2012) **816**:621–36. doi:10.1007/978-1-61779-415-5\_38
114. Kanis JA, McCloskey EV, Johansson H, Oden A, Melton LJ, Khaltaev N. A reference standard for the description of osteoporosis. *Bone* (2008) **42**(3):467–75. doi:10.1016/j.bone.2007.11.001
115. FitzGerald G, Boonen S, Compston JE, Pfeilschifter J, LaCroix AZ, Hosmer DW, et al. Differing risk profiles for individual fracture sites: evidence from the global longitudinal study of osteoporosis in women (GLOW). *J Bone Miner Res* (2012) **27**(9):1907–15. doi:10.1002/jbmr.1652
116. Lanyon L, Skerry T. Postmenopausal osteoporosis as a failure of bone's adaptation to functional loading: a hypothesis. *J Bone Miner Res* (2001) **16**(11):1937–47. doi:10.1359/jbmr.2001.16.11.1937
117. Hagino H, Raab DM, Kimmel DB, Akhter MP, Recker RR. Effect of ovariectomy on bone response to in vivo external loading. *J Bone Miner Res* (1993) **8**(3):347–57. doi:10.1002/jbmr.5650080312
118. Jagger CJ, Chow JW, Chambers TJ. Estrogen suppresses activation but enhances formation phase of osteogenic response to mechanical stimulation in rat bone. *J Clin Invest* (1996) **98**(10):2351–7. doi:10.1172/JCI119047
119. Sugiyama T, Galea GL, Lanyon LE, Price JS. Mechanical loading-related bone gain is enhanced by tamoxifen but unaffected by fulvestrant in female mice. *Endocrinology* (2010) **151**(12):5582–90. doi:10.1210/en.2010-0645
120. Turner RT, Wakley GK, Hannon KS, Bell NH. Tamoxifen inhibits osteoclast-mediated resorption of trabecular bone in ovarian hormone-deficient rats. *Endocrinology* (1988) **122**(3):1146–50. doi:10.1210/endo-122-3-1146
121. Saxon LK, Turner CH. Low-dose estrogen treatment suppresses periosteal bone formation in response to mechanical loading. *Bone* (2006) **39**(6):1261–7. doi:10.1016/j.bone.2006.06.030
122. Callewaert F, Bakker A, Schrooten J, Van Meerbeek B, Verhoeven G, Boonen S, et al. Androgen receptor disruption increases the osteogenic response to mechanical loading in male mice. *J Bone Miner Res* (2010) **25**(1):124–31. doi:10.1359/jbmr.091001
123. Börjesson AE, Windahl SH, Lagerquist MK, Engdahl C, Frenkel B, Movéare-Skrte S, et al. Roles of transactivating functions 1 and 2 of estrogen receptor-alpha in bone. *Proc Natl Acad Sci U S A* (2011) **108**(15):6288–93. doi:10.1073/pnas.1100454108
124. Saxon LK, Robling AG, Castillo AB, Mohan S, Turner CH. The skeletal responsiveness to mechanical loading is enhanced in mice with a null mutation in estrogen receptor-beta. *Am J Physiol Endocrinol Metab* (2007) **293**(2):E484–91. doi:10.1152/ajpendo.00189.2007
125. Lindberg MK, Weihua Z, Andersson N, Movéare S, Gao H, Vidal O, et al. Estrogen receptor specificity for the effects of estrogen in ovariectomized mice. *J Endocrinol* (2002) **174**(2):167–78. doi:10.1677/joe.0.1740167
126. Sunters A, Armstrong VJ, Zaman G, Kypta RM, Kawano Y, Lanyon LE, et al. Mechano-transduction in osteoblastic cells involves strain-regulated estrogen receptor alpha-mediated control of insulin-like growth factor (IGF) I receptor sensitivity to ambient IGF, leading to phosphatidylinositol 3-kinase/AKT-dependent Wnt/LRP5 receptor-independent activation of beta-catenin signaling. *J Biol Chem* (2010) **285**(12):8743–58. doi:10.1074/jbc.M109.027086
127. Galea GL, Price JS, Lanyon LE. Estrogen receptors' roles in the control of mechanically adaptive bone (re)modeling. *Bonekey Rep* (2013) **2**:413. doi:10.1038/bonekey.2013.147
128. Windahl SH, Börjesson AE, Farman HH, Engdahl C, Movéare-Skrte S, Sjögren K, et al. Estrogen receptor- $\alpha$  in osteocytes is important for trabecular bone formation in male mice. *Proc Natl Acad Sci U S A* (2013) **110**(6):2294–9. doi:10.1073/pnas.1220811110
129. Almeida M, Iyer S, Martin-Millan M, Bartell SM, Han L, Ambrogini E, et al. Estrogen receptor- $\alpha$  signaling in osteoblast progenitors stimulates cortical bone accrual. *J Clin Invest* (2012) **123**(1):394–404. doi:10.1172/JCI65910
130. Kondoh S, Inoue K, Igarashi K, Sugizaki H, Shirode-Fukuda Y, Inoue E, et al. Estrogen receptor  $\alpha$  in osteocytes regulates trabecular bone formation in female mice. *Bone* (2014) **60**:68–77. doi:10.1016/j.bone.2013.12.005
131. Sims NA, Dupont S, Krust A, Clement-Lacroix P, Minet D, Resche-Rigon M, et al. Deletion of estrogen receptors reveals a regulatory role for estrogen receptors-beta in bone remodeling in females but not in males. *Bone* (2002) **30**(1):18–25. doi:10.1016/S8756-3282(01)00643-3

**Conflict of Interest Statement:** The authors declare that the research was conducted in the absence of any commercial or financial relationships that could be construed as a potential conflict of interest. The Specialty Chief Editor Jonathan H. Tobias declares that, despite being affiliated to the same institution as the authors, the review process was handled objectively and no conflict of interest exists.

*Received: 28 July 2014; paper pending published: 17 August 2014; accepted: 12 September 2014; published online: 01 October 2014.*

*Citation: Meakin LB, Price JS and Lanyon LE (2014) The contribution of experimental in vivo models to understanding the mechanisms of adaptation to mechanical loading in bone. *Front. Endocrinol.* **5**:154. doi: 10.3389/fendo.2014.00154*

*This article was submitted to Bone Research, a section of the journal *Frontiers in Endocrinology*.*

*Copyright © 2014 Meakin, Price and Lanyon. This is an open-access article distributed under the terms of the Creative Commons Attribution License (CC BY). The use, distribution or reproduction in other forums is permitted, provided the original author(s) or licensor are credited and that the original publication in this journal is cited, in accordance with accepted academic practice. No use, distribution or reproduction is permitted which does not comply with these terms.*



# A new method to investigate how mechanical loading of osteocytes controls osteoblasts

**Marisol Vazquez<sup>1</sup>, Bronwen A. J. Evans<sup>2</sup>, Daniela Riccardi<sup>3</sup>, Sam L. Evans<sup>4</sup>, Jim R. Ralphs<sup>3</sup>, Christopher Mark Dillingham<sup>5</sup> and Deborah J. Mason<sup>3\*</sup>**

<sup>1</sup> Arthritis Research UK Biomechanics and Bioengineering Centre, School of Biosciences, Cardiff University, Cardiff, UK

<sup>2</sup> Institute of Molecular and Experimental Medicine, School of Medicine, Cardiff University, Cardiff, UK

<sup>3</sup> Division of Pathophysiology and Repair, School of Biosciences, Cardiff University, Cardiff, UK

<sup>4</sup> Institute of Mechanical and Manufacturing Engineering, School of Engineering, Cardiff University, Cardiff, UK

<sup>5</sup> School of Psychology, Cardiff University, Cardiff, UK

**Edited by:**

Jonathan H. Tobias, University of Bristol, UK

**Reviewed by:**

Andy Sunters, Royal Veterinary College, UK

Jonathan Gooi, The University of Melbourne, Australia

**\*Correspondence:**

Deborah J. Mason, Division of Pathophysiology and Repair, School of Biosciences, Cardiff University, Museum Avenue, Cardiff, CF10 3AX, UK  
e-mail: masondj@cardiff.ac.uk

Mechanical loading, a potent stimulator of bone formation, is governed by osteocyte regulation of osteoblasts. We developed a three-dimensional (3D) *in vitro* co-culture system to investigate the effect of loading on osteocyte–osteoblast interactions. MLO-Y4 cells were embedded in type I collagen gels and MC3T3-E1(14) or MG63 cells layered on top. Ethidium homodimer staining of 3D co-cultures showed 100% osteoblasts and 86% osteocytes were viable after 7 days. Microscopy revealed osteoblasts and osteocytes maintain their respective ovoid/pyriform and dendritic morphologies in 3D co-cultures. Reverse-transcriptase quantitative polymerase chain reaction (RT-qPCR) of messenger ribonucleic acid (mRNA) extracted separately from osteoblasts and osteocytes, showed that podoplanin (E11), osteocalcin, and runt-related transcription factor 2 mRNAs were expressed in both cell types. Type I collagen (*Col1a1*) mRNA expression was higher in osteoblasts ( $P < 0.001$ ), whereas, alkaline phosphatase mRNA was higher in osteocytes ( $P = 0.001$ ). Immunohistochemistry revealed osteoblasts and osteocytes express E11, type I pro-collagen, and connexin 43 proteins. In preliminary experiments to assess osteogenic responses, co-cultures were treated with human recombinant bone morphogenetic protein 2 (BMP-2) or mechanical loading using a custom built loading device. BMP-2 treatment significantly increased osteoblast *Col1a1* mRNA synthesis ( $P = 0.031$ ) in MLO-Y4/MG63 co-cultures after 5 days treatment. A 16-well silicone plate, loaded (5 min, 10 Hz, 2.5 N) to induce 4000–4500  $\mu\text{e}$  cyclic compression within gels increased prostaglandin E<sub>2</sub> (PGE<sub>2</sub>) release 0.5 h post-load in MLO-Y4 cells pre-cultured in 3D collagen gels for 48, 72 h, or 7 days. Mechanical loading of 3D co-cultures increased type I pro-collagen release 1 and 5 days later. These methods reveal a new osteocyte–osteoblast co-culture model that may be useful for investigating mechanically induced osteocyte control of osteoblast bone formation.

**Keywords:** osteocyte, osteoblast, 3 dimensional, co-culture, model, loading

## INTRODUCTION

Osteocytes are by far the most abundant bone cell type (90–95% of all bone cells) (1), forming a network of cells, connected by long cell processes that extend along canaliculi within the mineralized bone matrix. The adult human skeleton is continually being remodeled by bone forming osteoblasts and bone resorbing osteoclasts, whose activities are balanced in healthy individuals. Osteocytes are thought to integrate hormonal, growth factor, and mechanical stimuli to influence control of bone remodeling.

*In vivo*, osteocytes increase transcriptional and metabolic activities in response to short loading periods (2, 3), increase their dentin matrix protein 1 (DMP1) and matrix extracellular phosphoglycoprotein (MEPE) expression, controlling bone matrix mineral quality (4, 5), increase insulin growth factor 1 (IGF-1), and related proteins involved in mechanically induced bone formation

(6, 7), and stimulate nitric oxide (NO) production (8), an early mediator of mechanically induced bone formation (9). Osteocyte abundance, morphology, position within bone, and ability to form an extensive network are ideally suited to this mechanoresponsive role (10–14). Osteocytic processes and primary cilia detect mechanical stimuli (15–19) whereas, proteins involved in the connection of osteocytes to surrounding cells and/or the extracellular matrix (ECM), like focal adhesions, connexin 43 (CX43), and integrins, are involved in osteocyte response to mechanical stimuli (20, 21). Mechanically loaded osteocytes regulate osteoblast activity through various mechanisms including the downregulation of sclerostin (SOST) expression (22, 23), release of NO, which has an anabolic effect on osteoblast activity (9), and release of prostaglandin E<sub>2</sub> (PGE<sub>2</sub>), which regulates osteoblast proliferation and differentiation (24). Whilst the methodology developed here focuses on osteocyte control of osteoblasts, it is clear

that osteocytes regulate other cells activities in response to load (25–27).

A major problem with investigating osteocytes is the difficulty in isolation and culture of these cells *in vitro*. Studies using sequential digestion of bone to enrich for osteocytes have proved difficult and, so far, limited to chick (28–30), rat (31), and mouse (32). Mouse cell lines representing late osteoblast/early osteocytes (MLO-A5) (33) and osteocyte-like (MLO-Y4) (33, 34) cells have been developed to facilitate *in vitro* investigation of osteocytes, but these are routinely cultured in monolayer on type I collagen-coated plastic. More recently the IDG-SW3 mouse derived cells have been shown to replicate osteoblast-to-late osteocyte differentiation under both two-dimensional (2D) and three-dimensional (3D) collagen culture conditions *in vitro* (35).

There have been very few publications on co-culture of osteoblasts and osteocytes, despite the known physiological interactions between these cell types. Taylor et al. (36) describe a co-culture system in which the two cell types are grown in 2D, either side of a semi permeable cell culture insert membrane. Stimulation of the osteocyte layer by fluid shear enhanced alkaline phosphatase (ALP) expression by the osteoblasts, an effect at least partially dependent on cell–cell contact and gap junction communication (36). This system is useful but does not allow osteocytes to form a 3D network. The three-dimensionality of osteocyte environment is important; firstly embedding primary osteoblasts within 3D matrices induces differentiation to osteocyte-like cells *in vitro* (37), recapitulating the *in vivo* differentiation pathway, and secondly it facilitates a more realistic model of a 3D lacunocanicular system (LCS) of cells that can be subjected to appropriate mechanical cues.

*In vitro*, 3D bone models where bone cells are embedded in type I collagen gels have not been used to investigate osteocyte loading or osteocyte–osteoblast interactions (38–42). 3D cultures made out of polybicarbonate membranes (37) and scaffolds (43–46) do not embed cells within a 3D matrix, but instead attach them to the scaffold surface and therefore do not accurately capture the environment of an osteocyte within bone. Whilst these systems have proven the feasibility of reproducing the synthesis of an organized matrix (44) and cell-mediated matrix degradation (47–49), there are no models that co-culture osteoblasts and osteocytes in 3D under mechanical stimulation. This highlights a major gap in the understanding of the interactions that lead to mechanically induced bone formation.

Here, we describe the methodology for a new 3D co-culture model, cultured within a custom built multi-well silicone loading plate, to investigate how mechanical loading of osteocytes regulates osteoblast function. MLO-Y4 cells were cultured within type I collagen gels, with an osteoblast-like cell line [MC3T3-E1(14) or MG63] layered on top of the gel (**Figure 1**). Both osteoblasts and osteocytes maintain cell viability, morphology, and phenotype when cultured in 3D co-cultures and express CX43, a component of network formation. These co-cultures resulted in anabolic responses when stimulated with bone morphogenetic protein 2 (BMP-2) or mechanically loaded. This model will be useful in elucidating osteocyte-driven mechanical mechanisms that regulate bone formation.

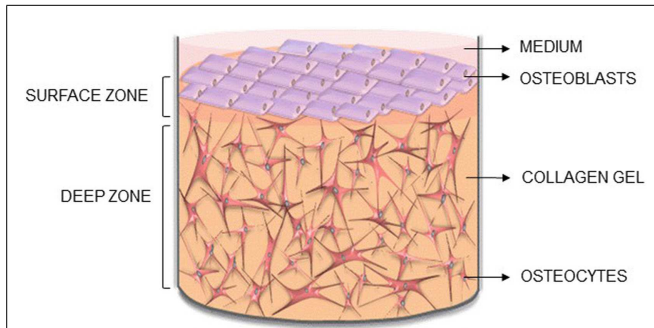


**FIGURE 1 | Novel 3D osteocyte–osteoblast co-culture model.** Diagram of the 3D *in vitro* model indicating the surface and deep zone, and positions of the surface osteoblasts and embedded osteocytes.

## MATERIALS AND METHODS

### CELLS

MLO-Y4 cells were a kind gift from Professor Lynda Bonewald, University of Missouri-Kansas City, USA. MC3T3-E1(14) and MG63 cells were obtained from the European Collection of Cell Cultures, Salisbury, UK.

MLO-Y4 cells (34) were cultured on collagen-coated flasks (rat tail tendon type I collagen, 0.15 mg/mL in 0.02 N glacial acetic acid) in alpha minimum essential medium (αMEM, Invitrogen) supplemented with 2.5% Heat Inactivated Fetal Bovine Serum (HIFBS, Invitrogen) and 2.5% Heat Inactivated Newborn Calf Serum (HINCS, Invitrogen) (50). MC3T3-E1(14) cells were cultured in αMEM supplemented with 10% FBS (Invitrogen) (51). MG63 cells were cultured in Dulbecco's Minimum Essential Medium (DMEM, Invitrogen) and supplemented with 5% FBS (Invitrogen). All three cell lines were supplemented with 100 U/mL penicillin and 100 µg/mL streptomycin and grown at 37°C in 5% CO<sub>2</sub>. At 70–80% (MLO-Y4) or 80–90% [MC3T3-E1(14) and MG63] confluence, cells were sub-cultured by treating with trypsin/ethylenediaminetetraacetic acid (EDTA) (0.25% w/v of each; Invitrogen).

### 3D CO-CULTURES

MLO-Y4 cells were incorporated within type I collagen gels and either MC3T3-E1(14) or MG63 cells layered on top. Rat tail tendon type I collagen (Sigma, in 7 mM glacial acetic acid) was mixed 4:1 with 5X MEM (Invitrogen) containing 11 g/L sodium bicarbonate on ice and neutralized [1 M tris(hydroxymethyl)aminomethane (Tris) base, pH 11.5] to give 2–2.6 mg/mL type I collagen gels. MLO-Y4 cells ( $1.5 \times 10^6$  cells/mL gel) diluted in αMEM (<10% of total gel volume) were added to the collagen on ice and 500 or 250 µL distributed into 24 or 48-well plastic plates, respectively for polymerization at 37°C for 1 h. MC3T3-E1(14) or MG63 cells ( $1.5 \times 10^5$  cells/well) in DMEM with 5% FBS (MG63) or 5% dialyzed FBS (DFBS) [MC3T3-E1(14)] were applied onto the surface of each gel after 1 h and incubated at 37°C for up to 1 week (**Figure 1**). Medium was changed after 24 h and every 2 days thereafter. To test cell responses, co-cultures were treated with human recombinant BMP-2 (250 ng/mL, Peprotech) for 5 days.

## CELL VIABILITY

Co-cultures grown in plastic plates were rinsed with phosphate buffered saline, pH 7.3 (PBS), incubated with 1 µM ethidium homodimer (Invitrogen) in serum free medium for 2 h at 4°C and then for a further 2.5 h at 37°C before washing overnight at 37°C in normal culture medium with gentle agitation. Positive controls co-cultures were freeze-thawed at -20°C three times, before treatment. For cell death analysis of the surface zone, confocal microscopy was performed directly on whole co-cultures. Samples were scanned using appropriate excitation and emission settings for simultaneous recording of 4',6-diamidino-2-phenylindole (DAPI) [358 nm Excitation ( $\text{Ex}_{(\max)}$ ); 461 nm Emission ( $\text{Em}_{(\max)}$ )] and ethidium homodimer [590 nm  $\text{Ex}_{(\max)}$ ; 617 nm  $\text{Em}_{(\max)}$ ]. Samples were optically sectioned, over five defined arbitrary regions per gel quarter, using a x10 objective lens with 2.32 zoom. 5 µm step size z-stack optical sections were reconstructed using Leica Confocal Software. Maximum intensity models were prepared showing detail of the surface zone. Counts were made of DAPI (blue) labeled nuclei (to give total number of cells) and ethidium homodimer and DAPI (purple) co-labeled nuclei (to give number of dead cells).

For deep zone viability, cultures were fixed with 1% paraformaldehyde (Sigma) in 0.05 M PBS for 30 min at 4°C and then washed in PBS. Some were labeled whole for filamentous actin and type I pro-collagen (see below). Cultures were infiltrated with 50% OCT compound (Tissue Tek) in PBS overnight at 4°C and then frozen in fresh OCT compound onto cryostat stubs using dry ice. Cryosections were cut at 20 µm using a Bright OTF5000 cryostat and collected on Polysine slides (VWR). Five random slides of each co-culture containing 4–6 sections each were mounted in Vectashield mounting medium with DAPI as a nuclear counterstain. One random section from each slide was observed under epi-fluorescence as above, and 10 random fields of view using the x20 objective photographed for each section under both DAPI and ethidium homodimer illumination. Counts were made as above.

## MICROSCOPY AND IMAGING OF CELLS AND CELL MARKERS

Osteocyte and osteoblast morphology was assessed in live cultures grown in plastic plates with a Leica DMRB inverted microscope equipped with a Moticam 2000 digital camera. For labeling procedures, 3D cultures were treated, fixed, frozen, and cryosectioned as previously outlined.

Filamentous actin was labeled by incubating fixed intact cultures or sections with 5 µM Atto488 conjugated phalloidin (Sigma) in PBS containing 0.1% tween 20 (PBST; Sigma) for 40 min at 4°C. Specimens were then washed thoroughly in PBST and mounted in Vectashield containing DAPI to label nuclei (Vector Laboratories). Labels for type I pro-collagen, gap junction protein CX43 and dendritic cell marker podoplanin (E11) were performed by indirect immunohistochemical procedures. In all cases, the primary antibody was replaced in control sections with PBST alone or with non-immune immunoglobulins (IgG), to reveal any non-specific binding. In all cases both PBST and IgG controls were negative. Type I pro-collagen was labeled using monoclonal antibody M38 recognizing the C-terminus of pro-collagen I in a wide range of species *except* mouse [5 µg/mL;

(52); Developmental Studies Hybridoma Bank], CX43 using monoclonal antibody CXN-6 (8 µg/mL; Sigma) and E11 with goat anti-mouse podoplanin (E11) primary antibody (2.5 µg/mL; R&D Systems). Sections were blocked with 5% goat serum (those stained with antibodies M38 and CXN-6; Dako) or 5% rabbit serum (E11; Dako) for 30 min and then incubated with primary antibodies overnight at 4°C (E11) or 1 h at room temperature (M38, CXN-6). After extensive washing with PBST, M38 and CXN-6 sections were incubated with AlexaFlour594 or AlexaFluor488 goat anti-mouse conjugates, for 30 min at room temperature. All sections were thoroughly washed and mounted in Vectashield/DAPI. E11 sections were incubated with a horseradish peroxidase rabbit anti-goat conjugate (Vector Laboratories; 1:800 dilution) for 30 min, washed in PBST and label visualized using a nickel-enhanced diaminobenzidine peroxidase substrate kit (Vector Laboratories). Fluorescence specimens were examined with an Olympus BX61 epi-fluorescence microscope equipped with an F-view camera and AnalySISimage capture and analysis software, or using a Leica TCS SP2 AOBS confocal scanning laser microscope and using the Leica Confocal Software, and peroxidase labels with a Leica DMRB microscope with a Moticam 2000 camera. Confocal microscopy was carried out on samples using appropriate excitation and emission settings for simultaneous recording of DAPI and ethidium homodimer as previously outlined, Phalloidin-Atto488 [495 nm  $\text{Ex}_{(\max)}$ , 519 nm  $\text{Em}_{(\max)}$ ], and Alexa 594 [590 nm  $\text{Ex}_{(\max)}$ , 617 nm  $\text{Em}_{(\max)}$ ]. Specimens were optically sectioned using a x63 objective with an arbitrary zoom (surface and deep zone actin filament stain, and CX43 immunofluorescence). 5 µm (surface zone) or 0.5 µm (deep zone) step size z-stack optical sections through the specimen were reconstructed using Leica Confocal Software. Maximum intensity models were prepared showing detail of the surface zone or deep zone.

## MOLECULAR ANALYSIS OF OSTEOCYTE AND OSTEOBLAST PHENOTYPE

Osteocyte and osteoblast phenotype was determined at the molecular level using reverse-transcriptase quantitative polymerase chain reaction (RT-qPCR). Ribonucleic acid (RNA) was extracted separately from surface and embedded cells of co-cultures grown in plastic plates by dispensing 1 mL Trizol (Invitrogen) onto the surface for 10 s to extract osteoblast RNA, and subsequently dissolving the underlying gel within a separate 1 mL Trizol aliquot to extract RNA from gel embedded cells. After RNA extraction according to manufacturer's protocol and DNase treatment (DNA-free, Ambion) RNA was re-precipitated with 3 M sodium acetate (pH 5.5, Ambion) and dissolved in molecular biology grade water (25 µL for surface cells, 50 µL for deep cells). RNA with  $A_{260}/A_{280}$  and  $A_{260}/A_{230}$  ratios of  $\geq 1.8$  was deemed good quality. RNA (1.7–253.3 ng for the surface zone; 108.8–1864.9 ng for the deep zone) was primed with random hexadeoxynucleotides (Promega, Southampton, UK) and reverse transcribed according to manufacturer's instructions (Superscript III, Invitrogen). Gene expression of E11, osteocalcin (OCN), runt-related transcription factor 2 (Runx2), type I collagen (*Col1a1*), ALP, and simian vacuolating virus 40 (SV40) large T-antigen were analyzed by RT-qPCR [SYBR Green I master mix (Sigma), 2.5 mM MgCl<sub>2</sub>, 200 nM each primer, Stratagene MX3000P]. All targets except OCN used intron-spanning primers (Table 1) and no template controls were

**Table 1 | Primer details.**

| Gene                            | Primers (5'-3')  | Amplicon size (bp) |
|---------------------------------|--|--------------------|
| GAPDH (human)<br>NM_002046.5    | Fwd – GGT ATC GTG GAA GGA CTC ATG A<br>Rev – GGC CAT CCA CAG TCT TCT G     | 68                 |
| HPRT1 (human)<br>NM_000194.2    | Fwd – GCA GAC TTT GCT TTC CTT GG<br>Rev – GTG GGG TCC TTT TCA CCA G        | 80                 |
| 18S rRNA<br>NR_003278.3         | Fwd – GCA ATT ATT CCC CAT GAA CG<br>Rev – GGC CTC ACT AAA CCA TCC AA       | 125                |
| E11 (human)<br>NM_006474.4      | Fwd – ACG GAG AAA GTG GAT GGA GA<br>Rev – ACG ATG ATT GCA CCA ATG AA       | 186                |
| RUNX2 (human)<br>NM_001024630.3 | Fwd – GTG GAC GAG GCA AGA GTT TC<br>Rev – TTC CCG AGG TCC ATC TAC TG       | 107                |
| COL1A1 (human)<br>NM_000088.3   | Fwd – CAG CCG CTT CAC CTA CAG C<br>Rev – TTT TGT ATT CAA TCA CTG TCT TGC C | 83                 |
| OCN (human)<br>NM_199173.4      | Fwd – GGC AGC GAG GTA GTG AAG AG<br>Rev – GAT CCG GGT AGG GGA CTG          | 73                 |
| Gapdh (mouse)<br>NM_001289726.1 | Fwd – GAC GGC CGC ATC TTC TTG TGC A<br>Rev – TGC AAA TGG CAG CCCTGG TGA C  | 114                |
| Hprt (mouse)<br>NM_013556.2     | Fwd – CGT GATTAGCGATGATGAACCAGGT<br>Rev – CCATCTCCTTCATGACATCTCGAGC        | 149                |
| E11 (mouse)<br>NM_010329.3      | Fwd – AAG ATG GCT TGC CAG TAG TCA<br>Rev – GGC GAG AAC CTT CCA GAA AT      | 118                |
| Runx2 (mouse)<br>NM_001146038.2 | Fwd – GAC GAG GCA AGA GTTTCA CC<br>Rev – GTCTGT GCC TTCTTG GTT CC          | 120                |
| Col1a1 (mouse)<br>NM_007742.3   | Fwd – ACT GCC CTC CTG ACG CAT GG<br>Rev – TCG CAC ACA GCC GTG CCATT        | 140                |
| OCN (mouse)<br>NM_007541.3      | Fwd – CCG CCTACAAACGCATCTAT<br>Rev – TTTTGGAGCTGCTGTGACAT                  | 153                |
| ALP (mouse)<br>NM_001287172.1   | Fwd – GCTGCCCTTGACCCCTCCA<br>Rev – ATCCGGAGGGCCACCTCCAC                    | 132                |
| SV40<br>YP_003708382.1          | Fwd – AGGGGGAGGTGTGGGAGGTTT<br>Rev – TCAGGCCCTCAGTCCTCAC                   | 100                |

included for all reactions. Thermocycling included 1 cycle of 95°C for 3 min, 40 cycles of 95°C for 20 s, 60°C for 40 s, 72°C for 20 s, and 1 cycle of 72°C for 10 min. Specificity of RT-qPCR was confirmed by melting curve analysis (Stratagene MX3000P) with complementary deoxyribonucleic acid (cDNA) standard curves of 90–110% efficiency and with an  $R^2$  value of  $\geq 0.99$  accepted as valid.

Relative quantification of messenger ribonucleic acid (mRNA) expression by RT-qPCR was calculated using the  $2^{-\Delta\Delta CT}$  method (53). In all cases, RT-qPCR was carried out using three reference

genes (RG), 18S rRNA, glyceraldehyde 3-phosphate dehydrogenase (GAPDH), and hypoxanthine–guanine phosphoribosyltransferase (HPRT1). The most stable RG was determined via NormFinder. Expression data for each gene in an experiment were transformed from  $\log_{10}$  to linear scale using a standard curve and then loaded into the NormFinder Microsoft Excel Add-In<sup>1</sup> (54). The most stable gene or combination of two genes, combined by calculating the geometric mean, was used for normalization and is clearly stated in the relevant figures. Target gene expression levels were expressed as relative expression units (REU), using the highest expresser within all samples as the calibrator sample.

## MECHANICAL LOADING

A 16-well loading plate (Figure 2A) was manufactured from solid silicone (Technovent TechSil 25)<sup>2</sup> so that the wells of the plate were of the same dimensions (10 mm diameter) as a standard Greiner (Stonehouse, UK) 48-well tissue culture plate but with a 150  $\mu$ m thick base. The spaces between the wells were filled with silicone and a series of holes were made on each side of the plate to accommodate hooks for attachment to a BOSE loading instrument. A Dantec Dynamics Digital Image Correlation (DIC) system was used to measure strain in the loading plate in order to calibrate the system. DIC compares two digital images of two different mechanical states of a particular object: a reference state and a deformed state. A previously applied speckle pattern (here applied using black face paint)<sup>3</sup> follows the strain of the object, and so the displacement that occurs between both reference and deformed state can be measured by matching the speckle pattern in small regions of the image (55, 56). By using two cameras (Limeess Messtechnik)<sup>4</sup> and matching speckle patterns in each image, the position and displacement in 3D can be obtained, after calibrating the system using a grid of known dimensions to determine the position of the cameras. DIC validated strains of 4000–4500  $\mu$ e in the majority of the wells of the loading plate when a force of 2.5 N was applied.

For mechanical loading the silicone plate was attached to a BOSE ElectroForce® 3200 (Kent, UK) loading instrument by a custom-made device (Figure 2B) in order to stretch the plate from one end causing cyclic compression in all wells. A 250 N load cell was used to apply a loading regime of 5 min, 10 Hz, 2.5 N to 3D osteocyte mono-cultures. Loading was controlled using WinTest® Software 4.1 with TuneIQ control optimization (BOSE).

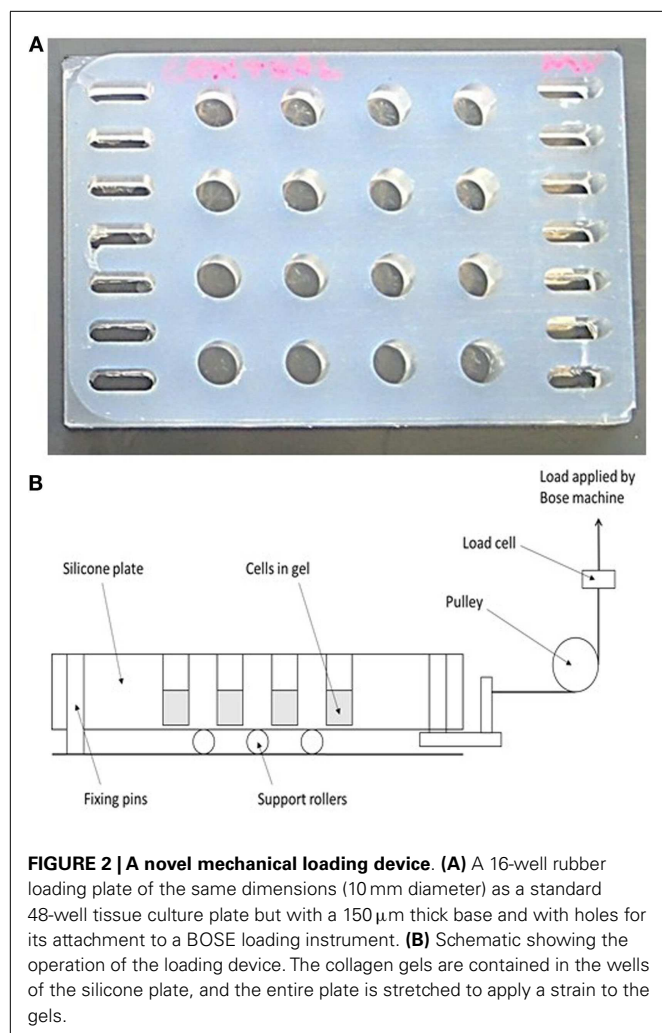
For loading, 3D osteocyte mono-cultures were prepared and cultured in the silicone plate in 800  $\mu$ l of DMEM GlutaMAX™ supplemented with 100 U/ml penicillin, 100  $\mu$ g/ml streptomycin, and 5% DFBS incubated at 37°C in 5% CO2/95% air atmosphere for 24, 48, or 72 h without changing culture medium prior to load, or 7 days where culture medium was changed every 2–3 days and prior to loading. 3D co-cultures were prepared and cultured in the silicone plate as described previously for plastic plates and cultured for 7 days prior to load, changing culture medium every 2–3 days and immediately prior to loading.

<sup>1</sup><http://www.mdl.dk/publicationsnormfinder.htm>

<sup>2</sup><http://www.technovent.com>

<sup>3</sup><http://www.snazaroo.co.uk>

<sup>4</sup><http://www.limeess.com>



Prostaglandin E<sub>2</sub> release was measured at 0, 0.5, 1, 3, 6, 12, and 24 h post-load using an Enzo Life Sciences PGE<sub>2</sub> kit (Exeter, UK) and following manufacturer's instructions. Experimental samples were diluted 1:64 (gels set up 24 h before loading), 1:16 (gels set up 48 and 72 h before loading), or 1:40 (gels set up 7 days before loading) in order to fit within the standard curve of the assay. All samples were within the standard curve range. The sensitivity of the assay is 8.26  $\mu\text{g}$  as stated by the manufacturer. Absorbance was recorded using a BMG Labtech FLUOstar Optima plate reader (Bucks, UK) and using the Optima Software for FLUOstar V2.00 R3 (BMG Labtech). PGE<sub>2</sub> concentration of the experimental samples was determined according to the standard curve. Data was normalized to total cell number by lysing cultures and performing LDH assay (CytoTox 96® Non-Radioactive Cytotoxicity Assay, Promega, Southampton, UK).

PINP (type I pro-collagen) synthesis was measured at day 1 and 5 post-load using a Rat/Mouse PINP Enzyme Immunoassay (EIA) kit (Immunodiagnostic systems, Tyne & Wear, UK) following the manufacturer's instructions. All samples were within the standard curve range. The sensitivity of the assay was 0.7 ng/ml as stated by the manufacturer. Data were normalized to total DNA content

(extracted using TRIzol® reagent and quantified after precipitation using a Quant-iT™ dsDNA High-Sensitivity Assay Kit, both following the manufacturer's instructions). The sensitivity of the DNA assay was 0.5 ng/ $\mu\text{l}$ .

## STATISTICS

Data are expressed as the mean  $\pm$  Standard Error of the Mean (SEM). Residuals were tested for normality (Anderson–Darling) and equal variance (Bartlett's and Levene's tests) and transformed if necessary, before applying analysis of variance (ANOVA) and *post hoc* Fisher's or Tukey's tests or General Linear Model (GLM) for crossed factors with pairwise comparisons where  $P < 0.05$  were recorded. Data were deemed to be significantly different when  $P < 0.05$ . 3D cultures prepared in individual wells within a plate, cultured for 1–12 days and loaded/treated were considered independent replicates. Group of independent replicates (3D cultures) prepared, cultured, and loaded/treated in separate plates on separate occasions were considered independent experiments.

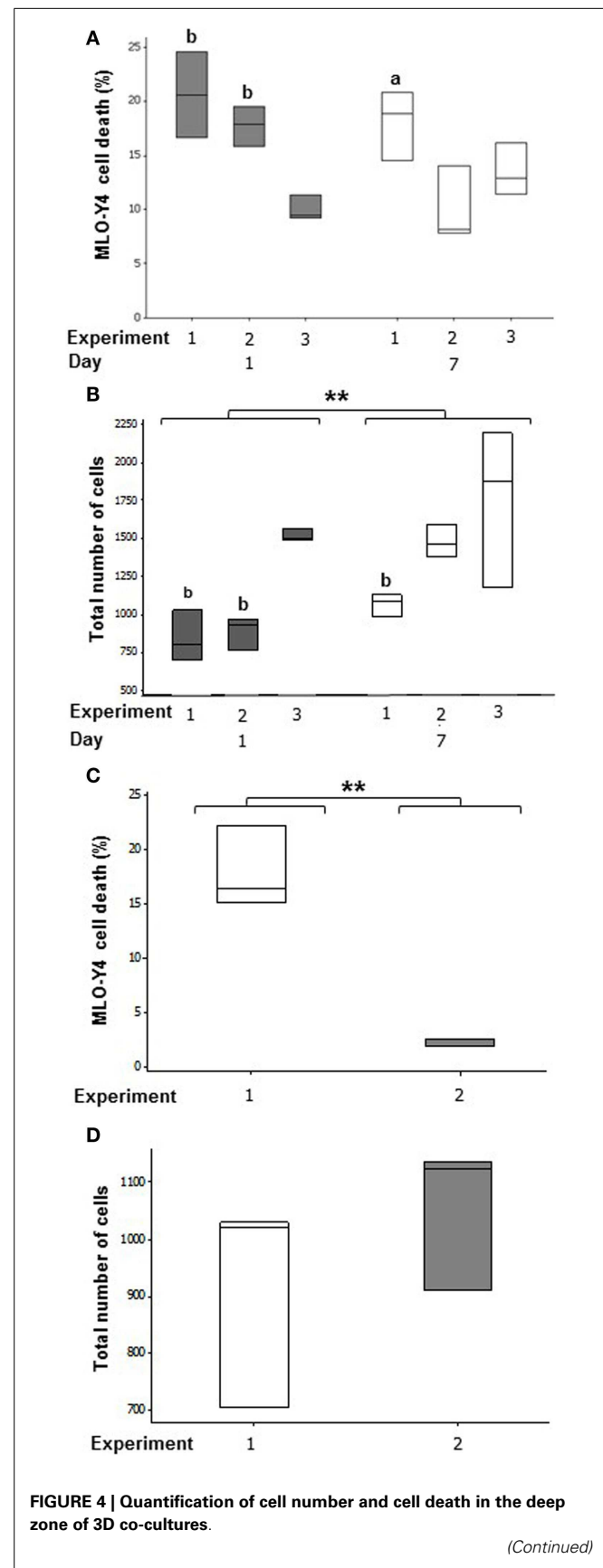
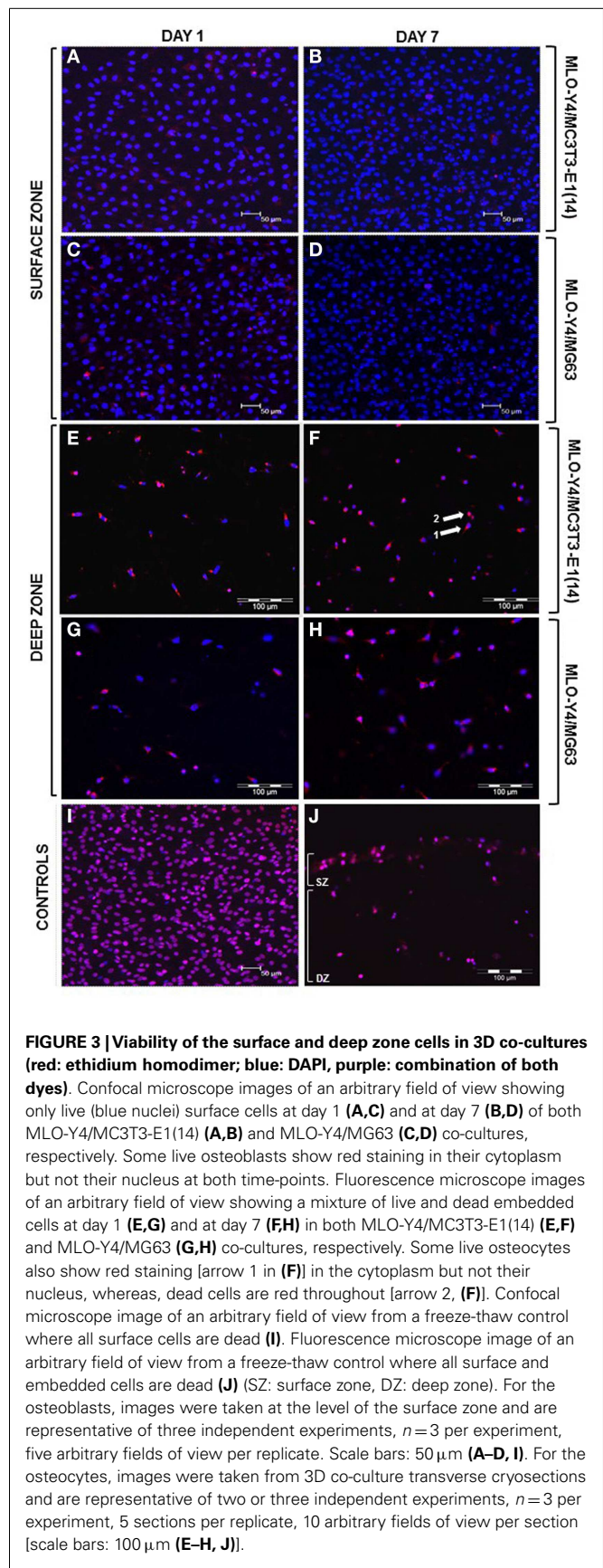
## RESULTS

### OSTEOCYTE AND OSTEOBLAST VIABILITY IN 3D CO-CULTURES

Confocal images of the surface zone across five arbitrary fields of view were taken for all replicates of both MLO-Y4/MC3T3-E1(14) (three independent experiments of  $n = 3$ ) or MLO-Y4/MG63 (two independent experiments of  $n = 3$ ) 3D co-cultures grown in plastic plates. At both day 1 and day 7, the viability of MC3T3-E1(14) (**Figures 3A,B**, respectively) or MG63 (**Figures 3C,D**, respectively) osteoblast-like cells was 100%. Freeze-thaw controls showed 100% death of the surface zone of the model (**Figure 3I**).

Ten arbitrary fields of view from five random transverse cryosections from all replicates were used for quantification of MLO-Y4 cell death as a proportion of total MLO-Y4 number in both MLO-Y4/MC3T3-E1(14) (three independent experiments of  $n = 3$ ) or MLO-Y4/MG63 (one independent experiment of  $n = 3$  for day 1; two independent experiments of  $n = 3$  for day 7) 3D co-cultures. At day 1 and day 7, a mixture of live and dead MLO-Y4 cells was observed for both MLO-Y4/MC3T3-E1(14) (**Figures 3E,F**, respectively) and MLO-Y4/MG63 (**Figures 3G,H**, respectively) co-cultures. Live osteocytes had a blue nucleus and dendritic morphology, whereas, a purple nucleus and rounded morphology was observed for dead osteocytes. Some live MLO-Y4 cells had red staining in their cytoplasm but not their nucleus (arrow 1, **Figure 3F**). Freeze-thaw controls showed 100% osteocyte death (**Figure 3J**).

In MLO-Y4/MC3T3-E1(14) co-cultures, an average of  $16.13 \pm 3.16\%$  osteocyte cell death was observed at day 1 and  $13.85 \pm 2.35\%$  at day 7 (**Figure 4A**). Mean MLO-Y4 cell death within 3D co-cultures did not differ between day 1 and day 7, however, MLO-Y4 cell death varied significantly between independent experiments (GLM,  $P = 0.002$ ) with a significant interaction between day and experiment (GLM,  $P = 0.018$ ). MLO-Y4 cell death at day 1 was significantly reduced in experiment 3 ( $10.04 \pm 1.14\%$ ) compared with experiment 1 ( $20.62 \pm 2.28\%$ ,  $P = 0.007$ ) and experiment 2 ( $17.32 \pm 1.43\%$ ,  $P = 0.004$ ) whereas, MLO-Y4 cell death at day 7 differed significantly between experiment 1 ( $18.08 \pm 1.86\%$ ) and experiment 2 ( $9.35 \pm 1.39\%$ ) ( $P = 0.041$ ).



(Continued)

**FIGURE 4 | Continued**

Boxplots of percentage cell death as a proportion of total number of cells at day 1 and day 7 in MLO-Y4/MC3T3-E1(14) (**A**) and MLO-Y4/MG63 (**C**) co-cultures. Boxplots showing total cell number counted for each replicate experiment at day 1 and day 7 in each independent experiment for MLO-Y4/MC3T3-E1(14) (**B**) and MLO-Y4/MG63 (**D**). For total cell number, significant differences obtained by GLM of  $\log_{10}$  data between day 1 and day 7 denoted by  $^{**}P < 0.01$ . Significant differences from pairwise comparisons, within each day, between independent experiments are shown by “a,” with respect to experiment 2; and “b,” with respect to experiment 3.

Total cell number increased between day 1 and day 7 (GLM,  $P = 0.003$  of  $\log_{10}$  data), and varied between replicate experiments (GLM,  $P < 0.001$  of  $\log_{10}$  data) in MLO-Y4/MC3T3-E1(14) co-cultures. At day 1, total cell number was 2-fold higher in experiment 3 when compared to experiment 1 (GLM,  $P = 0.009$  of  $\log_{10}$  data), and 1.5-fold higher when compared to experiment 2 (GLM,  $P = 0.019$  of  $\log_{10}$  data). At day 7, total cell number was 1.7-fold higher in experiment 3 when compared to experiment 1 (GLM,  $P = 0.049$  of  $\log_{10}$  data) (**Figure 4B**).

After 7 days of co-culture, the mean percentage of dead MLO-Y4 cells in MLO-Y4/MG63 co-cultures was  $9.98 \pm 3.66\%$  across both independent experiments. However, there was a significant difference observed between mean percentage death of experiments 1 ( $17.88 \pm 2.16\%$ ) and 2 ( $2.08 \pm 0.22\%$ ) (One-way ANOVA,  $P = 0.002$ ) (**Figure 4C**). There was no significant difference observed in total MLO-Y4 cell number at day 7 between experiments 1 and 2 in MLO-Y4/MG63 co-cultures (**Figure 4D**).

#### OSTEOCYTES AND OSTEOBLASTS ASSUME APPROPRIATE MORPHOLOGY IN CO-CULTURES

MLO-Y4 osteocyte-like cells embedded within a 3D type I collagen gel overlaid with either MC3T3-E1(14) or MG63 osteoblasts grown in plastic plates revealed a single osteoblast surface cell layer and dendritic MLO-Y4 cells embedded throughout the depth of the type I collagen gel (**Figure 5**).

In MLO-Y4/MC3T3-E1(14) co-cultures, MC3T3-E1(14) cells had a similar ovoid or pyriform morphology to those in monolayer cultures (**Figure 5A**). The MC3T3-E1(14) osteoblasts formed a thin pavement-like single cell layer on top of the 3D co-cultures, which were difficult to image under the inverse light microscope (**Figure 5B**). However, actin filament labeling (**Figure 5C**) revealed MC3T3-E1(14) osteoblast morphology more clearly, with stress-fibers throughout their cell bodies. With similar morphology to MG63 monolayer cultures (**Figure 5D**), MG63 cells formed a pavement-like single cell layer in MLO-Y4/MG63 co-cultures under both light microscopy (**Figure 5E**) and immunofluorescence, when filamentous actin was labeled (**Figure 5F**). MLO-Y4 dendritic morphology observed in monolayer cultures (**Figure 5G**) was similar in co-cultures (**Figure 5H**), although projections extended in three dimensions. Contacts between neighboring osteocytes were revealed by actin filament staining (**Figure 5I**).

#### OSTEOCYTES AND OSTEOBLASTS DISPLAY APPROPRIATE PHENOTYPE IN 3D CO-CULTURES

mRNA expression was assessed in both surface and deep zones of day 7 MLO-Y4/MC3T3-E1(14) 3D collagen co-cultures grown in

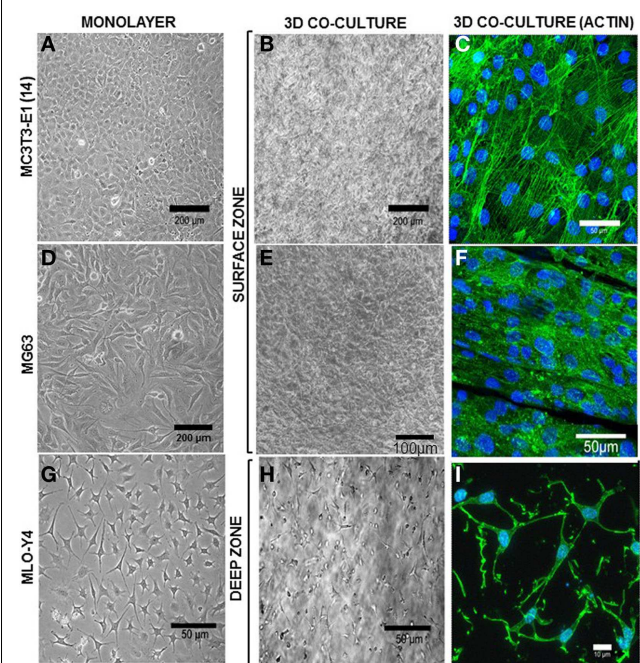


**FIGURE 5 | Morphology of surface and deep zone cells in 3D co-cultures.** Inverse light microscope images of MC3T3-E1(14) (**A**), MG63 (**D**), and MLO-Y4 (**G**) cells in monolayer. MC3T3-E1(14) and MG63 osteoblast-like cells present typical osteoblastic morphologies, mainly ovoid or pyriform, and MLO-Y4 osteocyte-like cells have a typical dendritic morphology. Inverse light microscope images taken from the surface zone (**B,E**) of the 3D model where a confluent monolayer of surface cells is observed, and halfway through the depth of a 3D co-culture (**H**) showing embedded cells with a similar dendritic morphology to that seen in MLO-Y4 monolayer cultures. Confocal microscope focusing directly onto the surface zone of a 3D co-culture at day 7 (**C,F**), where surface cells were stained to reveal actin filaments (Phalloidin-Atto488) and cell nuclei (DAPI). The image shows a pavement-like monolayer, with individual cells containing well-developed stress-fibers, and maintaining an osteoblastic morphology. Confocal microscope image stack of a 3D co-culture transverse cryosection at day 7 (**I**) where embedded cells were stained to reveal actin filaments (Phalloidin-Atto488) and cell nuclei (DAPI), showing a dendritic morphology and connections between neighboring cells. Images are arbitrary fields of view representative of three independent experiments,  $n = 3$  per experiment.

plastic plates by relative RT-qPCR using primers against osteoblast and osteocyte phenotypic markers. Data were expressed in REU and normalized to *Gapdh*, which was ranked as the most stable reference gene (NormFinder stability value = 0.398, intergroup variation = 0.376, and intragroup variation = 0.012). Data were analyzed from three independent experiments, each with three replicates for the surface zone, and four replicates for the deep zone, for all genes except *Colla1* (two independent experiments).

In MLO-Y4/MC3T3-E1(14) co-cultures, no significant difference in expression was detected between zones of the model for E11 (surface zone,  $0.264 \pm 0.072$  REU; deep zone,  $0.361 \pm 0.087$  REU) (**Figure 6A**), OCN (surface zone,  $0.212 \pm 0.076$  REU; deep zone,  $0.269 \pm 0.080$  REU) (**Figure 6B**), and Runx2 (surface zone,  $0.275 \pm 0.083$  REU; deep zone,  $0.157 \pm 0.025$ ) (**Figure 6C**). However, the surface zone of the model showed 6-fold increases in

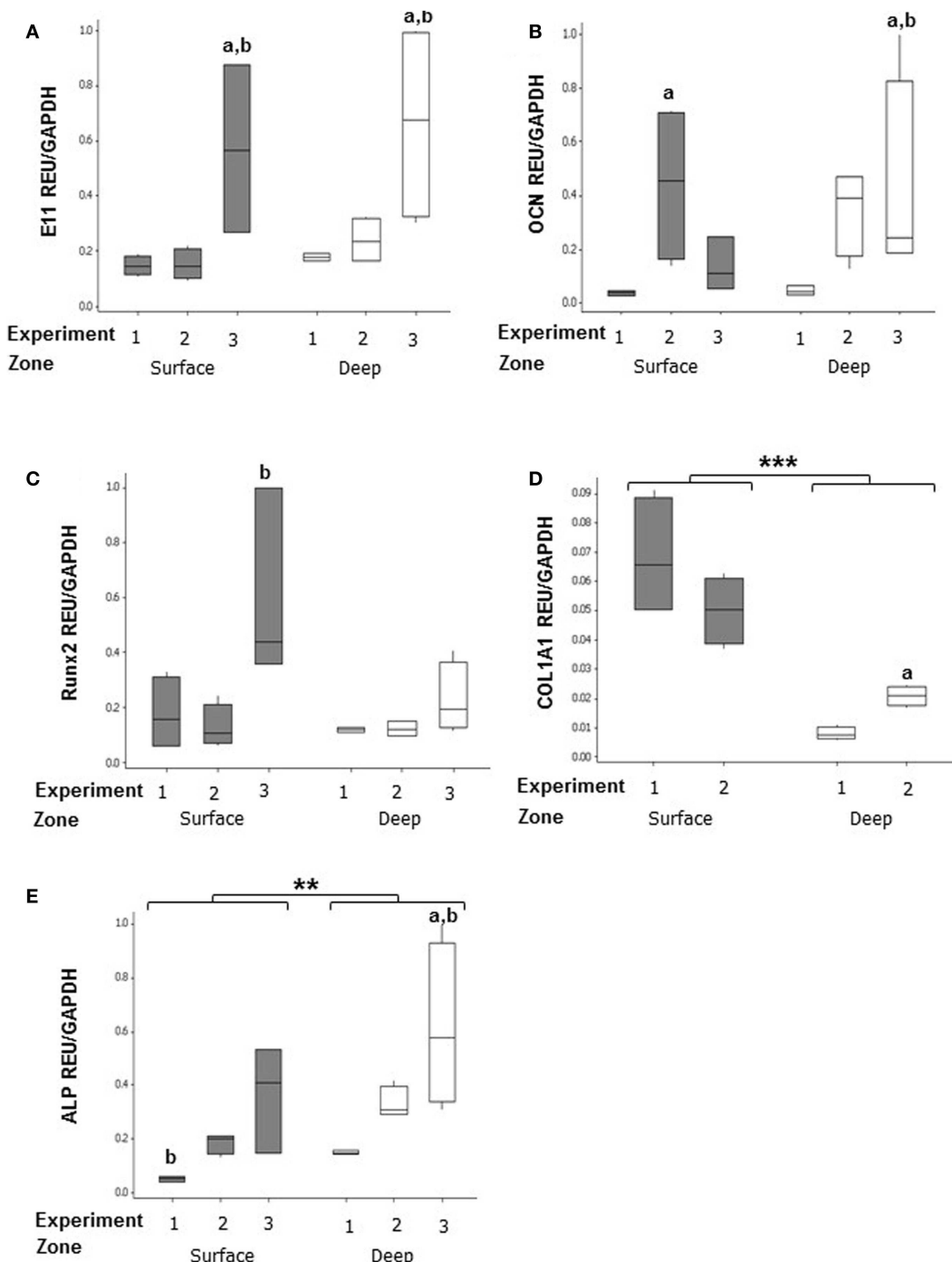


**FIGURE 6 | Gene expression of cellular markers in surface and deep zone cells in MLO-Y4/MC3T3-E1(14) 3D co-cultures.** Quantification of gene expression in the 3D co-culture after 7 days by relative RT-qPCR, boxplots of E11 (A), OCN (B), RUNX2 (C), *Col1a1* (D), and ALP (E) expressed as REU and normalized to *Gapdh* expression. Significant differences obtained by GLM of  $\log_{10}$  data (E11, *Col1a1*, and OCN) or ranked data (ALP and Runx2) between

surface and deep zones denoted by  $**P < 0.01$ ,  $***P < 0.0001$ . Significant differences from pairwise comparisons, within each zone, between independent experiments denoted by “a,” with respect to experiment 2; and “b,” with respect to experiment 3. Values derived from two (*Col1a1*) or three (all others) independent experiments,  $n = 3$  for surface and four for deep zones.

expression of *Col1a1* compared to the deep zone ( $0.168 \pm 0.085$  vs.  $0.028 \pm 0.007$  REU, GLM,  $P < 0.001$  of  $\log_{10}$  data) (Figure 6D). In contrast, the deep zone of the 3D co-culture showed

2-fold increases in ALP expression over the surface zone ( $0.366 \pm 0.075$  vs.  $0.185 \pm 0.047$  REU, GLM,  $P = 0.001$  of ranked data) (Figure 6E). Whilst REU of all genes varied significantly

between replicate experiments (GLM, E11, OCN, and *Colla1*,  $P < 0.001$  of  $\log_{10}$  data; Runx2  $P = 0.013$  of ranked data; ALP  $P < 0.001$  of ranked data;  $P < 0.05$  for all pairwise comparisons) the trend in terms of surface compared with deep REUs within each experiment was consistent. Consistent with this, RT-PCR of MLO-Y4/MG63 co-cultures, revealed surface osteoblasts and embedded osteocytes expressed E11, OCN, Runx2, and *COL1A1* mRNA (data not shown, three independent experiments of  $n = 3$  for both surface and deep zones). Quantification of mRNA expression could not be compared between surface MG63 and embedded MLO-Y4 cells as the respective human and mouse cDNA sequences are not sufficiently homologous to use the same primers.

Osteoblasts and osteocytes in MLO-Y4/MC3T3-E1(14) co-cultures showed strong, uniform immunolabelling for the dendrity marker E11 (Figures 7A,B). Intense E11 immunolabelling was also observed in embedded MLO-Y4 cells within the MLO-Y4/MG63 co-cultures, but not in surface MG63 cells (Figures 7C,D). In both 3D co-culture systems abundant CX43 immunostaining was observed in the cell membrane and cytoplasm of osteoblasts and in osteocytes along their processes, as well as within the cytoplasm, around the nucleus (Figures 7E–G) and in contacts between cells (Figures 7F inset; 7H). Immunohistochemistry images are representative of day 7, 3D co-cultures from three independent experiments where  $n = 3$  [MLO-Y4/MC3T3-E1(14)], or two independent experiments where  $n = 3$  (MLO-Y4/MG63). Four to six cryosections from all replicates were observed. PBST and IgG controls were negative.

### CELL MIGRATION IN CO-CULTURES

To detect whether MLO-Y4 cells moved to the surface zone, expression of the SV40 large T-antigen (only expressed by MLO-Y4 cells) was determined in MLO-Y4/MC3T3-E1(14) co-cultures grown in plastic plates (Figure 8). Whilst low levels of SV40 large T-antigen mRNA expression were detected in the surface zone (Figure 8A), SV40 large T-antigen immunolabelling was completely absent from the surface zone of the model (Figure 8B).

Osteoblast migration from surface to deep zone could be tracked in MLO-Y4/MG63 co-cultures, using a type I pro-collagen antibody that only detects human (i.e., MG63-derived) pro-collagen and not that expressed by mouse. Immunolocalization revealed that MG63 cells synthesizing human type I pro-collagen, whilst abundant in the upper layer of cells were also occasionally observed in cells up to 100  $\mu\text{m}$  beneath the surface zone (Figure 8C).

### BMP-2 TREATMENT REGULATES MG63 EXPRESSION OF TYPE I COLLAGEN IN CO-CULTURES

In order to determine whether osteoblasts in co-cultures could respond to an osteogenic signal, we stimulated the MLO-Y4/MG63 co-cultures grown in plastic plates with BMP-2 (Figure 9). We used the mouse/human model so that we could discriminate between MLO-Y4-derived and MG63-derived type I collagen expression. BMP-2 treatment significantly increased MG63 *COL1A1* mRNA expression at day 5 compared to day 1 (Figure 9A) (GLM of  $\log_{10}$  data,  $P = 0.03$ , two independent experiments of  $n = 3$ ). However, BMP-2 treatment had no effect on MLO-Y4 *Colla1* (Figure 9B),

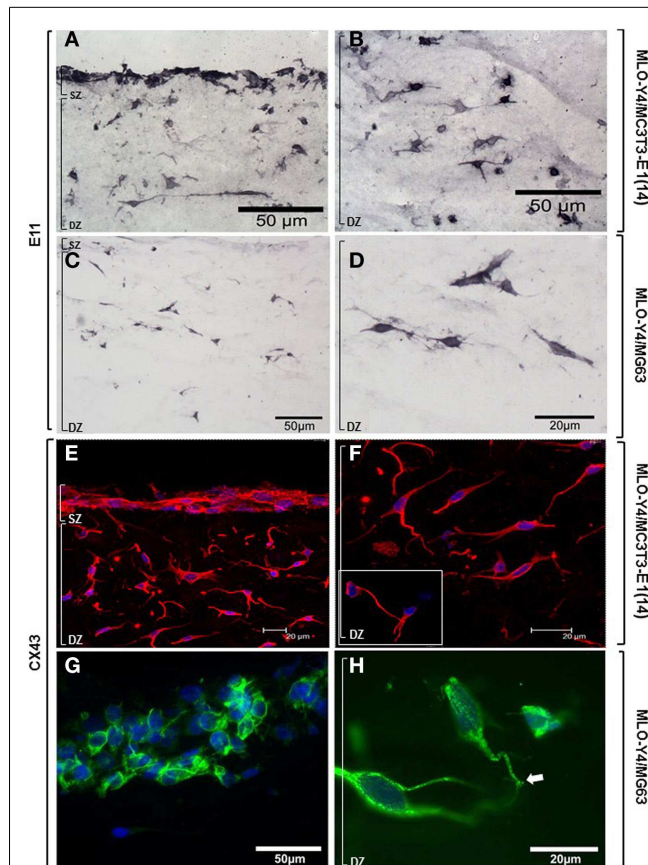


**FIGURE 7 | Protein expression of cellular markers in surface (SZ) and deep (DZ) zone cells of the 3D co-culture systems.** Brightfield photomicrographs showing immunostaining for the dendrity marker E11 in both surface and embedded cells (A) and showing E11 immunostaining in the osteocytes highlighting their morphology (B), in MLO-Y4/MC3T3-E1(14) 3D co-cultures. Light microscope images revealing immunostaining for the dendrity marker E11 in embedded cells (C,D) but not in surface cells (C), in MLO-Y4/MG63 co-cultures. Confocal microscope images showing CX43 (Dylight594) immunolabelling and cell nuclei stain (DAPI) in surface and deep zone cells (E) of MLO-Y4/MC3T3-E1(14) co-cultures. Image reveals abundant quantities of CX43 present in the cytoplasm and cell membranes of both cell types, around the nucleus of the embedded cells (F), and connections between neighboring cells [(F), inset] (inset scale bar: 10  $\mu\text{m}$ ). Fluorescent photomicrographs of surface (G) and deep (H) zone cells of MLO-Y4/MG63 co-cultures labeled for CX43 (green) and counterstained with DAPI (blue) reveals that the surface cell layer, in this case several cells thick, intensely labels for CX43 along cell–cell interfaces (G). High magnification of embedded cells within the same co-culture gel reveals extensive punctate labeling within the cytoplasm and at the cell surface, including at interfaces between cell processes (arrow) (H). Images are arbitrary fields of view taken from 3D co-culture transverse cryosections representative of two or three independent experiments,  $n = 3$  per experiment. In all cases, controls performed by omitting or substituting the primary antibody, showed no labeling.

MG63 or MLO-Y4 OCN (Figures 9C,D), and E11 (Figures 9E,F) mRNA expression.

Immunolabelling with monoclonal antibody M38 that recognizes the C-terminus of human type I pro-collagen (an epitope not present in the collagen used to make the gel) revealed that

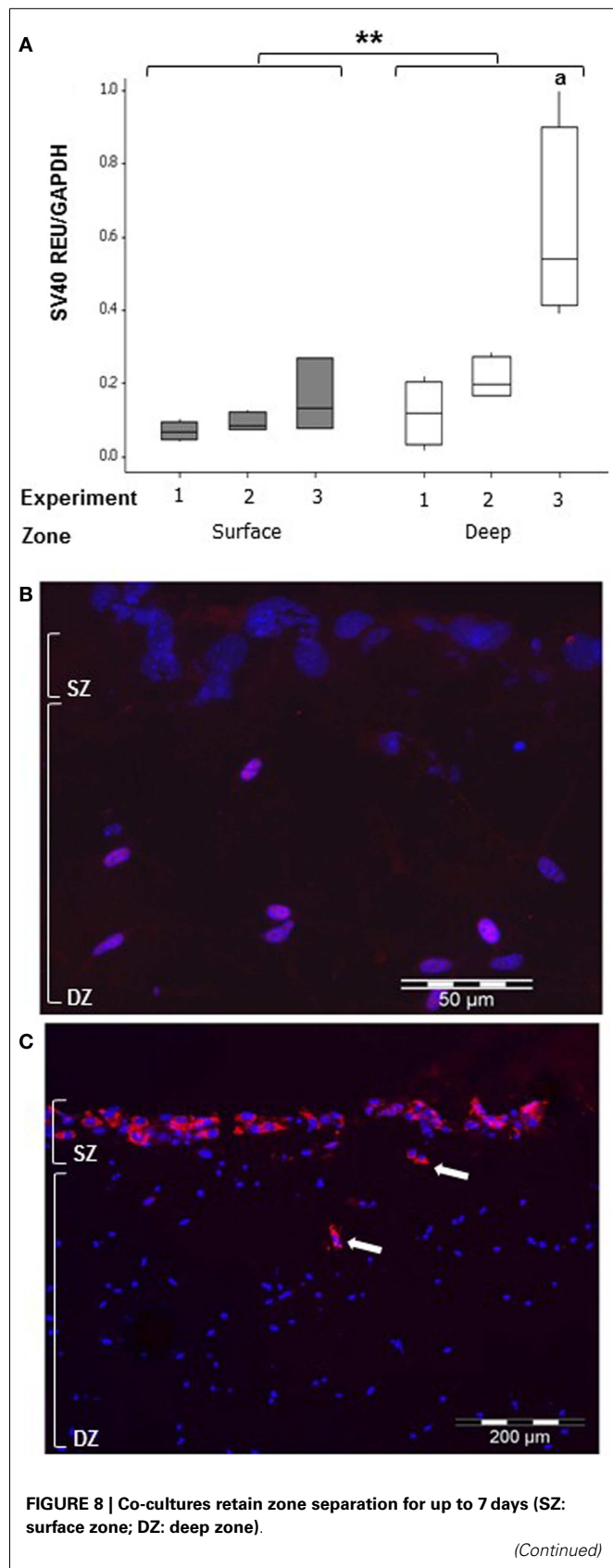


#### FIGURE 8 | Continued

Boxplot showing quantification of SV40 large T-antigen gene expression in the MLO-Y4/MC3T3-E1(14) co-culture after 7 days by relative RT-qPCR (A) expressed as REU and normalized to *Gapdh* expression. Significant differences obtained by GLM of  $\log_{10}$  data between surface and deep zones denoted by  $**P < 0.01$ . Significant differences from pairwise comparisons, within each zone, between independent experiments denoted by "a" with respect to experiment 1 (three independent experiments,  $n = 3$  for surface and 4 for deep zones). Fluorescent photomicrograph of transverse cryosection from day 7 MLO-Y4/MC3T3-E1(14) co-culture shows immunolabelling for SV40 large T-antigen (red) and cell nuclei stain (blue) in osteocytes only, represented by the purple color (red and blue co-localization) (B). However, no SV40 large T-antigen immunostaining in the osteoblasts was present (three independent experiments,  $n = 3$ ). SZ, surface zone; DZ, deep zone. Fluorescent photomicrograph of transverse cryosection from BMP-2 treated MLO-Y4/MG63 co-cultures at day 5 (C) revealed presence of type I pro-collagen in the upper layer of cells and in cells up to 100  $\mu\text{m}$  beneath the surface, which are all MG63 cells since M38 antibody does not recognize mouse type I pro-collagen (two independent experiments,  $n = 3$ ).

type I pro-collagen is abundant in surface MG63 cells after 5 days BMP-2 treatment (Figures 10A,B).

#### EMBEDDED MLO-Y4 CELLS RELEASE PGE<sub>2</sub> IN RESPONSE TO MECHANICAL LOADING

A pilot experiment to determine whether mechanical loading induced PGE<sub>2</sub> release in MLO-Y4 cells in 3D gels in the silicone plate, revealed that load (5 min, 10 Hz, 2.5 N) increased PGE<sub>2</sub> release between 0.5 and 24 h. Mean PGE<sub>2</sub> release was increased approximately 4-fold at 0.5 h post-load (control  $1206.55 \pm 37.32$  pg/ml; loaded  $4632.91 \pm 1773.78$  pg/ml;  $n = 2$  at each time) (Figure 11A).

To determine whether load-induced PGE<sub>2</sub> release was affected by MLO-Y4 culture time in 3D gels prior to loading, MLO-Y4 cells were pre-cultured in gels for 24, 48, or 72 h and PGE<sub>2</sub> measured 0.5 h after loading as before. After normalizing to cell number, PGE<sub>2</sub> was not detectable in loaded or control 3D MLO-Y4 mono-cultures pre-cultured for 24 h, whereas mean PGE<sub>2</sub> was increased in loaded osteocytes pre-cultured for 48 h and for 72 h compared with their respective unloaded controls (Figure 11B,  $n = 3$  per pre-culture time). When MLO-Y4 cells were pre-cultured for 7 days prior to mechanical loading, mean PGE<sub>2</sub> release, normalized to cell number, was also increased 0.5 h post-load [control  $1195.40 \pm 109.72$  pg/ml/OD<sub>492</sub> nm, loaded  $3152.26 \pm 435.20$  pg/ml/OD<sub>492</sub> nm;  $n = 2$  or 3 (Figure 11C)].

To determine whether mechanical loading could induce type I pro-collagen synthesis a pilot experiment assessed PINP synthesis 1 and 5 days post-load. This was carried out in 3D MLO-Y4/MC3T3-E1(14) co-cultures grown in the silicone plate pre-cultured for 7 days prior to load. Our preliminary findings reveal mean PINP release was increased in loaded 3D co-cultures when compared to control cultures at day 1 or 5 (Figure 11D,  $n = 2$  control and loaded).

#### DISCUSSION

This paper describes methodology for a novel *in vitro* 3D osteocyte–osteoblast co-culture model, which can be used to assess

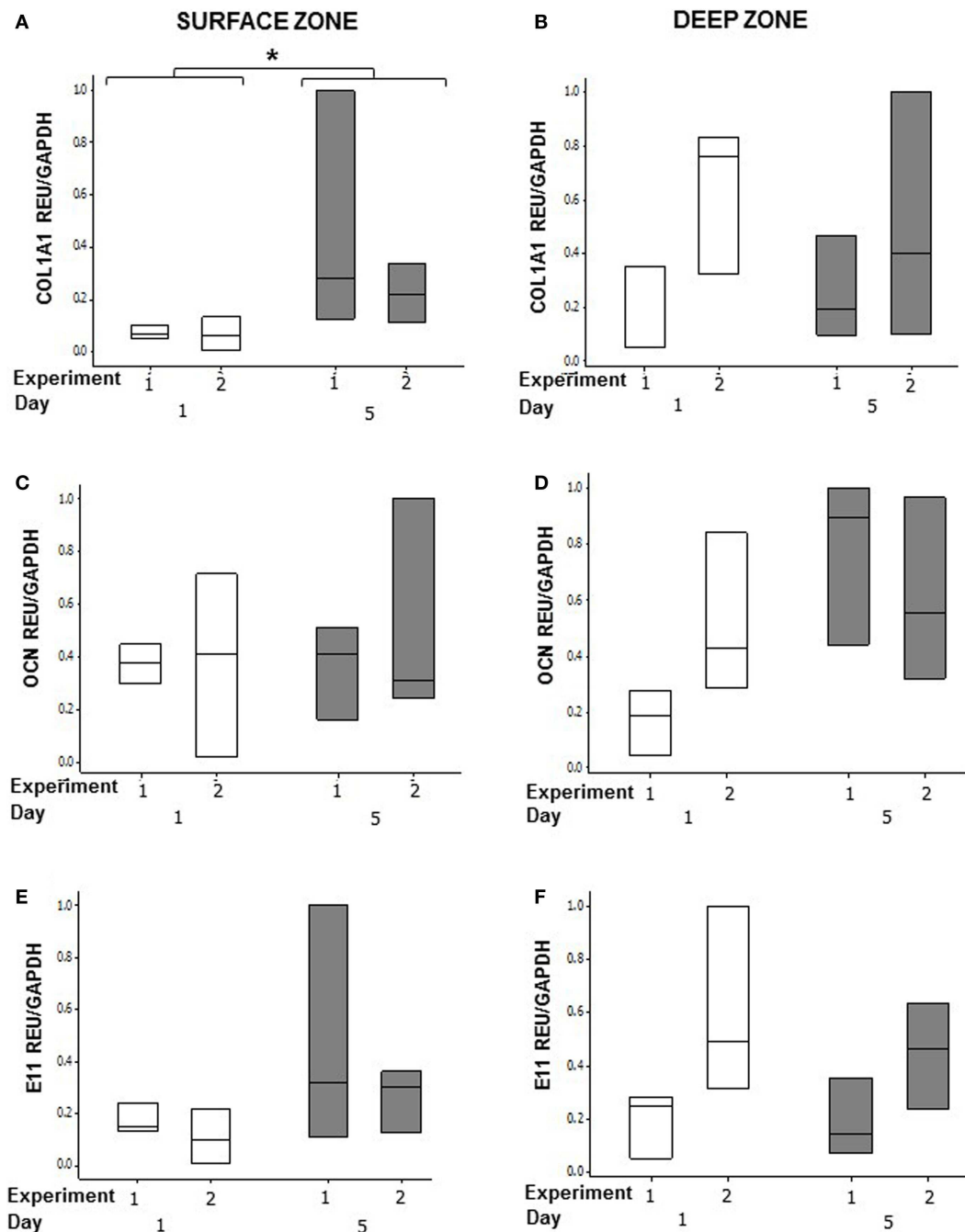


**FIGURE 9 | Effects of BMP-2 treatment on osteoblast and osteocyte phenotype in MLO-Y4/MG63 3D co-cultures.** Quantification of gene expression in surface and deep zone cells of 3D co-cultures at day 1 and 5 after BMP-2 treatment by relative RT-qPCR, boxplots of COL1A1 (A,B), OCN

(C,D), and E11 (E,F) expressed as REU and normalized to GAPDH expression. Significant differences obtained by GLM of  $\log_{10}$  data denoted by \* $P < 0.05$ . Data are from two independent experiments of  $n=3$  for surface and deep zones.

how osteocytes regulate osteoblasts in response to mechanical load. The model has been morphologically and phenotypically characterized, and methodology optimized based on responses to mechanical load. The model is a two-phase culture system where osteocytes are embedded within collagen gels and cultured overnight before osteoblasts were added to the surface of

the gel. In this model, cells were viable, expressed appropriate phenotypic markers and contacted neighboring cells. A 16-well silicone plate was developed to enable application of physiological and osteogenic forces within each gel. Our preliminary findings indicate that these 3D cultures increase PGE<sub>2</sub> synthesis and PINP release in response to mechanical loading.

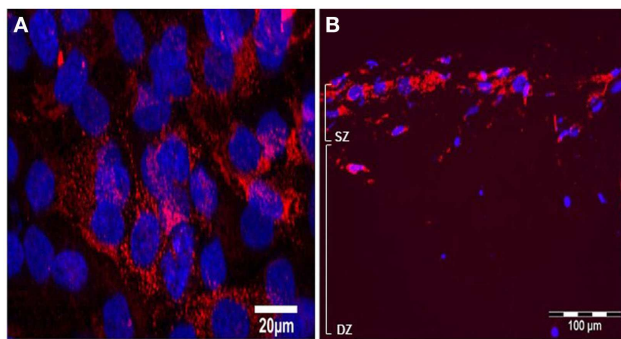


**FIGURE 10 | Effects of BMP-2 treatment on type I pro-collagen synthesis in co-cultures of MLO-Y4 and MG63 cells (type I pro-collagen: red; DAPI: blue).** Confocal microscope image of the surface cells from an untreated 3D co-culture revealed presence of particulate type I pro-collagen in all surface cells (**A**). Fluorescence microscope images of transverse cryosections from BMP-2 treated 3D co-cultures at day 5 (**B**) revealed presence of type I pro-collagen in the upper layer of cells and in cells up to 100  $\mu$ m beneath the surface, which are all MG63 cells since M38 antibody does not recognize mouse type I pro-collagen.

#### OSTEOCYTE AND OSTEOPHYTE VIABILITY IN 3D CO-CULTURES

In the 3D co-cultures, both MC3T3-E1(14) and MG63 surface osteoblasts were 100% viable. It is likely that osteoblasts on the surface of the co-culture behave like a monolayer of cells, with dead osteoblasts detaching from the top of the collagen gel and being replaced by new osteoblasts to maintain the single cell layer.

In the 3D co-cultures, embedded osteocytes displayed 16% death after 1 day of culture [MLO-Y4/MC3T3-E1(14)] and 10–14% death at day 7 (both co-culture systems). Osteocyte death is common in normal human bone (57) and increases from <1% at birth up to 75% by 80 years old (58–60). If there is a linear relationship between age and osteocyte death, 20% osteocyte death would occur in humans in their early 20s, consistent with osteocyte viability observed in both 3D models. Cells undergoing cell death are usually destroyed by neighboring or phagocytic cells (61), but dead osteocytes, embedded within a mineralized matrix are inaccessible, and can be detected within their lacunae *in vivo* (62, 63). In the 3D co-culture a similar percentage osteocyte cell death was observed at day 1 and day 7, which may reflect dead osteocyte retention within the matrix, but this remains to be determined.

#### OSTEOCYTE AND OSTEOPHYTE MORPHOLOGY IN 3D CO-CULTURES

In the 3D co-culture model, both MC3T3-E1(14) and MG63 cells displayed a range of osteoblastic, ovoid, and pyriform morphologies, when maintained for 7 days. They formed a pavement-like monolayer on top of the 3D culture with well-defined stress-fibers. Whilst both MC3T3-E1(14) (64) and MG63 (65) monolayer cultures show fibroblastic morphology during logarithmic growth *in vitro*, they assume a pyriform shape with prominent stress-fibers across their cell bodies when confluent (39, 64). *In vivo*, osteoblasts can be ovoid, rectangular, columnar, cuboidal, or pyriform (66). Osteoblasts form a pavement-like or “overlapping roof tiles” monolayer on the bone surface [Bidder, 1906 as cited in Bourne (66) and Sudo et al. (64)] overlaying osteocytes within the

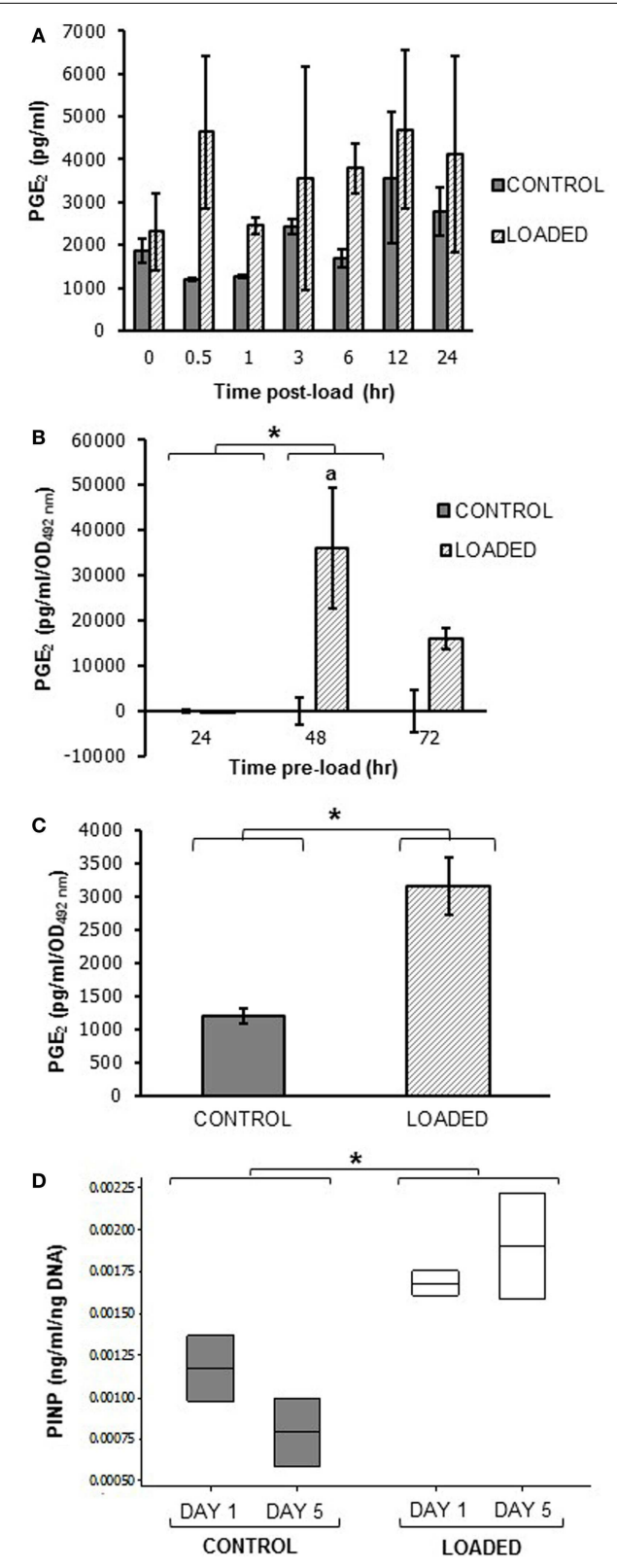


**FIGURE 11 | Prostaglandin E<sub>2</sub> and PINP release in mechanically loaded (5 min, 10 Hz, 2.5 N) 3D cultures by ELISA.**

(Continued)

**FIGURE 11 | Continued**

Graphs showing PGE<sub>2</sub> release from 3D osteocyte mono-cultures in a pilot experiment of 24 h cultures (**A**), categorized by time of culture (**B**), and 7 days cultures (**C**) at 0.5 h post-load unless other time-points are indicated. Data were normalized to the absorbance (OD<sub>492</sub> nm) of LDH lysates (cell number) (**B,C**). (**D**) Boxplot of PINP release from control and loaded MLO-Y4/MC3T3-E1(14) 3D co-cultures cultures at day 1 and day 5 post-load, normalized to total DNA. \**P* < 0.05 as obtained by GLM, GLM of ranked data (**B**) or one-way ANOVA (**C,D**). Significant differences as obtained by GLM pairwise comparisons denoted by “a” with respect to 24 h loaded cultures (**B**). Data presented are from (**A**) one independent experiment, *n* = 2 or 3; (**B**) one (48–72 h cultures) or two (24 h cultures) independent experiments, *n* = 3; (**C,D**) one independent experiment, *n* = 2 or 3.

bone matrix [Gegenbaur, 1864 as cited in Bourne (66)]. Osteoblast position is essential for osteocyte–osteoblast interactions, which ultimately regulate bone matrix formation (36, 67–69). Osteoblast morphology in the 3D co-culture is thus consistent with *in vitro* and *in vivo* observations.

In the 3D co-culture model, MLO-Y4 cells maintain their osteocytic morphology throughout all gel depths for 7 days, with cell projections from adjacent cells in contact. *In vivo*, osteocytes present a dendritic morphology that allows communication with neighboring osteocytes. This forms an extensive network known as the LCS (12, 70–73), which permits metabolic traffic and exchange within the mineralized environment of the bone matrix. *In vitro*, monolayer cultures of MLO-Y4 cells display a 2D dendritic morphology, which becomes 3D in collagen gel cultures (34, 39). Furthermore, IDG-SW3 cells also display dendritic morphology in 3D gels (35). The osteocyte morphology in the 3D co-cultures is consistent with both *in vivo* and *in vitro* observations, with morphological characteristics indicative of a 3D network throughout the co-culture.

**OSTEOCYTE AND OSTEOBLAST PHENOTYPE IN 3D CO-CULTURES**

In 3D co-cultures, MC3T3-E1(14) cells expressed E11 mRNA and protein and MG63 cells expressed E11 mRNA (antibody does not recognize human E11). E11 has been detected in mature osteoblasts and osteoblasts undergoing bone matrix synthesis (74–78). The E11 expression detected in the surface zone of the model suggests that osteoblasts may be sending out projections to connect with neighboring osteoblasts and/or embedded osteocytes. Previous studies have shown that osteoblasts have cytoplasmic processes connecting them to neighboring cells [Spuler, 1899 as cited in Bourne (66), Wetterwald et al. (75), and Schulze et al. (79)], with prominent stress-fibers that stretch across their cell bodies into small cytoplasmic processes (39).

OCN, Runx2, and *Col1a1* were also expressed in MC3T3-E1(14) and MG63 cells when in 3D co-cultures, consistent with *in vivo* and *in vitro* studies (51, 80–84). ALP mRNA expression was also found in MC3T3-E1(14) cells in 3D co-cultures consistent with previous reports (51, 80, 81, 84–86). CX43 protein expression was observed throughout osteoblast cytoplasm and cell membrane in both MC3T3-E1(14) and MG63 cells in 3D co-cultures, suggesting that the surface osteoblasts have the potential to connect to neighboring cells. Osteoblasts have been shown to express the gap junction CX43 protein (36, 87, 88), which is important in

responses to mechanical loading (21) and skeletal function (68, 89, 90).

In 3D co-cultures MLO-Y4 cells expressed mRNA and protein for the early osteocyte marker E11 (75–77, 79) consistent with previous data (75–77). OCN, Runx2, *Col1a1*, and ALP mRNAs were also detected in these cells in co-cultures. Osteocytes have been previously shown to express OCN, *Col1a1*, and ALP *in vivo* and *in vitro* (34, 91) and Runx2 *in vitro* (92).

Confocal imaging of osteocytes in 3D co-cultures showed the presence of CX43 throughout the cytoplasm, osteocytic processes, and around the nucleus. Osteocytes express CX43 both *in vivo* and *in vitro* (34, 36, 93, 94), which allows the formation of the LCS within the bone matrix, and connects osteocytes to surface osteoblasts (36, 95). CX43 gap junctions in osteocytes contribute to bone remodeling and formation (96) and they are also mediate load-induced PGE<sub>2</sub> release in osteocytes (97). The expression of CX43 indicates that osteocytes within the 3D co-culture are potentially able to form a network similar to the LCS, as well as connect to the osteoblasts on the surface.

In 3D co-cultures, MC3T3-E1(14) cells showed a significantly higher expression of *Col1a1* mRNA compared to the deep zone of the model. Interestingly, deep zone cells within the 3D co-cultures expressed significantly higher levels of ALP compared to the surface zone of the model. This suggests that under appropriate conditions the MLO-Y4 cells within the 3D model may contribute to mineralization the collagen matrix within which they are embedded, as previously seen in embedded IDG-SW3 cells (35).

**TESTING OSTEOGENIC RESPONSES IN THE 3D CO-CULTURE MODEL**

Pilot experiments were performed to see whether the co-culture methodology could reveal an osteogenic response. This was tested firstly by treatment with BMP-2 and secondly by testing responses to mechanical loading.

In the MLO-Y4/MG63 co-culture, osteoblasts were able to respond to BMP-2, by significantly increasing their *COL1A1* mRNA expression and showing abundant type I pro-collagen protein expression after 5 days of BMP-2 treatment. These data are consistent with previous *in vitro* studies, which showed that BMP-2 stimulates collagen synthesis in MC3T3-E1 cells (85).

To determine whether the osteocytes within the co-culture model responded to loading, we cultured MLO-Y4 in 3D collagen gels, without surface osteoblasts, and measured PGE<sub>2</sub> release in response to loading. To facilitate loading of the 3D model, a 16-well silicone plate was developed that applied uniform strain within each gel. The loading regime applied (5 min, 10 Hz, 2.5 N) was based on previous publications showing that 10 min of 10 Hz, 4000–4500  $\mu$ e loading is physiological and osteogenic *in vivo* (91, 98, 99). In 3D osteocyte mono-cultures, loading induced PGE<sub>2</sub> release over 24 h with maximum PGE<sub>2</sub> release occurred after 0.5 h. In osteocytes pre-cultured in 3D collagen gels for 48, 72 h, or 7 days, mechanical loading increased PGE<sub>2</sub> release 0.5 h post-load. No PGE<sub>2</sub> release occurred in osteocytes pre-cultured in 3D gels for 24 h. This suggests that the osteocytes may require at least 48 h in 3D collagen gels to develop an osteocytic phenotype, form dendrites and the CX43 gap junctions that are involved in the release of PGE<sub>2</sub> from osteocytes *in vitro* (100, 101). Others have shown that mechanically loaded osteocytes in monolayer increase

PGE<sub>2</sub> release (24, 93, 102, 103), as early as 0.5 h post-load (93) but no previous studies have investigated osteocyte response to load in 3D.

To determine whether mechanical loading in 3D co-cultures could elicit an osteogenic response, co-cultures were mechanically loaded as before and type I collagen synthesis quantified. In 3D co-cultures, mechanical loading increased PINP release, suggesting that mechanical stimuli of 3D co-cultures elicit an osteogenic response. PINP synthesis was measured from whole 3D co-cultures, therefore, PINP synthesis may not only be from surface osteoblasts, but also from embedded osteocytes. Both osteoblasts and osteocytes produce type I collagen *in vitro* (34, 104) although MLO-Y4 cells express reduced *Col1a1* mRNA compared to osteoblasts both in monolayer (34) and here in 3D co-cultures.

Our preliminary data showing that both BMP-2 and mechanical loading can induce type I collagen synthesis, reveals the potential for the new 3D co-culture and loading methodology described in this paper in investigating osteogenic responses regulated by osteocytes.

## LIMITATIONS OF THE 3D CO-CULTURE MODEL

### **Cell migration in co-cultures**

The 3D co-culture method is subject to the possibility of cross-contamination of RNA between surface osteoblasts and embedded osteocytes, due to the extraction protocol, or mixing of cell types between zones due to osteoblast and/or osteocyte migration. We used expression of the SV40 large T-antigen, exclusive to MLO-Y4 cells [derived from mice expressing the SV40 large T-antigen oncogene under the control of the OCN promoter (34)], and an antibody that detects human but not mouse type I pro-collagen, to investigate this. The expression of SV40 large T-antigen mRNA in RNA extracted from the surface zone, suggests that there is low level RNA cross-contamination from the osteocytes, or MLO-Y4 cell migration to the surface in MLO-Y4/MC3T3-E1(14) co-cultures. Since no SV40 large T-antigen immunostaining was observed in the surface zone of the model even after 7 days of co-culture, we conclude that no osteocytes migrated to the surface zone of the 3D co-culture and that the SV40 large T-antigen mRNA contamination in the surface zone is due to MLO-Y4 cells immediately underlying gel surface, lysing, and releasing RNA during extraction from surface cells. However, the human-specific type I pro-collagen antibody revealed that, although rare, some MG63 cells migrated from the surface to the deep zone of the model, in MLO-Y4/MG63 co-cultures.

### **Phenotype and function**

Whilst the 3D co-culture model described here has shown osteoblast and osteocyte cell viabilities (58–60, 105, 106), morphologies (66, 71, 107, 108), phenotypes (75, 81, 86, 91, 109–114), and loading (104) and osteogenic responses (115, 116) consistent with those found *in vivo*, the use of MLO-Y4 cells means that the important mechanically regulated factor, SOST, is not expressed in the osteocytes in the model. This limitation could be solved by replacing the MLO-Y4 cells with the IDG-SW3 cell line, which are able to differentiate into mature osteocytes and express SOST (35). Furthermore, the phenotypic characterization was performed in 3D co-cultures grown in plastic plates and it is possible that aspects

of the phenotype would be affected by growing cells in silicone plates.

Although the 3D model is designed to investigate mechanically induced osteogenesis in a similar *in vivo* physiological environment, it is not mineralized and so it would only represent interactions that occur in newly formed osteoid rather than mineralized bone. Previous studies have shown the mineralization of 3D collagen gels is possible with IDG-SW3 cells (35) during differentiation to osteocytes, and therefore the 3D co-culture could be mineralized. Mineralization of the 3D collagen gel would affect the properties of the matrix and cell–ECM interactions. Previous *in vitro* studies have shown that after mineralization the ECM of monolayer cultures became gradually stiffer (117). Furthermore, ECM composition has been shown to affect gene expression (118) and osteoblast differentiation and behavior (119). Therefore, mineralizing the 3D co-culture would make the collagen gels stiffer and alter phenotype, further mimicking a physiological environment. If the 3D co-culture was mineralized, further investigations should be done to test the mechanical properties of the mineralized 3D co-cultures as well as the viability and phenotype of the cells within the model and assess whether the medium nutrients can still diffuse to all areas of the 3D gel.

A technical challenge is to ensure that MLO-Y4 cells are evenly distributed within the collagen solution when gels are being set up, otherwise some 3D cultures will have more osteocytes than others. This will lead to cell number variability between experimental replicates, which could cause differences in osteocytic network and loading responses. This was further affected by a variation of up to 20% in the weight of collagen supplied by Sigma, meaning that, since the defined collagen mass was dissolved in a set volume of acid, the collagen gels varied from 2.0 to 2.6 mg/ml. These are potential explanations for differences in magnitude of responses across independent experiments and the essential 3D pre-culture time of at least 48 h for a consistent increase in PGE<sub>2</sub> in response to mechanical loading.

### **Mechanical loading device**

Currently, there are two devices similar to the one developed here (120, 121). Tata et al. (121) developed a silicone plate in a six-well plate format to mechanically load vascular smooth muscle cells (VSMCs) in monolayers, whereas, the device developed by Neidlinger-Wilke et al. (120) is a single-well silicone plate, which was designed to load 3D collagen cultures of intervertebral disk cells. Both devices applied cyclic mechanical stimuli by stretching in a similar fashion to the device described here, but used much higher strains at low frequency (Neidlinger-Wilke et al., 24 h, 0.1 Hz, 10,000  $\mu\epsilon$ ; Tata et al., 6–72 h, 1 Hz, 10–20% strain) (120, 121). Neidlinger-Wilke et al. (120) did not publish how they assessed strain associated with their device. Tata et al. (121) assessed the strain field at the bottom surface of the wells using finite element (FE) modeling, but did not validate this FE model with DIC, or any other methods. Therefore, our loading device is the first where the strains have been directly measured, albeit on the plate surface rather than within the gel.

Digital image correlation showed that when 2.5 N is applied to the silicone plate, the majority of the wells experienced strains of 4000–4500  $\mu\epsilon$ . Peak strain values in vertebrate bone range from

2000 to 3500  $\mu\text{e}$  (122–125), 4000–4500  $\mu\text{e}$  loading is physiological and osteogenic (91, 98, 99), whereas, 6000  $\mu\text{e}$  is pathophysiological (126). The strain testing performed was carried out on an empty plate. Testing a silicone plate with 3D cultures within the wells would further validate the loading plate. Whilst incorporation of particles into the 3D gels (127) would enable strains to be measured directly within the gels, we were unable to achieve this by DIC given the limited well size and the pink color and reflective properties of the gels. Further work is necessary to confirm the strain experienced by the cells in the gels is similar to that on the base of the plate.

## CONCLUSION

There is a great need for a fully characterized *in vitro* 3D matrix based bone model. The majority of the available 3D models involve culturing cells on scaffolds (44–46, 128), which does not represent the bone environment *in vivo* where osteocytes, are embedded within a matrix. Published models involving embedding osteoblasts (39, 129), MLO-Y4 (38, 39), primary osteocytes (42), or normal human bone-derived cells (NHBCs) (41) within a matrix showed maintenance of cell viability (38, 129), osteocyte cell morphology (38, 39, 41, 42), connectivity (38), and gene expression (41, 42). However, none of these models have been individually assessed in all key areas. Furthermore, none of the available 3D collagen based cultures involve co-culturing osteocytes and osteoblasts, nor they have been exposed to mechanical stimuli. Therefore, none investigate the important interactions between these cell types, which lead to mechanically induced bone formation.

This co-culture model facilitates a 3D network of osteocyte-like cells that can be subjected to appropriate anabolic and mechanical loading cues to act upon osteoblasts. Osteoblasts and osteocytes retain appropriate morphology, phenotype, and viability, and osteoblasts increase *COL1A1* expression when stimulated with BMP-2 and mechanical load. Furthermore, embedded osteocytes respond to mechanical loading by releasing PGE<sub>2</sub>. Potentially, this model may be useful in elucidating osteocyte-driven mechanisms that regulate bone formation as a result of mechanical loading, something other current 3D models do not provide (38, 39, 41, 42). The 3D co-culture, combined with a multi-well loading system could provide a novel platform for drug discovery and development for the treatment of age-related bone diseases.

## AUTHOR CONTRIBUTIONS

Conception and design: Marisol Vazquez, Bronwen A. J. Evans, Daniela Riccardi, Sam L. Evans, Jim R. Ralphs, Christopher M. Dillingham, Deborah J. Mason. Collection and assembly of data: Marisol Vazquez, Sam L. Evans, Jim R. Ralphs, Christopher M. Dillingham. Analysis and interpretation of data: Marisol Vazquez, Bronwen A. J. Evans, Daniela Riccardi, Sam L. Evans, Deborah J. Mason. Drafting of the manuscript: Marisol Vazquez, Deborah J. Mason. Critical revision: Marisol Vazquez, Bronwen A. J. Evans, Daniela Riccardi, Sam L. Evans, Deborah J. Mason. Final approval of the article: Marisol Vazquez, Bronwen A. J. Evans, Daniela Riccardi, Sam L. Evans, Jim R. Ralphs, Christopher M. Dillingham, Deborah J. Mason.

## ACKNOWLEDGMENTS

We would like to thank Professor Lynda Bonewald for the provision of the MLO-Y4 cell line, and Mrs. Carole Elford, Dr. Emma Blain, and Dr. Karen Brakspear for their contribution. This project was funded by Cardiff University and the Arthritis Research UK Biomechanics and Bioengineering Center.

## REFERENCES

- Franz-Odendaal TA, Hall BK, Witten PE. Buried alive: how osteoblasts become osteocytes. *Dev Dyn* (2006) **235**:176–90. doi:10.1002/dvdy.20603
- Pead MJ, Susillo R, Skerry TM, Vedi S, Lanyon LE. Increased 3H-uridine levels in osteocytes following a single short period of dynamic bone loading *in vivo*. *Calcif Tissue Int* (1988) **43**:92–6. doi:10.1007/BF02555153
- Skerry TM, Bitensky L, Chayen J, Lanyon LE. Early strain-related changes in enzyme activity in osteocytes following bone loading *in vivo*. *J Bone Miner Res* (1989) **4**:783–8. doi:10.1002/jbmr.5650040519
- Gluhak-Heinrich J, Ye L, Bonewald LF, Feng JQ, Macdougall M, Harris SE, et al. Mechanical loading stimulates dentin matrix protein 1 (DMP1) expression in osteocytes *in vivo*. *J Bone Miner Res* (2003) **18**:807–17. doi:10.1359/jbm.2003.18.5.807
- Harris SE, Gluhak-Heinrich J, Harris MA, Yang W, Bonewald LF, Riha D, et al. DMP1 and MEPE expression are elevated in osteocytes after mechanical loading *in vivo*: theoretical role in controlling mineral quality in the perilacunar matrix. *J Musculoskelet Neuronal Interact* (2007) **7**:313–5.
- Reijnders CM, Bravenboer N, Holzmann PJ, Bhoelan F, Blankenstein MA, Lips P. In vivo mechanical loading modulates insulin-like growth factor binding protein-2 gene expression in rat osteocytes. *Calcif Tissue Int* (2007) **80**:137–43. doi:10.1007/s00223-006-0077-4
- Reijnders CM, Bravenboer N, Tromp AM, Blankenstein MA, Lips P. Effect of mechanical loading on insulin-like growth factor-I gene expression in rat tibia. *J Endocrinol* (2007) **192**:131–40. doi:10.1677/joe.1.06880
- Zaman G, Pitsillides AA, Rawlinson SC, Susillo RF, Mosley JR, Cheng MZ, et al. Mechanical strain stimulates nitric oxide production by rapid activation of endothelial nitric oxide synthase in osteocytes. *J Bone Miner Res* (1999) **14**:1123–31. doi:10.1359/jbm.1999.14.7.1123
- Fox SW, Chambers TJ, Chow JW. Nitric oxide is an early mediator of the increase in bone formation by mechanical stimulation. *Am J Physiol* (1996) **270**:E955–60.
- Mullender MG, Huiskes R. Osteocytes and bone lining cells: which are the best candidates for mechano-sensors in cancellous bone? *Bone* (1997) **20**:527–32. doi:10.1016/S8756-3282(97)00036-7
- Nomura S, Takano-Yamamoto T. Molecular events caused by mechanical stress in bone. *Matrix Biol* (2000) **19**:91–6. doi:10.1016/S0945-053X(00)00050-0
- Plotkin LI, Manolagas SC, Bellido T. Transduction of cell survival signals by connexin-43 hemichannels. *J Biol Chem* (2002) **277**:8648–57. doi:10.1074/jbc.M108625200
- Turner CH, Robling AG, Duncan RL, Burr DB. Do bone cells behave like a neuronal network? *Calcif Tissue Int* (2002) **70**:435–42. doi:10.1007/s00223-001-1024-z
- Klein-Nulend J, Bakker AD, Bacabac RG, Vatsa A, Weinbaum S. Mechanosensation and transduction in osteocytes. *Bone* (2013) **54**:182–90. doi:10.1016/j.bone.2012.10.013
- You L, Cowin SC, Schaffler MB, Weinbaum S. A model for strain amplification in the actin cytoskeleton of osteocytes due to fluid drag on pericellular matrix. *J Biomech* (2001) **34**:1375–86. doi:10.1016/S0021-9290(01)00107-5
- McGarry JG, Klein-Nulend J, Prendergast PJ. The effect of cytoskeletal disruption on pulsatile fluid flow-induced nitric oxide and prostaglandin E2 release in osteocytes and osteoblasts. *Biochem Biophys Res Commun* (2005) **330**:341–8. doi:10.1016/j.bbrc.2005.02.175
- Hoey DA, Kelly DJ, Jacobs CR. A role for the primary cilium in paracrine signaling between mechanically stimulated osteocytes and mesenchymal stem cells. *Biochem Biophys Res Commun* (2011) **412**:182–7. doi:10.1016/j.bbrc.2011.07.072
- Xiao Z, Dallas M, Qiu N, Nicollie D, Cao L, Johnson M, et al. Conditional deletion of Pkd1 in osteocytes disrupts skeletal mechanosensing in mice. *FASEB J* (2011) **25**:2418–32. doi:10.1096/fj.10-180299

19. Nguyen AM, Jacobs CR. Emerging role of primary cilia as mechanosensors in osteocytes. *Bone* (2013) **54**:196–204. doi:10.1016/j.bone.2012.11.016
20. Litzenberger JB, Kim JB, Tummala P, Jacobs CR. Beta1 integrins mediate mechanosensitive signaling pathways in osteocytes. *Calcif Tissue Int* (2010) **86**:325–32. doi:10.1007/s00223-010-9343-6
21. Zhang Y, Paul EM, Sathyendra V, Davison A, Sharkey N, Bronson S, et al. Enhanced osteoclastic resorption and responsiveness to mechanical load in gap junction deficient bone. *PLoS One* (2011) **6**:e23516. doi:10.1371/journal.pone.0023516
22. Robling AG, Niziolek PJ, Baldridge LA, Condon KW, Allen MR, Alam I, et al. Mechanical stimulation of bone in vivo reduces osteocyte expression of SOST/sclerostin. *J Biol Chem* (2008) **283**:5866–75. doi:10.1074/jbc.M705092200
23. Tu X, Rhee Y, Condon KW, Bivi N, Allen MR, Dwyer D, et al. SOST downregulation and local Wnt signaling are required for the osteogenic response to mechanical loading. *Bone* (2012) **50**:209–17. doi:10.1016/j.bone.2011.10.025
24. Li L, Yang Z, Zhang H, Chen W, Chen M, Zhu Z. Low-intensity pulsed ultrasound regulates proliferation and differentiation of osteoblasts through osteocytes. *Biochem Biophys Res Commun* (2012) **418**:296–300. doi:10.1016/j.bbrc.2012.01.014
25. Tan SD, Kuijpers-Jagtman AM, Semeins CM, Bronckers ALJJ, Maltha JC, Hoff JW, et al. Fluid shear stress inhibits TNF $\alpha$ -induced osteocyte apoptosis. *J Dent Res* (2006) **85**:905–9. doi:10.1177/154405910608501006
26. Nakashima T, Hayashi M, Fukunaga T, Kurata K, Oh-Hora M, Feng JQ, et al. Evidence for osteocyte regulation of bone homeostasis through RANKL expression. *Nat Med* (2011) **17**:1231–4. doi:10.1038/nm.2452
27. Xiong J, Onal M, Jilka RL, Weinstein RS, Manolagas SC, O’brien CA. Matrix-embedded cells control osteoclast formation. *Nat Med* (2011) **17**:1235–41. doi:10.1038/nm.2448
28. Nijweide PJ, Van Der Plas A, Alblas MJ, Klein-Nulend J. Osteocyte isolation and culture. *Methods Mol Med* (2003) **80**:41–50.
29. Van Der Plas A, Nijweide PJ. JBMR anniversary classic. Isolation and purification of osteocytes. A van der Plas A, PJ Nijweide. Originally published in Volume 7, Number 4, pp 389–96 (1992). *J Bone Miner Res* (2005) **20**(4):706–14. doi:10.1002/jbmr.5650070406
30. Semeins CM, Bakker AD, Klein-Nulend J. Isolation of primary avian osteocytes. *Methods Mol Biol* (2012) **816**:43–53. doi:10.1007/978-1-61779-415-5\_4
31. Gu G, Nars M, Hentunen TA, Metsikko K, Vaananen HK. Isolated primary osteocytes express functional gap junctions in vitro. *Cell Tissue Res* (2006) **323**:263–71. doi:10.1007/s00441-005-0066-3
32. Halleux C, Kramer I, Allard C, Kneissel M. Isolation of mouse osteocytes using cell fractionation for gene expression analysis. *Methods Mol Biol* (2012) **816**:55–66. doi:10.1007/978-1-61779-415-5\_5
33. Kato Y, Boskey A, Spevak L, Dallas M, Hori M, Bonewald LF. Establishment of an osteoid preosteocyte-like cell MLO-A5 that spontaneously mineralizes in culture. *J Bone Miner Res* (2001) **16**:1622–33. doi:10.1359/jbmr.2001.16.9.1622
34. Kato Y, Windle JJ, Koop BA, Mundy GR, Bonewald LF. Establishment of an osteocyte-like cell line, MLO-Y4. *J Bone Miner Res* (1997) **12**:2014–23. doi:10.1359/jbmr.1997.12.12.2014
35. Woo SM, Rosser J, Dusevich V, Kalajzic I, Bonewald LF. Cell line IDG-SW3 replicates osteoblast-to-late-osteocyte differentiation in vitro and accelerates bone formation in vivo. *J Bone Miner Res* (2011) **26**:2634–46. doi:10.1002/jbmr.465
36. Taylor AF, Saunders MM, Shingle DL, Cimbala JM, Zhou Z, Donahue HJ. Mechanically stimulated osteocytes regulate osteoblastic activity via gap junctions. *Am J Physiol Cell Physiol* (2007) **292**:C545–52. doi:10.1152/ajpcell.00611.2005
37. Boukhechba F, Balaguer T, Michiels JF, Ackermann K, Quincey D, Bouler JM, et al. Human primary osteocyte differentiation in a 3D culture system. *J Bone Miner Res* (2009) **24**:1927–35. doi:10.1359/jbmr.090517
38. Kurata K, Heino TJ, Higaki H, Vaananen HK. Bone marrow cell differentiation induced by mechanically damaged osteocytes in 3D gel-embedded culture. *J Bone Miner Res* (2006) **21**:616–25. doi:10.1359/jbmr.060106
39. Murshid SA, Kamioka H, Ishihara Y, Ando R, Sugawara Y, Takano-Yamamoto T. Actin and microtubule cytoskeletons of the processes of 3D-cultured MC3T3-E1 cells and osteocytes. *J Bone Miner Metab* (2007) **25**:151–8. doi:10.1007/s00774-007-0772-x
40. Qi J, Chi L, Faber J, Koller B, Banes AJ. ATP reduces gel compaction in osteoblast-populated collagen gels. *J Appl Physiol* (2007) **102**:1152–60. doi:10.1152/japplphysiol.00535.2006
41. Atkins GJ, Welldon KJ, Holding CA, Haynes DR, Howie DW, Findlay DM. The induction of a catabolic phenotype in human primary osteoblasts and osteocytes by polyethylene particles. *Biomaterials* (2009) **30**:3672–81. doi:10.1016/j.biomaterials.2009.03.035
42. Honma M, Ikebuchi Y, Kariya Y, Suzuki H. Establishment of optimized in vitro assay methods for evaluating osteocyte functions. *J Bone Miner Metab* (2014). doi:10.1007/s00774-013-0555-5
43. Santos MI, Unger RE, Sousa RA, Reis RL, Kirkpatrick CJ. Crosstalk between osteoblasts and endothelial cells co-cultured on a polycaprolactone-starch scaffold and the in vitro development of vascularization. *Biomaterials* (2009) **30**:4407–15. doi:10.1016/j.biomaterials.2009.05.004
44. Tortelli F, Pujic N, Liu Y, Laroche N, Vico L, Cancedda R. Osteoblast and osteoclast differentiation in an in vitro three-dimensional model of bone. *Tissue Eng Part A* (2009) **15**:2373–83. doi:10.1089/ten.tea.2008.0501
45. Barron MJ, Tsai CJ, Donahue SW. Mechanical stimulation mediates gene expression in MC3T3 osteoblastic cells differently in 2D and 3D environments. *J Biomech Eng* (2010) **132**:041005. doi:10.1115/1.4001162
46. Krishnan V, Dhurjati R, Vogler EA, Mastro AM. Osteogenesis in vitro: from pre-osteoblasts to osteocytes: a contribution from the Osteobiology Research Group, The Pennsylvania State University. *In vitro Cell Dev Biol Anim* (2010) **46**:28–35. doi:10.1007/s11626-009-9238-x
47. Nakagawa K, Abukawa H, Shin MY, Terai H, Troulis MJ, Vacanti JP. Osteoclastogenesis on tissue-engineered bone. *Tissue Eng* (2004) **10**:93–100. doi:10.1089/107632704322791736
48. Domaschke H, Gelinsky M, Burmeister B, Fleig R, Hanke T, Reinstorf A, et al. In vitro ossification and remodeling of mineralized collagen I scaffolds. *Tissue Eng* (2006) **12**:949–58. doi:10.1089/ten.2006.12.949
49. Tortelli F, Cancedda R. Three-dimensional cultures of osteogenic and chondrogenic cells: a tissue engineering approach to mimic bone and cartilage in vitro. *Eur Cell Mater* (2009) **17**:1–14.
50. Kitase Y, Barragan L, Qing H, Kondoh S, Jiang JX, Johnson ML, et al. Mechanical induction of PGE2 in osteocytes blocks glucocorticoid-induced apoptosis through both the beta-catenin and PKA pathways. *J Bone Miner Res* (2010) **25**:2657–68. doi:10.1002/jbmr.168
51. Wang D, Christensen K, Chawla K, Xiao G, Krebsbach PH, Franceschi RT. Isolation and characterization of MC3T3-E1 preosteoblast subclones with distinct in vitro and in vivo differentiation/mineralization potential. *J Bone Miner Res* (1999) **14**:893–903. doi:10.1359/jbmr.1999.14.6.893
52. Mcdonald JA, Broekelmann TJ, Mattheke ML, Crouch E, Koo M, Kuhn C III. A monoclonal antibody to the carboxyterminal domain of procollagen type I visualizes collagen-synthesizing fibroblasts. Detection of an altered fibroblast phenotype in lungs of patients with pulmonary fibrosis. *J Clin Invest* (1986) **78**:1237–44. doi:10.1172/JCI112707
53. Livak KJ, Schmittgen TD. Analysis of relative gene expression data using real-time quantitative PCR and the 2-(Delta Delta C(T)) method. *Methods* (2001) **25**:402–8. doi:10.1006/meth.2001.1262
54. Andersen CL, Jensen JL, Orntoft TF. Normalization of real-time quantitative reverse transcription-PCR data: a model-based variance estimation approach to identify genes suited for normalization, applied to bladder and colon cancer data sets. *Cancer Res* (2004) **64**:5245–50. doi:10.1158/0008-5472.CAN-04-0496
55. Peters WH, Ranson WF. Digital imaging techniques in experimental stress analysis. *Opt Eng* (1982) **21**:213427–213427. doi:10.1117/12.797295
56. Chu T, Ranson W, Sutton M. Applications of digital-image-correlation techniques to experimental mechanics. *Exp Mech* (1985) **25**:232–44. doi:10.1016/j.jmbbm.2013.02.006
57. Noble BS, Stevens H, Loveridge N, Reeve J. Identification of apoptotic changes in osteocytes in normal and pathological human bone. *Bone* (1997) **20**:273–82. doi:10.1016/S8756-3282(96)00365-1
58. Frost HM. In vivo osteocyte death. *J Bone Joint Surg* (1960) **42**:138–43.
59. Mullender MG, Van Der Meer DD, Huiskes R, Lips P. Osteocyte density changes in aging and osteoporosis. *Bone* (1996) **18**:109–13. doi:10.1016/8756-3282(95)00444-0

60. Tomkinson A, Reeve J, Shaw RW, Noble BS. The death of osteocytes via apoptosis accompanies estrogen withdrawal in human bone. *J Clin Endocrinol Metab* (1997) **82**:3128–35. doi:10.1210/jc.82.9.3128
61. Gregory CD, Pound JD. Cell death in the neighbourhood: direct microenvironmental effects of apoptosis in normal and neoplastic tissues. *J Pathol* (2011) **223**:178–95. doi:10.1002/path.2792
62. Tomkinson A, Gevers EF, Wit JM, Reeve J, Noble BS. The role of estrogen in the control of rat osteocyte apoptosis. *J Bone Miner Res* (1998) **13**:1243–50. doi:10.1359/jbmr.1998.13.8.1243
63. Weinstein RS, Nicholas RW, Manolagas SC. Apoptosis of osteocytes in glucocorticoid-induced osteonecrosis of the hip. *J Clin Endocrinol Metab* (2000) **85**:2907–12. doi:10.1210/jc.85.8.2907
64. Sudo H, Kodama HA, Amagai Y, Yamamoto S, Kasai S. In vitro differentiation and calcification in a new clonal osteogenic cell line derived from newborn mouse calvaria. *J Cell Biol* (1983) **96**:191–8. doi:10.1083/jcb.96.1.191
65. Billiau A, Edy VG, Heremans H, Van Damme J, Desmyter J, Georgiades JA, et al. Human interferon mass production in a newly established cell line, MG-63. *Antimicrob Agents Chemother* (1977) **12**:11–5. doi:10.1128/AAC.12.1.11
66. Bourne GH. *The Biochemistry and Physiology of Bone*. 2nd ed. New York, NY: Academic Press (1972). p. 21–40.
67. Heino TJ, Hentunen TA, Vaananen HK. Conditioned medium from osteocytes stimulates the proliferation of bone marrow mesenchymal stem cells and their differentiation into osteoblasts. *Exp Cell Res* (2004) **294**:458–68. doi:10.1016/j.yexcr.2003.11.016
68. Rhee Y, Allen MR, Condon K, Lezcano V, Ronda AC, Galli C, et al. PTH receptor signaling in osteocytes governs periosteal bone formation and intracortical remodeling. *J Bone Miner Res* (2011) **26**:1035–46. doi:10.1002/jbmr.304
69. Zarrinkalam MR, Mulaibrahimovic A, Atkins GJ, Moore RJ. Changes in osteocyte density correspond with changes in osteoblast and osteoclast activity in an osteoporotic sheep model. *Osteoporos Int* (2012) **23**:1329–36. doi:10.1007/s00198-011-1672-4
70. Doty SB. Morphological evidence of gap junctions between bone cells. *Calcif Tissue Int* (1981) **33**:509–12. doi:10.1007/BF02409482
71. Menton DN, Simmons DJ, Chang SL, Orr BY. From bone lining cell to osteocyte – an SEM study. *Anat Rec* (1984) **209**:29–39. doi:10.1002/ar.1092090105
72. Palumbo C, Palazzini S, Marotti G. Morphological study of intercellular junctions during osteocyte differentiation. *Bone* (1990) **11**:401–6. doi:10.1016/8756-3282(90)90134-K
73. Bonewald LF. Establishment and characterization of an osteocyte-like cell line, MLO-Y4. *J Bone Miner Metab* (1999) **17**:61–5. doi:10.1007/s00740050066
74. Nose K, Saito H, Kuroki T. Isolation of a gene sequence induced later by tumor-promoting 12-O-tetradecanoylphorbol-13-acetate in mouse osteoblastic cells (MC3T3-E1) and expressed constitutively in ras-transformed cells. *Cell Growth Differ* (1990) **1**:511–8.
75. Wetterwald A, Hoffstetter W, Cecchini MG, Lanske B, Wagner C, Fleisch H, et al. Characterization and cloning of the E11 antigen, a marker expressed by rat osteoblasts and osteocytes. *Bone* (1996) **18**:125–32. doi:10.1016/S8756-3282(95)00457-2
76. Hadjigargyrou M, Rightmire EP, Ando T, Lombardo FT. The E11 osteoblastic lineage marker is differentially expressed during fracture healing. *Bone* (2001) **29**:149–54. doi:10.1016/S8756-3282(01)00489-6
77. Zhang K, Barragan-Adjeman C, Ye L, Kotha S, Dallas M, Lu Y, et al. E11/gp38 selective expression in osteocytes: regulation by mechanical strain and role in dendrite elongation. *Mol Cell Biol* (2006) **26**:4539–52. doi:10.1128/MCB.02120-05
78. Jahn K, Richards RG, Archer CW, Stoddart MJ. Pellet culture model for human primary osteoblasts. *Eur Cell Mater* (2010) **20**:149–61.
79. Schulze E, Witt M, Kasper M, Lowik CW, Funk RH. Immunohistochemical investigations on the differentiation marker protein E11 in rat calvaria, calvaria cell culture and the osteoblastic cell line ROS 17/2.8. *Histochem Cell Biol* (1999) **111**:61–9. doi:10.1007/s004180050334
80. Collin P, Nefussi JR, Wetterwald A, Nicolas V, Boy-Lefevre ML, Fleisch H, et al. Expression of collagen, osteocalcin, and bone alkaline phosphatase in a mineralizing rat osteoblastic cell culture. *Calcif Tissue Int* (1992) **50**:175–83. doi:10.1007/BF00298797
81. Zhou H, Choong P, McCarthy R, Chou ST, Martin TJ, Ng KW. In situ hybridization to show sequential expression of osteoblast gene markers during bone formation in vivo. *J Bone Miner Res* (1994) **9**:1489–99. doi:10.1002/jbmr.5650090922
82. Shi S, Kirk M, Kahn AJ. The role of type I collagen in the regulation of the osteoblast phenotype. *J Bone Miner Res* (1996) **11**:1139–45. doi:10.1002/jbmr.5650110813
83. Katopodis H, Philippou A, Tenta R, Doillon C, Papachroni KK, Papavassiliou AG, et al. MG-63 osteoblast-like cells enhance the osteoprotegerin expression of PC-3 prostate cancer cells. *Cancer Res* (2009) **29**:4013–8.
84. Tsai SW, Liou HM, Lin CJ, Kuo KL, Hung YS, Weng RC, et al. MG63 osteoblast-like cells exhibit different behavior when grown on electrospun collagen matrix versus electrospun gelatin matrix. *PLoS One* (2012) **7**:e31200. doi:10.1371/journal.pone.0031200
85. Takuwa Y, Ohse C, Wang EA, Wozney JM, Yamashita K. Bone morphogenetic protein-2 stimulates alkaline phosphatase activity and collagen synthesis in cultured osteoblastic cells, MC3T3-E1. *Biochem Biophys Res Commun* (1991) **174**:96–101. doi:10.1016/0006-291X(91)90490-X
86. Whyte MP. Hypophosphatasia and the role of alkaline phosphatase in skeletal mineralization. *Endocr Rev* (1994) **15**:439–61. doi:10.1210/edrv-15-4-439
87. Lecanda F, Warlow PM, Sheikh S, Furlan F, Steinberg TH, Civitelli R. Connexin43 deficiency causes delayed ossification, craniofacial abnormalities, and osteoblast dysfunction. *J Cell Biol* (2000) **151**:931–44. doi:10.1083/jcb.151.4.931
88. Yamaguchi DT, Ma D. Mechanism of pH regulation of connexin 43 expression in MC3T3-E1 cells. *Biochem Biophys Res Commun* (2003) **304**:736–9. doi:10.1016/S0006-291X(03)00633-8
89. Stains JP, Civitelli R. Gap junctions in skeletal development and function. *Biochem Biophys Acta* (2005) **1719**:69–81. doi:10.1016/j.bbapm.2005.10.012
90. Sharroff AC, Li Y, Micsenyi A, Griswold RD, Wells A, Monga SS, et al. Modulation of osteoblast gap junction connectivity by serum, TNFalpha, and TRAIL. *Exp Cell Res* (2008) **314**:297–308. doi:10.1016/j.yexcr.2007.10.010
91. Mason DJ, Hillam RA, Skerry TM. Constitutive in vivo mRNA expression by osteocytes of beta-actin, osteocalcin, connexin-43, IGF-I, c-fos and c-jun, but not TNF-alpha nor tartrate-resistant acid phosphatase. *J Bone Miner Res* (1996) **11**:350–7. doi:10.1002/jbmr.5650110308
92. Fujita T, Izumo N, Fukuyama R, Meguro T, Nakamura H, Kohno T, et al. Phosphate provides an extracellular signal that drives nuclear export of Runx2/Cbfα1 in bone cells. *Biochem Biophys Res Commun* (2001) **280**:348–52. doi:10.1006/bbrc.2000.4108
93. Cheng B, Kato Y, Zhao S, Luo J, Sprague E, Bonewald LF, et al. PGE(2) is essential for gap junction-mediated intercellular communication between osteocyte-like MLO-Y4 cells in response to mechanical strain. *Endocrinology* (2001) **142**:3464–73. doi:10.1210/endo.142.8.8338
94. Cheng B, Zhao S, Luo J, Sprague E, Bonewald LF, Jiang JX. Expression of functional gap junctions and regulation by fluid flow in osteocyte-like MLO-Y4 cells. *J Bone Miner Res* (2001) **16**:249–59. doi:10.1359/jbmr.2001.16.2.249
95. Shalhoub V, Shatzen E, Henley C, Boedigheimer M, Mcninch J, Manoukian R, et al. Calcification inhibitors and Wnt signaling proteins are implicated in bovine artery smooth muscle cell calcification in the presence of phosphate and vitamin D sterols. *Calcif Tissue Int* (2006) **79**:431–42. doi:10.1007/s00223-006-0126-z
96. Bivi N, Condon KW, Allen MR, Farlow N, Passeri G, Brun LR, et al. Cell autonomous requirement of connexin 43 for osteocyte survival: consequences for endocortical resorption and periosteal bone formation. *J Bone Miner Res* (2012) **27**:374–89. doi:10.1002/jbmr.548
97. Chan ME, Lu XL, Huo B, Baik AD, Chiang V, Guldberg RE, et al. A trabecular bone explant model of osteocyte–osteoblast co-culture for bone mechanobiology. *Cell Mol Bioeng* (2009) **2**:405–15. doi:10.1007/s12195-009-0075-5
98. Hillam RA, Skerry TM. Inhibition of bone resorption and stimulation of formation by mechanical loading of the modeling rat ulna in vivo. *J Bone Miner Res* (1995) **10**:683–9. doi:10.1002/jbmr.5650100503
99. Rubin CT, Sommerfeld DW, Judex S, Qin Y-X. Inhibition of osteopenia by low magnitude, high-frequency mechanical stimuli. *Drug Discov Today* (2001) **6**:848–58. doi:10.1016/S1359-6446(01)01872-4
100. Jiang JX, Cherian PP. Hemichannels formed by connexin 43 play an important role in the release of prostaglandin E(2) by osteocytes in response to mechanical strain. *Cell Commun Adhes* (2003) **10**:259–64. doi:10.1080/cac.10.4-6.259.264
101. Cherian PP, Siller-Jackson AJ, Gu S, Wang X, Bonewald LF, Sprague E, et al. Mechanical strain opens connexin 43 hemichannels in osteocytes: a novel mechanism for the release of prostaglandin. *Mol Biol Cell* (2005) **16**:3100–6. doi:10.1091/mbc.E04-10-0912

102. Jiang JX, Cheng B. Mechanical stimulation of gap junctions in bone osteocytes is mediated by prostaglandin E2. *Cell Commun Adhes* (2001) **8**:283–8. doi:10.3109/15419060109080738
103. Saini V, Yadav S, McCormick S. Low-intensity pulsed ultrasound modulates shear stress induced PGHS-2 expression and PGE2 synthesis in MLO-Y4 osteocyte-like cells. *Ann Biomed Eng* (2011) **39**:378–93. doi:10.1007/s10439-010-0156-6
104. Yang M, Huang L, Xiao L, Liao E. [Effects of mechanical stimulation on proliferation and differentiation in MG-63 osteoblast-like cells]. *Sheng Wu Yi Xue Za Zhi* (2012) **29**:894–7.
105. Parfitt A. Bone-forming cells in clinical conditions. In: Bk H, editor. *Bone: The Osteoblast and Osteocyte*. Boca Raton, FL: Telford Press and CRC Press (1990). p. 351–429.
106. Jilka RL, Weinstein RS, Bellido T, Parfitt AM, Manolagas SC. Osteoblast programmed cell death (apoptosis): modulation by growth factors and cytokines. *J Bone Miner Res* (1998) **13**:793–802. doi:10.1359/jbmr.1998.13.5.793
107. Doty SB, Robinson RA, Schofield B. Morphology of bone and histochemical staining characteristics of bone cells. In: Greep RO, Astwood EB, editors. *Handbook of Physiology*. Washington, DC: American Physiological Society (1976). 3 p.
108. Palumbo C. A three-dimensional ultrastructural study of osteoid-osteocytes in the tibia of chick embryos. *Cell Tissue Res* (1986) **246**:125–31. doi:10.1007/BF00219008
109. Dodds RA, Ali N, Peat MJ, Lanyon LE. Early loading-related changes in the activity of glucose 6-phosphate dehydrogenase and alkaline phosphatase in osteocytes and periosteal osteoblasts in rat fibulae in vivo. *J Bone Miner Res* (1993) **8**:261–7. doi:10.1002/jbmr.5650080303
110. Duxy P, Zhang R, Geoffroy V, Ridall AL, Karsenty G. Osf2/Cbfa1: a transcriptional activator of osteoblast differentiation. *Cell* (1997) **89**:747–54. doi:10.1016/S0092-8674(00)80257-3
111. Komori T, Yagi H, Nomura S, Yamaguchi A, Sasaki K, Deguchi K, et al. Targeted disruption of Cbfa1 results in a complete lack of bone formation owing to maturational arrest of osteoblasts. *Cell* (1997) **89**:755–64. doi:10.1016/S0092-8674(00)80258-5
112. Otto F, Thornell AP, Crompton T, Denzel A, Gilmour KC, Rosewell IR, et al. Cbfa1, a candidate gene for cleidocranial dysplasia syndrome, is essential for osteoblast differentiation and bone development. *Cell* (1997) **89**:765–71. doi:10.1016/S0092-8674(00)80259-7
113. Schwab W, Schulze E, Witt M, Funk RH, Kasper M. Immunohistochemical localization of the differentiation marker E11 in dental development of rats. *Acta Histochem* (1999) **101**:431–6. doi:10.1016/S0065-1281(99)80043-9
114. Li X, Ominsky MS, Niu QT, Sun N, Daugherty B, D'agostin D, et al. Targeted deletion of the sclerostin gene in mice results in increased bone formation and bone strength. *J Bone Miner Res* (2008) **23**:860–9. doi:10.1359/jbmr.080216
115. Chen X, Yang L, Tian W. [Heterotopic osteogenesis of autogenous marrow stromal cells with recombinant human bone morphogenetic protein 2 gene transfection and porous calcium phosphate ceramic as a scaffold]. *Hua Xi Kou Qiang Yi Xue Za Zhi* (2003) **21**:419–21.
116. Chen G, Deng C, Li YP. TGF-beta and BMP signaling in osteoblast differentiation and bone formation. *Int J Biol Sci* (2012) **8**:272–88. doi:10.7150/ijbs.2929
117. Meng Y, Qin YX, Dimasi E, Ba X, Rafailovich M, Pernodet N. Biominerization of a self-assembled extracellular matrix for bone tissue engineering. *Tissue Eng Part A* (2009) **15**:355–66. doi:10.1089/ten.tea.2007.0371
118. Bissell MJ, Hall HG, Parry G. How does the extracellular matrix direct gene expression? *J Theor Biol* (1982) **99**:31–68. doi:10.1016/0022-5193(82)90388-5
119. Prideaux M, Loveridge N, Pitsillides AA, Farquharson C. Extracellular matrix mineralization promotes E11/gp38 glycoprotein expression and drives osteocytic differentiation. *PLoS One* (2012) **7**:e36786. doi:10.1371/journal.pone.0036786
120. Neidlinger-Wilke C, Wurtz K, Liedert A, Schmidt C, Borm W, Ignatius A, et al. A three-dimensional collagen matrix as a suitable culture system for the comparison of cyclic strain and hydrostatic pressure effects on intervertebral disc cells. *J Neurosurg Spine* (2005) **2**:457–65. doi:10.3171/spi.2005.2.4.0457
121. Tata U, Xu H, Rao SMN, Chuong C-J, Nguyen KT, Chiao JC. A novel multiwell device to study vascular smooth muscle cell responses under cyclic strain. *J Nanotechnol Eng Med* (2011) **2**:021007–021007. doi:10.1115/1.4003928
122. Rubin CT. Skeletal strain and the functional significance of bone architecture. *Calcif Tissue Int* (1984) **36**(Suppl 1):S11–8. doi:10.1007/BF02406128
123. Rubin CT, Lanyon LE. Dynamic strain similarity in vertebrates: an alternative to allometric limb bone scaling. *J Theor Biol* (1984) **107**:321–7. doi:10.1016/S0022-5193(84)80031-4
124. Rubin CT, Lanyon LE. Regulation of bone formation by applied dynamic loads. *J Bone Joint Surg Am* (1984) **66**:397–402.
125. Rubin CT, Mcleod KJ, Bain SD. Functional strains and cortical bone adaptation: epigenetic assurance of skeletal integrity. *J Biomech* (1990) **23**(Suppl 1):43–54. doi:10.1016/0021-9290(90)90040-A
126. Bailey DA, Faulkner RA, Mckay HA. Growth, physical activity, and bone mineral acquisition. *Exerc Sport Sci Rev* (1996) **24**:233–66.
127. Sutton MA, Orteu J, Schreier HW. Digital image correlation (DIC). *Image Correlation for Shape, Motion and Deformation Measurements: Basic Concepts, Theory and Applications*. New York: Springer (2009).
128. Papadimitropoulos A, Scherberich A, Guven S, Theilgaard N, Crooijmans HJ, Santini F, et al. A 3D in vitro bone organ model using human progenitor cells. *Eur Cell Mater* (2011) **21**:445–58.
129. Maeno S, Niki Y, Matsumoto H, Morioka H, Yatabe T, Funayama A, et al. The effect of calcium ion concentration on osteoblast viability, proliferation and differentiation in monolayer and 3D culture. *Biomaterials* (2005) **26**:4847–55. doi:10.1016/j.biomaterials.2005.01.006

**Conflict of Interest Statement:** The authors declare that the research was conducted in the absence of any commercial or financial relationships that could be construed as a potential conflict of interest.

*Received: 16 October 2014; paper pending published: 03 November 2014; accepted: 18 November 2014; published online: 09 December 2014.*

*Citation: Vazquez M, Evans BAJ, Riccardi D, Evans SL, Ralphs JR, Dillingham CM and Mason DJ (2014) A new method to investigate how mechanical loading of osteocytes controls osteoblasts. *Front. Endocrinol.* **5**:208. doi: 10.3389/fendo.2014.00208*

*This article was submitted to Bone Research, a section of the journal *Frontiers in Endocrinology*.*

*Copyright © 2014 Vazquez, Evans, Riccardi, Evans, Ralphs, Dillingham and Mason. This is an open-access article distributed under the terms of the Creative Commons Attribution License (CC BY). The use, distribution or reproduction in other forums is permitted, provided the original author(s) or licensor are credited and that the original publication in this journal is cited, in accordance with accepted academic practice. No use, distribution or reproduction is permitted which does not comply with these terms.*



# Mechanical regulation of bone regeneration: theories, models, and experiments

Duncan Colin Betts and Ralph Müller \*

Institute for Biomechanics, ETH Zürich, Zürich, Switzerland

**Edited by:**

Jonathan H. Tobias, University of Bristol, UK

**Reviewed by:**

Jan Josef Stepan, Charles University, Czech Republic

Sarah Taylor, Stanford University, USA

**\*Correspondence:**

Ralph Müller, Institute for Biomechanics, ETH Zurich, Vladimir-Prelog-Weg 3, Zurich 8093, Switzerland

e-mail: ram@ethz.ch

How mechanical forces influence the regeneration of bone remains an open question. Their effect has been demonstrated experimentally, which has allowed mathematical theories of mechanically driven tissue differentiation to be developed. Many simulations driven by these theories have been presented, however, validation of these models has remained difficult due to the number of independent parameters considered. An overview of these theories and models is presented along with a review of experimental studies and the factors they consider. Finally limitations of current experimental data and how this influences modeling are discussed and potential solutions are proposed.

**Keywords:** bone regeneration, fracture healing, mechanobiology, simulation

## INTRODUCTION

Bone's capability of "perfect" regeneration is unique, unlike other tissues it is capable of recovering its form without permanent scars. However not all fractures heal spontaneously, it has been found that 20 per 100,000 people per year will have delayed healing or a non-union, where the fractured bone fails to fuse (1). It is known that mechanical forces can influence the pathways through which healing occurs; several studies have shown that changes in the mechanical environment can modulate the time taken to heal, change the proportions of different tissue type as well as gene expression patterns of cells in the healing bone (2, 3). The exact mechanism through which mechanical stimuli are sensed and incorporated in the healing process is not fully understood and still remains an open question. Answering this question will lead to improved treatment methods for bone fracture repair, reducing the amount of time patients are hospitalized. To this end, we have compiled a summary of literature on the topic examining the experimental studies and numerical theories.

Depending on the stability of the bone fragments the healing can progress down two paths, rigidly fixed fragments with only a small fracture gap can heal through primary bone healing, where the bone remodeling units, responsible for the adaption of the cortical bone, bridge the gap; secondary fracture healing occurs when relative motion occurs between the bone fragments, causing a callus to form. Secondary fracture healing can be divided into three overlapping stages as described in **Figure 1**, the reactive, reparative, and remodeling phases. Immediately post-fracture there is an inflammatory response, termed the reactive phase, in which blood vessels, which have ruptured fill the injured area with blood forming clot called the fracture hematoma. The fracture hematoma is infiltrated by fibroblasts and small blood vessels, becoming granulation tissue. The initial callus is thus a mixture of hematoma, fibrous tissues, and infiltrating blood vessels. The reparative phase begins once bone and cartilage form, the bone is initially formed through intramembranous ossification initiating on the existing cortical bone and progressing with time toward the plane of the

fracture, while the cartilage forms in regions of low oxygen tension (4, 5). Once the blood supply is sufficient enough, cartilage is calcified and converted into woven bone through endochondral ossification. The stability of a fracture influences the amount of intramembranous and endochondral ossification, with more cartilage being formed in less stable fractures and thus more endochondral ossification (6). Bony bridging, the union of the hard callus from either side of the fracture, occurs making the structure extremely stable. The remodeling phase begins during the reparative stage, with the bone structure being adapted back to its original load bearing form. The cortical bone is also remodeled with the cortical bone adjacent to the fracture becoming woven bone, likely as the vasculature within this bone is damaged during the fracture, causing hypoxia (7–9). Hypoxia has been shown to up regulate the formation, size, and activity of osteoclasts, the cells responsible for the resorption of bone (10). The remodeling phase concludes with the callus being completely remodeled into the shape of the original bone, recovering the original strength, and functionality. The events are driven through intercellular signaling, levels of oxygen tension and the mechanical environment directing mesenchymal stem cells to differentiate into osteoblasts, chondrocytes, or fibroblasts each of these cells being responsible for the production of particular tissues (7). In this review, we concentrate explicitly on the mechanical factors influencing bone regeneration, what has been experimentally observed as well as theories and models, which have been developed to explain this.

## EXPERIMENTAL STUDIES

Mechanical loads are applied at the organ level and propagate to a level where cells can sense them, which in turn results in changes at the tissue level. Many studies have investigated applying different forces to fractured bones *in vivo* and quantifying the tissue produced or the mechanical competence of the bone. Loads applied to bone cause non-homogenous strains throughout the healing tissue, resulting in a variety of tissues forming. Experimentally, these strains cannot be quantified *in vivo* preventing

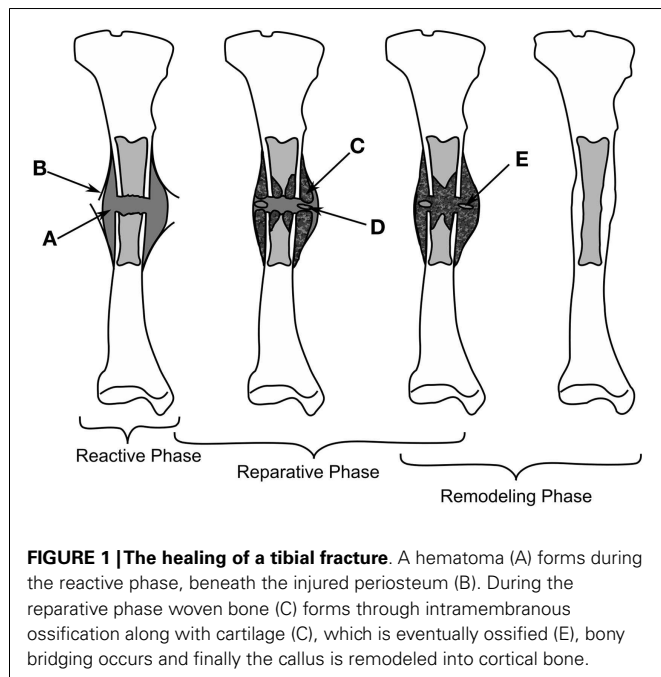


**FIGURE 1 | The healing of a tibial fracture.** A hematoma (A) forms during the reactive phase, beneath the injured periosteum (B). During the reparative phase woven bone (C) forms through intramembranous ossification along with cartilage (D), which is eventually ossified (E), bony bridging occurs and finally the callus is remodeled into cortical bone.

the direct development of mechanobiological rules, however, the result of organ level loading is important for validating fracture healing models, as an accurate rule set should predict the outcomes of such studies. Experimental studies investigating the effect of inter-fragmentary movement (IFM) and fixator stability/stiffness are essentially referring to how loading effects fracture healing outcome. IFM is ambiguously used to describe either axial tension/compression of the bone defect, shear movement in the plane of the defect, relative axial rotation of the fragments, or a bending. Here, we will distinguish between these different modes using the following terms: inter-fragmentary compression (IFC), inter-fragmentary tension (IFT), inter-fragmentary bending (IFB), and inter-fragmentary shear (IFS). The different loading modes are illustrated in **Figures 2A–E** with the exception of IFT, which is just the opposite of IFC. The cases of shear movement and rotation both create a non-uniform shear loading within the tissue, therefore we combine both of these loading states as IFS.

To study the effect of each mode of movement demands the precise control and measurement of bone fragment movement requiring the use of some form of fixation. There are two categories of fixation used in biomechanical research, external and internal fixation, which can be seen in **Figures 2F–I**. External fixation is commonly used in large animal studies often with modifications to the fixator or to the surgical technique so as to change the stability of the fixator, or be instrumented to measure the fragment displacements (11). In contrast, internal fixators are simpler in design and technique. An intramedullary nail for example is guided by the medullary cavity and can be a single piece, which has made them much more commonly used in small animal studies (12–15). The fixation method has a large effect on the loads, which can be applied, external fixation allows for controlled movements or fixed forces, whereas, internal fixation typically limits the load to an applied force. The fragile nature of the soft tissue means

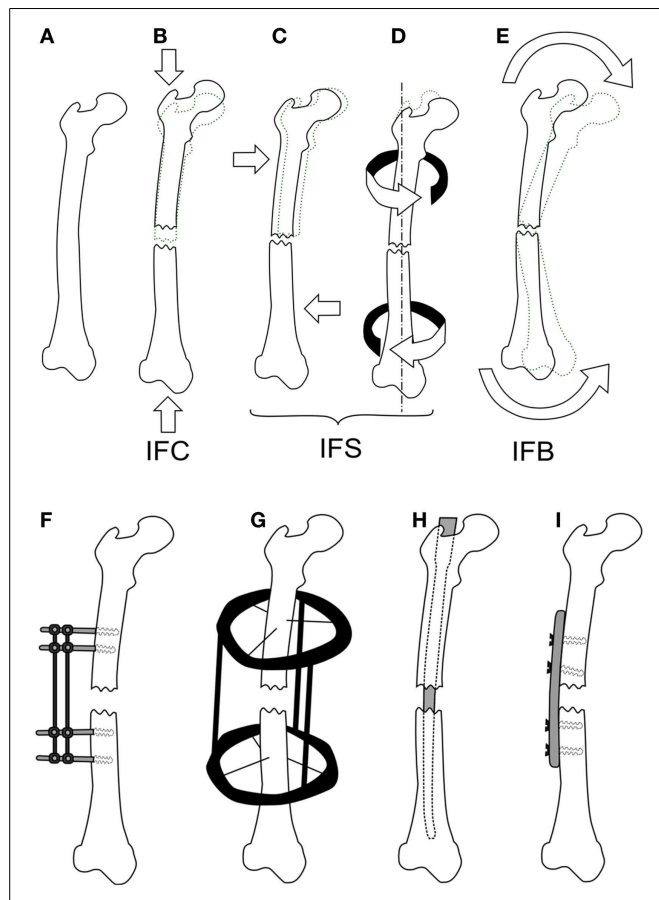


**FIGURE 2 | The different loading modes for a fracture, shown on a femur (A).** IFC causes in a narrowing of the fracture gap (B), IFS is a shear movement (C) across the gap plane, or a relative torsional movement around the axis of the bone (D), and IFB is a bending movement (E) centered around the fracture. Fixation methods for fractures are shown in (F–I), external fixator (F), the ring fixator (G), intramedullary nailing (H), and plating (I).

that constant loading throughout a study is not always possible, thus some studies will define a maximum load and displacement. For example, Goodship and Kenwright (16) apply a 33% inter-fragmentary strain or a 360 N load, as initially such a load would induce strains in the hematoma that inhibited healing, whereas, once bony bridging occurs, this level of strain would damage the new bone.

There exists no standard methodology for loading during fracture healing. Studies can either use active loading like Goodship and Kenwright (16) passively allow a limited amount of movement as done by Claes et al. (11) or use a fixator structure or orientation with a different stiffness as done by Klein et al. (17) and Schell et al. (18). While it is often possible to compare initial loading of the callus, the loading is altered as the tissue distribution changes. This can lead to diverging results making comparisons between how bone heals in relation to loading difficult between studies. We attempt to provide a summary of how different organ level loadings affect the healing outcome and were possible highlight variations in fixation and loading between studies.

## INTER-FRAGMENTARY COMPRESSION AND INTER-FRAGMENTARY TENSION

There are a substantial number of studies, which have investigated the effects of IFC on bone healing, several are summarized within **Table 1**. It is widely accepted that a certain amount of IFC has a positive effect on the healing process, which was first shown by Goodship and Kenwright (16). The timing of the load is also critical with Gardner et al. (12) showing that immediate application of loading post-surgery resulted in reduced healing potential compared to those applied 4 days after. They also demonstrated that too high an IFC force can be detrimental to healing. However, as they used an intramedullary nail and applied a force rather than a displacement, it is difficult to compare the results. Rate dependence with respect to the application of IFC has been identified by Goodship et al. (19) showing that for the same number of cycles a strain rate of 40 mm/s showed superior healing compared to 2 and 400 mm/s. High frequency low amplitude IFC was investigated by Goodship et al. (20) demonstrating an increase in the callus stiffness.

Inter-fragmentary tension is movement applied in the opposite direction to compression, causing an increase in gap size. Cheal et al. (25) showed that high tensile loads lead to reduced healing with even cortical resorption occurring, while lower tensile loads lead to callus formation.

## INTER-FRAGMENTARY SHEAR

How IFS affects the bone regeneration process remains controversial, with studies showing that it can inhibit healing and others showing that it can have a positive effect. Several studies in this area are summarized in **Table 2**, with Bishop et al. (27) and Park et al. (28) showing neutral or positive effects and the others showing negative outcomes. These differences are likely due to the loading conditions. Park et al. (28) studied rabbits in which the femur was fractured instead of the more common method of cutting a discrete unit of bone out with a saw, i.e., osteotomy. They compared compression and shear loading showing an increase in periosteal cartilage formation and a significantly stiffer callus after 4 weeks. It is possible that traumatic injury will solicit a different biological response, which osteotomies do not cause. In addition, fracture planes will not have been as uniform and perhaps will have influenced the tissue loading.

Bishop et al. (27), for example, applied torsion using a custom designed fixator aiming to produce a principal strain of 25% between the fragments and compared it to equivalent principal strain produced through IFC, he reports torsion having stimulated intercortical mineralization. The complex loading condition presented through shear loading confounds such a comparison, as the pure shear loading produced an equal maximum and minimum principal strains of  $\pm 25\%$ , whereas as compression produces a single negative principle strain of  $-25\%$ . Thus the gap tissue stored twice the amount of elastic energy in the case of IFS as IFC. Additionally, the rotation of  $7.2^\circ$  with a cortical radius of 10 mm and a gap of 2.4 mm would have induced principal strains of 52%, not the 25% stated within the paper. Bishop et al. (27) assumed their torsional fixator to be completely rigid axially with no IFC, in comparison Schell et al. (18) measure both the IFS and IFC for their flexible fixator, when considering just the IFS they calculated a

principal strain of  $\pm 26\%$ , while including it they received  $+18.5\%$  and  $-33\%$ , respectively. It is possible that compliance of the fixator and physiological loading created a beneficial amount of IFC, which was not considered by Bishop et al. (27) in their study. The conclusion which can be drawn is that pure shear motion applied to the whole organ is not pure shear within the healing tissue. It seems inappropriate to compare tissue strain between loading cases using a single value from the strain tensor, a solution would be through using a scalar valued function such as strain energy density (SED), or a combination of deviatoric and volumetric strain.

## INTER-FRAGMENTARY BENDING

The case of IFB has not be sufficiently investigated to form a conclusion, the two studies, which consider this are summarized in **Table 3**. What has been shown is that asymmetric bending, results in asymmetric callus formation. Healing appears to be inhibited on the tensile side of the callus and promoted on the compressive side (33). This is in agreement with studies looking at axial compression and tension individually as shown before. Cyclic bending appears to cause bone healing to take a different pathway. It has been shown that cyclic bending induces changes in gene expression, where genes responsible for bone morphogenetic proteins are down regulated while genes responsible for cartilage production are up regulated. More cartilage within the callus was observed compared to the unloaded case indicating that the balance of tissue production during the reparative phase was altered (3). The increased level of cartilage indicates that the stimulated callus is not as vascularized as the fixed callus, and the healing will progress along the endochondral ossification pathway rather than through endochondral ossification.

## THEORIES AND MODELS

In this section, different theories for tissue differentiation are described followed by an overview of the simulations, which have been performed using them (summary of these data can be found in **Table 4**). Experimental evidence demonstrates that mechanical forces can direct the healing process, i.e., tissue differentiation is mechanobiologically regulated. There are several theories as to which mechanical quantities are the stimuli for differentiation such as SED, deviatoric and volumetric strain, or relative fluid flow between cells and the matrix. Due to the complicated geometries, which occur in fracture healing it is not possible to analytically apply these theories. Instead they are applied as components of simulations, we concentrate here on mechanically driven simulations, which typically consist of five parts summarized in **Figure 3**; the geometries of bone, defect and callus; the boundary conditions; finite element analysis used to determine the mechanical signal in the callus; the tissue differentiation rules, through which a new callus geometry is created; and finally most simulations consider an additional “biological aspect,” which adds a temporal scale and directs spatially where the ossification occurs. A simulation will go through several iterations changing the tissues composing the callus until a state of equilibrium is reached.

The callus geometries are typically assumed to be constant and ellipsoidal, so simulations of fracture healing start at the reparative phase once the soft callus has formed. The only exception

**Table 1 | Experimental studies considering the effects of inter-fragmentary compression on fracture healing.**

| Author                      | Study (n)  | Method  | Outcome  |
|-----------------------------|------------|---|--|
| Goodship and Kenwright (16) | Sheep (12) | A osteotomy gap of 1 mm in the tibia, fixed with frame fixator, loaded through 33% IFC or 360 N force applied at a frequency of 0.5 Hz  | Stimulated callus was significantly stiffer 12 weeks post-surgery compared to rigidly fixed  |
| Claes et al. (11)           | Sheep (42) | Six groups with osteotomy gaps of 1.0, 2.0, or 6.0 mm of the tibia and a maximum IFC of 7 or 31%. Fractures fixed with instrumented ring fixator, which measured IFC throughout the experiment  | Increased osteotomy gap delayed healing, for 1 mm gap early bony bridging occurred. For larger gaps increased IFC did not enhance healing  |
| Claes and Heigle (4)        | Sheep (7)  | Osteotomy gap of 3 mm with max allowable IFC of 1.0 mm, fracture fixed with instrumented ring fixator, which monitored IFC over the course of healing. Calcein green injected at 4 weeks and reverin at 8 weeks   | IFC reduced over the course of healing. Histological sections appeared to show bone advanced along a path from the cortical surface  |
| Kenwright et al. (21)       | Human (85) | Frame fixator applied to tibial fractures, IFC of 0.5–2.0 mm applied at 0.5 Hz for 30 min a day   | Group with micro-movements showed a significantly reduced healing time (17.9 vs. 23.2 weeks, $p = 0.0027$ )  |
| Kenwright et al. (22)       | Human (80) | Frame fixator applied to tibial fractures, IFC of 1.0 mm applied at 0.5 Hz for 30 min a day. Initial loading limited to 12 kg   | Healing time to unsupported weight bearing was significantly reduced (23 vs. 29 weeks, $p < 0.01$ ). Additionally, higher callus stiffness was observed  |
| Gardner et al. (12)         | Mice (80)  | Tibial osteotomy fixed with an intramedullary nail, loaded with compressive vibrations with a maximum load of 1, 2, and 4 N and amplitudes 0.5, 1, and 2 N where applied. Immediate onset of loading regime was compared to a delayed onset of 4 days   | The lowest load case with delayed onset for loading resulted in a significantly higher callus strength. Immediate loading resulted in significantly reduced strength in all cases, and higher loads either in comparable or lower strength                                       |
| Claes et al. (23)           | Sheep (10) | Osteotomy of 2.0 mm mid tibia, two groups 10 and 50% maximum IFC. Fractures fixed with instrumented ring fixator, which measured IFC throughout the experiment. Sacrificed at week 9  | Higher IFM resulted in greater fibrocartilage formation, and less bone. No significance in the distribution of blood vessels   |
| Claes et al. (24)           | Sheep (10) | Tibial osteotomy of 2.1 or 5.7 mm, both groups had same IFC strain of 30%. Fixation through ring fixator  | Larger gap led to fewer blood vessels, less bone formation, and more fibrocartilage  |
| Goodship et al. (19)        | Sheep (24) | Mid-diaphyseal tibial osteotomy gap of 3.0 mm, stabilized with a frame fixator. An IFC of 33% or force of 200 N was applied cyclically at 0.5 Hz at strain rates of 2, 40, and 400 mm/s commencing 1 week post-operatively. A secondary study considered the application of the 400 mm/s strain rate 6 weeks post-operatively | The strain rate of 40 mm/s applied 1 week post-operatively showed more mature, stiffer, and stronger callus with a higher BMD when compared to the other groups. There was no significance between 400 and 2 mm/s  |
| Goodship et al. (20)        | Sheep (8)  | Mid-diaphyseal tibial osteotomy gap of 3.0 mm, stabilized with a frame fixator. IFC was applied at 30 Hz  | High frequency loading led to a 3.6-fold stiffer, 2.5-fold stronger, and 29% larger callus compared to controls  |
| Cheal et al. (25)           | Sheep (11) | Mid-diaphyseal tibial osteotomy gap of 1.0 mm, stabilized with a flexible plate. A transducer was attached opposite the plate producing a tensile strain gradient from 10 to 100% across the gap  | Areas with higher strain led to cortical resorption, while areas with lower strain showed callus development   |
| Mark et al. (26)            | Rats (84)  | Mid-diaphyseal femoral osteotomy was performed and the gap adjusted from 0–2.0 mm. Axial stiffness was measured at $265 \pm 34$ N/mm for the 0 mm gap and $30.38 \pm 2.07$ mm for the 2.0 mm gap  | The group with larger gap and less stiffness resulted in a late onset for bone formation and greater endochondral bone formation. Full ossification of the callus was delayed, however, early in the healing stage no difference was found between the two groups histologically |

(Continued)

**Table 1 | Continued**

| Author            | Study (n)  | Method   | Outcome  |
|-------------------|------------|--|--|
| Klein et al. (17) | Sheep (12) | Mid-diaphyseal tibial osteotomy was performed and fixed with a gap of 3.0 mm. The fixation plane varied between the two groups mounted either in the medial plane or anteromedial plane. This lead to differential stiffness between the groups with anteromedial fixation leading to significantly higher IFS and IFC | The group with larger IFM resulted in a stiffer, smaller callus when compared to rigid fixation. The larger IFM group also presented signs of significant remodeling of the callus indicating a more advanced stage of healing |

**Table 2 | Experimental studies considering the effects of inter-fragmentary shear on fracture healing.**

| Author             | Subjects (n) | Method  | Outcome   |
|--------------------|--------------|---|---|
| Schell et al. (29) | Sheep (40)   | Mid-diaphyseal tibial osteotomy was performed and fixed with a gap of 3.0 mm. Two fixators were used, a rigid fixator and a fixator with high axial rigidity and no resistance to shear motion  | The group with free shear movement had significantly reduced torsional strength and stiffness at every time point. Three animals in this group presented hypertrophic non-unions after 6 months   |
| Vetter et al. (9)  | Sheep (64)   | Mid-diaphyseal tibial osteotomy was performed and fixed with a gap of 3.0 mm. The animals were divided into two groups, one with rigid fixation, and the other with a fixator, which allowed greater shear movement   | Histological slices were categorized as belonging to one of six different healing stages based on topological features present. Rigid fixation resulted in a faster progression in healing, this could also be seen in the ratio of bone area to total area which was higher for rigid fixation |
| Bishop et al. (27) | Sheep (18)   | Mid-diaphyseal tibial osteotomy was performed and fixed with a gap of 2.4 mm. Three groups one with rigid fixation, one with torsional shear, and one with IFC. Movement was stimulated to cause 25% principal strain   | The group with torsional shear motion had a greater callus area and similar stiffness when compared to the group with no motion, while IFC produced small callus, less advanced with little bridging  |
| Schell et al. (18) | Sheep (64)   | Mid-diaphyseal femoral osteotomy was performed and fixed with a gap of 3.0 mm. Two different fixators were used of different stiffness. This resulted in greater IFS within the less stable group   | Throughout the healing significantly more cartilage formed with the less rigid fixation group. The rigid group had a larger callus formation. At 9 weeks, there was no significant difference between the two groups  |
| Park et al. (28)   | Rabbit (56)  | Two cohorts with oblique and transverse tibial fractures each consisting of a rigid fixation and a sliding fixation group. The sliding fixator allowed IFC while the transverse group and IFS in the oblique group  | The oblique IFS group showed accelerated healing compared to the other three groups, the torsional strength by 4 weeks exceeded that of intact bone   |
| Klein et al. (30)  | Sheep (12)   | Mid-diaphyseal femoral osteotomy was performed and fixed with a gap of 3.0 mm. One group of animals was fixed through un-reamed medullary nailing allowing torsional rotation of 10°, the other with a rigid frame fixator. The IFMs were measured throughout | The nailed group showed significantly inferior healing compared to the rigidly fixed group, when comparing mechanical properties and histological sections of the callus after 9 weeks  |
| Lienau et al. (31) | Sheep (64)   | Mid-diaphyseal tibial osteotomy gap of 3.0 mm stabilized with a frame fixator. Test group received a fixator, which allowed increased IFS compared to control   | Group with higher IFS initially showed a lower blood supply, the healing stage for this group lagged behind, presenting lower stiffness at 6 weeks, this was compensated after 9 weeks. However, the rigid group appeared to have entered the remodeling phase, whereas, the IFS group had not  |
| Epari et al. (32)  | Sheep (64)   | Mid-diaphyseal tibial osteotomy gap of 3.0 mm, stabilized with a frame fixator. Test group a fixator, which allowed increased IFS compared to control   | IFS induced a larger amount of cartilage formation compared control, while also have a more compliant callus. The remodeling process was initiated earlier for rigidly fixed fractures  |

**Table 3 | Experimental studies considering the effects of inter-fragmentary bending on fracture healing.**

| Author               | Subjects ( <i>n</i> ) | Method  | Outcome   |
|----------------------|-----------------------|---|---|
| Hente et al. (33)    | Sheep (18)            | Mid-diaphyseal femoral osteotomy was performed and fixed with a gap of 2.0 mm. Using a custom fixator bending cycles lasting 0.8 s creating a 50% inter-fragmentary strain at the endosteum was applied. The number of loading cycles was varied, the control received no loading, while the first group received 10 bending cycles per day and a second group received 1000 cycles per day | The compressive side of the osteotomy gap resulted in 25-fold greater periosteal callus formation. Greater cycle number showed again a 10-fold difference to the lower cycle number. Bridging occurred exclusively at the compressed side.                  |
| Palomares et al. (3) | Rats (85)             | Mid-diaphyseal femoral osteotomy of 1.5 mm, the animal were fixed with an external frame, which allowed bending, approximately centered on the gap, the experimental group had stimulated $-25/+35^\circ$ bending applied at 1 Hz for 15 min per day starting 10 days post-surgery  | Stimulation up regulated cartilage related genes, and down regulated several genes responsible for bone morphogenetic proteins (BMPs). Serial sectioning showed a much more prolific presence of cartilage and less mineralized callus compared to control. |

to this is the model of Gomez-Benito et al. (44) who presented a model, which allows the callus boundaries to evolve over time. Boundary conditions are based upon the loading described by the experimental study the authors aim to replicate.

#### TISSUE DIFFERENTIATION THEORIES

In 1960, Pauwels first proposed that tissue differentiation within a fracture callus was governed by mechanical stimuli. He theorized that cartilage formed as a result of local hydrostatic pressure causing mesenchymal stem cells to become chondroblasts, whereas, bone and fibrous tissues resulted from shear strains causing mesenchymal stem cells to differentiate into osteoblasts and fibroblasts, respectively (68). Perren and Cordey (69) defined the upper limits of mechanical stimulation of fracture healing. Their inter-fragmentary strain theory states that the tissue within the fracture gap must be capable of withstanding the strain produced by the IFM. They then suggested that rigid fixation of fractures should result in the healing process commencing at a later stage. This was later contradicted by the study of Goodship and Kenwright (16) that showed that a certain level of micro-movement accelerated aspects of the healing process. However, their inter-fragmentary strain theory certainly governs what tissues can exist and is particularly important in cases where tension is dominant.

The theory of Pauwels (68) was numerically investigated by Carter et al. (70). As a fracture callus is an internal three dimensional structure, it was not possible to study the strain *in vivo*. Using a finite element model of an idealized fracture geometry with soft callus they investigated what they called the osteogenic index, a relationship between hydrostatic pressure and octahedral shear stress.

$$I = \sum_{i=1}^c n_i (S_i + kD_i)$$

Where  $I$  is the osteogenic index,  $c$  is the number of load cases,  $n$  is the number of loading cycles,  $S_i$  is the cyclic octahedral shear stress,  $D_i$  is the cyclic hydrostatic pressure, and  $k$  is a scaling factor relating the two. They also recognized that the load applied to a fracture would not be constant, but vary between different

load cases. The osteogenic index was therefore a summation of the mechanical signals at these different load cases. The proposed theory also considered a distinction between tissues with poor and good bloody supply, with good blood supply being capable of forming all tissue types, but requiring significant hydrostatic pressure to form cartilage, whereas, tissue with poor blood supply formed either connective tissue or cartilage (70).

Prendergast and Huiskes (71) studied how the osteogenic index differed between the use of linear-elastic or poro-elastic material properties for the healing tissues. The aqueous nature of biological tissues, particularly soft tissues, means that representing them as a mixture of fluid and solid phases describes the tissue behavior more accurately than linear-elastic models. Using the experiments of Søballe et al. (35), where a loadable bone chamber was implanted in the femoral condyle of canines and the tissues, which formed under different loadings quantified cross-sectionally over a number of weeks, Prendergast and Huiskes (71) were able to determine that the poro-elastic model predicted the osteogenic index more appropriately when compared to tissue distributions in the experiment. They expanded on this work by developing a new theory, that the relative velocity between fluid, solid, and shear strain, rather than hydrostatic pressure and shear strain where the stimuli for tissue differentiation as described by **Figure 4A** (72).

$$S = \gamma/a + v/b$$

$$\text{Condition for bone : } S < S_{\text{bone}}$$

$$\text{Condition for cartilage : } S_{\text{bone}} < S < S_{\text{cartilage}}$$

$$\text{Condition for fibrous connective tissue : } S > S_{\text{cartilage}}$$

where  $\gamma$  is the deviatoric shear strain,  $v$  is the solid/fluid velocity, and  $a$  and  $b$  are empirically derived constants varying for each tissue type.

The relationship was defined as a summation of maximal distortional strain and relative velocity between fluid and solid (34). It is important to reiterate that this theory was developed from experiments using a bone chamber, which has a simple geometry known *a priori* that can be easily represented in finite element simulations with the applied loads being known. In contrast, the

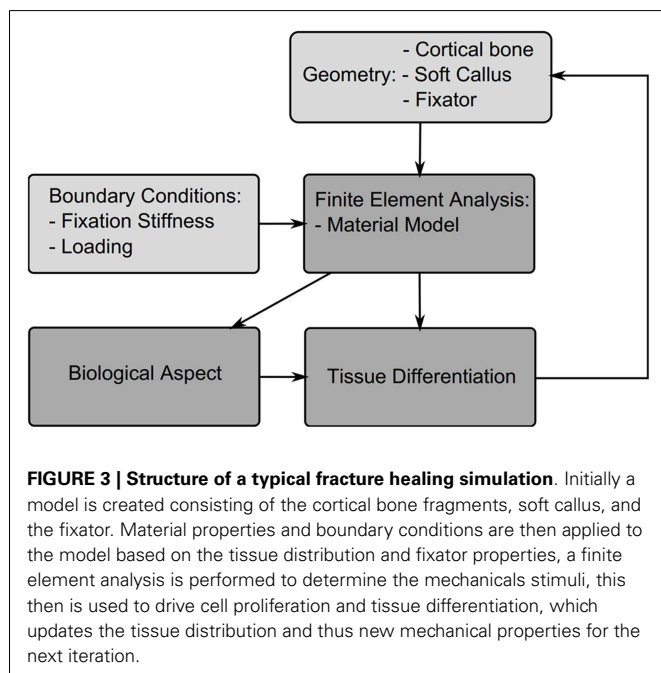
**Table 4 | Numerical studies.**

| <b>Author</b>                                 | <b>Application</b>                              | <b>Stimuli</b>                                  | <b>Validation/comparison</b>                  |
|---|---|---|---|
| Huiskes et al. (34)                           | Bone chamber                                    | Fluid/solid velocity<br>Shear strain            | Søballe et al. (35)                           |
| Ament and Hofer (36),<br>Palomares et al. (3) | Mid-diaphyseal fracture                         | Strain energy density                           | Claes et al. (11)                             |
| Lacroix and Prendergast (37)                  | Mid-diaphyseal fracture                         | Fluid/solid velocity<br>Shear strain            | Claes et al. (38)                             |
| Lacroix et al. (39)                           | Mid-diaphyseal fracture                         | Fluid/solid velocity<br>Shear strain            | None  |
| Bailón-Plaza and van der<br>Meulen (40)       | Mid-diaphyseal fracture                         | Dilatational strains<br>Deviatoric strains      | Goodship and Kenwright (16)                   |
| Geris et al. (41)                             | Bone chamber                                    | Fluid/solid velocity<br>Shear strain            | Unpublished pilot study and Geris et al. (41) |
| Shefelbine et al. (42)                        | Trabecular bone                                 | Dilatational strains<br>Deviatoric strains      | None  |
| Kelly and Prendergast (43)                    | Osteochondral defect                            | Fluid/solid velocity<br>Shear strain            | None  |
| Gomez-Benito et al. (44)                      | Mid-diaphyseal fracture                         | Second invariant of deviatoric<br>strain tensor | Claes et al. (38)                             |
| Pérez and Prendergast (45)                    | Bone-implant interface                          | Fluid/solid velocity<br>Shear strain            | None  |
| Isaksson et al. (46, 47)                      | Mid-diaphyseal fracture                         | Fluid/solid velocity<br>Shear strain            | None  |
| Geris et al. (48)                             | Bone chamber                                    | Fluid/solid velocity<br>Shear strain            | Geris et al. (48)                             |
| Chen et al. (49)                              | Mid-diaphyseal fracture                         | Dilatational strains<br>Deviatoric strains      | Claes et al. (11)                             |
| Hayward and Morgan (50)                       | Mid-diaphyseal fracture,<br>mouse               | Fluid/solid velocity<br>Shear strain            | Cullinane et al. (51)                         |
| Khayyeri et al. (52)                          | Bone chamber                                    | Fluid/solid velocity<br>Shear strain            | Tägil and Aspenberg (53)                      |
| Checa and Prendergast (54)                    | Total hip replacement,<br>stem–bone integration | Fluid/solid velocity<br>Shear strain            | None  |
| Isaksson et al. (55)                          | Mid-diaphyseal fracture                         | Fluid/solid velocity<br>Shear strain            | None  |
| Geris et al. (56)                             | Mid-diaphyseal fracture                         | Fluid/solid velocity<br>Hydrostatic pressure    | None  |
| Wehner et al. (57)                            | Tibial fracture                                 | Dilatational strains<br>Deviatoric strains      | Wehner et al. (57)                            |
| Simon et al. (58)                             | Mid-diaphyseal fracture                         | Dilatational strains<br>Deviatoric strains      | Claes et al. (11)                             |
| Byrne et al. (59)                             | Tibial fracture                                 | Fluid/solid velocity<br>Shear strain            | Richardson et al. (60)                        |

(Continued)

**Table 4 | Continued**

| Author               | Application             | Stimuli                                      | Validation/comparison  |
|----------------------|-------------------------|--|--|
| Witt et al. (61)     | Tibial fracture         | Principal strain with largest absolute value | Witt et al. (61)   |
| Burke and Kelly (62) | Mid-diaphyseal fracture | Substrate stiffness                          | Vetter et al. (9)  |
| Vetter et al. (63)   | Mid-diaphyseal fracture | Various                                      | Vetter et al. (9)  |
| Steiner et al. (64)  | Mid-diaphyseal fracture | Dilatational strains<br>Deviatoric strains   | Vetter et al. (9)  |
| Steiner et al. (65)  | Mid-diaphyseal fracture | Dilatational strains<br>Deviatoric strains   | Epari et al. (66), Bottlang et al. (67), Schell et al. (29), Hente et al. (33), Bishop et al. (27) |



boundaries of the callus are not known exactly and the loading is an approximation of the physiological condition.

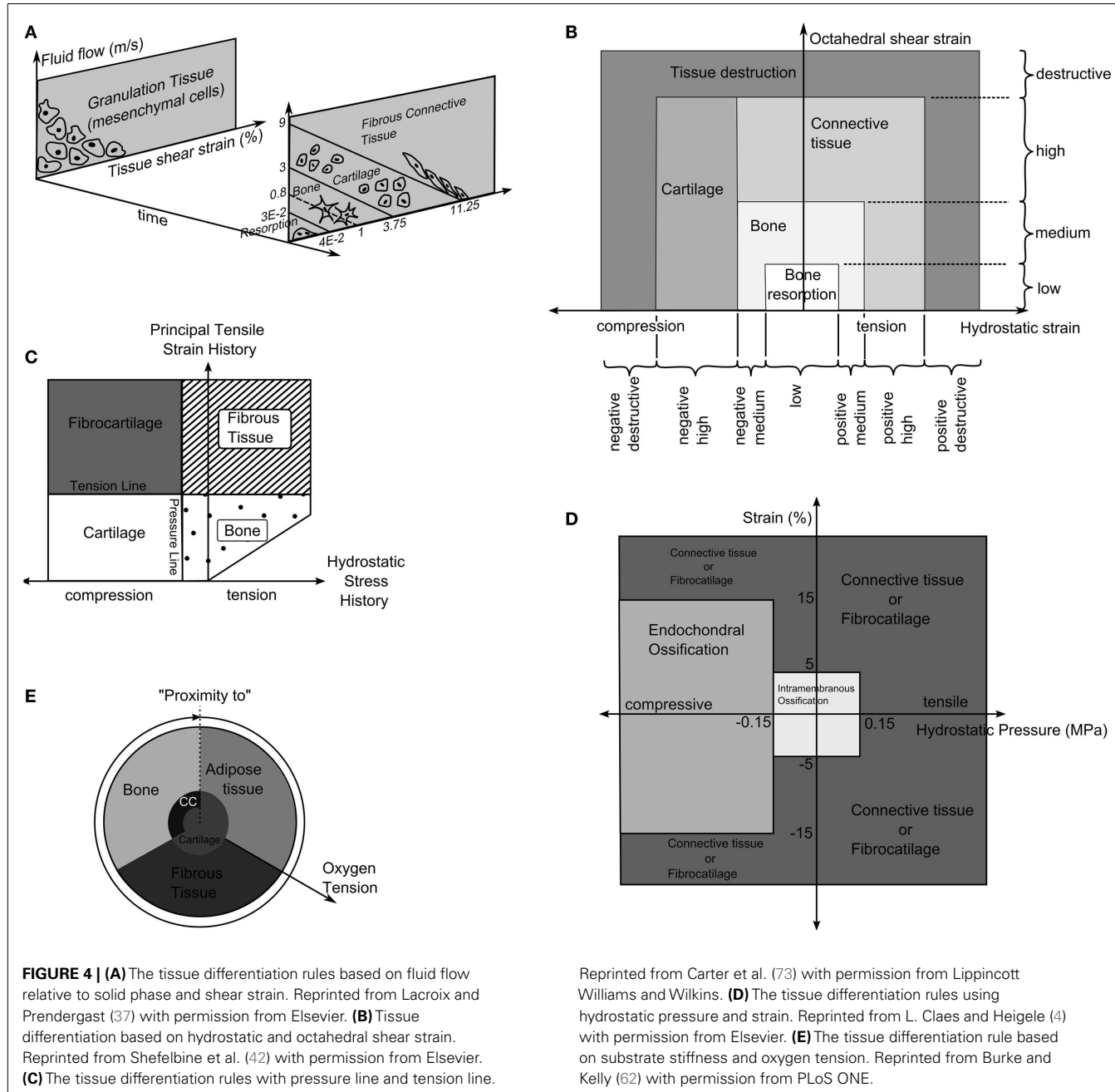
Carter et al. (73) proposed that tissue differentiation was determined through tensile principal strain and hydrostatic pressure as shown in **Figure 4C**. High principal tensile strains result in fibrous tissue when pressure is low and fibrocartilage when pressure is high, whereas, low principal tensile strains results in bone and cartilage when pressure is low or high, respectively.

The theory of Pauwels (68) was revisited by Claes et al. (38) who in a large interdisciplinary study compared the tissue distribution of healing tibial fractures in an animal study and equivalent finite element study. They attempted to determine the values of hydrostatic pressure and axial strains, which caused differing tissue differentiation. They determined that below a hydrostatic pressure of 0.15 MPa and strain <5% stimulate intramembranous ossification, compressive hydrostatic pressure >0.15 MPa and strain <15% stimulated endochondral ossification and that pressure and strain outside of these regions resulted in fibrous tissue or cartilage,

as shown in **Figure 4D**. Claes and Heigle (4) then proposed ossification only occurs on an existing bony surface. While they did not develop a simulation, they created FE models, which represented the healing callus at different stages and correlated the stress and strain from these models with histological sections from an animal study, which was performed in parallel.

Ament and Hofer (36) presented a simulation using a fuzzy logic controller with nine linguistic rules, which defined how levels of SED and the concentration of bone in neighboring elements to control the differentiation of elements into three tissue types, cartilage, bone, and fibrous connective tissue. The SED could be within four different levels; low, physiological, increased, and pathological. These were independent of the tissue type, as SED is relatively invariant to tissue type. Results were compared with the experiments of Claes et al. (11) and showed strong similarities in the reduction of IFM over time.

Fuzzy logic was again used by Shefelson et al. (42), modeling trabecular regeneration. Their model was based on the proposed relationship of Claes and Heigle (4). However, they modified the tissue differentiation theory replacing the hydrostatic pressure criteria with an equivalent volumetric strain. Thus, the mechanical stimuli became volumetric strain and octahedral shear strain, described in **Figure 4B**. This model had 21 linguistic rules to describe how tissue differentiated; it considered three tissue types, bone, cartilage, and fibrous tissue. In addition, vascularization was also modeled using fuzzy rules. The simulation required the strains in a particular element to reach a certain range before tissue within the element began differentiating, for bone to form the elements must also have sufficient vascularity while cartilage formed independently of vascularity. The vascularity was also driven mechanically only advancing to elements within an acceptable strain level. The model was implemented as a three dimensional linear-elastic simulation. While this model can capture the events of bone regeneration, Steiner et al. (65) conducted a parameter study of fixator stiffness, which encompassed values used several *in vivo* studies and achieved comparable outcomes, it is a linguistic representation of observed phenomenon. Thus it is entirely phenomenological and does not encompass any underlying mechanism in physical or chemical terms. This raises issues with regards scaling, should the resolution of the model or length of the iteration change, as there is no governing equation.



## BIOLOGICAL ASPECTS

The majority of simulations included an additional level often described as the biological aspect. As Claes and Heigle (4) observed the front of healing bone follows a path, starting at the original cortical faces and advancing toward the fracture gap. The inclusion of biological aspects in the form of cell, revascularization, nutrient supply, or oxygen tension, allows ossification to follow such a path. These biological elements are typically modeled as diffusive processes (39), random walks (45, 74), or through logical association of neighboring elements (36, 42). While cell proliferation and revascularization are vital aspects of fracture healing, the interplay between mechanical forces and these processes are not

fully understood, in addition there is limited experimental data available so the validation of such model becomes much more difficult.

How the biologic aspect influences the course of fracture healing can vary, Lacroix et al. (39) considered cells diffusing within the callus and scaled the tissue stiffness according to cell destiny within an element. An issue exists with this approach, as the maturity of the tissue is determined purely by the cell number within and the tissue phenotype by the mechanical stimuli this allows mature cartilage to switch directly to mature bone. Kelly and Prendergast (43) similarly applied a scaling, but considered multiple cell phenotypes and so multiple tissues within a single element removing

this issue. Shefelbine et al. (42) considered nutrient supply to be the critical biological factor in bone development, and so bone could only form in areas with good vascularization. This was again used by Wehner et al. (57) and Simon et al. (58). Chen et al. (49) added an additional level to this considering nutrient diffusion from the developing vasculature.

Burke and Kelly (62) proposed a theory in which tissue differentiation is indirectly driven by mechanical forces. Revascularization is allowed on in elements where the deviatoric strain is below a level of 6%. The blood vessels were assumed to diffuse into the tissue.

$$\int_{\Omega_{\gamma<0.06}} \frac{dV}{dt} dx = \int_{\Omega_{\gamma<0.06}} 0.5 \times \Delta V dx$$

Where  $V$  is the vascularity,  $\gamma$  is the deviatoric strain, and  $\Omega$  is the computational domain with all elements where this strain was  $<6\%$ . The oxygen is then assumed to diffuse from the vasculature without any dependence on the local mechanical environment.

$$\int_{\Omega} \frac{dO_2}{dt} dx = \int_{\Omega} D \Delta O_2 - Q \cdot n^{\max} n dx$$

Here  $O_2$  is the oxygen concentration,  $D$  is the diffusion coefficient of oxygen in the tissue,  $Q$  is the oxygen consumption rate of cells in the tissue, and  $n$  represents the number of cells in the element and  $n^{\max}$  the maximum cell density. The tissues then differentiated based on the oxygen tension and the stiffness of neighboring elements as described in **Figure 4E**.

Several models exist which consider purely biological factors in fracture healing, Bailon-Plaza and Van Der Meulen (75) first proposed a model for bone regeneration, which included diffusion of stem cells, and various growth factors, but no mechanical feedback. Geris et al. (76) applied this model to simulate the healing of tibial fractures in mice, finding that the model could predict the course of healing, but was sensitive to initial levels of growth factor production. Geris et al. (56) investigated if mechanical regulation of angiogenesis and growth factor production could improve this model and account for load induced non-unions, and concluded that mechanical feedback for both angiogenesis and osteogenesis was required to correctly predict unions and non-unions. Later changes to this model have excluded mechanics and focused on more detailed representations of angiogenesis (77, 78).

These theories consider cell density in homogenous tissue elements and apply rules for motion, differentiation, and proliferation to the cell population based upon tissue level stimuli. *In vivo*, the structure of tissues within callus is microscopically heterogeneous, thus mechanical stimuli at the tissue level are not easily translated to the cellular level. While at the tissue level, strains and perfusion of interstitial fluid (ISF) in the callus can be accurately determined, the stimulation they cause at the cellular level will be different for each cell within a tissue element due to the heterogeneity. This has not yet been quantified *in vivo*, however, fluid dynamic studies of perfusion bioreactors can lend insights as to the heterogeneity of mechanical stimuli when fluid is perfused through a structure at physiological rates. Zermatten et al. (79) used high resolution micro computed tomography (micro-CT)

images of bone tissue engineering scaffolds. Fluid dynamic simulations of medium perfusion showed the wall shear stress within a scaffold had a wide range of values. It has been known for some time that *in vitro* osteoblastic differentiation and bone formation are augmented with ISF flow (80), however, application of this biological information *in silico* will require more detailed models of the tissue structure.

The features all these biological aspects share are the boundary conditions, considering the periosteum of the cortical fragments and the surrounding tissue at the source of cells, nutrients, or vascular tissue. The propagation of these are mainly all diffusive processes, though for ease of implementation and to reduce computational power required implementations have varied, the random walk used by Pérez and Prendergast (45) and fuzzy logic of Shefelbine et al. (42) allowed diffusive behavior without the computational cost of solving the diffusion equation numerically.

## COMPARISON OF MODEL PERFORMANCE

Validation of models has remained a significant problem, looking at **Table 4** approximately half of the studies have no experimental reference. The study of Claes et al. (11) has frequently been used as a comparison due to clear experimental method and inclusion of IFC values longitudinally as well as histological slices obtained cross-sectionally. However, while the IFC data are available no quantitative comparison has been made between simulations and the results, instead visually comparing general trends and histological slices has predominated. In **Figure 5**, we see simulation results from (A) Burke and Kelly (62), (B) Lacroix and Prendergast (37), and (C) Steiner et al. (65) these all consist of a uniform cortical bone and callus geometry, which is made up of non-uniform finite elements, in the case of Burke and Kelly (62) and Lacroix and Prendergast (37) they are two dimensional axisymmetric simulations and in Steiner et al. (65) three dimensional. **Figure 5D** is a histological section from an *in vivo* study by Claes and Heigle (4); we see the callus is non-uniform and asymmetric. This mismatch between the asymmetric callus in the histological images and uniformly simulated calluses complicates direct comparison, additionally axisymmetric boundary conditions implies the simulation should match every quadrant of the histological slice, which is clearly impossible, when using three dimensional models like Steiner et al. (65) one must also find the correct slice of the model to compare to the histology. Vetter et al. (63) compared the use of volumetric strain, deviatoric strain, greatest-shear strain, and principal strain as stimuli for tissue differentiation. Through carrying out a parametric study they found that all of these could accurately predict bone healing within a range of thresholds. They used quantitative metrics to assess the accuracy, comparing averaged histological sections from Vetter et al. (9) with simulated images. This allowed the comparison of volume fraction and number of co-located pixels. However, this work was in two dimensions and thus did not consider IFS or IFB. The data of Vetter et al. (9) were later used a visual comparison by Burke and Kelly (62), who showed their simulations appeared to agree well with the results, however, no quantitative comparison was used.

There are several studies comparing the performance of the different tissue differentiation theories. Isaksson et al. (81) and Epari et al. (82) both compared the models of Prendergast and Huiskes

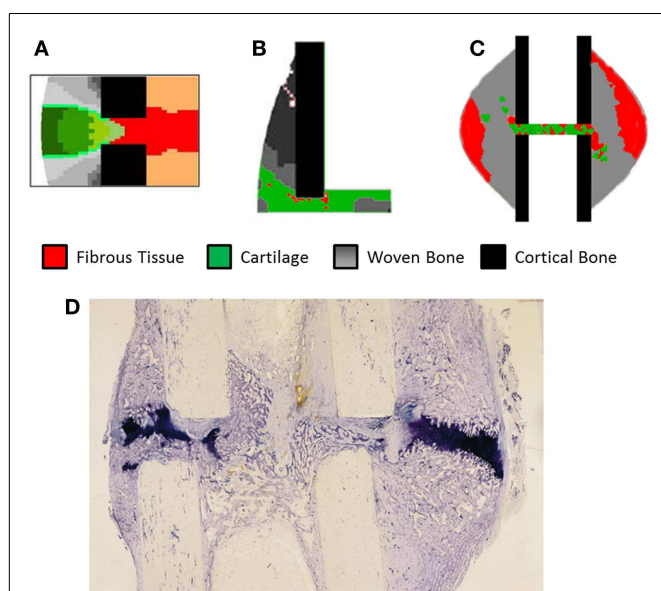


**FIGURE 5 |**The results of fracture healing simulations, **(A)** Burke and Kelly (62) reprinted with permission from PLoS ONE. **(B)** Lacroix and Prendergast (37) reprinted with permission from Elsevier. **(C)** Steiner et al. (65) reprinted with permission from PLoS ONE. **(D)** Histological section of healing ovine tibia, new woven bone is lightly stained, while cartilage is darkly stained. Reprinted with permission from Elsevier.

(71) and Claes and Heigele (4). Both used three dimensional models with poro-elastic element properties, however, different results were presented for similar load cases. Isaksson et al. (81) found that under  $7.2^\circ$  of torsion only the model of Prendergast and Huiskes (71) correctly predicted healing. While Epari et al. (82) found that for  $10^\circ$  of torsion both models predicted fracture healing. The differences can possibly be explained through differences in material properties, with Isaksson et al. (81) using an elastic modulus for the granulation tissue an order of magnitude larger than Epari et al. (82). However, the mechanical properties for all of the tissues included by Epari et al. (82) are not listed, making a complete comparison not possible. One further erroneous element is the formation of unconnected bone in both studies when using the Claes and Heigele (4) differentiation theory. This theory explicitly states that ossification occurs in the soft tissue contacting the surface of existing bone, and that the rest of the callus is fibrous tissue unless a pressure of  $-0.15$  MPa is present and then it becomes cartilage. The formation of unconnected bone can only imply that both implementations did not consider this aspect of the differentiation rules, and applied the surface ossification rules throughout the callus. To complicate this further Klein et al. (30) and Bishop et al. (27) found contradictory results for healing under torsional loading. The theory of Shefelbine et al. (42) is essentially an equivalent theory to Claes and Heigele (4) except it uses deviatoric and dilatational stress and strain rather than stress. This model has been used by Steiner et al. (64), Wehner et al. (57), and Simon et al. (58). Steiner et al. (64) demonstrated that with the correct threshold values the model could predict union for the cases of IFC and IRF, but non-union for IFS.

Isaksson et al. (83) again compared the theories of Claes and Heigele (4) and Prendergast and Huiskes (71), as well as Carter et al. (73). They found the theories predicted extremely similar temporal and spatial patterns in healing. In addition, they compared the volumetric components (relative fluid solid velocity and pore pressure) of the theories with the distortional components, finding that deviatoric strain alone could also predict similar tissue formations, whereas, volumetric components such as pore pressure and fluid velocity could not predict healing by themselves. This is however contradicted by Isaksson et al. (81) who found that the tissue formation predicted by deviatoric strain alone did not match *in vivo* data.

Hayward and Morgan (50) implemented a model using Prendergast and Huiskes (71) theory of tissue differentiation. They used three dimensional models based on micro-CT images of a mouse femur. The model correctly predicted a mechanically induced non-union and larger volume of cartilage formed due to the loading, but was not completely accurate in the patterns of tissue formation, predicting an excess of bone formation within the gap. Checa et al. (84) investigated if the Prendergast and Huiskes (71) theory could be directly applied different species, specifically rats and sheep. They reported that differences in healing between the species observed *in vivo* cannot be purely attributed to differences in loading and animal size, but also the thresholds for formation are different between, for sheep a larger mechanical stimuli was capable of forming bone, which in the case of the rat would result in cartilage. Given that Hayward and Morgan (50) did not scale these parameters for mice, this is a limitation of their study, which was not considered.

Another form of validation is possible; instead of using results directly from fracture healing one can compare how algorithms perform when modeling a bone chamber. Geris et al. (48) compared the differentiation rules of Prendergast and Huiskes (71), Carter et al. (73), and Claes and Heigele (4) against tissue formation in a bone chamber. They concluded that the models only partially matched experimental findings, with models predicting cartilage formation, which was not observed experimentally. The implementation of Prendergast and Huiskes (71) algorithm did not consider bone resorption, which is found in the implementation of Lacroix and Prendergast (37). As the other algorithms do not include resorption this modification is understandable to enable comparison between them, however, it would be interesting to see if its inclusion increased or decreased the accuracy.

## OUTLOOK

Mechanical forces and bone regeneration are intrinsically linked. While there has been a vast amount of research on this topic, experimental comparison between studies is extremely difficult. The greatest difficulty comes from non-standard experimental setups, specifically, different defect sizes and use of modified and non-standard fixators. While great efforts have been made to characterize the movements and stiffness of devices, without knowing the true bone geometry and exact tissue composition it is difficult to determine the precise strains tissues are experiencing. These factors play a part in the validation of simulations using this data, as differences in geometry between simulation and experiments should cause different mechanical stimuli.

Validation of models with experimental data is crucial for all simulation work, and is the distinguishing factor between simulation and animation. What is clear is that in the field of bone regeneration, comparing the results of *in silico* studies with *in vivo* studies is not trivial. It is impossible to measure every factor simultaneously, yet models for fracture healing have become increasingly complicated. More factors are considered such as cellular events, revascularization, and even protein secretion. While validation of such models is not impossible it requires large cross-sectional studies, which have yet to be performed. To compound this, current models of bone regeneration all consider tissues as homogenous continuum, while woven bone is a macroscopically porous structure. The theories of Carter et al. (73), Claes and Heigele (4), and Prendergast et al. (72) are based on comparing the results of continuum finite element analyzes with histological data, and correlating the areas where bone has formed with the local mechanical environment. The histological data were the result of cross-sectional studies, so while they could observe the formation of woven bone, they could not see how individual structures evolved. One solution to this problem lies in *in vivo* micro-CT. Micro-CT uses two dimensional X-ray images of a sample taken from multiple directions to reconstruct a three dimensional image of the sample. The application of *in vivo* micro-CT means time-lapsed longitudinal studies can be performed, where the same animals can be imaged at several time points. These images can then be compared, highlighting the changes in the regenerating tissue. When combined with a well-defined loading regime an equivalent finite element analysis can be performed using the micro-CT images as a basis. The results of which can be compared to the changes in tissue observed *in vivo*, allowing the validation or falsification of current theories for tissue differentiation.

The development and maturation of the callus (reactive and reparative phase) is a single aspect of fracture healing, eventually the bone must remodel to its original form, while Lacroix and Prendergast (37) include this, it has never been shown that this is the correct mechanism. Schell et al. (8) have shown that early in the healing process osteoclasts are present, and that cortical bone closest to the defect gets remodeled into woven bone, then back to cortical. With *in vivo* micro-CT based studies this remodeling can be quantified. With quantitative data remodeling theories can be corroborated. Such a study could provide a window into the relationship between cortical remodeling and trabecular remodeling and what causes the differentiation between the two.

Subject specific simulations are a necessity, allowing direct comparison between simulations and experimental results on a sample by sample basis. Currently, no study has performed an animal specific simulation and determined if the simulation produces results without a significant difference to the *in vivo* results. This will remove the any error associated with averaging experimental results so they can be compared to simulations using idealized geometry. Additionally simulations using realistic geometry and loading conditions will allow the effects of the non-uniform bone geometry and strain distribution within the callus to be quantified. In **Figure 5D**, we can see clearly how asymmetric the callus is, and that on the left side of the bone cartilage has formed within the osteotomy gap whereas on the right side of the image the cartilage is bridging the larger hard callus. The asymmetry of the

bone, callus, and loading cannot be captured in axisymmetric models and only partially using idealized models of the geometry. This geometric information will be the product of studies using *in vivo* micro-CT. What parameters should be compared between such models is an open question, which must be addressed first. Work already presented in the field of bone remodeling and adaptation (85) provides a basis for what can be measured, and models for bone remodeling such as Schulte et al. (86) may also be incorporated in simulations, representing the remodeling phase.

## CONCLUSION

This review has presented how the mechanical models and experiments of fracture healing have developed since Pauwels (68) first proposed his theory. The differences between the types of data produced by simulations and experimental studies remains an obstacle for advancing the field. Existing rules without exception have all been derived from two dimensional continuum finite element models, though associating the simulated mechanical stimuli to tissue growth seen in histological section from cross-sectional a study. As more detailed, quantitative and longitudinal data are being gathered experimentally these rules must be re-examined, their accuracy assessed using longitudinal time-lapsed data. With simulations there is a need for simulations to move away from simplified representations of the geometry with continuum material properties, toward real bone microstructural geometries measured through micro-CT, so as to allow direct and quantitative comparison of their predicted tissue distribution directly to the results of *in vivo* studies, rather than a visual comparison with single histological slices.

## ACKNOWLEDGMENTS

The authors gratefully acknowledge financial support from the European Union (BIODESIGN FP7-NMP-2012-262948).

## REFERENCES

1. Mills LA, Simpson AHRW. The relative incidence of fracture non-union in the Scottish population (5.17 million): a 5-year epidemiological study. *BMJ Open* (2013) 3:e002276. doi:10.1136/bmopen-2012-002276
2. Carter DR. Mechanical loading history and skeletal biology. *J Biomech* (1987) 20(11):1095–109. doi:10.1016/0021-9290(87)90027-3
3. Palomares KTS, Gleason RE, Mason ZD, Cullinane DM, Einhorn TA, Gerstenfeld LC, et al. Mechanical stimulation alters tissue differentiation and molecular expression during bone healing. *J Orthop Res* (2009) 27(9):1123–32. doi:10.1002/jor.20863
4. Claes L, Heigele C. Magnitudes of local stress and strain along bony surfaces predict the course and type of fracture healing. *J Biomech* (1999) 32(3):255–66. doi:10.1016/S0021-9290(98)00153-5
5. Taylor DK, Meganck JA, Terkhorn S, Rajani R, Naik A, O’Keefe RJ, et al. Thrombospondin-2 influences the proportion of cartilage and bone during fracture healing. *J Bone Miner Res* (2009) 24(6):1043–54. doi:10.1359/jbmr.090101
6. Thompson Z, Miclau T, Hu D, Helms JA. A model for intramembranous ossification during fracture healing. *J Orthop Res* (2002) 20(5):1091–8. doi:10.1016/S0736-0266(02)00017-7
7. Einhorn TA. The cell and molecular biology of fracture healing. *Clin Orthop Relat Res* (1998) 355:S7–21. doi:10.1097/00003086-199810001-00003
8. Schell H, Lienau J, Epari DR, Seebek P, Exner C, Muchow S, et al. Osteoclastic activity begins early and increases over the course of bone healing. *Bone* (2006) 38(4):547–54. doi:10.1016/j.bone.2005.09.018
9. Vetter A, Epari DR, Seidel R, Schell H, Fratzl P, Duda GN, et al. Temporal tissue patterns in bone healing of sheep. *J Orthop Res* (2010) 28(11):1440–7. doi:10.1002/jor.21175

10. Utting JC, Flanagan AM, Brandao-Burch A, Orriss IR, Arnett TR. Hypoxia stimulates osteoclast formation from human peripheral blood. *Cell Biochem Funct* (2010) **28**(5):374–80. doi:10.1002/cbf.1660
11. Claes L, Augat P, Suger G, Wilke H-J. Influence of size and stability of the osteotomy gap on the success of fracture healing. *J Orthop Res* (1997) **15**(4):577–84. doi:10.1002/jor.1100150414
12. Gardner MJ, van der Meulen MC, Demetrikopoulos D, Wright TM, Myers ER, Bostrom MP. In vivo cyclic axial compression affects bone healing in the mouse tibia. *J Orthop Res* (2006) **24**(8):1679–86. doi:10.1002/jor.20230
13. Gardner MJ, Putnam SM, Wong A, Streubel PN, Kotiya A, Silva MJ. Differential fracture healing resulting from fixation stiffness variability: a mouse model. *J Orthop Sci* (2011) **16**(3):298–303. doi:10.1007/s00776-011-0051-5
14. Garcia P, Holstein JH, Maier S, Schaumlöffel H, Al-Marrawi F, Hannig M, et al. Development of a reliable non-union model in mice. *J Surg Res* (2008) **147**(1):84–91. doi:10.1016/j.jss.2007.09.013
15. Holstein JH, Matthys R, Histing T, Becker SC, Fiedler M, Garcia P, et al. Development of a stable closed femoral fracture model in mice. *J Surg Res* (2009) **153**(1):71–5. doi:10.1016/j.jss.2008.02.042
16. Goodship A, Kenwright J. The influence of induced micromovement upon the healing of experimental tibial fractures. *J Bone Joint Surg Br* (1985) **67**(4):650–5.
17. Klein P, Schell H, Streitparth F, Heller M, Kassi J-P, Kandziora F, et al. The initial phase of fracture healing is specifically sensitive to mechanical conditions. *J Orthop Res* (2003) **21**(4):662–9. doi:10.1016/S0736-0266(02)00259-0
18. Schell H, Epari D, Kassi J, Bragulla H, Bail H, Duda G. The course of bone healing is influenced by the initial shear fixation stability. *J Orthop Res* (2005) **23**(5):1022–8. doi:10.1016/j.orthres.2005.03.005
19. Goodship AE, Cunningham JL, Kenwright J. Strain rate and timing of stimulation in mechanical modulation of fracture healing. *Clin Orthop Relat Res* (1998) **355**:S105–15. doi:10.1097/00003086-199810001-00012
20. Goodship AE, Lawes TJ, Rubin CT. Low-magnitude high-frequency mechanical signals accelerate and augment endochondral bone repair: preliminary evidence of efficacy. *J Orthop Res* (2009) **27**(7):922–30. doi:10.1002/jor.20824
21. Kenwright J, Goodship A, Kelly D, Newman J, Harris J, Richardson J, et al. Effect of controlled axial micromovement on healing of tibial fractures. *Lancet* (1986) **328**(8517):1185–7. doi:10.1016/S0140-6736(86)92196-3
22. Kenwright J, Richardson J, Cunningham J, White S, Goodship A, Adams M, et al. Axial movement and tibial fractures. A controlled randomised trial of treatment. *J Bone Joint Surg Br* (1991) **73**(4):654–9.
23. Claes L, Eckert-Hübner K, Augat P. The effect of mechanical stability on local vascularization and tissue differentiation in callus healing. *J Orthop Res* (2002) **20**(5):1099–105. doi:10.1016/S0736-0266(02)00044-X
24. Claes L, Eckert-Hübner K, Augat P. The fracture gap size influences the local vascularization and tissue differentiation in callus healing. *Langenbecks Arch Surg* (2003) **388**(5):316–22. doi:10.1007/s00423-003-0396-0
25. Cheal E, Mansmann K, DiGioia A III, Hayes W, Perren S. Role of interfragmen-tary strain in fracture healing: ovine model of a healing osteotomy. *J Orthop Res* (1991) **9**(1):131–42. doi:10.1002/jor.1100090116
26. Mark H, Nilsson A, Nannmark U, Rydevik B. Effects of fracture fixation stability on ossification in healing fractures. *Clin Orthop Relat Res* (2004) **419**:245–50. doi:10.1097/00003086-200402000-00040
27. Bishop N, Van Rhijn M, Tami I, Corveleijn R, Schneider E, Ito K. Shear does not necessarily inhibit bone healing. *Clin Orthop Relat Res* (2006) **443**:307–14. doi:10.1097/01.blo.0000191272.34786.09
28. Park S-H, O'CONNOR K, McKellop H, Sarmiento A. The influence of active shear or compressive motion on fracture-healing\*. *J Bone Joint Surg Am* (1998) **80**(6):868–78.
29. Schell H, Thompson MS, Bail HJ, Hoffmann J-E, Schill A, Duda GN, et al. Mechanical induction of critically delayed bone healing in sheep: radiological and biomechanical results. *J Biomech* (2008) **41**(14):3066–72. doi:10.1016/j.biomech.2008.06.038
30. Klein P, Opitz M, Schell H, Taylor W, Heller M, Kassi J-P, et al. Comparison of unreamed nailing and external fixation of tibial diastases – mechanical conditions during healing and biological outcome. *J Orthop Res* (2004) **22**(5):1072–8. doi:10.1016/j.orthres.2004.02.006
31. Lienau J, Schell H, Duda GN, Seebeck P, Muchow S, Bail HJ. Initial vascularization and tissue differentiation are influenced by fixation stability. *J Orthop Res* (2005) **23**(3):639–45. doi:10.1016/j.orthres.2004.09.006
32. Epari DR, Schell H, Bail HJ, Duda GN. Instability prolongs the chondral phase during bone healing in sheep. *Bone* (2006) **38**(6):864–70. doi:10.1016/j.bone.2005.10.023
33. Hente R, Füchtmeier B, Schlegel U, Ernstberger A, Perren S. The influence of cyclic compression and distraction on the healing of experimental tibial fractures. *J Orthop Res* (2004) **22**(4):709–15. doi:10.1016/j.orthres.2003.11.007
34. Huiskes R, Van Driel W, Prendergast P, Søballe K. A biomechanical regulatory model for periprosthetic fibrous-tissue differentiation. *J Mater Sci Mater Med* (1997) **8**(12):785–8.
35. Søballe K, Hansen ES, B-Rasmussen H, Jørgensen PH, Bünger C. Tissue ingrowth into titanium and hydroxyapatite-coated implants during stable and unstable mechanical conditions. *J Orthop Res* (1992) **10**(2):285–99. doi:10.1002/jor.1100100216
36. Ament C, Hofer E. A fuzzy logic model of fracture healing. *J Biomech* (2000) **33**(8):961–8. doi:10.1016/S0021-9290(00)00049-X
37. Lacroix D, Prendergast P. A mechano-regulation model for tissue differentiation during fracture healing: analysis of gap size and loading. *J Biomech* (2002) **35**(9):1163–71. doi:10.1016/S0021-9290(02)00086-6
38. Claes LE, Heigle CA, Neidlinger-Wilke C, Kaspar D, Seidl W, Margevicius KJ, et al. Effects of mechanical factors on the fracture healing process. *Clin Orthop Relat Res* (1998) **355**:S132–47. doi:10.1097/00003086-199810001-00015
39. Lacroix D, Prendergast P, Li G, Marsh D. Biomechanical model to simulate tissue differentiation and bone regeneration: application to fracture healing. *Med Biol Eng Comput* (2002) **40**(1):14–21. doi:10.1007/BF02347690
40. Bailón-Plaza A, van der Meulen MC. Beneficial effects of moderate, early loading and adverse effects of delayed or excessive loading on bone healing. *J Biomech* (2003) **36**(8):1069–77. doi:10.1016/S0021-9290(03)00117-9
41. Geris L, Andreykiv A, Oosterwyck HV, Sloten JV, Keulen F, van Duyck J, et al. Numerical simulation of tissue differentiation around loaded titanium implants in a bone chamber. *J Biomech* (2004) **37**(5):763–9. doi:10.1016/j.jbiomech.2003.09.026
42. Shefelbine SJ, Augat P, Claes L, Simon U. Trabecular bone fracture healing simulation with finite element analysis and fuzzy logic. *J Biomech* (2005) **38**(12):2440–50. doi:10.1016/j.jbiomech.2004.10.019
43. Kelly D, Prendergast PJ. Mechano-regulation of stem cell differentiation and tissue regeneration in osteochondral defects. *J Biomech* (2005) **38**(7):1413–22. doi:10.1016/j.jbiomech.2004.06.026
44. Gomez-Benito M, Garcia-Aznar J, Kuiper J, Doblaré M. Influence of fracture gap size on the pattern of long bone healing: a computational study. *J Theor Biol* (2005) **235**(1):105–19. doi:10.1016/j.jtbi.2004.12.023
45. Pérez M, Prendergast P. Random-walk models of cell dispersal included in mechanobiological simulations of tissue differentiation. *J Biomech* (2007) **40**(10):2244–53. doi:10.1016/j.jbiomech.2006.10.020
46. Isaksson H, van Donkelaar CC, Huiskes R, Yao J, Ito K. Determining the most important cellular characteristics for fracture healing using design of experiments methods. *J Theor Biol* (2008) **255**(1):26–39. doi:10.1016/j.jtbi.2008.07.037
47. Isaksson H, van Donkelaar CC, Huiskes R, Ito K. A mechano-regulatory bone-healing model incorporating cell-phenotype specific activity. *J Theor Biol* (2008) **252**(2):230–46. doi:10.1016/j.jtbi.2008.01.030
48. Geris L, Vandamme K, Naert I, Vander Sloten J, Duyck J, Van Oosterwyck H. Application of mechanoregulatory models to simulate peri-implant tissue formation in an *in vivo* bone chamber. *J Biomech* (2008) **41**(1):145–54. doi:10.1016/j.jbiomech.2007.07.008
49. Chen G, Niemeyer F, Wehner T, Simon U, Schuetz M, Pearcey M, et al. Simulation of the nutrient supply in fracture healing. *J Biomech* (2009) **42**(15):2575–83. doi:10.1016/j.jbiomech.2009.07.010
50. Hayward LNM, Morgan EF. Assessment of a mechano-regulation theory of skeletal tissue differentiation in an *in vivo* model of mechanically induced cartilage formation. *Biomech Model Mechanobiol* (2009) **8**(6):447–55. doi:10.1007/s10237-009-0148-3
51. Cullinane DM, Fredrick A, Eisenberg SR, Pacicca D, Elman MV, Lee C, et al. Induction of a neoarthrosis by precisely controlled motion in an experimental mid-femoral defect. *J Orthop Res* (2002) **20**(3):579–86. doi:10.1016/S0736-0266(01)00131-0
52. Khayyeri H, Checa S, Tägil M, Prendergast PJ. Corroboration of mechanobiological simulations of tissue differentiation in an *in vivo* bone chamber using

- a lattice-modeling approach. *J Orthop Res* (2009) **27**(12):1659–66. doi:10.1002/jor.20926
53. Tägil M, Aspenberg P. Cartilage induction by controlled mechanical stimulation in vivo. *J Orthop Res* (1999) **17**(2):200–4. doi:10.1002/jor.1100170208
54. Checa S, Prendergast PJ. A mechanobiological model for tissue differentiation that includes angiogenesis: a lattice-based modeling approach. *Ann Biomed Eng* (2009) **37**(1):129–45. doi:10.1007/s10439-008-9594-9
55. Isaksson H, Van Donkelaar CC, Ito K. Sensitivity of tissue differentiation and bone healing predictions to tissue properties. *J Biomech* (2009) **42**(5):555–64. doi:10.1016/j.jbiomech.2009.01.001
56. Geris L, Vander Sloten J, Van Oosterwyck H. Connecting biology and mechanics in fracture healing: an integrated mathematical modeling framework for the study of nonunions. *Biomech Model Mechanobiol* (2010) **9**(6):713–24. doi:10.1007/s10237-010-0208-8
57. Wehner T, Claes L, Niemeyer F, Nolte D, Simon U. Influence of the fixation stability on the healing time – a numerical study of a patient-specific fracture healing process. *Clin Biomech* (2010) **25**(6):606–12. doi:10.1016/j.clinbiomech.2010.03.003
58. Simon U, Augat P, Utz M, Claes L. A numerical model of the fracture healing process that describes tissue development and revascularisation. *Comput Methods Biomed Eng Biomed Engin* (2011) **14**(01):79–93. doi:10.1080/10255842.2010.499865
59. Byrne DP, Lacroix D, Prendergast PJ. Simulation of fracture healing in the tibia: mechanoregulation of cell activity using a lattice modeling approach. *J Orthop Res* (2011) **29**(10):1496–503. doi:10.1002/jor.21362
60. Richardson J, Cunningham J, Goodship A, O’Connor B, Kenwright J. Measuring stiffness can define healing of tibial fractures. *J Bone Joint Surg Br* (1994) **76**(3):389–94.
61. Witt F, Petersen A, Seidel R, Vetter A, Weinkamer R, Duda GN. Combined in vivo/in silico study of mechanobiological mechanisms during endochondral ossification in bone healing. *Ann Biomed Eng* (2011) **39**(10):2531–41. doi:10.1007/s10439-011-0338-x
62. Burke DP, Kelly DJ. Substrate stiffness and oxygen as regulators of stem cell differentiation during skeletal tissue regeneration: a mechanobiological model. *PLoS One* (2012) **7**(7):e40737. doi:10.1371/journal.pone.0040737
63. Vetter A, Witt F, Sander O, Duda G, Weinkamer R. The spatio-temporal arrangement of different tissues during bone healing as a result of simple mechanobiological rules. *Biomech Model Mechanobiol* (2012) **11**(1–2):147–60. doi:10.1007/s10237-011-0299-x
64. Steiner M, Claes L, Ignatius A, Niemeyer F, Simon U, Wehner T. Prediction of fracture healing under axial loading, shear loading and bending is possible using distortional and dilatational strains as determining mechanical stimuli. *J R Soc Interface* (2013) **10**:20130389. doi:10.1098/rsif.2013.0389
65. Steiner M, Claes L, Ignatius A, Simon U, Wehner T. Numerical simulation of callus healing for optimization of fracture fixation stiffness. *PLoS One* (2014) **9**(7):e101370. doi:10.1371/journal.pone.0101370
66. Epari DR, Kassi J-P, Schell H, Duda GN. Timely fracture-healing requires optimization of axial fixation stability. *J Bone Joint Surg Am* (2007) **89**(7):1575–85. doi:10.2106/JBJS.F.00247
67. Bottlang M, Lesser M, Koerber J, Doornink J, von Rechenberg B, Augat P, et al. Far cortical locking can improve healing of fractures stabilized with locking plates. *J Bone Joint Surg Am* (2010) **92**(7):1652–60. doi:10.2106/JBJS.I.01111
68. Pauwels F. Eine neue Theorie über den Einfluß mechanischer Reize auf die Differenzierung der Stützgewebe. *Zeitschrift für Anatomie und Entwicklungsgeschichte* (1960) **121**(6):478–515. doi:10.1007/BF00523401
69. Perren SM, Cordey J. The concept of interfragmentary strain. In: Uhthoff HK, Stahl E, editors. *Current Concepts of Internal Fixation of Fractures*. New York, NY: Springer (1980). p. 63–77.
70. Carter D, Blenman P, Beaupre G. Correlations between mechanical stress history and tissue differentiation in initial fracture healing. *J Orthop Res* (1988) **6**(5):736–48. doi:10.1002/jor.1100060517
71. Prendergast P, Huiskes R. Finite element analysis of fibrous tissue morphogenesis: a study of the osteogenic index using a biphasic approach. *Mech Comp Mater* (1996) **32**(2):209–18. doi:10.1007/BF02254782
72. Prendergast P, Huiskes R, Søballe K. Biophysical stimuli on cells during tissue differentiation at implant interfaces. *J Biomech* (1997) **30**(6):539–48. doi:10.1016/S0021-9290(96)00140-6
73. Carter DR, Beaupré GS, Giori NJ, Helms JA. Mechanobiology of skeletal regeneration. *Clin Orthop Relat Res* (1998) **355**:S41–55. doi:10.1097/00003086-199810001-00006
74. Byrne DP, Lacroix D, Planell JA, Kelly DJ, Prendergast PJ. Simulation of tissue differentiation in a scaffold as a function of porosity, Young’s modulus and dissolution rate: application of mechanobiological models in tissue engineering. *Biomaterials* (2007) **28**(36):5544–54. doi:10.1016/j.biomaterials.2007.09.003
75. Bailon-Plaza A, Van Der Meulen MC. A mathematical framework to study the effects of growth factor influences on fracture healing. *J Theor Biol* (2001) **212**(2):191–209. doi:10.1006/jtbi.2001.2372
76. Geris L, Gerisch A, Maes C, Carmeliet G, Weiner R, Vander Sloten J, et al. Mathematical modeling of fracture healing in mice: comparison between experimental data and numerical simulation results. *Med Biol Eng Comput* (2006) **44**(4):280–9. doi:10.1007/s11517-006-0040-6
77. Peiffer V, Gerisch A, Vandepitte D, Van Oosterwyck H, Geris L. A hybrid bioregulatory model of angiogenesis during bone fracture healing. *Biomech Model Mechanobiol* (2011) **10**(3):383–95. doi:10.1007/s10237-010-0241-7
78. Carlier A, Geris L, Bentley K, Carmeliet G, Carmeliet P, Van Oosterwyck H. MOSAIC: a multiscale model of osteogenesis and sprouting angiogenesis with lateral inhibition of endothelial cells. *PLoS Comput Biol* (2012) **8**(10):e1002724. doi:10.1371/journal.pcbi.1002724
79. Zermatten E, Vetsch JR, Ruffoni D, Hofmann S, Müller R, Steinfield A. Micro-computed tomography based computational fluid dynamics for the determination of shear stresses in scaffolds within a perfusion bioreactor. *Ann Biomed Eng* (2014) **42**(5):1085–94. doi:10.1007/s10439-014-0981-0
80. Hillsley M, Frangos J. Review: bone tissue engineering: the role of interstitial fluid flow. *Biotechnol Bioeng* (1994) **43**(7):573–81. doi:10.1002/bit.260430706
81. Isaksson H, van Donkelaar CC, Huiskes R, Ito K. Corroboration of mechanoregulatory algorithms for tissue differentiation during fracture healing: comparison with in vivo results. *J Orthop Res* (2006) **24**(5):898–907. doi:10.1002/jor.20118
82. Epari DR, Taylor WR, Heller MO, Duda GN. Mechanical conditions in the initial phase of bone healing. *Clin Biomech* (2006) **21**(6):646–55. doi:10.1016/j.clinbiomech.2006.01.003
83. Isaksson H, Wilson W, van Donkelaar CC, Huiskes R, Ito K. Comparison of biophysical stimuli for mechano-regulation of tissue differentiation during fracture healing. *J Biomech* (2006) **39**(8):1507–16. doi:10.1016/j.jbiomech.2005.01.037
84. Checa S, Prendergast PJ, Duda GN. Inter-species investigation of the mechanoregulation of bone healing: comparison of secondary bone healing in sheep and rat. *J Biomech* (2011) **44**(7):1237–45. doi:10.1016/j.jbiomech.2011.02.074
85. Levchuk A, Zwahlen A, Weigt C, Lambers FM, Badilatti SD, Schulte FA, et al. The Clinical Biomechanics Award 2012 – presented by the European Society of Biomechanics: large scale simulations of trabecular bone adaptation to loading and treatment. *Clin Biomech* (2014) **29**(4):355–62. doi:10.1016/j.clinbiomech.2013.12.019
86. Schulte FA, Zwahlen A, Lambers FM, Kuhn G, Ruffoni D, Betts D, et al. Strain-adaptive in silico modeling of bone adaptation: a computer simulation validated by in vivo micro-computed tomography data. *Bone* (2013) **52**(1):485–92. doi:10.1016/j.bone.2012.09.008

**Conflict of Interest Statement:** The authors declare that the research was conducted in the absence of any commercial or financial relationships that could be construed as a potential conflict of interest.

*Received: 17 October 2014; paper pending published: 05 November 2014; accepted: 23 November 2014; published online: 10 December 2014.*

*Citation: Betts DC and Müller R (2014) Mechanical regulation of bone regeneration: theories, models, and experiments. *Front. Endocrinol.* 5:211. doi:10.3389/fendo.2014.00211*

*This article was submitted to Bone Research, a section of the journal Frontiers in Endocrinology.*

*Copyright © 2014 Betts and Müller. This is an open-access article distributed under the terms of the Creative Commons Attribution License (CC BY). The use, distribution or reproduction in other forums is permitted, provided the original author(s) or licensor are credited and that the original publication in this journal is cited, in accordance with accepted academic practice. No use, distribution or reproduction is permitted which does not comply with these terms.*



# The effect of altering the mechanical loading environment on the expression of bone regenerating molecules in cases of distraction osteogenesis

**Mohammad M. Alzahrani<sup>1,2</sup>, Emad A. Anam<sup>1,3</sup>, Asim M. Makhdum<sup>1,3</sup>, Isabelle Villemure<sup>4,5</sup> and Reggie Charles Hamdy<sup>1\*</sup>**

<sup>1</sup> Division of Orthopaedic Surgery, Shriners Hospital for Children, Montreal Children Hospital, McGill University, Montreal, QC, Canada

<sup>2</sup> Department of Orthopaedic Surgery, University of Dammam, Dammam, Saudi Arabia

<sup>3</sup> Department of Orthopaedic Surgery, King Abdulaziz University, Jeddah, Saudi Arabia

<sup>4</sup> Department of Mechanical Engineering, École Polytechnique de Montréal, Montréal, QC, Canada

<sup>5</sup> Sainte-Justine University Hospital Center, Montréal, QC, Canada

**Edited by:**

Jonathan H. Tobias, University of Bristol, UK

**Reviewed by:**

Bronwen Evans, Cardiff University, UK  
Lee B. Meakin, University of Bristol, UK

**\*Correspondence:**

Reggie Charles Hamdy, Division of Orthopaedic Surgery, Shriners Hospital for Children, McGill University, 1529 Cedar Avenue, Montréal, QC H3G 1A6, Canada  
e-mail: rhamdy@shriners.mcgill.ca

Distraction osteogenesis (DO) is a surgical technique where gradual and controlled separation of two bony fragments following an osteotomy leads to the induction of new bone formation in the distracted gap. DO is used for limb lengthening, correction of bony deformities, and the replacement of bone loss secondary to infection, trauma, and tumors. Although DO gives satisfactory results in most cases, one major drawback of this technique is the prolonged period of time the external fixator has to be kept on until the newly formed bone consolidates thus leading to numerous complications. Numerous attempts at accelerating bone formation during DO have been reported. One specific approach is manipulation of the mechanical environment during DO by applying changes in the standard protocol of distraction. Attempts at changing this mechanical environment led to mixed results. Increasing the rate or applying acute distraction, led to poor bone formation in the distracted zone. On the other hand, the addition of compressive forces (such as weight bearing, alternating distraction with compression or by over-lengthening, and then shortening) has been reported to increase bone formation. It still remains unclear why these alterations may lead to changes in bone formation. While the cellular and molecular changes occurring during the standard DO protocol, specifically increased expression of transforming growth factor- $\beta$ 1, platelet-derived growth factor, insulin-like growth factor, basic fibroblast growth factor, vascular endothelial growth factor, and bone morphogenic proteins have been extensively investigated, the literature is sparse on the changes occurring when this protocol is altered. It is the purpose of this article to review the pertinent literature on the changes in the expression of various proteins and molecules as a result of changes in the mechanical loading technique in DO and try to define potential future research directions.

**Keywords:** mechanical loading, growth factor, distraction osteogenesis, bone regeneration, bone regenerating molecule

## INTRODUCTION

Distraction osteogenesis (DO) is a surgical technique first described by the Russian physician Ilizarov in the early 1950s (1, 2). This technique consists of performing an osteotomy to a bone that needs to be lengthened followed by gradual and controlled distraction of the two ends of the osteotomized bone. These mechanical forces of distraction lead to the induction and formation of new bone in the distracted gap (Figures 1 and 2) (1, 2). When the desired amount of lengthening is reached, the distraction is stopped but the external fixator is kept on until the newly formed bone in the distracted gap consolidates and becomes strong enough to withstand external forces after removal of the external fixator without bending or fracturing. The surgical technique of DO involves several temporal phases outlined below (3).

## LATENCY PHASE

The latency phase starts immediately following the osteotomy and lasts between 5 and 7 days. It allows the formation and organization of the hematoma and facilitates the recruitment of inflammatory cells and mesenchymal stem cells (4). This stage resembles the acute stage of fracture healing, including hematoma formation, immediate inflammatory response, and subsequent differentiation of stem cells into chondrocytes and osteoblasts (4).

## DISTRACTION PHASE

In this phase, following the latency period, distraction of the two bone segments is started at a specific rate and rhythm of 1.0 mm a day, divided into four increments. This protocol was shown – experimentally and clinically – by Ilizarov to be the optimal rate and rhythm of distraction for bone formation. Higher rates of

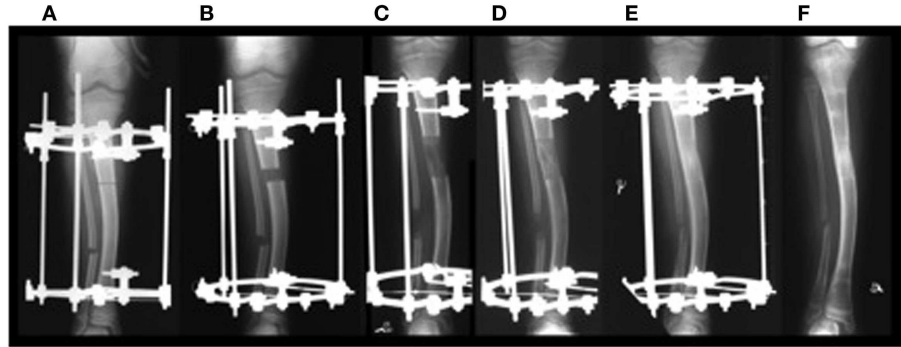


**FIGURE 1 | (A)** Application of distractor; **(B)** start of distraction; **(C)** end of distraction; **(D,E)** consolidation phase without any distraction until bone in the distraction gap consolidates; **(F)** removal of distractor. ©2012 Hamdy et al. (7).

distraction lead to poor or delayed regenerate bone formation while slower rates of distraction lead to premature consolidation (3). This phase is characterized by the formation of a radiolucent central fibrous interzone (FIZ) in the middle of the distracted gap (**Figure 2**). The fibroblast cells and collagen fibers are arranged longitudinally along the axis of distraction. In addition, one of the hallmarks of this phase is formation of new blood vessels with intense angiogenesis, neoangiogenesis, recruitment of osteoblasts, and new bone formation (5).

#### CONSOLIDATION PHASE

Once the desired amount of lengthening is obtained, distraction ceases, and the newly formed bone gradually bridges the gap between the two ends of the osteotomy (**Figure 2**). This new regenerate bone arises from the periosteum (hence, the importance of avoiding damage to the periosteum), the medullary canal, and the surrounding soft tissues (6). This phase is the longest phase in DO, about 1 month for each centimeter lengthened (1). In addition, it lasts until the newly formed bone in the distracted gap becomes biomechanically strong enough to allow removal of the fixator.

#### ADVANTAGES OF DO OVER OTHER TECHNIQUES OF BONE REGENERATION

Distraction osteogenesis is widely considered the best *in vivo* tissue engineering and has numerous advantages over other bone graft techniques, such as autografts, allografts, vascularized fibular grafts, and various artificial bone substitutes (7). With the technique of DO, very large and almost unlimited amounts of new bone can be generated and this newly formed bone is vascularized and of the same micro and macrostructure as the native bone. Furthermore, DO leads to the generation of new bone in a reproducible and predictable manner. One other major advantage of DO is the simultaneous regeneration and lengthening of all soft tissues surrounding the lengthened bone, including skin, subcutaneous tissues, blood vessels, nerves, and muscles (8).

#### CLINICAL APPLICATIONS OF DO

Nowadays, the technique of DO is widely used worldwide in the management of numerous orthopedic conditions including gradual correction of bony deformities, limb lengthening, and

management of bone loss secondary to infection, trauma, and tumors (**Figure 3**) (7,9). Currently, this technique has been applied in maxillofacial surgery for mandibular lengthening and in the treatment of craniofacial deformities (10). DO has also gained popularity in the field of dental surgery (11–13).

#### PROBLEMS ASSOCIATED WITH DO

Although DO gives satisfactory results in most cases, one of the drawbacks of this technique is the prolonged length of time the external fixator has to be kept in place until the newly formed bone in the distracted gap consolidates. For every centimeter lengthened, the fixator has to be kept in place for about a month. For example, a child undergoing a 6.0 cm lengthening will require the fixator to be kept in place for about 6 months. This prolonged length of time during which the fixator is kept in place, may increase the risk of complications, such as pin site infections, pain, discomfort, and psychological complications (**Figure 4**) (14, 15).

Numerous methods have been described in an attempt to accelerate the consolidation of the newly formed bone and hence allow early removal of the fixator (16). Most of these techniques are invasive and involve the local application of substances such as osteogenic growth factors, allografts, autografts, mesenchymal stem cells, various synthetic bone substitutes (such as TCP – tricalcium phosphates), the systemic application of bone stimulating pharmacological agents or the use of external stimulation such as electromagnetic fields (17).

One area that has been surprisingly less extensively investigated in this context is the mechanical loading environment in DO and whether changes in this mechanical environment during the process of DO may have an impact on bone formation and consolidation (**Figure 5**) (18–20). Ilizarov discovered that when gradual and controlled distraction is applied to the two ends of an osteotomized bone, new bone would form in the distraction gap (1, 6). He called this phenomenon the “Law of Tension Stress.” In fact, without knowing it and long before the term mechanotransduction was coined for the first time by Harold Frost in the 1960s (21), Ilizarov laid the foundation of the whole field of mechanotransduction, where the mechanical forces of distraction applied during the process of DO are translated into molecular signals that lead to the induction of new regenerate bone (the tension

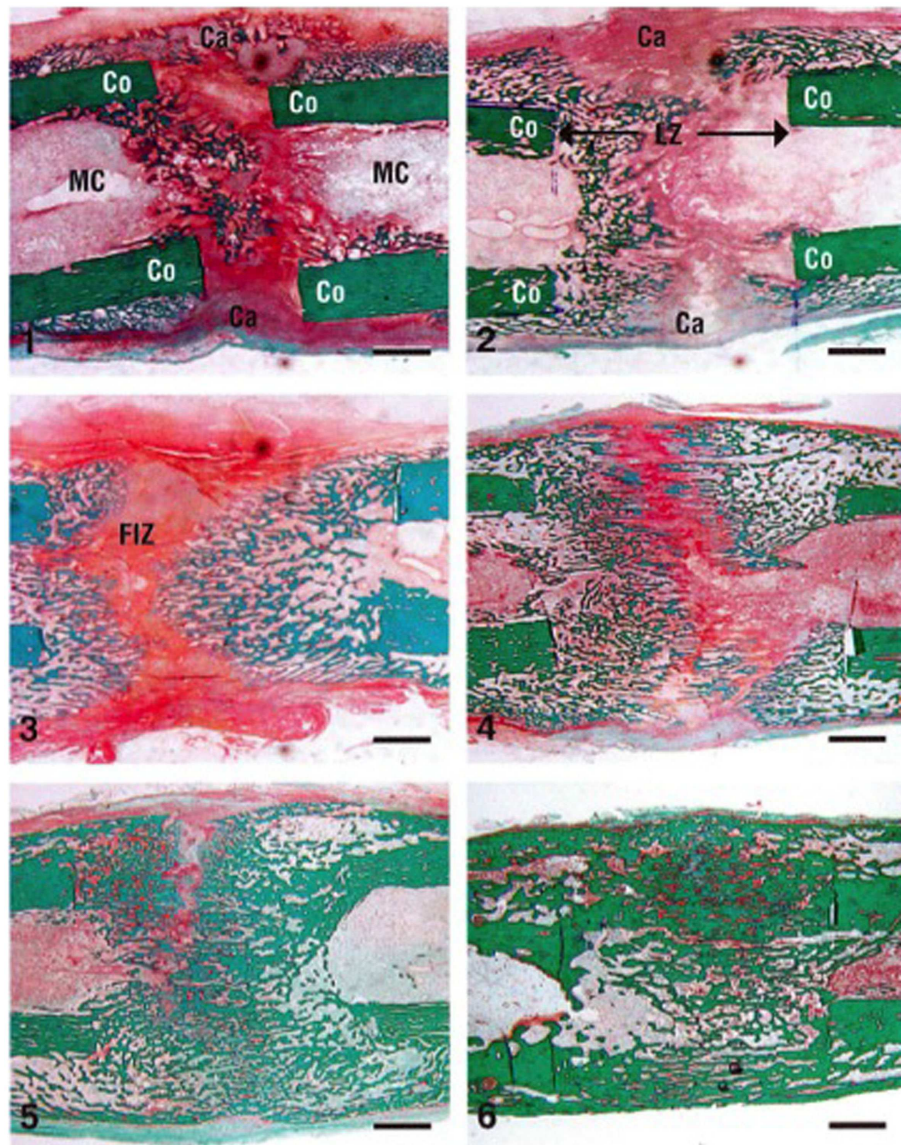


**FIGURE 2 | Cellular changes in a rabbit DO model during distraction osteogenesis of the tibia (stain is Trichrome staining).** The numbers indicate the number of weeks after the distraction process was started (1–3

are during the distraction phase and 4–6 are during the consolidation phase). Co, cortex; LZ, lengthened zone; Ca, callus; FIZ, fibrous interzone. Bar scale = 2 mm. Reprinted from Rauch et al. (34), with permission from Elsevier.

of the distraction forces causes stress in the distracted tissue). This controlled distraction protocol described by Ilizarov more than 60 years ago consists of a rate and rhythm of distraction of 0.25 mm four times a day and does not include any compressive forces besides those of distraction. This unique type of mechanical loading in the context of bone regeneration, revolutionized the field of bone regeneration, and continues to be followed almost to the letter worldwide in both long bone DO (9, 22) and mandibular DO (23).

It is surprising that in the present time and knowing the beneficial and anabolic effects of compressive forces and loading on skeletal tissue, this protocol remains largely unchallenged (2). In an attempt to accelerate bone formation in DO, several authors have

analyzed the effects of applying various changes in the standard protocol by changing the rate or rhythm of distraction or by the addition of compressive forces that alternate with the distraction cycles (accordion technique). Some of these attempts – specifically, the addition of compressive forces – were successful in accelerating bone formation while others (increasing the rate of distraction) were not.

Although bone formation using standard protocol in DO has been extensively investigated at both the cellular and molecular levels, there have been very few reports analyzing the changes in the molecular expression of various proteins and molecules secondary to changes in the mechanical environment. It is the aim of this study to review the pertinent literature on that topic,



**FIGURE 3 |** Distraction osteogenesis is used to manage multiple orthopedic conditions including congenital short femur (A) and fibular hemimelia (B).

try to identify potential therapeutic targets for accelerating bone formation and define future research directions.

### MOLECULAR CHANGES DURING STANDARD DISTRACTION RATE AND RHYTHM

The expression of various proteins and molecules and signaling pathways during the process of DO using the standard protocol – 1.0 mm distraction a day divided into four equal increments – has been extensively investigated in both human beings and animal models of DO (4, 27, 28). Compared to simple osteotomy without distraction, systemic up-regulation of transforming growth factor- $\beta$ 1 (TGF- $\beta$ 1), platelet-derived growth factor (PDGF), insulin-like growth factor (IGF), basic fibroblast growth factor (bFGF), vascular endothelial growth factor (VEGF), and its receptors VEGFR 1 and 2 have been reported by multiple investigators suggesting that these changes are caused by the distraction process (29–31).

Using a standard DO protocol in various animal models (mice, rats, rabbits, dogs, and sheep), we and others have shown that the expression of numerous factors related to osteogenesis and chondrogenesis is mostly upregulated during the distraction phase, when the mechanical forces of distraction are applied and then, the expression of these factors is downregulated once the mechanical forces of distraction cease at the end of the distraction phase. These proteins include bone morphogenic proteins (BMPs); an extensively studied protein in the context of DO (**Figure 6**), in addition to TGF- $\beta$ 1, FGF, IGF, and PDGF (4, 28, 32–36).

In addition, the expression of extracellular matrix proteins collagen type 1, 2, 4, and 10, osteocalcin, osteopontin, and osteonectin during the various phases of DO has been reported in the literature, and showed highest expression during the distraction phase of this process and decreased expression toward the end of the lengthening process (33, 37–40).



**FIGURE 4 |** Ilizarov ring fixator frame applied for distraction osteogenensis of the femur.

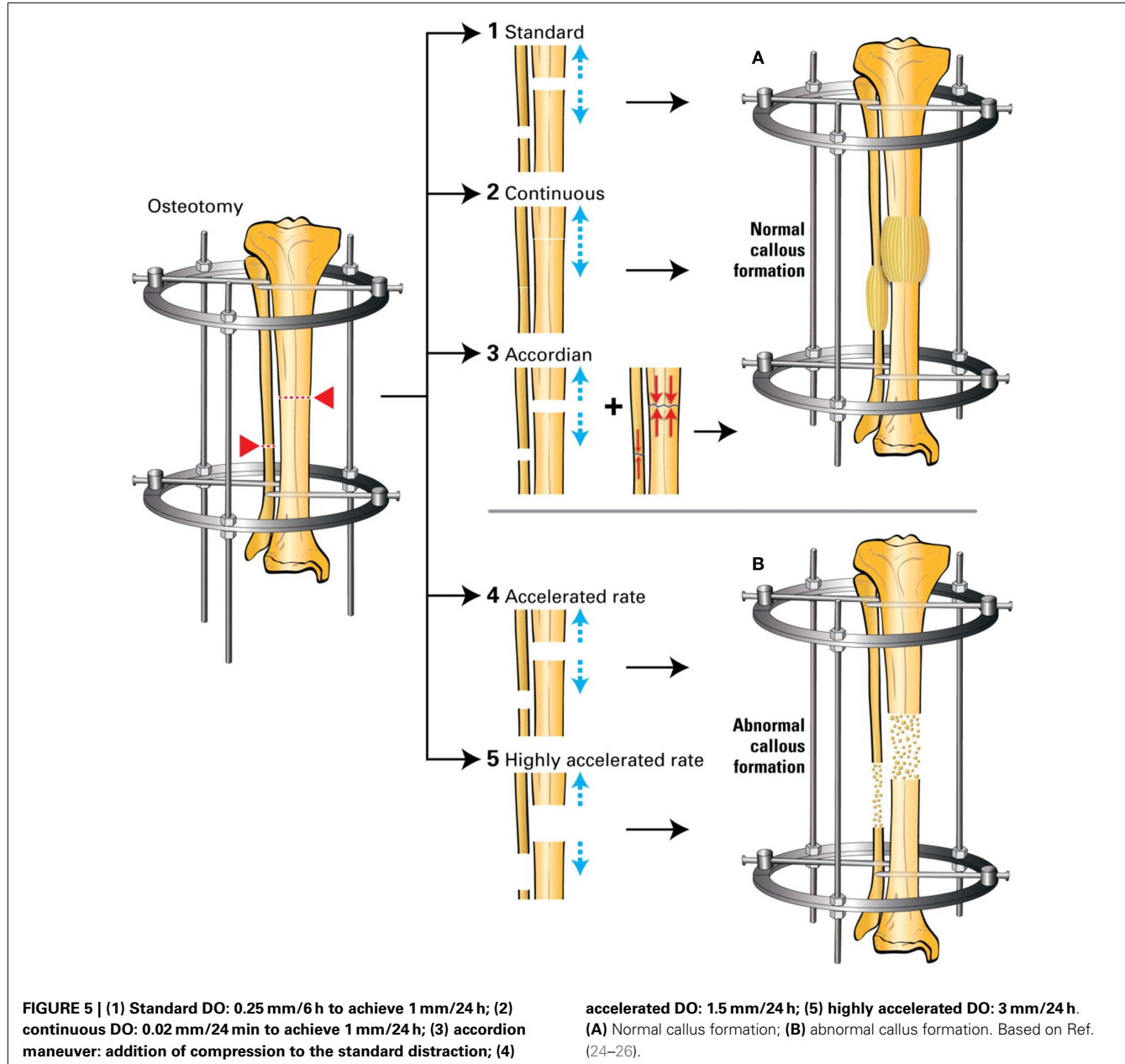
Angiogenesis and neoangiogenesis factors have also been identified in the distraction zone during DO, specifically members of the VEGF and angiopontin signaling pathways (5, 41–45).

Pro-inflammatory cytokines involved in bone repair [interleukin-6 (IL-6) and tumor necrosis factor (TNF)] have been found to be expressed during the DO process, especially during the latency phase (46). The expression of bone resorption factors was investigated in the rabbit model of DO and showed diminished expression during the consolidation phase of DO (47, 48).

The expression of mechanotransduction factors during the distraction process has also been reported and includes extracellular signal-regulated kinase (ERK), proto-oncogene tyrosine-protein kinase Src (c-Src), integrin pathway, and focal adhesion kinase (FAK) (49–51).

### EFFECT OF THE MECHANICAL ENVIRONMENT IN OTHER BONE MODELS

Although DO attracted most of the attention in the literature when assessing the effect of the mechanical environment on molecular signaling, there have been numerous studies on these effects in



other bone models, including normal and fractured bones. The addition of mechanical loading in these models leads to an alteration of the protein and molecular signaling in the loaded segment, especially during the early loading phases (52–57). In a study by Mantila Roosa et al., they found increased bone matrix genes when loading was applied to the intact forelimb of rats compared to the contralateral unloaded limb (56). In the same study, the loaded limb also showed up-regulation of TGF- $\beta$ 1, PDGF, and bFGF (56). In the same animal model, but in intact hindlimb loading, Raab-Cullen et al. also showed up-regulation of TGF- $\beta$ 1 and IGF when a mechanical load was applied (58). These findings were further proven by multiple *in vivo* and *in vitro* studies where levels of these growth factors were found to be stimulated when loading

was applied (53, 59). On the other hand, a downregulation of sclerostin was observed in axially loaded bones thus leading to decreased inhibition of the Wnt/ $\beta$ -catenin signaling pathway and ultimately improving bone quality (55, 57).

In the fractured bones, mechanical loading also showed an agonist effect on bone formation. Palomares et al. studied these effects on protein and molecular signaling during fracture healing in their rat femoral model and found up-regulation of collagen type 2 in the loaded segment of the fracture (60). In his model, BMP 3 was also upregulated by the loading process (60). In other studies, stimulation of BMPs was observed when mechanical loading was applied, but this stimulation was mostly attributed to an indirect effect of the loading process through the Wnt/ $\beta$ -catenin signaling

pathway which also showed up-regulation when mechanical stimulation was applied (52–54).

## METHODS OF ALTERING THE MECHANICAL ENVIRONMENT

It has been previously shown that alterations of the mechanical environment may have an effect on the healing process of DO (18–20).

Changes in the mechanical environment include addition of compression forces to the distraction forces applied, changes in the technique of distraction (acute or gradual), changes in the rate of distraction (continuous or intermittent), or changes in the rhythm of distraction (for example, accelerated distraction).

### ADDITION OF COMPRESSION FORCES

In the context of DO, addition of compression forces to the distraction protocol may take one of several forms, including weight bearing on the distracted limb, alternate cycles of distraction and compression (accordion), over-lengthening, and then shortening or fixator dynamization (18, 19).

#### Weight bearing

Weight bearing during the process of DO has been shown to be an important stimulus for regenerate formation and maturation in DO (1, 6, 61, 62). Radiographical and histological evidence of significantly improved bone formation has been shown when weight bearing was applied in a goat tibial model of DO (63). In a rat model of DO, Radomisli et al. showed that in the weight bearing group BMP2/4, collagen type 1, and osteocalcin expression was

more abundant (64). Leung et al. also showed increased expression of TGF- $\beta$ 1 when weight bearing was applied in the lengthened bone thus emphasizing the importance of early weight bearing in DO (63). Although the exact mechanism of increased weight bearing is still not fully understood, the findings in the studies of Radomisli and Leung – specifically, the increased expression of collagen type 1, suggest that weight bearing may have a more significant effect on osteogenesis than chondrogenesis, as it is associated with early collagen type 1 and osteocalcin expression (64).

#### **Distraction with addition of compression forces**

When examining the impact of adding compression forces to the distraction protocol on molecular signaling the literature is scarce in this aspect (**Table 1**). In addition, there is no consensus on a standard compression-distraction protocol.

Several studies – mostly anecdotal – have shown that the addition of compressive forces alternating with the standard distraction protocol – known as the accordion technique – stimulates bone formation in the distracted gap (67–70). The accordion technique has also been successful after bone transport in obtaining union at the docking site and thus managing the bone defect (71, 72). It is believed that compression forces favor intramembranous bone formation, whereas distraction (tensile) forces favor endochondral bone formation (**Figure 7**) (38, 73–75). Hence, the combination of these two different types of mechanical loading may stimulate bone formation more than either type of loading alone. The literature lacks in studies examining the molecular effect of the accordion maneuver in DO, as most of the studies apply compression at the end of the distraction process and not in an alternating pattern.

**Table 1 | Factor expression in distraction and compression forces in rabbit DO model.**

| Factor                | Outcome   | Reference                     |
|-----------------------|---|-------------------------------|
| BMP-4 (mRNA)          | Acceleration of expression of BMP-4 when compression applied                              | Kim et al. (65) <sup>a</sup>  |
| TGF- $\beta$ 1 (mRNA) | Increased and sustained expression of TGF- $\beta$ 1 when compression applied             | Kim et al. (65) <sup>a</sup>  |
| Osteonectin (mRNA)    | Sustained expression of osteonectin up to 3 weeks post-compression in the accordion group | Kim et al. (65) <sup>a</sup>  |
| VEGF (protein)        | Increased expression of VEGF in the compression group                                     | Mori et al. (66) <sup>b</sup> |

DO, distraction osteogenesis; BMP, bone morphogenic protein; VEGF, vascular endothelial growth factor; TGF- $\beta$ 1, transforming growth factor beta.

<sup>a</sup>Control group (distraction of 1 mm/day for 8 days) and experimental group (distraction of 1 mm/day for 10 days followed by a 3-day latency period after which they compressed 1 mm/day for 2 days) – rabbit mandibular DO.

<sup>b</sup>Control group (distraction of 0.7 mm/day for 14 days) and experimental group (distraction of 0.7 mm/day for 14 days then compression of 0.7 mm/day for 3 days) – rabbit tibial DO.

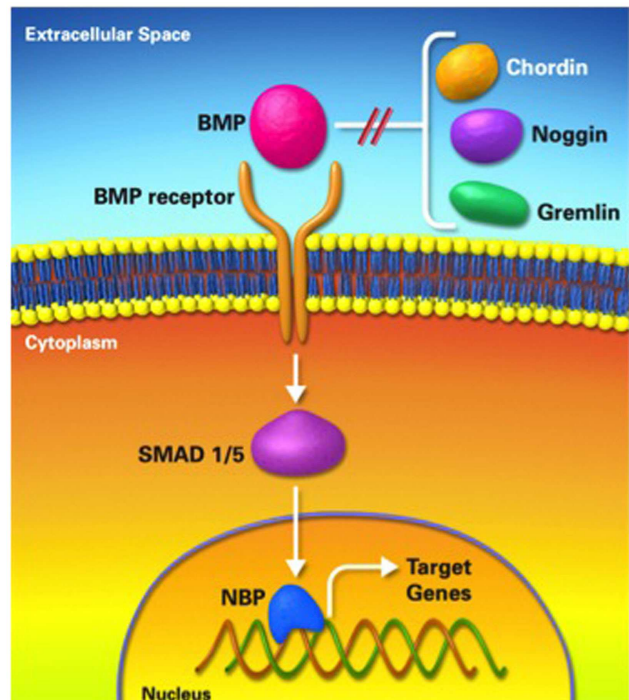
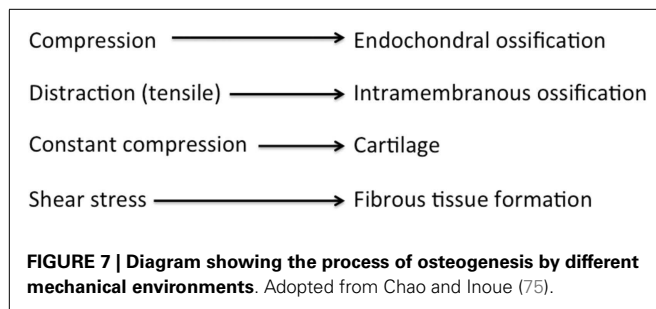


**FIGURE 6 | Bone morphogenic protein pathway.** BMP, bone morphogenic protein, NBP, nuclear binding protein.



Another method of adding compressive forces is the protocol of over distracting the bone by a few millimeters, beyond the planned amount of lengthening followed by gradual shortening (or compression) equivalent to the amount of over-lengthening. One well-designed study by Kim et al. examined the effect of the addition of compressive forces (distraction followed by compression) on BMP-4 in the mandible DO rabbit model (65). They divided their experiment into a control group (distraction of 1 mm/day for 8 days) and an experimental group (distraction of 1 mm/day for 10 days followed by a 3-day latency period after which they compressed 1 mm/day for 2 days). The level of BMP-4 expression increased in both groups at the end of the distraction process, but in the experimental group the expression accelerated when compression was applied and was maintained for 2 weeks post-compression. In the same study, it was reported that the expression of TGF- $\beta$ 1 not only markedly increased when compression was applied but also continued until 2 weeks after compression, whereas in the control group, there was only moderate elevation and remained elevated for a significantly shorter period of the DO process (65). Hamanishi et al. also applied this method in a rabbit model of tibia DO and found histologically increased proliferation of osteoblasts in the distraction gap (76). Surprisingly, this was associated with decreased vascularity, which they attributed to the compression forces causing vascular lumen collapse (76). Also, in a rabbit DO model, Mori et al. demonstrated that although there was collapse of the vascular lumen when compression was applied, VEGF and hypoxia inducible factor-1a (HIF-1a) showed marked increase in expression (66). They concluded that this method enhanced membranous bone formation in the distraction gap.

### ACUTE VERSUS GRADUAL DISTRACTION

Compared to gradual distraction (GD), acute distraction (AD) is a less favorable method for bone regeneration in DO (Table 2) (25, 51, 77). At the molecular level, studies comparing GD and AD in the context of DO are limited. Warren et al. found a low expression of collagen type 1 and osteocalcin in the mandibular DO rat model during the consolidation phase of the AD group compared with the control (25). Fang et al. compared FGF expression in GD with AD and found that expression of FGF increased in GD more than AD (77).

### CONTINUOUS VERSUS INTERMITTENT DISTRACTION

Several experimental studies have shown improved bone regeneration using continuous versus intermittent DO (Table 3) (78–80). Continuous distraction leads to up-regulation of several genes

**Table 2 | Factor expression in acute versus gradual distraction osteogenesis in rat mandibles.**

| Factor  | Outcome   | Reference                       |
|---|---|---------------------------------|
| ERK 1/2, BMP 2/4 (protein)                        | GD → ↑ ERK1/2+ ↑ BMP2/4<br>AD → no ERK1/2   | Rhee et al. (51) <sup>a</sup>   |
| VEGF/FGF (protein)                                | GD → ↑ VEGF and FGF<br>AD → absence of GF   | Fang et al. (77) <sup>b</sup>   |
| Osteocalcin, collagen type 1, TIMP-1, VEGF (mRNA) | GD → ↑ osteocalcin<br>Collagen type 1 and TIMP-1 compared to AD<br>Both protocols had no effect on VEGF | Warren et al. (25) <sup>c</sup> |

DO, distraction osteogenesis; GD, gradual distraction; AD, acute distraction; ERK1/2 extracellular signal-related kinase; BMP, bone morphogenic protein; VEGF, vascular endothelial growth factor; FGF, fibroblast growth factor; GF, growth factors; TIMP-1, tissue inhibitor metalloproteinase's-1.

<sup>a</sup>Gradual distraction group (distraction of 0.6 mm/day for 8.5 days), Acute distraction groups (intra-operative separation of 2.1 mm in group 1 and 5.1 mm in group 2).

<sup>b</sup>Gradual distraction group (distraction of 0.5 mm/day for 8 days) and acute distraction group (intra-operative separation of 4 mm).

<sup>c</sup>Gradual distraction group (distraction of 0.5 mm/day for 6 days) and acute distraction group (intra-operative separation of 3 mm).

more than intermittent traction (78, 79, 81). In a mandibular DO rabbit model comparing continuous versus intermittent distraction, Zheng et al. found that VEGF was significantly upregulated at the early stage of distraction phase and remained elevated throughout the consolidation phase, while FGF was significantly higher at the early stage of distraction phase only and no significant difference was established between the two groups in the other stages. Also, there was advanced bone formation and partial bone healing in continuous DO based on histological examination (78). In the same model, Zheng et al. also reported that, compared to intermittent DO, the mRNA level for BMP-2 in rabbits undergoing continuous distraction, was significantly higher throughout the distraction phase, whereas no significant difference was noted in the consolidation phase (79). Furthermore, the mRNA expression of TGF- $\beta$ 1 was significantly higher at the early stage of distraction phase in the continuous distraction group, although no significant difference was found between two groups in other stages (79).

Contradicting the previously mentioned positive results of continuous distraction, a recent clinical study by Bright et al. showed no significant difference between intermittent (0.25 mm 4 times/day) and continuous distraction (1/1440 mm 1400 times/day) in time to union or complication rate (82).

### VARIABLE DISTRACTION RATE AND RHYTHM

The effect of the rate and rhythm used in the applied DO protocol has a significant effect on the expression of factors involved in the DO process (Table 4). Cheung et al. examined the expression of BMP-2, -4, and -7 with routine (0.9 mm/day) and rapid (2.7 mm/day) distraction in the mandible DO rabbit model (83).

They showed that in the early consolidation phase there was intense signaling of BMP-2 and BMP-4 at the edges of the distraction regenerate in the routine group, which spread to the primary trabecule as the consolidation phase progressed, whereas in the rapid group there were only weak signals of these BMPs in the area of the distraction regenerate and no extension to other parts of the bone throughout the consolidation phase. In both groups, BMP-7 was not detected throughout the experimental periods.

Schiller et al. studied the alteration of expression of various growth factors in rapid distraction (0.75 mm twice/day) compared to routine (0.25 mm twice/day). They found that there was decreased cellular staining of FGF, VEGF, and PDGF in the rapid distraction group starting on the first day of lengthening (26).

**Table 3 | Factor expression in continuous versus intermittent distraction osteogenesis in rabbit mandibles.**

| Factor                      | Outcome  | Reference                          |
|-----------------------------|--|------------------------------------|
| TIMP-1 (mRNA)               | Up-regulating TIMP-1 in continuous DO  | Liu et al. (80, 81) <sup>a</sup>   |
| TGF- $\beta$ 1/BMP 2 (mRNA) | High level of TGF- $\beta$ 1 and BMP 2 in continuous DO  | Zheng et al. (78, 79) <sup>a</sup> |
| VEGF/bFGF (mRNA)            | Continuous DO → proper mechanical environment for angiogenesis through up-regulation of the angiogenic mediators | Zheng et al. (78, 79) <sup>a</sup> |

DO, distraction osteogenesis; TIMP-1, tissue inhibitor metalloproteinase's-1; BMP, bone morphogenic protein; TGF- $\beta$ 1, transforming growth factor beta; bFGF, basic fibroblast growth factor; VEGF, vascular endothelial growth factor.

<sup>a</sup>Continuous distraction group (0.9 mm/day for 11 days at a rate of 8 times/s) and intermittent distraction group (0.9 mm/day for 11 days at a rate of once per day).

## DISCUSSION

The beneficial effects of mechanical loading on bone formation have been known for more than a century, when Wolff developed the concept that bone adapts to its environment (75). However, of all the forms of mechanical loading – compression, tension (or distraction), bending, torsion, and shear – only compression forces were mostly recognized as having an anabolic effect on bone formation. It was Ilizarov, in the 1950s, who was the first one to introduce the concept that distraction (tension) forces could also lead to bone formation, provided these forces are applied in a controlled environment, and that was the key to the success of the technique of DO (1, 6). As previously mentioned, although DO is a very successful technique in generating large amounts of new bone, the long period of time the external fixator has to be kept on until the newly formed bone consolidates, presented a major problem of this technique. The question then arises: how to accelerate newly formed bone in the distracted gap? Numerous techniques have been described to accelerate bone formation, however, manipulation of the mechanical loading environment is probably the most attractive as it is non-invasive, easily applicable, and furthermore adds no cost to the technique. This led some authors to challenge the standard distraction protocol developed by Ilizarov. Several reports in the literature have shown that the addition of compressive forces to the distraction protocol, specifically the accordion technique, could be beneficial in accelerating bone formation in the distracted gap (67–70, 84). However, there has been no detailed analysis of this technique: how much compression should be applied, which phase of DO should the compression be added and for how long? More importantly, it still remains largely unknown how the effects of compression forces differ from those of distraction forces at the molecular level in stimulating bone formation in the context of DO.

The expression of multiple growth factors has been identified in context of standard DO protocol, including TGF- $\beta$ , PDGF, IGF, bFGF, and VEGF. While alteration of the mechanical environment

**Table 4 | Factor expression in variable distraction rates and rhythms of distraction osteogenesis.**

| Factor                              | Distraction protocol                               | Model                    | Outcome  | Reference            |
|-------------------------------------|--|--------------------------|--|----------------------|
| BMP-2/4/7 (protein)                 | 0.9 mm/day versus 2.7 mm/day                       | Mandibular DO in rabbits | Increased Expression of BMP-2/4 in 0.9 mm/day group<br>No BMP-7 in both groups   | Cheung et al. (83)   |
| FGF/VEGF/PDGF (protein)             | 0.5 mm/day versus 1.5 mm/day                       | Femur DO in rats         | Increased expression of VEGF, FGF and PDGF in 0.5 mm/day group   | Schiller et al. (26) |
| Endothelial cells antigen (protein) | Four varying rates (0.3, 0.7, 1.3, and 2.7 mm/day) | Tibia DO in rabbits      | The vascularization process was maximally stimulated at distraction rates of 0.7 and 1.3 mm/day. While impaired in 0.3 mm/day and not maximally stimulated in 2.7 mm/day | Li et al. (24, 38)   |
| Collagen type 4 (protein)           | Four varying rates (0.3, 0.7, 1.3, and 2.7 mm/day) | Tibia DO in rabbits      | Collagen type 4 expression was highest at rates of 0.7 mm/day and 1.3 mm/day   | Li et al. (24, 38)   |

DO, distraction osteogenesis; BMP, bone morphogenic protein; VEGF, vascular endothelial growth factor; FGF, fibroblast growth factor; PDGF, platelet-derived growth factor.

lead to variable changes in expression of these factors. Except for the BMP pathway, we were unable to identify any other specific protein, molecule or pathway that clearly characterizes specific changes in signaling when the biomechanical loading environment is altered. The BMP pathway has been extensively studied in the context of bone regeneration and DO and we and others have shown that it plays a significant role in DO using the standard protocol (28, 32, 36, 85). We have also shown (**Tables 1–4**) that the expression of BMPs changes when the mechanical loading environment is altered, specifically an increased expression of BMPs when compression forces are added to the standard protocol and when continuous distraction is applied. More research needs to be done in that area to identify which specific combination of biomechanical forces leads to optimal expression of BMPs.

Another possible explanation on the beneficial effects of compression loading on bone formation in DO at the molecular level is related to the expression of sclerostin and the difference in sclerostin inhibition with various types of loading. The emergence of the Wnt pathway as a major player in bone regeneration, along with its alteration when sclerostin is inhibited led to extensive research in that area (86, 87). We know today that sclerostin inhibition is one of the numerous pathways through which mechanotransduction may lead to new bone formation (55, 88). In our laboratory, we have demonstrated in a mouse model of DO that various members of the Wnt signaling pathway are expressed during the distraction process (86) and that systemic application of sclerostin antibodies caused increased bone formation in the distracted gap (87). However, to the best of our knowledge, there has been no study evaluating the effects of altering the mechanical loading environment in the context of DO on the expression of Wnt pathway members and the degree of sclerostin inhibition. The only study we were able to find comparing the effects of compression versus distraction on the expression of sclerostin, was by Robling et al., who showed in an ulnar loading model in the rat that compression loading causes 80% suppression of sclerostin, while distraction loading caused only 20% inhibition of sclerostin (55). This is an extremely important observation as it supports the hypothesis that the addition of compressive loading to the distraction protocol may be beneficial to bone formation by suppressing more sclerostin than distraction forces only. We believe that future research should also focus on analyzing the effects of altering the biomechanical loading environment on the expression of various members of this pathway and hence try to identify the optimal “non-invasive tissue engineering” method to enhance bone formation in DO.

## ACKNOWLEDGMENTS

The authors would like to thank Dr. Sebastian Rendon, orthopedic researcher at Shriners Hospital for children for his valuable contribution in literature review. Also, we would like to thank Guylaine Bédard graphic artist and photographer in Shriners Hospital for children for her participation in image and pictures design.

## REFERENCES

- Ilizarov GA. The tension-stress effect on the genesis and growth of tissues: part II. The influence of the rate and frequency of distraction. *Clin Orthop Relat Res* (1989) **239**:263–85.
- Ilizarov GA. Clinical application of the tension-stress effect for limb lengthening. *Clin Orthop Relat Res* (1990) **250**:8–26.
- Green SA. The Ilizarov method of distraction osteogenesis. In: Hamdy RC, McCarthy J, editors. *Management of Limb Length Discrepancy*. Rosemont, IL: American Academy of Orthopaedic Surgeons (2011). p. 39–44.
- Al-Aql ZS, Alagl AS, Graves DT, Gerstenfeld LC, Einhorn TA. Molecular mechanisms controlling bone formation during fracture healing and distraction osteogenesis. *J Dent Res* (2008) **87**:107–18. doi:10.1177/154405910808700215
- Choi IH, Chung CY, Cho TJ, Yoo WJ. Angiogenesis and mineralization during distraction osteogenesis. *J Korean Med Sci* (2002) **17**:435–47. doi:10.3346/jkms.2002.17.4.435
- Ilizarov GA. The tension-stress effect on the genesis and growth of tissues. Part I. The influence of stability of fixation and soft-tissue preservation. *Clin Orthop Relat Res* (1989) **238**:249–81.
- Hamdy RC, Rendon JS, Tabrizian M. Distraction osteogenesis and its challenges in bone regeneration. In: Tal H, editor. *Bone Regeneration*. InTech (2012):185–212. doi:10.5772/32229. Available from: <http://www.intechopen.com/books/bone-regeneration/distraction-osteogenesis-and-its-challenges-in-bone-regeneration>
- Codivilla A. The classic: on the means of lengthening, in the lower limbs, the muscles and tissues which are shortened through deformity. 1905. *Clin Orthop Relat Res* (2008) **466**:2903–9. doi:10.1007/s11999-008-0518-7
- Birch JG, Samchukov ML. Use of the Ilizarov method to correct lower limb deformities in children and adolescents. *J Am Acad Orthop Surg* (2004) **12**:144–54.
- McCarthy JG, Schreiber J, Karp N, Thorne CH, Grayson BH. Lengthening the human mandible by gradual distraction. *Plast Reconstr Surg* (1992) **89**:1–8. doi:10.1097/00006534-199201000-00001
- Margaride LA, Breuer J. Transmaxillary osteogenic distraction with intraoral tooth-borne distractors. *J Craniofac Surg* (2012) **23**:1425–7. doi:10.1097/SCS.0b013e31824ef7b4
- Ohba S, Tobita T, Tajima N, Matsuo K, Yoshida N, Asahina I. Correction of an asymmetric maxillary dental arch by alveolar bone distraction osteogenesis. *Am J Orthod Dentofacial Orthop* (2013) **143**:266–73. doi:10.1016/j.ajodo.2011.09.013
- Uribe F, Agarwal S, Janakiraman N, Shafer D, Nanda R. Bidimensional dentoalveolar distraction osteogenesis for treatment efficiency. *Am J Orthod Dentofacial Orthop* (2013) **144**:290–8. doi:10.1016/j.ajodo.2012.09.023
- Paley D. Problems, obstacles, and complications of limb lengthening by the Ilizarov technique. *Clin Orthop Relat Res* (1990) **250**:81–104.
- Garcia-Cimbrela E, Olsen B, Ruiz-Yague M, Fernandez-Baillo N, Munuera-Martinez L. Ilizarov technique. Results and difficulties. *Clin Orthop Relat Res* (1992) **283**:116–23.
- Sabharwal S. Enhancement of bone formation during distraction osteogenesis: pediatric applications. *J Am Acad Orthop Surg* (2011) **19**:101–11.
- Makhdom AM, Hamdy RC. The role of growth factors on acceleration of bone regeneration during distraction osteogenesis. *Tissue Eng Part B Rev* (2013) **19**:442–53. doi:10.1089/ten.TEB.2012.0717
- Aronson J, Harp JH. Mechanical forces as predictors of healing during tibial lengthening by distraction osteogenesis. *Clin Orthop Relat Res* (1994) **301**:73–9.
- Waanders NA, Richards M, Steen H, Kuhn JL, Goldstein SA, Goulet JA. Evaluation of the mechanical environment during distraction osteogenesis. *Clin Orthop Relat Res* (1998) **349**:225–34. doi:10.1097/00003086-199804000-00028
- Saunders MM, Lee JS. The influence of mechanical environment on bone healing and distraction osteogenesis. *Atlas Oral Maxillofac Surg Clin North Am* (2008) **16**:147–58. doi:10.1016/j.cxom.2008.04.006
- Frost HM. *The Utah Paradigm of Skeletal Physiology* Vol. 1–2. ISMNI (1960).
- Li G, Simpson AH, Kenwright J, Triffitt JT. Assessment of cell proliferation in regenerating bone during distraction osteogenesis at different distraction rates. *J Orthop Res* (1997) **15**:765–72. doi:10.1002/jor.1100150520
- Mofid MM, Manson PN, Robertson BC, Tufaro AP, Elias JJ, Vander Kolk CA. Craniofacial distraction osteogenesis: a review of 3278 cases. *Plast Reconstr Surg* (2001) **108**:1103–14. doi:10.1097/00003086-200110000-00001
- Li G, Simpson AH, Kenwright J, Triffitt JT. Effect of lengthening rate on angiogenesis during distraction osteogenesis. *J Orthop Res* (1999) **17**:362–7. doi:10.1002/jor.1100170310
- Warren SM, Mehrara BJ, Steinbrech DS, Paccione MF, Greenwald JA, Spector JA, et al. Rat mandibular distraction osteogenesis: part III. Gradual distraction versus acute lengthening. *Plast Reconstr Surg* (2001) **107**:441–53. doi:10.1097/00006534-200102000-00001
- Schiller JR, Moore DC, Ehrlich MG. Increased lengthening rate decreases expression of fibroblast growth factor 2, platelet-derived growth factor, vascular

- endothelial growth factor, and CD31 in a rat model of distraction osteogenesis. *J Pediatr Orthop* (2007) **27**:961–8. doi:10.1097/BPO.0b013e3181558c37
27. Bouletrau PJ, Warren SM, Longaker MT. The molecular biology of distraction osteogenesis. *J Craniomaxillofac Surg* (2002) **30**:1–11. doi:10.1054/jcms.2001.0263
28. Haque T, Hamade F, Alam N, Kotsiopifitis M, Lauzier D, St-Arnaud R, et al. Characterizing the BMP pathway in a wild type mouse model of distraction osteogenesis. *Bone* (2008) **42**:1144–53. doi:10.1016/j.bone.2008.01.028
29. Holbein O, Neidlinger-Wilke C, Suger G, Kinzl L, Claes L. Ilizarov callus distraction produces systemic bone cell mitogens. *J Orthop Res* (1995) **13**:629–38. doi:10.1002/jor.1100130420
30. Lammens J, Liu Z, Aerssens J, Dequeker J, Fabry G. Distraction bone healing versus osteotomy healing: a comparative biochemical analysis. *J Bone Miner Res* (1998) **13**:279–86. doi:10.1359/jbmr.1998.13.2.279
31. Weiss S, Baumgart R, Jochum M, Strasburger CJ, Bidlingmaier M. Systemic regulation of distraction osteogenesis: a cascade of biochemical factors. *J Bone Miner Res* (2002) **17**:1280–9. doi:10.1359/jbmr.2002.17.7.1280
32. Li G, Berven S, Simpson H, Triffitt JT. Expression of BMP-4 mRNA during distraction osteogenesis in rabbits. *Acta Orthop Scand* (1998) **69**:420–5. doi:10.3109/17453679808999060
33. Sato M, Yasui N, Nakase T, Kawahata H, Sugimoto M, Hirota S, et al. Expression of bone matrix proteins mRNA during distraction osteogenesis. *J Bone Miner Res* (1998) **13**:1221–31. doi:10.1359/jbmr.1998.13.8.1221
34. Rauch F, Lauzier D, Croteau S, Travers R, Glorieux FH, Hamdy R. Temporal and spatial expression of bone morphogenetic protein-2, -4, and -7 during distraction osteogenesis in rabbits. *Bone* (2000) **27**:453–9. doi:10.1016/S8756-3282(00)00337-9
35. Haque T, Amako M, Nakada S, Lauzier D, Hamdy RC. An immunohistochemical analysis of the temporal and spatial expression of growth factors FGF 1, 2 and 18, IGF 1 and 2, and TGFbeta1 during distraction osteogenesis. *Histol Histopathol* (2007) **22**:119–28.
36. Alam N, St-Arnaud R, Lauzier D, Rosen V, Hamdy RC. Are endogenous BMPs necessary for bone healing during distraction osteogenesis? *Clin Orthop Relat Res* (2009) **467**:3190–8. doi:10.1007/s11999-009-1065-6
37. Tajana GF, Morandi M, Zembo MM. The structure and development of osteogenic repair tissue according to Ilizarov technique in man. Characterization of extracellular matrix. *Orthopedics* (1989) **12**:515–23.
38. Li G, Simpson AH, Triffitt JT. The role of chondrocytes in intramembranous and endochondral ossification during distraction osteogenesis in the rabbit. *Calcif Tissue Int* (1999) **64**:310–7. doi:10.1007/s002239900625
39. Knabe C, Nicklin S, Yu Y, Walsh WR, Radlanski RJ, Marks C, et al. Growth factor expression following clinical mandibular distraction osteogenesis in humans and its comparison with existing animal studies. *J Craniomaxillofac Surg* (2005) **33**:361–9. doi:10.1016/j.jcms.2005.07.003
40. Feng X, Tuo X, Chen F, Wu W, Ding Y, Duan Y, et al. Ultrastructural cell response to tension stress during mandibular distraction osteogenesis. *Br J Oral Maxillofac Surg* (2008) **46**:527–32. doi:10.1016/j.bjoms.2008.03.005
41. Pacicca DM, Patel N, Lee C, Salisbury K, Lehmann W, Carvalho R, et al. Expression of angiogenic factors during distraction osteogenesis. *Bone* (2003) **33**:889–98. doi:10.1016/j.bone.2003.06.002
42. Sojo K, Sawaki Y, Hattori H, Mizutani H, Ueda M. Immunohistochemical study of vascular endothelial growth factor (VEGF) and bone morphogenetic protein-2, -4 (BMP-2, -4) on lengthened rat femurs. *J Craniomaxillofac Surg* (2005) **33**:238–45. doi:10.1016/j.jcms.2005.02.004
43. Byun JH, Park BW, Kim JR, Lee JH. Expression of vascular endothelial growth factor and its receptors after mandibular distraction osteogenesis. *Int J Oral Maxillofac Surg* (2007) **36**:338–44. doi:10.1016/j.ijom.2006.10.013
44. Jacobsen KA, Al-Aql ZS, Wan C, Fitch JL, Stapleton SN, Mason ZD, et al. Bone formation during distraction osteogenesis is dependent on both VEGFR1 and VEGFR2 signaling. *J Bone Miner Res* (2008) **23**:596–609. doi:10.1359/jbmr.080103
45. Mandu-Hrit M, Seifert E, Kotsiopifitis M, Lauzier D, Haque T, Rohlicek C, et al. OP-1 injection increases VEGF expression but not angiogenesis in a rabbit model of distraction osteogenesis. *Growth Factors* (2008) **26**:143–51. doi:10.1080/08977190802106154
46. Cho TJ, Kim JA, Chung CY, Yoo WJ, Gerstenfeld LC, Einhorn TA, et al. Expression and role of interleukin-6 in distraction osteogenesis. *Calcif Tissue Int* (2007) **80**:192–200. doi:10.1007/s00223-006-0240-y
47. Wang LC, Takahashi I, Sasano Y, Sugawara J, Mitani H. Osteoclastogenic activity during mandibular distraction osteogenesis. *J Dent Res* (2005) **84**:1010–5. doi:10.1177/154405910508401108
48. Ge WL, Xie ZJ, He JF. Expression of c-fos, OPG, OPGL in rabbit mandibular distraction osteogenesis zone. *Zhejiang Da Xue Xue Bao Yi Xue Ban* (2006) **35**:496–500.
49. Tong L, Buchman SR, Ignelzi MA Jr, Rhee S, Goldstein SA. Focal adhesion kinase expression during mandibular distraction osteogenesis: evidence for mechanotransduction. *Plast Reconstr Surg* (2003) **111**:211–22. doi:10.1097/00006534-200301000-00037
50. Rhee ST, Buchman SR. Colocalization of c-Src (pp60src) and bone morphogenetic protein 2/4 expression during mandibular distraction osteogenesis: in vivo evidence of their role within an integrin-mediated mechanotransduction pathway. *Ann Plast Surg* (2005) **55**:207–15. doi:10.1097/01.sap.0000164576.10754.aa
51. Rhee ST, El-Bassiony L, Buchman SR. Extracellular signal-related kinase and bone morphogenetic protein expression during distraction osteogenesis of the mandible: in vivo evidence of a mechanotransduction mechanism for differentiation and osteogenesis by mesenchymal precursor cells. *Plast Reconstr Surg* (2006) **117**:2243–9. doi:10.1097/01.pr.0000224298.93486.1b
52. Hens JR, Wilson KM, Dann P, Chen X, Horowitz MC, Wysolmerski JJ. TOP-GAL mice show that the canonical Wnt signaling pathway is active during bone development and growth and is activated by mechanical loading in vitro. *J Bone Miner Res* (2005) **20**:1103–13. doi:10.1359/JBMR.050210
53. Lau KH, Kapur S, Kesavan C, Baylink DJ. Up-regulation of the Wnt, estrogen receptor, insulin-like growth factor-I, and bone morphogenetic protein pathways in C57BL/6J osteoblasts as opposed to C3H/HeJ osteoblasts in part contributes to the differential anabolic response to fluid shear. *J Biol Chem* (2006) **281**:9576–88. doi:10.1074/jbc.M509205200
54. Robinson JA, Chatterjee-Kishore M, Yaworsky PJ, Cullen DM, Zhao W, Li C, et al. Wnt/beta-catenin signaling is a normal physiological response to mechanical loading in bone. *J Biol Chem* (2006) **281**:31720–8. doi:10.1074/jbc.M602308200
55. Robling AG, Niziolek PJ, Baldridge LA, Condon KW, Allen MR, Alam I, et al. Mechanical stimulation of bone in vivo reduces osteocyte expression of Sost/sclerostin. *J Biol Chem* (2008) **283**:5866–75. doi:10.1074/jbc.M705092200
56. Mantila Roosa SM, Liu Y, Turner CH. Gene expression patterns in bone following mechanical loading. *J Bone Miner Res* (2011) **26**:100–12. doi:10.1002/jbmr.193
57. Moustafa A, Sugiyama T, Prasad J, Zaman G, Gross TS, Lanyon LE, et al. Mechanical loading-related changes in osteocyte sclerostin expression in mice are more closely associated with the subsequent osteogenic response than the peak strains engendered. *Osteoporos Int* (2012) **23**:1225–34. doi:10.1007/s00198-011-1656-4
58. Raab-Cullen DM, Thiede MA, Petersen DN, Kimmel DB, Recker RR. Mechanical loading stimulates rapid changes in periosteal gene expression. *Calcif Tissue Int* (1994) **55**:473–8. doi:10.1007/BF00298562
59. Lean JM, Jagger CJ, Chambers TJ, Chow JW. Increased insulin-like growth factor I mRNA expression in rat osteocytes in response to mechanical stimulation. *Am J Physiol* (1995) **268**:E318–27.
60. Palomares KT, Gleason RE, Mason ZD, Cullinane DM, Einhorn TA, Gerstenfeld LC, et al. Mechanical stimulation alters tissue differentiation and molecular expression during bone healing. *J Orthop Res* (2009) **27**:1123–32. doi:10.1002/jor.20863
61. Green SA. Postoperative management during limb lengthening. *Orthop Clin North Am* (1991) **22**:723–34.
62. Fink B, Krieger M, Schneider T, Menkhaus S, Fischer J, Ruther W. Factors affecting bone regeneration in Ilizarov callus distraction. *Unfallchirurg* (1995) **98**:633–9.
63. Leung KS, Cheung WH, Yeung HY, Lee KM, Fung KP. Effect of weightbearing on bone formation during distraction osteogenesis. *Clin Orthop Relat Res* (2004) **419**:251–7. doi:10.1097/00003086-200402000-00041
64. Radomisli TE, Moore DC, Barrach HJ, Keeping HS, Ehrlich MG. Weight-bearing alters the expression of collagen types I and II, BMP 2/4 and osteocalcin in the early stages of distraction osteogenesis. *J Orthop Res* (2001) **19**:1049–56. doi:10.1016/S0736-0266(01)00044-4
65. Kim UK, Park SJ, Seong WJ, Heo J, Hwang DS, Kim YD, et al. Expression of TGF-beta1, osteonectin, and BMP-4 in mandibular distraction osteogenesis with compression stimulation: reverse transcriptase-polymerase chain reaction study and biomechanical test. *J Oral Maxillofac Surg* (2010) **68**:2076–84. doi:10.1016/j.joms.2009.09.070

66. Mori S, Akagi M, Kikuyama A, Yasuda Y, Hamanishi C. Axial shortening during distraction osteogenesis leads to enhanced bone formation in a rabbit model through the HIF-1alpha/vascular endothelial growth factor system. *J Orthop Res* (2006) **24**:653–63. doi:10.1002/jor.20076
67. Perren SM, Huggler A, Russenberger M, Allgower M, Mathys R, Schenk R, et al. The reaction of cortical bone to compression. *Acta Orthop Scand Suppl* (1969) **125**:19–29.
68. Krishnan A, Pamecha C, Patwa JJ. Modified Ilizarov technique for infected nonunion of the femur: the principle of distraction-compression osteogenesis. *J Orthop Surg (Hong Kong)* (2006) **14**:265–72.
69. Claes L, Augat P, Schorlemmer S, Konrads C, Ignatius A, Ehrnhaller C. Temporary distraction and compression of a diaphyseal osteotomy accelerates bone healing. *J Orthop Res* (2008) **26**:772–7. doi:10.1002/jor.20588
70. Ozgul S, Akdeniz ZD, Celebiler O, Alcan T, Sav A. The effect of 2 different distraction-compression models on new bone generation. *J Oral Maxillofac Surg* (2012) **70**:e490–9. doi:10.1016/j.joms.2012.05.022
71. Tsuchiya H, Tomita K, Minematsu K, Mori Y, Asada N, Kitano S. Limb salvage using distraction osteogenesis. A classification of the technique. *J Bone Joint Surg Br* (1997) **79**:403–11. doi:10.1302/0301-620X.79B3.7198
72. Iacobellis C, Berizzi A, Aldegheri R. Bone transport using the Ilizarov method: a review of complications in 100 consecutive cases. *Strategies Trauma Limb Reconstr* (2010) **5**:17–22. doi:10.1007/s11751-010-0085-9
73. Hamdy RC, Silvestri A, Rivard CH, Ehrlich M. Histologic evaluation of bone regeneration in cases of limb lengthening by Ilizarov's technique. An experimental study in the dog. *Ann Chir* (1997) **51**:875–83.
74. Yasui N, Sato M, Ochi T, Kimura T, Kawahata H, Kitamura Y, et al. Three modes of ossification during distraction osteogenesis in the rat. *J Bone Joint Surg Br* (1997) **79**:824–30. doi:10.1302/0301-620X.79B5.7423
75. Chao EY, Inoue N. Biophysical stimulation of bone fracture repair, regeneration and remodelling. *Eur Cell Mater* (2003) **6**:72–84.
76. Hamanishi C, Yoshii T, Totani Y, Tanaka S. Lengthened callus activated by axial shortening. Histological and cytomorphometrical analysis. *Clin Orthop Relat Res* (1994) **307**:250–4.
77. Fang TD, Salim A, Xia W, Nacamuli RP, Guccione S, Song HM, et al. Angiogenesis is required for successful bone induction during distraction osteogenesis. *J Bone Miner Res* (2005) **20**:1114–24. doi:10.1359/jbmr.050301
78. Zheng LW, Ma L, Cheung LK. Angiogenesis is enhanced by continuous traction in rabbit mandibular distraction osteogenesis. *J Craniomaxillofac Surg* (2009) **37**:405–11. doi:10.1016/j.jcms.2009.03.007
79. Zheng LW, Ma L, Cheung LK. Comparison of gene expression of osteogenic factors between continuous and intermittent distraction osteogenesis in rabbit mandibular lengthening. *Oral Surg Oral Med Oral Pathol Oral Radiol Endod* (2009) **108**:496–9. doi:10.1016/j.tripleo.2009.05.038
80. Liu XL, Zhang HX, Ma L, Peng L, Cheung LK, Zheng LW. Responses of distraction regenerate to high-frequency traction at a rapid rate. *J Trauma Acute Care Surg* (2012) **72**:1035–9. doi:10.1097/TA.0b013e31823cc867
81. Liu XL, Cheung LK, Zhang HX, Li JY, Ma L, Zheng LW. Comparison of gene expression of tissue inhibitor of matrix metalloproteinase-1 between continuous and intermittent distraction osteogenesis: a quantitative study on rabbits. *J Craniomaxillofac Surg* (2012) **40**:e185–8. doi:10.1016/j.jcms.2011.10.005
82. Bright AS, Herzenberg JE, Paley D, Weiner I, Burghardt RD. Preliminary experience with motorized distraction for tibial lengthening. *Strategies Trauma Limb Reconstr* (2014) **9**(2):97–100. doi:10.1007/s11751-014-0191-1
83. Cheung LK, Zheng LW, Ma L. Effect of distraction rates on expression of bone morphogenetic proteins in rabbit mandibular distraction osteogenesis. *J Craniomaxillofac Surg* (2006) **34**:263–9. doi:10.1016/j.jcms.2006.02.004
84. Kim UK, Chung IK, Lee KH, Swift JQ, Seong WJ, Ko CC. Bone regeneration in mandibular distraction osteogenesis combined with compression stimulation. *J Oral Maxillofac Surg* (2006) **64**:1498–505. doi:10.1016/j.joms.2006.03.028
85. Farhadieh RD, Gianoutsos MP, Yu Y, Walsh WR. The role of bone morphogenetic proteins BMP-2 and BMP-4 and their related postreceptor signaling system (Smads) in distraction osteogenesis of the mandible. *J Craniofac Surg* (2004) **15**:714–8. doi:10.1097/00001665-200409000-00003
86. Kasai B, Moffatt P, Al-Salmi L, Lauzier D, Lessard L, Hamdy RC. Spatial and temporal localization of WNT signaling proteins in a mouse model of distraction osteogenesis. *J Histochem Cytochem* (2012) **60**:219–28. doi:10.1369/0022155411432010
87. Makhdum AM, Rauch F, Lauzier D, Hamdy RC. The effect of systemic administration of sclerostin antibody in a mouse model of distraction osteogenesis. *J Musculoskelet Neuronal Interact* (2014) **14**:124–30.
88. Morse A, McDonald M, Kelly N, Melville K, Schindeler A, Kramer I, et al. Mechanical load increases in bone formation via a sclerostin-independent pathway. *J Bone Miner Res* (2014) **29**(11):2456–67. doi:10.1002/jbmr.2278

**Conflict of Interest Statement:** The authors declare that the research was conducted in the absence of any commercial or financial relationships that could be construed as a potential conflict of interest.

**Received:** 16 September 2014; **accepted:** 26 November 2014; **published online:** 10 December 2014.

**Citation:** Alzahrani MM, Anam EA, Makhdum AM, Villemure I and Hamdy RC (2014) The effect of altering the mechanical loading environment on the expression of bone regenerating molecules in cases of distraction osteogenesis. *Front. Endocrinol.* **5**:214. doi: 10.3389/fendo.2014.00214

This article was submitted to Bone Research, a section of the journal *Frontiers in Endocrinology*.

Copyright © 2014 Alzahrani, Anam, Makhdum, Villemure and Hamdy. This is an open-access article distributed under the terms of the Creative Commons Attribution License (CC BY). The use, distribution or reproduction in other forums is permitted, provided the original author(s) or licensor are credited and that the original publication in this journal is cited, in accordance with accepted academic practice. No use, distribution or reproduction is permitted which does not comply with these terms.



# New insights into Wnt–Lrp5/6– $\beta$ -catenin signaling in mechanotransduction

Kyung Shin Kang<sup>1</sup> and Alexander G. Robling<sup>1,2,3\*</sup>

<sup>1</sup> Department of Anatomy and Cell Biology, Indiana University School of Medicine, Indianapolis, IN, USA

<sup>2</sup> Department of Biomedical Engineering, Indiana University–Purdue University at Indianapolis, Indianapolis, IN, USA

<sup>3</sup> Richard L. Roudebush VA Medical Center, Indianapolis, IN, USA

**Edited by:**

Jonathan H. Tobias, University of Bristol, UK

**Reviewed by:**

Matt Pridéaux, University of Missouri-Kansas City, USA

Noam Levao, Ben-Gurion University of the Negev, Israel

**\*Correspondence:**

Alexander G. Robling, Department of Anatomy and Cell Biology, Indiana University School of Medicine, 635 Barnhill Drive, MS 5035, Indianapolis, IN 46202, USA  
e-mail: arobling@iupui.edu

Mechanical loading is essential to maintain normal bone metabolism and the balance between bone formation and resorption. The cellular mechanisms that control mechanotransduction are not fully defined, but several key pathways have been identified. We discuss the roles of several components of the Wnt signaling cascade, namely Lrp5, Lrp6, and  $\beta$ -catenin in mechanical loading-induced bone formation. Lrp5 is an important Wnt co-receptor for regulating bone mass and mechanotransduction, and appears to function principally by augmenting bone formation. Lrp6 also regulates bone mass but its action might involve resorption as well as formation. The role of Lrp6 in mechanotransduction is unclear. Studies addressing the role of  $\beta$ -catenin in bone metabolism and mechanotransduction highlight the uncertainties in downstream modulators of Lrp5 and Lrp6. Taken together, these data indicate that mechanical loading might affect bone regulation triggering the canonical Wnt signaling (and perhaps other pathways) not only via Lrp5 but also via Lrp6. Further work is needed to clarify the role of the Wnt signaling pathway in Lrp5 and/or Lrp6-mediated mechanotransduction, which could eventually lead to powerful therapeutic agents that might mimic the anabolic effects of mechanical stimulation.

**Keywords:** Wnt, Lrp5, Lrp6, Sost, mechanotransduction

## INTRODUCTION

Mechanical loading is essential to maintain normal bone metabolism and the balance between bone formation and resorption (1, 2). Disuse of bone or insufficient loading can cause reduced bone formation as well as increased bone turnover, which can be appreciated in astronauts that have spent significant time in space, among patients restricted to bed rest, and in people suffering from muscle paralysis (3). Conversely, exposure to frequent, high-impact loading results in active bone formation (4). A good example of this effect can be seen among competitive racquet sports players, in whom the upper limb bones of the dominant (playing) arm is generally more robust compared to the non-playing skeletal elements (5). These effects are consequences of Wolff's law (6) and have been verified in numerous murine models of mechanotransduction, such as ulna- and tibia-loading models, the tail suspension model, and the botulinum toxin paralysis model (7–9). However, the precise physical and biological mechanisms that drive adaptation to disuse/overuse have not been completely elucidated.

Although the biological mechanisms that control mechanotransduction are far from certain, considerable progress has been made in identification of some of the key players in this process. For example, very early after a mechanical signal is received by bone cells, adenosine triphosphate (ATP) is released from stimulated cells and intracellular  $\text{Ca}^{2+}$  concentration increases within 1 min after loading (10–12). Subsequently, at least two other essential second messengers, prostaglandin E2 (PGE2) and nitric oxide (NO), are released from the mechanically stimulated cells (13–15).

(Figure 1). Those events lead to the induction of MAP-kinase signaling (ERK 1/2) and C-fos expression (16, 17). Later, inhibition of Sost and Dkk1 expression, along with increased expression of IGF-I and other bone matrix-related genes such as osteopontin and collagen have been documented (18, 19).

In this process, the Wnt pathway has been reported to play an important role in transmitting mechanical signaling in bone remodeling through both activating and inactivating several signaling cascades (20). The canonical Wnt pathway is initiated when released Wnt proteins bind to receptor complexes including a seven pass transmembrane co-receptor called Frizzled, and either low-density lipoprotein-related receptor-5 (Lrp5) or -6 (Lrp6). Formation of this receptor complex at the cell surface eventually leads to increased  $\beta$ -catenin-induced transcriptional activity via increased  $\beta$ -catenin levels in the cytoplasm.

Over the past decade, this Wnt/ $\beta$ -catenin signaling pathway has been identified as an essential component of mechanically induced signal transduction. Heterozygous deletion of  $\beta$ -catenin in osteocytes has been reported to significantly reduce loading-induced anabolic responses in bone (21). Wnt/ $\beta$ -catenin signaling in bone remodeling is proposed to be regulated by both Lrp5 and Lrp6 (22–25). Although Lrp5 and Lrp6 have common properties, such as sequence and structural similarity within this subfamily of the LDL receptor-related proteins (26–28), their molecular downstream events might be different in the context of bone remodeling. In this review, we discuss the roles of both Lrp5 and Lrp6 in mechanical loading-induced Wnt/ $\beta$ -catenin signaling pathways in the process of bone remodeling.

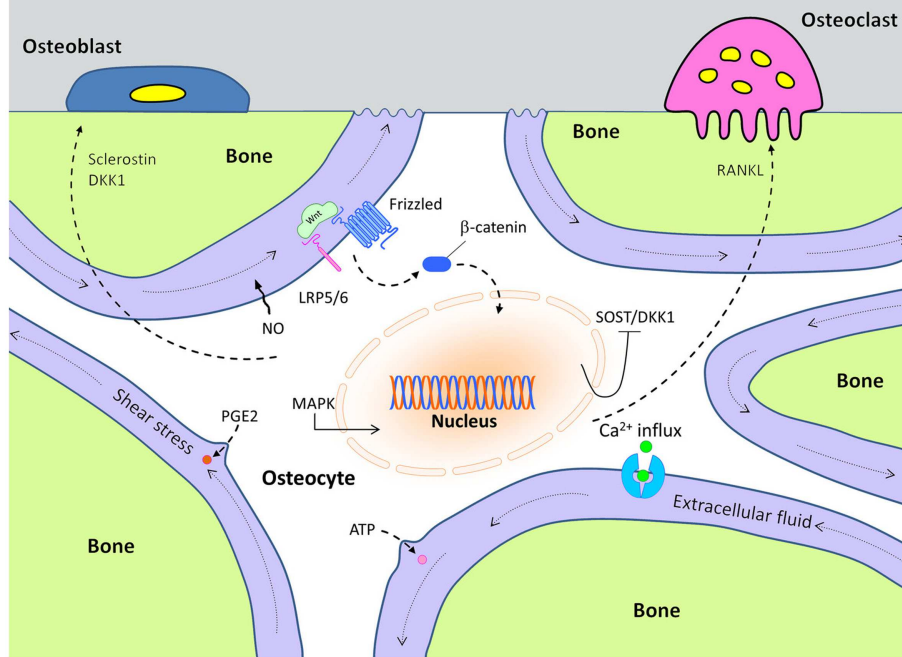


**FIGURE 1 |** Cellular mechanisms of action in mechanically stimulated osteocytes, which control osteoblast and osteoclast activity.

## LRP5

### LOSS-OF-FUNCTION STUDIES

Experiments performed on mice engineered with loss-of-function mutations in Lrp5 have revealed that Lrp5 is important to transfer the mechanical loading-induced signals in mechanosensory bone cells. Sawakami et al. investigated the crucial role of Lrp5 on skeletal mechanotransduction using mice with loss-of-function mutations (Lrp5-null) (25). Similar to the human patients with loss-of-function mutations in LRP5, the loss of Lrp5 signaling in mice yielded a significant decrease in bone-mineral density and bone strength. Mechanotransduction studies in these mice showed a reduced osteogenic response to mechanical loading, which was due to a reduction in load-induced synthesis of bone matrix, but not due to osteoblast recruitment and/or activation on the surfaces. Saxon et al. confirmed that Lrp5 has an important role in mechanotransduction using a different Lrp5<sup>-/-</sup> mouse model and a different skeletal loading modality. Among the experiments they reported that where their control mice (Lrp5<sup>+/+</sup>) exhibited dose-responsiveness to loading, they observed a loss of responsiveness in the Lrp5 mutants (29).

Based on the positive effects of the mechanical loading on bone formation, we can surmise that loading might either increase expression of Wnt stimulatory molecules, reduce expression of inhibitory molecules, or both. One of the more notable inhibitors of bone formation is sclerostin, which is known to participate in the Wnt signaling pathway (Figure 1). Sclerostin is an Lrp5/Lrp6 antagonist that is encoded by the Sost gene. It is primarily expressed in the osteocyte population, and loss-of-function mutations in Sost (or in its regulatory elements) are known to cause sclerosing bone disorders such as sclerosteosis and Van Buchem

disease (30–32). Sost transcript expression and sclerostin protein levels are dramatically decreased as a result of mechanical loading, especially in the high strain regions of the bone (8). Conversely, skeletal disuse causes an increase in Sost expression. The functional role of Sost regulation during mechanical loading was addressed by Tu et al., who showed that if the normal decrease in Sost expression that occurs during loading was prevented, the anabolic effects of loading were abolished (33). They accomplished this effect by loading engineered mice that harbored a transgene comprising an 8 kb Dmp1 promoter driving a human SOST cDNA. In these mice, the normal drop in endogenous Sost levels that occurs during loading was countered by an increase in human SOST during loading, owing to the load-sensitive Dmp1 promoter that regulated the hSOST cDNA.

### GAIN-OF-FUNCTION STUDIES

Other mutations in LRP5 have been identified in the human population that, rather than causing loss-of-function and very low bone mass, were found to cause abnormally high bone mass (HBM). Engineered mice have been generated to study the effect of these gain-of-function missense mutations in LRP5, including transgenic and knock-in models. Published reports from these mouse models demonstrate that the gain-of-function mutations in Lrp5 are associated with an HBM phenotype (24, 29). The mechanotransduction phenotype observed in the loss-of-function (Lrp5<sup>-/-</sup>) mice prompted several investigators to ask whether the HBM-causing mutations in Lrp5 also affect mechanotransduction, perhaps in the converse (beneficial) direction. To this end, Robinson et al. conducted ulnar loading experiments in mice harboring a human cDNA for LRP5 that included the G171V-causing

nucleotide substitution (34). The cDNA was driven by the 2.3 kb Col1a1 promoter, which provided specificity of the HBM allele to mature osteoblasts and osteocytes. They showed that Wnt/β-catenin target gene expression was increased after loading and this effect was associated with increased cell responsiveness to mechanical loading. This result was confirmed by Saxon et al., who reported the same mouse model (2.3 kb Col1a1 – G171V) subjected to tibial loading produced an increased osteogenic response to mechanical loading (29). They also indicated that these HBM transgenic mice had increased resistance to bone loss associated with disuse compared to wild type (WT) controls.

The effect of HBM-causing mutations in Lrp5 on mechanotransduction were further probed by Niziolek et al., who used two novel HBM knock-in models to elucidate the role of Lrp5 in the loading response. Those investigators used a different approach than the G171V transgenic approach used by Robinson et al. (34) and Saxon et al. (29). Rather than overexpressing cDNAs for HBM-causing alleles only in osteoblastic cells, Niziolek et al. knocked in the G171V and A214V HBM-causing mutations into the endogenous loci. This strategy allowed for normal expression levels and tissue distribution, owing to the undisturbed promoter and regulatory elements. These mice are therefore a more orthologous model to two of the human HBM families (7). When axial tibia loading was applied for 3 days to mature male Lrp5 G171V and Lrp5 A214V knock-in mice and to their WT controls, fluorochrome-labeling results showed that this loading resulted in a significantly enhanced periosteal response in the A214V knock-in mice, whereas the G171V knock-in mice exhibited greater bone formation on the endocortical surface. This bone formation difference in two different HBM-inducing Lrp5 mutations indicated that these types of mutations can alter the mechanisms responsible for anabolic mechanotransduction, and also, that a portion of the HBM phenotype observed in human patients carrying gain-of-function mutations in LRP5 might be at least partially due to enhanced mechanoresponsiveness in their skeletons.

## LRP6

Lrp6 is similar in sequence and structure to Lrp5, and these two receptors have been proposed to function largely in the same contexts and signaling pathways. However, there are some important differences between the two receptors. The most obvious difference is that whereas Lrp5<sup>-/-</sup> mice are viable and fertile (albeit with low bone mass), Lrp6<sup>-/-</sup> mice exhibit an embryonic lethal phenotype. Those observations suggest that either (1) the timing, location, and/or level of embryonic expression is different between Lrp5 and Lrp6, (2) the ligands, inhibitors, and/or downstream cascades differ between these two receptors, or (3) some combination of those two possibilities. For example, Lrp6 appears to be crucially important for bone's anabolic response to intermittent parathyroid hormone (PTH) treatment, whereas Lrp5 appears to be uninvolved. Li et al. showed that deletion of a floxed Lrp6 allele in osteoblasts, using osteocalcin-driven Cre recombinase, disrupts the bone anabolic activity of PTH by reducing number of osteoblasts (23). Wan et al. showed direct interaction between Lrp6 and the PTH 1 receptor using fluorescence resonance energy transfer (35). While Lrp6 appears to be important for PTH signaling, at least two published reports indicate that Lrp5 is not essential

for transducing PTH signaling (25, 36). These data suggested that Lrp5 and Lrp6 might participate selectively and differently in Wnt and/or other hormonal signaling. On the other hand, while Lrp5 is crucial for mechanotransduction, there is to date no clear evidence indicating that Lrp6 participates in mechanical loading-induced activation of Wnt signaling pathway.

Although both Lrp5 and Lrp6 are required to develop normal postnatal bone, available evidence indicates that their roles in this process might differ. Lrp6 has been reported to play a role in bone resorption and formation, whereas Lrp5 appears to affect bone formation but not bone resorption (22–25). These observations come from a number of studies that have looked at cell-specific effects of Lrp5 and Lrp6 in bone. For example, Kubota et al. reported the discovery of a naturally occurring mutation in Lrp6, which conferred hypomorphic properties to the receptor (referred to as the "rs" mutation). In a careful analysis of these mice, they found that canonical Wnt signaling was severely impaired in cells harvested from the rs/rs mice compared to WT mice (22). As expected, the rs/rs mice displayed low bone mass *in vivo*, but the phenotype was primarily due to increased bone resorption, with no detectable change in bone formation. This result stands in stark contrast to that reported for Lrp5<sup>-/-</sup> mice, in which bone resorption is normal but bone formation is reduced considerably. While both Lrp5 and Lrp6 can regulate Wnt signaling, the receptors might be active in osteoblasts over different time windows. A recent report indicates that Lrp6 might affect early osteogenic differentiation, whereas Lrp5 seems to affect late osteogenic differentiation (24). It should also be noted that the resorption/formation phenotype observed in the Lrp6 hypomorphic mice was not confirmed in an osteoblast-specific deletion model (Ocn-Cre with Lrp5<sup>fl/fl</sup>/fl mice); in fact, the opposite mechanism was reported, i.e., reduced bone formation and no change in resorption (23, 24). Li et al. observed that Lrp6 KO mice showed little change in the osteoclast number but reduced the osteoblast number compared with the WT littermates (23).

Another remarkable point of difference between Lrp5 and Lrp6 function is that the bone compartment affected might be different, although both Lrp5 and Lrp6 can both influence cortical bone remodeling. Sawakami et al. showed that the cross-sectional area of ulnas from Lrp5-deficient mice was reduced compared to WT mice (25), whereas Lrp6 appeared to be involved preferentially in trabecular bone development (22). This suggests that the developmental role of Lrp5 and Lrp6 might be different across bone surfaces. Other examples of compartment-specific effects have been reported for the Wnt cascade. For example, Liu et al. observed a surface-specific influence of Wnt signaling on bone metabolism. They found that Wnt16 deletion decreased cortical bone thickness and increased cortical bone porosity, while very minor changes were observed in trabecular bone in mice lacking Wnt16 (37).

## β-CATENIN

A major canonical downstream target of both Lrp5 and Lrp6 is β-catenin. Inactivation of β-catenin in osteoblasts (e.g., 2.3 kb Col1a1-Cre crossed to β-catenin<sup>fl/fl</sup>) causes osteopenia by affecting bone resorption rather than bone formation (38). The resorption phenotype in these mice has been replicated using Dmp1-Cre, a Cre driver that is active later in the osteoblast

differentiation pathway, i.e., late-stage osteoblasts and osteocytes. Osteocyte-specific  $\beta$ -catenin-deficient mice showed a low bone mass phenotype via increased osteoclast number and activity, while osteoblastic function was normal (39). Mechanistically, downregulated osteoprotegerin (OPG) expression was implicated in osteoclastic resorptive activity effect of those mice. Because  $\beta$ -catenin is downstream of Lrp5/6, this result is consistent with the Kubota et al. report on the Lrp6 hypomorphic mouse, but is inconsistent with the reports on Lrp5<sup>-/-</sup> and osteoblastic Lrp6<sup>-/-</sup> mice. It is interesting to note that the  $\beta$ -catenin resulted in a more severe bone phenotype than lack of either Lrp5 or Lrp6, indicating that there might be a combined (or synergistic) effect of Lrp5 and Lrp6 on bone regulation. Holmen et al. showed this possibility by comparing mice lacking various combinations of Lrp5 and Lrp6 (40). Additionally,  $\beta$ -catenin receives input from other proteins (e.g., mTOR, Pi3K), so it might be unreasonable to expect that  $\beta$ -catenin deletion would phenocopy the deletion of Lrp5/6. Regarding the role of  $\beta$ -catenin in mechanotransduction, it was recently shown that both copies of  $\beta$ -catenin are required in osteocytes and/or late-stage osteoblasts for mechanotransduction to occur; mice haploinsufficient for  $\beta$ -catenin in those cell populations showed no measurable response to mechanical stimulation *in vivo* (21).

Based on the various evidences regarding the Lrp5 function on bone formation and the Lrp6 role on bone regulation via bone resorption, we can hypothesize that the mechanical loading might affect bone regulation triggering the canonical Wnt signaling not only via Lrp5 (bone formation) but also via Lrp6 (perhaps both bone resorption and formation). In normal conditions, Wnt signaling pathways probably are influenced by both Lrp5 and Lrp6 at the same time, but in different ways and their roles might be synergistic. Further investigation on the role of Lrp6 in mechanical loading-induced signaling pathways and the synergistic effect of Lrp5 and Lrp6 could show more clearly the mechanism of Wnt signaling, via both Lrp5 and Lrp6, in mechanotransduction.

## CONCLUSION

Mechanical loading is a powerful modulator of bone modeling and remodeling. The exact cellular and molecular mechanisms by which this process occurs are still unclear. Substantial evidence indicates that the Wnt signaling pathway participates in the transduction of mechanical signals at the cell surface and ultimately leads to the regulation of bone metabolism. Lrp5 is intricately involved in bone cell mechanotransduction, but there is no indication at this time whether Lrp6 has any role in this process. Further studies are needed to clarify the role of the Wnt signaling pathway in Lrp5 and/or Lrp6-mediated mechanotransduction, which could eventually lead to powerful therapeutic agents that might mimic the anabolic effects of mechanical stimulation.

## REFERENCES

1. Robling AG, Castillo AB, Turner CH. Biomechanical and molecular regulation of bone remodeling. *Annu Rev Biomed Eng* (2006) **8**:455–98. doi:10.1146/annurev.bioeng.8.061505.095721
2. Rubin CT, Lanyon LE. Regulation of bone mass by mechanical strain magnitude. *Calcif Tissue Int* (1985) **37**(4):411–7. doi:10.1007/BF02553711
3. Leblanc AD, Schneider VS, Evans HJ, Engelbreton DA, Krebs JM. Bone-mineral loss and recovery after 17 weeks of bed rest. *J Bone Miner Res* (1990) **5**(8):843–50. doi:10.1002/jbmr.5650050807
4. Robling AG, Hinant FM, Burr DB, Turner CH. Improved bone structure and strength after long-term mechanical loading is greatest if loading is separated into short bouts. *J Bone Miner Res* (2002) **17**(8):1545–54. doi:10.1359/jbmr.2002.17.8.1545
5. Jones HH, Priest JD, Hayes WC, Tichenor CC, Nagel DA. Humeral hypertrophy in response to exercise. *J Bone Joint Surg* (1977) **59**(2):204–8.
6. Wolff J. *The Law of Bone Transformation*. Berlin: A. Hirschwald (1892).
7. Niziolek PJ, Warman ML, Robling AG. Mechanotransduction in bone tissue: the A214V and G171V mutations in Lrp5 enhance load-induced osteogenesis in a surface-selective manner. *Bone* (2012) **51**(3):459–65. doi:10.1016/j.bone.2012.05.023
8. Robling AG, Niziolek PJ, Baldridge LA, Condon KW, Allen MR, Alam I, et al. Mechanical stimulation of bone *in vivo* reduces osteocyte expression of Sost/sclerostin. *J Biol Chem* (2008) **283**(9):5866–75. doi:10.1074/jbc.M705092200
9. Warner SE, Sanford DA, Becker BA, Bain SD, Srinivasan S, Gross TS. Botox induced muscle paralysis rapidly degrades bone. *Bone* (2006) **38**(2):257–64. doi:10.1016/j.bone.2005.08.009
10. Hung CT, Allen FD, Pollack SR, Brighton CT. Intracellular Ca<sup>2+</sup> stores and extracellular Ca<sup>2+</sup> are required in the real-time Ca<sup>2+</sup> response of bone cells experiencing fluid flow. *J Biomech* (1996) **29**(11):1411–7. doi:10.1016/0021-9290(96)84536-2
11. Genets DC, Geist DJ, Liu D, Donahue HJ, Duncan RL. Fluid shear-induced ATP secretion mediates prostaglandin release in MC3T3-E1 osteoblasts. *J Bone Miner Res* (2005) **20**(1):41–9. doi:10.1359/JBMR.041009
12. Reich KM, McAllister TN, Gudi S, Frangos JA. Activation of G proteins mediates flow-induced prostaglandin E(2) production in osteoblasts. *Endocrinology* (1997) **138**(3):1014–8. doi:10.1210/endo.138.3.4999
13. Forwood MR, Kelly WL, Worth NF. Localisation of prostaglandin endoperoxide H synthase (PGHS)-1 and PGHS-2 in bone following mechanical loading *in vivo*. *Anat Rec* (1998) **252**(4):580–6. doi:10.1002/(SICI)1097-0185(199812)252:4<580::AID-AR8>3.0.CO;2-S
14. Rawlinson SC, el-Haj AJ, Minter SL, Tavares IA, Bennett A, Lanyon LE. Loading-related increases in prostaglandin production in cores of adult canine cancellous bone *in vitro* – a role for prostacyclin in adaptive bone remodeling. *J Bone Miner Res* (1991) **6**(12):1345–51. doi:10.1002/jbmr.5650061212
15. Rawlinson SC, Pitsillides AA, Lanyon LE. Involvement of different ion channels in osteoblasts' and osteocytes' early responses to mechanical strain. *Bone* (1996) **19**(6):609–14. doi:10.1016/S8756-3282(96)00260-8
16. Jessop HL, Rawlinson SC, Pitsillides AA, Lanyon LE. Mechanical strain and fluid movement both activate extracellular regulated kinase (ERK) in osteoblast-like cells but via different signaling pathways. *Bone* (2002) **31**(1):186–94. doi:10.1016/S8756-3282(02)00797-4
17. Pavalko FM, Norvell SM, Burr DB, Turner CH, Duncan RL, Bidwell JP. A model for mechanotransduction in bone cells: the load-bearing mechanosomes. *J Cell Biochem* (2003) **88**(1):104–12. doi:10.1002/jcb.10284
18. Lean JM, Mackay AG, Chow JW, Chambers TJ. Osteocytic expression of mRNA for c-fos and IGF-I: an immediate early gene response to an osteogenic stimulus. *Am J Physiol* (1996) **270**(6):E937–45.
19. Robling AG, Turner CH. Mechanical signaling for bone modeling and remodeling. *Crit Rev Eukar Gene Expr* (2009) **19**(4):319–38. doi:10.1615/CritRevEukarGeneExpr.v19.i4.50
20. Burgers TA, Williams BO. Regulation of Wnt/beta-catenin signaling within and from osteocytes. *Bone* (2013) **54**(2):244–9. doi:10.1016/j.bone.2013.02.022
21. Javaheri B, Stern AR, Lara N, Dallas M, Zhao H, Liu Y, et al. Deletion of a single beta-catenin allele in osteocytes abolishes the bone anabolic response to loading. *J Bone Miner Res* (2014) **29**(3):705–15. doi:10.1002/jbmr.2064
22. Kubota T, Michigani T, Sakaguchi N, Kokubu C, Suzuki A, Namba N, et al. Lrp6 hypomorphic mutation affects bone mass through bone resorption in mice and impairs interaction with Mesd. *J Bone Miner Res* (2008) **23**(10):1661–71. doi:10.1359/jbmr.080512
23. Li C, Xing Q, Yu B, Xie H, Wang W, Shi C, et al. Disruption of LRP6 in osteoblasts blunts the bone anabolic activity of PTH. *J Bone Miner Res* (2013) **28**(10):2094–108. doi:10.1002/jbmr.1962
24. Riddle RC, Diegel CR, Leslie JM, Van Koevering KK, Faugere MC, Clemens TL, et al. Lrp5 and Lrp6 exert overlapping functions in osteoblasts during postnatal bone acquisition. *PLoS One* (2013) **8**(5):e63323. doi:10.1371/journal.pone.0063323

25. Sawakami K, Robling AG, Ai M, Pitner ND, Liu D, Warden SJ, et al. The Wnt co-receptor LRP5 is essential for skeletal mechanotransduction but not for the anabolic bone response to parathyroid hormone treatment. *J Biol Chem* (2006) **281**(33):23698–711. doi:10.1074/jbc.M601000200
26. Chen D, Lathrop W, Dong Y. Molecular cloning of mouse Lrp7(Lr3) cDNA and chromosomal mapping of orthologous genes in mouse and human. *Genomics* (1999) **55**(3):314–21. doi:10.1006/geno.1998.5688
27. Brown SD, Twells RC, Hey PJ, Cox RD, Levy ER, Soderman AR, et al. Isolation and characterization of LRP6, a novel member of the low density lipoprotein receptor gene family. *Biochem Biophys Res Commun* (1998) **248**(3):879–88. doi:10.1006/bbrc.1998.9061
28. Hey PJ, Twells RC, Phillips MS, Yusuke N, Brown SD, Kawaguchi Y, et al. Cloning of a novel member of the low-density lipoprotein receptor family. *Gene* (1998) **216**(1):103–11. doi:10.1016/S0378-1119(98)00311-4
29. Saxon LK, Jackson BF, Sugiyama T, Lanyon LE, Price JS. Analysis of multiple bone responses to graded strains above functional levels, and to disuse, in mice in vivo show that the human Lrp5 G171V high bone mass mutation increases the osteogenic response to loading but that lack of Lrp5 activity reduces it. *Bone* (2011) **49**(2):184–93. doi:10.1016/j.bone.2011.03.683
30. Staehling-Hampton K, Proll S, Paepke BW, Zhao L, Charmley P, Brown A, et al. A 52-kb deletion in the SOST-MEOX1 intergenic region on 17q12-q21 is associated with van Buchem disease in the Dutch population. *Am J Med Genet* (2002) **110**(2):144–52. doi:10.1002/ajmg.10401
31. Balemans W, Patel N, Ebeling M, Van Hul E, Wuyts W, Lacza C, et al. Identification of a 52 kb deletion downstream of the SOST gene in patients with van Buchem disease. *J Med Genet* (2002) **39**(2):91–7. doi:10.1136/jmg.39.2.91
32. Balemans W, Ebeling M, Patel N, Van Hul E, Olson P, Dioszegi M, et al. Increased bone density in sclerosteosis is due to the deficiency of a novel secreted protein (SOST). *Hum Mol Genet* (2001) **10**(5):537–43. doi:10.1093/hmg/10.5.537
33. Tu X, Rhee Y, Condon KW, Bivi N, Allen MR, Dwyer D, et al. Sost downregulation and local Wnt signaling are required for the osteogenic response to mechanical loading. *Bone* (2012) **50**(1):209–17. doi:10.1016/j.bone.2011.10.025
34. Robinson JA, Chatterjee-Kishore M, Yaworsky PJ, Cullen DM, Zhao W, Li C, et al. Wnt/beta-catenin signaling is a normal physiological response to mechanical loading in bone. *J Biol Chem* (2006) **281**(42):31720–8. doi:10.1074/jbc.M602308200
35. Wan M, Yang C, Li J, Wu X, Yuan H, Ma H, et al. Parathyroid hormone signaling through low-density lipoprotein-related protein 6. *Gene Dev* (2008) **22**(21):2968–79. doi:10.1101/gad.1702708
36. Iwaniec UT, Wronski TJ, Liu J, Rivera MF, Arzaga RR, Hansen G, et al. PTH stimulates bone formation in mice deficient in Lrp5. *J Bone Miner Res* (2007) **22**(3):394–402. doi:10.1359/jbmr.061118
37. Liu X, Nagano K, Saito H, Baron R, Gori F. Wnt16 deletion differentially affects cortical and trabecular bone: increase cortical bone resorption, porosity and fracture in Wnt16 knockout mice. *ASBMR 2013 Annual Meeting*. Baltimore: Baltimore Convention Center (2013).
38. Glass DA II, Bialek P, Ahn JD, Starbuck M, Patel MS, Clevers H, et al. Canonical Wnt signaling in differentiated osteoblasts controls osteoclast differentiation. *Dev Cell* (2005) **8**(5):751–64. doi:10.1016/j.devcel.2005.02.017
39. Kramer I, Halleux C, Keller H, Pegurri M, Gooi JH, Weber PB, et al. Osteocyte Wnt/beta-catenin signaling is required for normal bone homeostasis. *Mol Cell Biol* (2010) **30**(12):3071–85. doi:10.1128/MCB.01428-09
40. Holmen SL, Giambardini TA, Zylstra CR, Buckner-Berghuis BD, Resau JH, Hess JF, et al. Decreased BMD and limb deformities in mice carrying mutations in both Lrp5 and Lrp6. *J Bone Miner Res* (2004) **19**(12):2033–40. doi:10.1359/jbmr.040907

**Conflict of Interest Statement:** The authors declare that the research was conducted in the absence of any commercial or financial relationships that could be construed as a potential conflict of interest.

Received: 16 October 2014; paper pending published: 13 November 2014; accepted: 31 December 2014; published online: 20 January 2015.

Citation: Kang KS and Robling AG (2015) New insights into Wnt-Lrp5/6- $\beta$ -catenin signaling in mechanotransduction. *Front. Endocrinol.* **5**:246. doi:10.3389/fendo.2014.00246

This article was submitted to Bone Research, a section of the journal *Frontiers in Endocrinology*.

Copyright © 2015 Kang and Robling. This is an open-access article distributed under the terms of the Creative Commons Attribution License (CC BY). The use, distribution or reproduction in other forums is permitted, provided the original author(s) or licensor are credited and that the original publication in this journal is cited, in accordance with accepted academic practice. No use, distribution or reproduction is permitted which does not comply with these terms.



# Improvement of skeletal fragility by teriparatide in adult osteoporosis patients: a novel mechanostat-based hypothesis for bone quality

Toshihiro Sugiyama<sup>1\*</sup>, Tetsuya Torio<sup>1</sup>, Tsuyoshi Sato<sup>2</sup>, Masahito Matsumoto<sup>3</sup>, Yoon Taek Kim<sup>1</sup> and Hiromi Oda<sup>1</sup>

<sup>1</sup> Department of Orthopaedic Surgery, Saitama Medical University, Saitama, Japan

<sup>2</sup> Department of Oral and Maxillofacial Surgery, Saitama Medical University, Saitama, Japan

<sup>3</sup> Division of Functional Genomics and Systems Medicine, Research Center for Genomic Medicine, Saitama Medical University, Saitama, Japan

\*Correspondence: tsugiym@saitama-med.ac.jp

**Edited and reviewed by:**

Jonathan H. Tobias, University of Bristol, UK

**Keywords:** bone, parathyroid hormone, mechanostat, mechanical strain, bone quality

## SKELETAL ADAPTATION TO MECHANICAL STRAIN IN HUMANS

Several lines of clinical evidence (1–3) suggest that the adult skeleton in humans continuously responds to change in mechanical environment to maintain resultant “elastic” deformation (strain) of bone; increased or decreased bone strain would normally induce bone gain or loss, respectively. Indeed, skeletal adaptation to mechanical strain, known as the mechanostat (4–6), plays a significant role in the treatment of osteoporosis. For example, bone strain from habitual physical activity decreases when an osteoporosis drug increases bone strength, indicating that the effect of osteoporosis therapy is limited by mechanical strain-related feedback control; this mechanostat-based logic is consistent with various clinical data (3). Approaches to reduce the limitation of osteoporosis therapy include pharmacologically enhancing skeletal response to mechanical loading, and earlier experimental studies using external mechanical loading models show that intermittent treatment with parathyroid hormone has such a possibility (7, 8). Importantly, treatment with teriparatide could synergistically produce bone gain with even low, physiological levels of mechanical loading in humans (9) as well as animals (10). The present article concisely discusses the effects of daily or weekly treatment with teriparatide and proposes a new mechanostat-based hypothesis for bone quality associated with mineral versus collagen.

## DAILY OR WEEKLY TREATMENT WITH TERIPARATIDE IN OSTEOPOROSIS

In Japan, not only daily subcutaneous injection of teriparatide (20 µg/day) (11–13) but also weekly subcutaneous injection of teriparatide (56.5 µg/week) (14, 15) has been approved for the treatment of adult osteoporosis patients with high risk of fracture. Interestingly, there are marked differences in the effects of these two treatments on circulating markers of bone formation and resorption. The daily injection results in a rapid and sustained increase in bone formation markers followed by a delayed increase in bone resorption markers (12); the period of time during which the increase in bone formation is superior to that in bone resorption is called the anabolic window (16). In contrast, the weekly injection induces only a transient increase in bone formation markers without an increase in bone resorption markers (14).

Formation and resorption occur on different surfaces during bone modeling, and thus modeling-based bone formation and resorption are not coupled; such uncoupling factors include mechanical loading that stimulates bone formation and suppresses bone resorption. Modeling-based bone formation by histomorphometry (17, 18) as well as an increase in bone formation markers and a decrease in bone resorption markers in blood (19) are observed during the first month of daily treatment with teriparatide, which is consistent with clinical finding suggesting that daily treatment with teriparatide and normal physical activity synergistically produce bone gain (9). A rapid but transient increase

in bone formation markers without an increase in bone resorption markers (14) implies that weekly treatment with teriparatide also stimulates modeling-based bone formation.

On the other hand, long-term daily, but not weekly, treatment with teriparatide causes increases in both bone formation and resorption markers (12, 14). These systemic changes agree with histomorphometric data showing that 1 or 2 years of daily treatment with teriparatide results in an increase in remodeling-based bone formation (20); resorption followed by formation occurs on the same surface during bone remodeling and thus remodeling-based bone resorption and formation are coupled. Increased or decreased bone remodeling lowers or raises, respectively, the degree of mineralization (21), and cortical volumetric bone mineral density (BMD) is decreased after daily treatment with teriparatide (13). In contrast, weekly treatment with teriparatide is unlikely to increase bone remodeling because neither an increase in bone resorption markers nor a decrease in cortical volumetric BMD is not found (14, 15).

## PERSPECTIVES ON THE EFFECTS OF TERIPARATIDE ON BONE FRAGILITY

An important goal of osteoporosis therapy is to prevent hip fracture associated with significant morbidity and mortality. The latest systematic review suggests that bone fragility at the hip is improved by daily treatment with teriparatide (22); the effect of weekly treatment with teriparatide on non-vertebral fracture risk

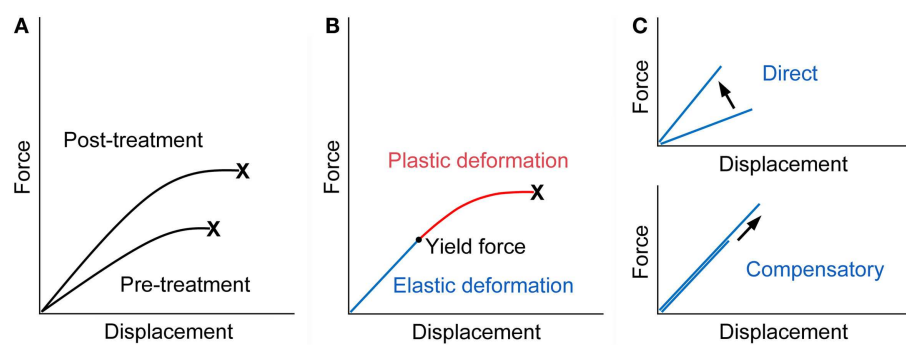


**FIGURE 1 | Force displacement curve of a bone.** **(A)** Treatment with an ideal osteoporosis drug improves bone fragility by increasing both of the force and displacement at failure (23). X denotes fracture. **(B)** The curve would consist of the pre-yield “elastic” deformation associated with mineral and the post-yield “plastic” deformation associated with collagen. Consequently, mechanical strain-related feedback control, the mechanostat, could work against mineral-related, but not collagen-related,

impairment of bone quality. X denotes fracture. **(C)** The pre-yield “elastic” deformation can be modified by osteoporosis therapy that (i) directly enhances the response to mechanical loading and increases the slope of the curve (upper) or (ii) lowers mineral-related bone quality and results in compensatory bone gain by the mechanostat to maintain the slope of the curve (lower). Note that, in the latter case, the yield force can be increased if compensated efficiently.

is under investigation. Here, we present mechanostat-based perspectives on this topic.

Fall-related fracture occurs if the energy from the fall is higher than that the bone can absorb. Force displacement curve obtained from a biomechanical test, in which a bone is loaded until it fractures, shows that work to failure (energy absorption), the area under the curve, represents bone fragility, and an ideal strategy for the improvement of bone fragility is to increase both the force and displacement at failure (23) (**Figure 1A**).

From a material point of view, stiffness and toughness of bone tissue generally depend on mineral and collagen, respectively (24). There is a yield force at which a bone begins to deform plastically, and mechanical strain from normal physical activity would be linked to the pre-yield “elastic” deformation associated with mineral but not to the post-yield “plastic” deformation associated with collagen (**Figure 1B**). Consequently, mechanical strain-related feedback control could compensate mineral-related, but not collagen-related, impairment of bone quality to maintain “elastic” deformation. Indeed, this theory is compatible with clinical data relating to bone quality. Examples of the mechanostat-based compensation for mineral-related impairment of bone quality would include rickets/osteomalacia and use of warfarin (3, 25–27), while the impairment of bone quality associated

with collagen cross-links significantly contributes to skeletal fragility in diabetes (28–30).

It is possible to speculate that treatment with teriparatide improves bone fragility at the hip through the mechanostat-based “modeling-related direct” and “remodeling-related compensatory” mechanisms (**Figure 1C**). Both daily and weekly treatments are expected to have the former effect by the enhancement of skeletal response to mechanical loading (7–10). In contrast, the latter effect is linked to daily treatment; a decrease in the degree of mineralization after daily but not weekly treatment (13, 15) might act to improve bone fragility if compensated efficiently, because compensatory bone gain by the mechanostat to maintain the pre-yield “elastic” deformation could increase the yield force at which a bone begins to deform plastically and thus the energy that the bone can absorb. This possibility is supported by histomorphometric data showing that one or two years of the treatment results in increases in modeling- and remodeling-based bone formation (20), because the mechanostat suggests that the former “modeling-related direct” effect does not continue for a long time (3).

Finally, the mechanostat-based theory appears to be inconsistent with clinical data that daily or weekly treatment with teriparatide stimulates bone accrual at the endosteal rather than periosteal surface, because the strain level would be lower

at the former site; endosteal as well as trabecular, but not periosteal, bone apposition is detected by computed tomography after daily (13) and weekly (15) treatments. Teriparatide-induced bone modeling is dose-dependent (17, 18), implying higher concentrations of the agent at the trabecular and endosteal surfaces. Regardless of the mechanism, the mechanostat suggests that inner bone gain could limit outer bone gain, because bone gain in the inner compartments is likely to decrease bone strain in the outer compartment.

## REFERENCES

- Christen P, Ito K, Ellouz R, Boutroy S, Sornay-Rendu E, Chapurlat RD, et al. Bone remodelling in humans is load-driven but not lazy. *Nat Commun* (2014) 5:4855. doi:10.1038/ncomms5855
- Bhatia VA, Edwards WB, Johnson JE, Troy KL. Short-term bone formation is greatest within high strain regions of the human distal radius: a prospective pilot study. *J Biomech Eng* (2015) 137:011001. doi:10.1115/1.4028847
- Sugiyama T, Kim YT, Oda H. Osteoporosis therapy: a novel insight from natural homeostatic system in the skeleton. *Osteoporos Int* (2015). doi:10.1007/s00198-014-2923-y
- Frost HM. Bone’s mechanostat: a 2003 update. *Anat Rec A Discov Mol Cell Evol Biol* (2003) 275:1081–101. doi:10.1002/ar.a.10119
- Skerry TM. The response of bone to mechanical loading and disuse: fundamental principles and influences on osteoblasts/osteocyte homeostasis. *Arch Biochem Biophys* (2008) 473:117–23. doi:10.1016/j.abb.2008.02.028
- Meakin LB, Price JS, Lanyon LE. The contribution of experimental in vivo models to understanding the mechanisms of adaptation to mechanical loading in bone. *Front Endocrinol* (2014) 5:154. doi:10.3389/fendo.2014.00154

7. Chow JW, Fox S, Jagger CJ, Chambers TJ. Role for parathyroid hormone in mechanical responsiveness of rat bone. *Am J Physiol* (1998) **274**: E146–54.
8. Hagino H, Okano T, Akhter MP, Enokida M, Teshima R. Effect of parathyroid hormone on cortical bone response to in vivo external loading of the rat tibia. *J Bone Miner Metab* (2001) **19**:244–50. doi:10.1007/s007740170027
9. Poole KE, Treece GM, Ridgway GR, Mayhew PM, Borggreve J, Gee AH. Targeted regeneration of bone in the osteoporotic human femur. *PLoS One* (2011) **6**:e16190. doi:10.1371/journal.pone.0016190
10. Sugiyama T, Saxon LK, Zaman G, Moustafa A, Sunters A, Price JS, et al. Mechanical loading enhances the anabolic effects of intermittent parathyroid hormone (1-34) on trabecular and cortical bone in mice. *Bone* (2008) **43**:238–48. doi:10.1016/j.bone.2008.04.012
11. Neer RM, Arnaud CD, Zanchetta JR, Prince R, Gaich GA, Reginster JY, et al. Effect of parathyroid hormone (1-34) on fractures and bone mineral density in postmenopausal women with osteoporosis. *N Engl J Med* (2001) **344**:1434–41. doi:10.1056/NEJM200105103441904
12. Miyauchi A, Matsumoto T, Sugimoto T, Tsujimoto M, Warner MR, Nakamura T. Effects of teriparatide on bone mineral density and bone turnover markers in Japanese subjects with osteoporosis at high risk of fracture in a 24-month clinical study: 12-month, randomized, placebo-controlled, double-blind and 12-month open-label phases. *Bone* (2010) **47**:493–502. doi:10.1016/j.bone.2010.05.022
13. Borggreve J, Graeff C, Nickelsen TN, Marin F, Gluer CC. Quantitative computed tomographic assessment of the effects of 24 months of teriparatide treatment on 3D femoral neck bone distribution, geometry, and bone strength: results from the EUROFORS study. *J Bone Miner Res* (2010) **25**:472–81. doi:10.1359/jbmr.090820
14. Nakamura T, Sugimoto T, Nakano T, Kishimoto H, Ito M, Fukunaga M, et al. Randomized Teriparatide [human parathyroid hormone (PTH) 1-34] once-weekly efficacy research (TOWER) trial for examining the reduction in new vertebral fractures in subjects with primary osteoporosis and high fracture risk. *J Clin Endocrinol Metab* (2012) **97**:3097–106. doi:10.1210/jc.2011-3479
15. Ito M, Oishi R, Fukunaga M, Sone T, Sugimoto T, Shiraki M, et al. The effects of once-weekly teriparatide on hip structure and biomechanical properties assessed by CT. *Osteoporos Int* (2014) **25**:1163–72. doi:10.1007/s00198-013-2596-y
16. Rubin MR, Bilezikian JP. The anabolic effects of parathyroid hormone therapy. *Clin Geriatr Med* (2003) **19**:415–32. doi:10.1016/S0749-0690(02)00074-5
17. Lindsay R, Cosman F, Zhou H, Bostrom MP, Shen VW, Cruz JD, et al. A novel tetracycline labeling schedule for longitudinal evaluation of the short-term effects of anabolic therapy with a single iliac crest bone biopsy: early actions of teriparatide. *J Bone Miner Res* (2006) **21**:366–73. doi:10.1359/JBMR.051109
18. Lindsay R, Zhou H, Cosman F, Nieves J, Dempster DW, Hodzman AB. Effects of a one-month treatment with PTH(1-34) on bone formation on cancellous, endocortical, and periosteal surfaces of the human ilium. *J Bone Miner Res* (2007) **22**:495–502. doi:10.1359/jbmr.070104
19. Glover SJ, Eastell R, McCloskey EV, Rogers A, Garner P, Lowery J, et al. Rapid and robust response of biochemical markers of bone formation to teriparatide therapy. *Bone* (2009) **45**:1053–8. doi:10.1016/j.bone.2009.07.091
20. Ma YL, Zeng Q, Donley DW, Ste-Marie LG, Gallagher JC, Dalsky GP, et al. Teriparatide increases bone formation in modeling and remodeling osteons and enhances IGF-II immunoreactivity in postmenopausal women with osteoporosis. *J Bone Miner Res* (2006) **21**:855–64. doi:10.1359/jbmr.060314
21. Roschger P, Misof B, Paschalis E, Fratzl P, Klaushofer K. Changes in the degree of mineralization with osteoporosis and its treatment. *Curr Osteoporos Rep* (2014) **12**:338–50. doi:10.1007/s11914-014-0218-z
22. Eriksen EF, Keaveny TM, Gallagher ER, Krege JH. Literature review: the effects of teriparatide therapy at the hip in patients with osteoporosis. *Bone* (2014) **67**:246–56. doi:10.1016/j.bone.2014.07.014
23. Turner CH. Biomechanics of bone: determinants of skeletal fragility and bone quality. *Osteoporos Int* (2002) **13**:97–104. doi:10.1007/s001980200000
24. Fratzl P, Gupta HS, Paschalis EP, Roschger P. Structure and mechanical quality of the collagen-mineral nano-composite in bone. *J Mater Chem* (2004) **14**:2115–23. doi:10.1039/b402005g
25. Sugiyama T, Tanaka S, Miyajima T, Kim YT, Oda H. Vitamin D supplementation and fracture risk in adults: a new insight. *Osteoporos Int* (2014) **25**:2497–8. doi:10.1007/s00198-014-2798-y
26. Sugiyama T, Yoshioka H, Sakaguchi K, Kim YT, Oda H. An evidence-based perspective on vitamin D and the growing skeleton. *Osteoporos Int* (2015). doi:10.1007/s00198-014-2975-z
27. Sugiyama T, Kugimiya F, Kono S, Kim YT, Oda H. Warfarin use and fracture risk: an evidence-based mechanistic insight. *Osteoporos Int* (2015). doi:10.1007/s00198-014-2912-1
28. Leslie WD, Rubin MR, Schwartz AV, Kanis JA. Type 2 diabetes and bone. *J Bone Miner Res* (2012) **27**:2231–7. doi:10.1002/jbmr.1759
29. Garner P. The contribution of collagen crosslinks to bone strength. *Bonekey Rep* (2012) **1**:182. doi:10.1038/bonekey.2012.182
30. Saito M, Marumo K. Bone quality in diabetes. *Front Endocrinol* (2013) **4**:72. doi:10.3389/fendo.2013.00072

**Conflict of Interest Statement:** The authors declare that the research was conducted in the absence of any commercial or financial relationships that could be construed as a potential conflict of interest.

Received: 05 December 2014; accepted: 13 January 2015; published online: 30 January 2015.

**Citation:** Sugiyama T, Torio T, Sato T, Matsumoto M, Kim YT and Oda H (2015) Improvement of skeletal fragility by teriparatide in adult osteoporosis patients: a novel mechanostat-based hypothesis for bone quality. *Front. Endocrinol.* **6**:6. doi: 10.3389/fendo.2015.00006  
This article was submitted to Bone Research, a section of the journal *Frontiers in Endocrinology*.

Copyright © 2015 Sugiyama, Torio, Sato, Matsumoto, Kim and Oda. This is an open-access article distributed under the terms of the Creative Commons Attribution License (CC BY). The use, distribution or reproduction in other forums is permitted, provided the original author(s) or licensor are credited and that the original publication in this journal is cited, in accordance with accepted academic practice. No use, distribution or reproduction is permitted which does not comply with these terms.



# Ethnic differences in bone health

Ayse Zengin<sup>1</sup>, Ann Prentice<sup>1,2</sup> and Kate Anna Ward<sup>1\*</sup>

<sup>1</sup> Medical Research Council Human Nutrition Research, Cambridge, UK

<sup>2</sup> Medical Research Council, Keneba, Gambia

**Edited by:**

Jonathan H. Tobias, University of Bristol, UK

**Reviewed by:**

Jennifer Tickner, University of Western Australia, Australia

Mark H. Edwards, MRC Lifecourse Epidemiology Unit, UK

**\*Correspondence:**

Kate Anna Ward, MRC Human Nutrition Research, Elsie Widdowson Laboratory, Fulbourn Road, Cambridge CB1 9NL, UK  
e-mail: kate.ward@mrc-hnr.cam.ac.uk

There are differences in bone health between ethnic groups in both men and in women. Variations in body size and composition are likely to contribute to reported differences. Most studies report ethnic differences in areal bone mineral density (aBMD), which do not consistently parallel ethnic patterns in fracture rates. This suggests that other parameters beside aBMD should be considered when determining fracture risk between and within populations, including other aspects of bone strength: bone structure and microarchitecture, as well as muscle strength (mass, force generation, anatomy) and fat mass. We review what is known about differences in bone-densitometry-derived outcomes between ethnic groups and the extent to which they account for the differences in fracture risk. Studies are included that were published primarily between 1994 and 2014. A “one size fits all approach” should definitely not be used to understand better ethnic differences in fracture risk.

**Keywords:** ethnic groups, bone, muscle, pQCT, DXA, fracture, skeletal, bone mineral density

## INTRODUCTION

There are differences in fracture risk between ethnic groups in both men and in women across the globe. It is important to understand the underlying phenotype that contributes to these differences in order to be able to determine strategies for the prevention of osteoporosis and bone fragility in an ever-changing environment. Most studies report ethnic differences in areal bone mineral density (aBMD), which do not consistently parallel ethnic patterns in fracture rates. Variations in body size and composition are likely to contribute to reported differences.

Traditionally, aBMD ( $\text{g}/\text{cm}^2$ ) measured by single and dual energy x-ray absorptiometry (DXA) or photon absorptiometry (SPA/DPA) is used as a surrogate for bone strength and fracture risk. DXA superseded SPA/DPA over 30 years ago. DXA has many advantages, including good precision, low radiation dose, and ability to scan skeletal sites most prone to osteoporotic fracture. Areal BMD predicts fracture and in Western White older adults, a 1-SD decrease in aBMD leads to 2.6-fold greater fracture risk (1). However, DXA only measures aBMD ( $\text{g}/\text{cm}^2$ ), projectional bone area ( $\text{cm}^2$ ), and bone mineral content (BMC, g) and as such does not fully account for bone size because it cannot account for differences in bone depth. Additionally, DXA is an average value across all bony elements within the periosteal envelope and so does not assess the separate compartments within bone (cortical or trabecular), bone structure (size and shape), organization within the periosteal envelope (e.g., cortical thickness), microarchitecture (e.g., trabecular thickness, number, cortical porosity), or bone metabolism, all of which are important components of bone strength. The aforementioned limitations are thought to be the basis for the inadequacies of aBMD in predicting fracture in different ethnic groups (2). The advancement of imaging technology to include central, peripheral, and high-resolution peripheral quantitative computed tomography (QCT, pQCT, and HRpQCT) has enabled the measurement of volumetric bone mineral density

(vBMD), the structural dimensions, and internal organization of cortical and trabecular bone and to give *in vivo* estimates of bone strength. With its greater spatial resolution ( $82 \mu\text{m}$ ), HRpQCT also measures trabecular and cortical microarchitecture; it measures trabecular number directly and provides indirect estimates of trabecular bone volume, trabecular thickness, trabecular separation, and bone strength (3).

Throughout this review, ethnicity has been used to group individuals according to a mix of cultural and other factors including geography, language, diet, religion, ancestry, and physical features traditionally associated with race. The glossary in **Table 1** has summarized and defined each ethnic group that is discussed in this review.

This review focuses on evidence from studies using bone-densitometry techniques and those reporting fracture incidences. With the aforementioned technical developments and the recognition of the limitations of DXA, recent studies have focused on describing ethnic differences in bone structure and bone microarchitecture and the extent to which these may contribute to differences in fracture risk. However, as this review highlights, there are still relatively few data available outside of US, particularly in populations where fracture incidence is predicted to rise over the coming decades.

## FRACTURE INCIDENCE AND BMD ACROSS THE GLOBE

Global data on adults suggest that, compared to age-matched White-American or British/European populations, other ethnic groups have a lower incidence of fracture (**Figure 1**). There is a >10-fold variation in age-standardized hip fracture risk across 63 countries and a notable divide between Western and Eastern populations (4–6). Most recently, Cauley et al. (5) showed greater variability in incidence and geographic pattern for clinical vertebral fractures than for hip fracture; it should be noted that for radiographically confirmed vertebral fractures the global pattern

**Table 1 | Classification of ethnic groups.**

| Ethnic group           | Definition   |
|------------------------|--|
| White-American         | European ancestral origins living in US  |
| Black-American         | African ancestral origins living in US   |
| Asian-American         | Collective group of eastern Asian (Japanese, Chinese) ancestral origins living in US     |
| Chinese-American       | Chinese ancestral origins living in US   |
| Japanese-American      | Japanese ancestral origins living in US  |
| White-British          | English, Welsh, Scottish, and Northern Irish living in UK                                |
| South-Asian British    | Indian, Pakistani, and Bangladeshi ancestral roots living in UK                          |
| Afro-Caribbean British | African ancestral origins whose forebears were in the Caribbean before immigrating to UK |
| Gambian                | Sub-Saharan African ancestral origins, primarily Mandinka, living in The Gambia          |
| Gambian-British        | Sub-Saharan African ancestral origins, primarily Mandinka, living in UK                  |
| Chinese                | Chinese ancestral origins living in China  |

incidence was similar to that for hip fracture (5). Globally, the lowest fracture rates are in populations with African ancestry (6), but there is a sparsity of data from the African continent, particularly Sub-Saharan Africa (5, 7, 8). In the late 1960s, Solomon et al. described differences between White and Bantu populations in adult fracture incidence to be similar to those reported in North-America between Black- and White-Americans (9). Data from Cameroon suggest similarities to populations from the developed world because women have higher incidence than men of low trauma fracture to the hip and wrist (10). Further data are required to confirm the generalizability of this observation. With a rising life expectancy, increasing “Westernization” of African populations, better survival for individuals with HIV, and increasing non-communicable disease risk fracture incidence is also expected to rise and should be better characterized (5, 7, 10, 11). In Asian populations, a 15-fold increase in hip fracture incidences was reported in studies from Japan and Hong Kong (12, 13). Compared to Western populations, there also appear to be sex differences in the patterns of incidence where in China there were no sex differences and in Thailand, men have greater hip fracture incidence (14, 15).

To date, the majority of large population studies have used aBMD measured by DXA as a proxy for fracture risk to study ethnic differences in bone health. In men, data from the third National Health and Nutrition Examination Survey (NHANES III) showed that Black-Americans had a higher mean femoral neck and total hip aBMD compared to White-American men (16); these differences were similar to reported fracture rates between these ethnic groups (17). The osteoporotic fractures in men study (MrOS) used QCT and showed that Black-American and East Asian-American men had higher bone strength compared to White-American men

due to greater vBMD at the femoral neck (18). Data from UK-cohort of the European Male Aging Study (EMAS) compared White-British men to a group of Afro-Caribbean British and South-Asian British men. The Afro-Caribbean British group had higher aBMD at all sites compared to South-Asian British and White-British, both before and after adjustment for body size (19). However, vBMD of the distal radius assessed using pQCT was not different between the groups (20).

One of the largest multi-ethnic studies, the National Osteoporosis Risk Assessment (NORA) study (NORA) showed that Black-American women had higher, and Asian-Americans<sup>1</sup> lower, aBMD in the study population (2). Even after adjusting for body weight and other risk factor covariates, the greater aBMD in Black-American women persisted; however, Asian-American women had similar values to White-American women (2). Despite lower aBMD in Asian-American women, studies have shown lower rates of fracture compared to White-American women (2). In UK, South-Asian women had lower aBMD than White-British women before appropriate adjustment for body or bone size, thereafter there were no differences between groups (21, 22). Similarly, Chinese women had lower aBMD than White-British women; after adjustment for body size, these differences were attenuated (23). Furthermore, despite a lower size-adjusted BMC at the lumbar spine, hip, and radius in Gambian women compared to White-British women (independent of height and weight), there was a lower incidence of fracture among Gambian women (24), suggesting that there are other factors contributing to the lower fracture risk seen in Gambian women. Taken together, all of the studies discussed in this section suggest that there may be other components of bone strength that should be studied to help to better predict fracture risk in different populations.

## ETHNIC DIFFERENCES IN BONE STRUCTURE

Earlier studies of bone structure show differences in body-segment proportions (sitting and standing height) and also in cortical parameters measured using histomorphometry, which may contribute to ethnic differences in fracture rates (25, 26). The most recent studies also demonstrate that bone structure and microarchitecture are different in ethnic groups and these variations are likely to contribute to the ethnic differences in fracture rates.

## DUAL ENERGY X-RAY ABSORPTIOMETRY

The Study of Womens Health Across the Nation (SWAN) study reported no differences in aBMD between Chinese-American, Japanese-American, and White-American women, but bone structure varied greatly (27). Femoral neck cross-sectional area (total bone surface in a cross-section, exclusive of soft tissue spaces and pores) and section modulus of the hip, measured by DXA, were higher in Japanese-American compared to White-American women (27). A greater section modulus in Japanese-American women would give better resistance to axial compressive and bending stresses. In the previously described studies of Gambian and Chinese women, compared to White-British women, ethnic differences in hip axis length (HAL) have been reported, in addition to

<sup>1</sup>Residing in US, i.e., predominantly East Asian population

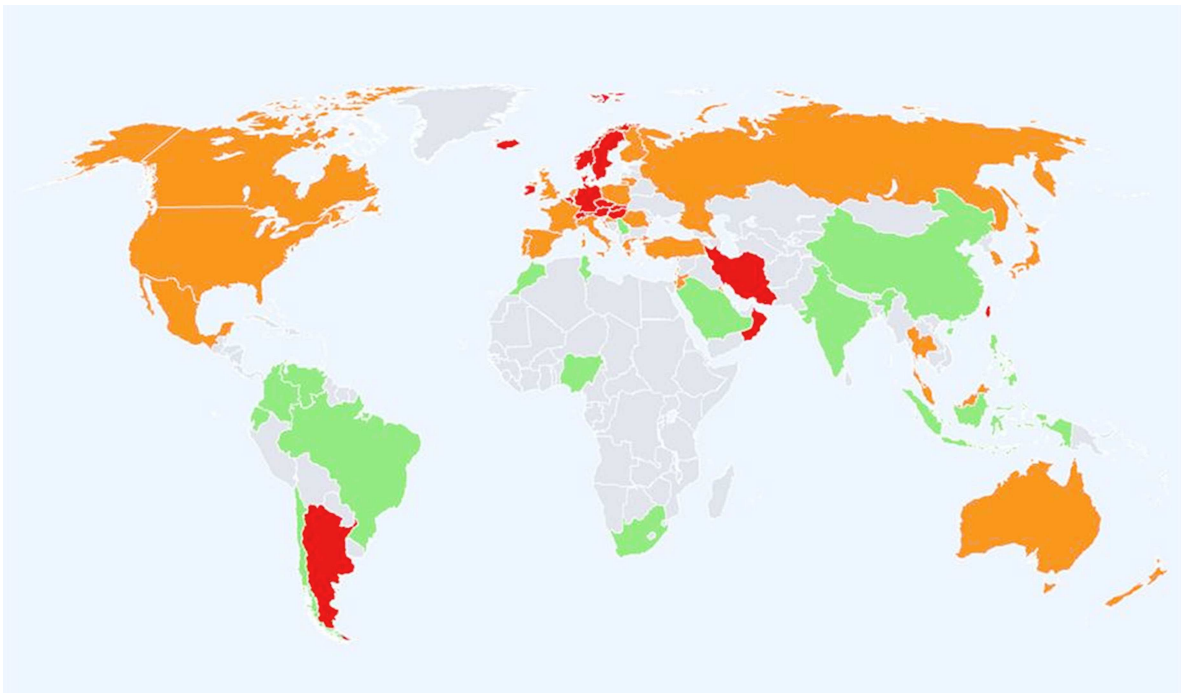


**FIGURE 1 | Hip fracture rates for men and women combined in different countries of the world categorized by risk.** Where estimates are available, countries are color coded red (annual incidence  $>250/100,000$ ), orange ( $150\text{--}250/100,000$ ), or green ( $<150/100,000$ ) (6).

the aBMD differences (23, 28, 29). Of the three groups, Gambian women had the shortest HAL after correction for height. Similarly, in a study in British men, HAL was shorter in Afro-Caribbean British men compared to White-British and South-Asian British men (19); similar results were reported in Gambian-British compared to White-British men after correcting for weight and height (28). A longer HAL has been associated with a higher risk of hip fracture, and is considered to be a risk predictor for hip fracture (30). And so, it is likely that these structural differences, in part, explain differences between ethnic groups of hip fracture incidence (28, 31).

#### QUANTITATIVE COMPUTED TOMOGRAPHY

In UK, there are only sparse data on bone structure measured by axial or peripheral QCT. Pre-menopausal South-Asian British women had lower cortical vBMD, BMC, and thinner cortices at the radial diaphysis compared to White-British women; this was independent of age, height, and weight (32). Despite lower BMC in the South-Asian British women, bone strength, as estimated using the strength strain index (SSI) was similar. This suggests that bones of pre-menopausal South-Asian British women may be efficiently adapted to a lower BMC as a result of a different distribution of bone mineral within the periosteal envelope, thereby preserving bone strength (32, 33). In contrast, another study has shown that post-menopausal South-Asian British women have lower SSI and fracture load at the radius and tibia despite having thicker cortices and higher vBMD; bone cross-sectional area was smaller (34).

In MrOS, Black-American and Asian-American men had thicker cortices, measured using axial QCT, than

White-Americans, which led to greater bone strength at the hip (18). Similarly, greater estimated bone strength was found in Afro-Caribbean British and South-Asian British men compared to White-British men. Lower strength in the White-British men was due to smaller bone size at the mid-shaft radius (20).

#### HIGH-RESOLUTION pQCT

Due to the relatively recent introduction of HRpQCT, there are only limited data using this technology. In a comparison of pre-menopausal women from US, Chinese-American women were shown to have smaller bones, with higher cortical vBMD and different trabecular microarchitecture than White-American women (35, 36). They appeared to have a structural advantage in their trabecular microarchitecture compared to White-American women, with larger, more plate-like trabeculae, and a greater plate-rod junction density, which indicates the number of trabecular network connections (35). As plate-like structure contributes to a greater proportion of bone strength than the rods, these structural differences may explain the lower fracture risk in this group of women. Currently, there are no other data using HRpQCT to compare differences in bone structure. Lower fracture risk in African-American women is likely due to thicker cortices and better trabecular microarchitecture, both of which would be reflected in higher aBMD (a composite measurement of trabecular and cortical bone) previously reported in this ethnic group (37).

#### ETHNIC DIFFERENCES IN BODY COMPOSITION

There are major differences in body habitus (fat mass, muscle mass, height, and weight) between ethnic groups (Table 2),

**Table 2 | Ethnic differences in body composition in women and men.**

|           |             | Chinese-American | South-Asian British | Black-American | Tobago       | South-African | Mexican-American |
|-----------|-------------|------------------|---------------------|----------------|--------------|---------------|------------------|
| Women     | Body weight | ↓                | ↑                   | ↑              | ↑            | =             | =                |
|           | Height      | ↓                | ↓                   | =              | ↑            | ↓             | ↓                |
|           | BMI         | ↓                | ↑                   | ↑              | ↑            | ↑             | ↑                |
|           | Fat mass    | ↓                | ↑                   | ↑              |              |               | ↑                |
|           | Muscle mass | ↓                | ↓                   | ↑              |              |               | ↓                |
| Men       | Body weight | ↓ <sup>a</sup>   | ↓                   | =              | =            | ↓             | ↓                |
|           | Height      | ↓ <sup>a</sup>   | ↓                   | =              | =            | ↓             | ↓                |
|           | BMI         | = <sup>a</sup>   | =                   | =              | ↓            | ↓             | =                |
|           | Fat mass    | ↑ <sup>a</sup>   | ↑ <sup>b</sup>      | ↓              | ↓            |               | ↓                |
|           | Muscle mass |                  | ↓ <sup>b</sup>      | ↑              |              |               |                  |
| Reference |             | (23, 50)         | (32, 34, 51, 52)    | (40, 53)       | (45, 54, 55) | (56, 57)      | (40, 58)         |

All parameters are compared to White individuals.

<sup>a</sup>Chinese ancestral origins living in China.

<sup>b</sup>South-Asian ancestral origins living in New Zealand.

which should be considered when studying differences in bone between and within different ethnic groups (38). For example, Chinese-American and Gambian women have a low BMI, which is a risk factor for fracture (Table 2) (2, 24). In post-menopausal women, a higher body weight is considered to be protective against fracture due to increased load (from greater muscle and fat mass) on the skeleton and also with fat accumulation providing padding during a fall (39). This is indicated in Black-American women who have greater fat and lean mass and aBMD, and lower fracture risk, compared to White-American women (40) (Table 2). A recent meta-analysis reported that muscle mass exerts a greater positive influence on aBMD than fat mass in men and women combined (41). However, increased weight appears to provide only partial protection, with an audit of fracture cases in UK and results from the Global Longitudinal Study of Osteoporosis in Women showing that obesity was a risk factor for fracture (42, 43). Those who fractured did not have a low aBMD (43), indicating the insensitivity of aBMD to predict fracture.

The NORA and SWAN studies (2, 44) emphasized the importance of taking into account body weight when quantifying differences in aBMD between Asian-American (Chinese and Japanese) and White-American women. Correcting for body weight decreased or reversed the differences in the total hip or spine aBMD between Asian-American (Chinese and Japanese) and White-American women (2, 44, 45). Similarly, correcting for body size attenuated differences in aBMD at the hip, lumbar spine, and total body in South-Asian British (Pakistani and Gujarati) women compared to White-British women (22, 46).

There is a gap in the literature regarding the differences in body composition between men of different ethnicities (Table 2). The studies mentioned in Table 2 demonstrate that there are differences in muscle mass between ethnic groups. These studies also show that it is important to interpret aBMD from DXA with caution if bone area, height, and weight (or its component parts) are not adequately accounted for, as it may lead to misinterpretation of results (46).

## ETHNIC DIFFERENCES IN THE MUSCLE–BONE RELATIONSHIP

Muscle strength is a composite term that describes muscle mass and anatomy (including intramuscular fat accumulation), force generating capacity and power (33). Muscle contractions are considered as the primary source of load upon the skeleton, more so than body weight, even in weight bearing bones (47). Given the differences in lean mass discussed in the previous section, it is likely that muscle force and power will also be different between ethnic groups, which are likely to contribute to differences in vBMD, size, shape, and distribution of bone. Measurements of muscle mass or cross-sectional area incompletely represent changes in muscle strength (48). Techniques to quantify the functional aspects of muscle strength include grip force, jumping mechanography, dynamometry, and electromyography. These dynamic tests give more accurate estimations of muscle strength than using muscle mass alone (46). Preliminary data from the EMAS demonstrated ethnic differences in the relationship between muscle force and power and age (20, 49).

There is a gap in the literature, because no studies published to date have investigated the relationships of muscle mass and function with vBMD, bone size and shape, and/or microarchitecture between ethnic populations. Differences in muscle force and power may partly underlie the ethnic differences in fracture incidence.

## CONCLUSION

Fracture incidence varies between ethnic groups. Despite its many advantages, it is now recognized that the variance in fracture rates between ethnic groups cannot solely be explained by DXA. The studies described in this review highlights that “one size does not fit all” and there is a need to understand differences in skeletal phenotype at different stages of life (e.g., pre- versus post-menopausal) and in different populations both within and across continents (33). The separate measurement of cortical and trabecular bone compartments, and bone shape, size, microarchitecture, and metabolism is important to fully understand the differences of bone strength between ethnic groups. This requires technologies that move beyond measurements aBMD/BMC by DXA and use of

three-dimensional imaging devices like pQCT and HRpQCT. The investigation of muscle and bone relationships in ethnic groups is also critical to the development of more effective strategies to improve musculoskeletal health and function. Future studies are required to identify how differences in nutrition, cultural preferences, socioeconomic factors, sunshine exposure, and physical activity levels affect bone health between ethnic groups.

## ACKNOWLEDGMENTS

This research is funded by the Medical Research Council (MRC) (program codes U105960371, U123261351) and the Department for International Development (DFID) under the MRC/DFID Concordat agreement.

## REFERENCES

- Marshall D, Johnell O, Wedel H. Meta-analysis of how well measures of bone mineral density predict occurrence of osteoporotic fractures. *BMJ* (1996) **312**:1254–9. doi:10.1136/bmj.312.7041.1254
- Barrett-Connor E, Siris ES, Wehren LE, Miller PD, Abbott TA, Berger ML, et al. Osteoporosis and fracture risk in women of different ethnic groups. *J Bone Miner Res* (2005) **20**:185–94. doi:10.1359/JBMR.041007
- Bouxsein ML. Bone structure and fracture risk: do they go arm in arm? *J Bone Miner Res* (2011) **26**:1389–91. doi:10.1002/jbmr.442
- Ballane G, Cauley JA, Luckey MM, Fuleihan Gel H. Secular trends in hip fractures worldwide: opposing trends East versus West. *J Bone Miner Res* (2014) **29**:1745–55. doi:10.1002/jbmr.2218
- Cauley JA, Chalhoub D, Kassem AM, Fuleihan Gel H. Geographic and ethnic disparities in osteoporotic fractures. *Nat Rev Endocrinol* (2014) **10**:338–51. doi:10.1038/nrendo.2014.51nrendo.2014.51
- Kanis JA, Oden A, McCloskey EV, Johansson H, Wahl DA, Cooper C. A systematic review of hip fracture incidence and probability of fracture worldwide. *Osteoporos Int* (2012) **23**:2239–56. doi:10.1007/s00198-012-1964-3
- Prentice A. Diet, nutrition and the prevention of osteoporosis. *Public Health Nutr* (2004) **7**:227–43. doi:10.1079/PHN2003590
- Prentice A, Ward KA, Schoenmakers I, Goldberg GR, editors. *Bone Growth in African Children and Adolescents*. Boca Raton, FL: Taylor & Francis Group (2012).
- Solomon L. Osteoporosis and fracture of the femoral neck in the South African Bantu. *J Bone Joint Surg Br* (1968) **50**:2–13.
- Zebaze RM, Seeman E. Epidemiology of hip and wrist fractures in Cameroon, Africa. *Osteoporos Int* (2003) **14**:301–5. doi:10.1007/s00198-002-1356-1
- Cooper C, Campion G, Melton LJ III. Hip fractures in the elderly: a world-wide projection. *Osteoporos Int* (1992) **2**:285–9. doi:10.1007/BF01623184
- Tsang SW, Kung AW, Kanis JA, Johansson H, Oden A. Ten-year fracture probability in Hong Kong Southern Chinese according to age and BMD femoral neck T-scores. *Osteoporos Int* (2009) **20**:1939–45. doi:10.1007/s00198-009-0906-1
- Orimo H, Yaegashi Y, Onoda T, Fukushima Y, Hosoi T, Sakata K. Hip fracture incidence in Japan: estimates of new patients in 2007 and 20-year trends. *Arch Osteoporos* (2009) **4**:71–7. doi:10.1007/s11657-009-0031-y
- Lau EM, Lee JK, Suriwongpaisal P, Saw SM, Das De S, Khir A, et al. The incidence of hip fracture in four Asian countries: the Asian Osteoporosis Study (AOS). *Osteoporos Int* (2001) **12**:239–43. doi:10.1007/s001980170135
- Yan L, Zhou B, Prentice A, Wang X, Golden MH. Epidemiological study of hip fracture in Shenyang, People's Republic of China. *Bone* (1999) **24**:151–5. doi:10.1016/S8756-3282(98)00168-9
- Looker AC, Wahner HW, Dunn WL, Calvo MS, Harris TB, Heyse SP, et al. Updated data on proximal femur bone mineral levels of US adults. *Osteoporos Int* (1998) **8**:468–89. doi:10.1007/s001980050093
- Shin MH, Zmuda JM, Barrett-Connor E, Sheu Y, Patrick AL, Leung PC, et al. Race/ethnic differences in associations between bone mineral density and fracture history in older men. *Osteoporos Int* (2014) **25**:837–45. doi:10.1007/s00198-013-2503-6
- Marshall LM, Zmuda JM, Chan BK, Barrett-Connor E, Cauley JA, Ensrud KE, et al. Race and ethnic variation in proximal femur structure and BMD among older men. *J Bone Miner Res* (2008) **23**:121–30. doi:10.1359/jbmr.070908
- Pye S, Ward K, Adams J, Finn J, Wu F, O'Neill T. Influence of ethnicity on bone mineral density and HIP axis length in UK men. In: Society BR, editor. *Bone Research Society/British Orthopaedic Research Society – Joint Meeting*. Oxford: Frontiers Media SA (2013). 96 p.
- Ward K, Jeffery M, Pye S, Adams J, Boonen S, Vanderschueren D, et al. Abstracts of the osteoporosis conference 2010. November 28–December 1, 2010, Liverpool, United Kingdom. *Osteoporos Int* (2010) **21**:S443–518. doi:10.1007/s00198-010-1388-x
- Mehta G, Taylor P, Petley G, Dennison EM, Cooper C, Walker-Bone K. Bone mineral status in immigrant Indo-Asian women. *Q J Med* (2004) **97**:97–9. doi:10.1093/qjmed/hch017
- Roy D, Swarbrick C, King Y, Pye S, Adams J, Berry J, et al. Differences in peak bone mass in women of European and South Asian origin can be explained by differences in body size. *Osteoporos Int* (2005) **16**:1254–62. doi:10.1007/s00198-005-1837-0
- Yan L, Crabtree NJ, Reeve J, Zhou B, Dequeker J, Nijs J, et al. Does hip strength analysis explain the lower incidence of hip fracture in the People's Republic of China? *Bone* (2004) **34**:584–8. doi:10.1016/j.bone.2003.12.005
- Aspray TJ, Prentice A, Cole TJ, Sawo Y, Reeve J, Francis RM. Low bone mineral content is common but osteoporotic fractures are rare in elderly rural Gambian women. *J Bone Miner Res* (1996) **11**:1019–25. doi:10.1002/jbmr.5650110720
- Aspray TJ, Prentice A, Cole TJ. The bone mineral content of weight-bearing bones is influenced by the ratio of sitting to standing height in elderly Gambian women. *Bone* (1995) **17**:261–3. doi:10.1016/8756-3282(95)98407-E
- Schnitzler CM, Pettifor JM, Mesquita JM, Bird MD, Schnaid E, Smyth AE. Histomorphometry of iliac crest bone in 346 normal black and white South African adults. *Bone Miner* (1990) **10**:183–99. doi:10.1016/0169-6009(90)90261-D
- Danielson ME, Beck TJ, Lian Y, Karlamangla AS, Greendale GA, Ruppert K, et al. Ethnic variability in bone geometry as assessed by hip structure analysis: findings from the hip strength across the menopausal transition study. *J Bone Miner Res* (2013) **28**:771–9. doi:10.1002/jbmr.1781
- Dibba B, Prentice A, Laskey MA, Stirling DM, Cole TJ. An investigation of ethnic differences in bone mineral, hip axis length, calcium metabolism and bone turnover between West African and Caucasian adults living in the United Kingdom. *Ann Hum Biol* (1999) **26**:229–42. doi:10.1080/030144699282732
- Prentice A, Shaw J, Laskey MA, Cole TJ, Fraser DR. Bone mineral content of British and rural Gambian women aged 18–80+ years. *Bone Miner* (1991) **12**:201–14. doi:10.1016/0169-6009(91)90033-V
- Wang Q, Teo JW, Ghasem-Zadeh A, Seeman E. Women and men with hip fractures have a longer femoral neck moment arm and greater impact load in a sideways fall. *Osteoporos Int* (2009) **20**:1151–6. doi:10.1007/s00198-008-0768-y
- Duboeuf F, Hans D, Schott AM, Kotzki PO, Favier F, Marcelli C, et al. Different morphometric and densitometric parameters predict cervical and trochanteric hip fracture: the EPIDOS Study. *J Bone Miner Res* (1997) **12**:1895–902. doi:10.1359/jbmr.1997.12.11.1895
- Ward KA, Roy DK, Pye SR, O'Neill TW, Berry JL, Swarbrick CM, et al. Forearm bone geometry and mineral content in UK women of European and South-Asian origin. *Bone* (2007) **41**:117–21. doi:10.1016/j.bone.2007.03.013
- Ward K. Musculoskeletal phenotype through the life course: the role of nutrition. *Proc Nutr Soc* (2012) **71**:27–37. doi:10.1017/S0029665111003375
- Darling AL, Hakim OA, Horton K, Gibbs MA, Cui L, Berry JL, et al. Adaptations in tibial cortical thickness and total volumetric bone density in postmenopausal South Asian women with small bone size. *Bone* (2013) **55**:36–43. doi:10.1016/j.bone.2013.03.006
- Liu XS, Walker MD, McMahon DJ, Udesky J, Liu G, Bilezikian JP, et al. Better skeletal microstructure confers greater mechanical advantages in Chinese-American women versus white women. *J Bone Miner Res* (2011) **26**:1783–92. doi:10.1002/jbmr.378
- Walker MD, Liu XS, Stein E, Zhou B, Bezati E, McMahon DJ, et al. Differences in bone microarchitecture between postmenopausal Chinese-American and white women. *J Bone Miner Res* (2011) **26**:1392–8. doi:10.1002/jbmr.352
- Putman MS, Yu EW, Lee H, Neer RM, Schindler E, Taylor AP, et al. Differences in skeletal microarchitecture and strength in African-American and white women. *J Bone Miner Res* (2013) **28**:2177–85. doi:10.1002/jbmr.1953
- Baker JE, Davis M, Alexander R, Zemel BS, Mostoufi-Moab S, Shults J, et al. Associations between body composition and bone density and structure in men and women across the adult age spectrum. *Bone* (2013) **53**:34–41. doi:10.1016/j.bone.2012.11.035

39. De Laet C, Kanis JA, Oden A, Johanson H, Johnell O, Delmas P, et al. Body mass index as a predictor of fracture risk: a meta-analysis. *Osteoporos Int* (2005) **16**:1330–8. doi:10.1007/s00198-005-1863-y
40. Nelson DA, Beck TJ, Wu G, Lewis CE, Bassford T, Cauley JA, et al. Ethnic differences in femur geometry in the women's health initiative observational study. *Osteoporos Int* (2011) **22**:1377–88. doi:10.1007/s00198-010-1349-4
41. Ho-Pham LT, Nguyen UD, Nguyen TV. Association between lean mass, fat mass, and bone mineral density: a meta-analysis. *J Clin Endocrinol Metab* (2014) **99**:30–8. doi:10.1210/jc.2013-3190
42. Compston JE, Watts NB, Chapurlat R, Cooper C, Boonen S, Greenspan S, et al. Obesity is not protective against fracture in postmenopausal women: GLOW. *Am J Med* (2011) **124**:1043–50. doi:10.1016/j.amjmed.2011.06.013
43. Premaor MO, Pilbrow L, Tonkin C, Parker RA, Compston J. Obesity and fractures in postmenopausal women. *J Bone Miner Res* (2010) **25**:292–7. doi:10.1359/jbmr.091004
44. Finkelstein JS, Lee ML, Sowers M, Ettinger B, Neer RM, Kelsey JL, et al. Ethnic variation in bone density in premenopausal and early perimenopausal women: effects of anthropometric and lifestyle factors. *J Clin Endocrinol Metab* (2002) **87**:3057–67. doi:10.1210/jcem.87.7.8654
45. Nam HS, Kweon SS, Choi JS, Zmuda JM, Leung PC, Lui LY, et al. Racial/ethnic differences in bone mineral density among older women. *J Bone Miner Metab* (2013) **31**:190–8. doi:10.1007/s00774-012-0402-0
46. Prentice A, Parsons T, Cole T. Uncritical use of bone mineral density in absorptiometry may lead to size-related artifacts in the identification of bone mineral determinants. *Am J Clin Nutr* (1994) **60**:837–42.
47. Frost H. Bone "mass" and the "mechanostat": a proposal. *Anat Rec* (1987) **219**:1–9. doi:10.1002/ar.1092190104
48. Rittweger J, Schiessl H, Felsenberg D, Runge M. Reproducibility of the jumping mechanography as a test of mechanical power output in physically competent adult and elderly subjects. *J Am Geriatr Soc* (2004) **52**:128–31. doi:10.1111/j.1532-5415.2004.52022.x
49. Jeffrey M. Age-related change and ethnic differences in neuromuscular function. *8th International Workshop For Musculoskeletal & Neuronal Interactions*. Ipswich (2012).
50. Khan UI, Wang D, Sowers MR, Mancuso P, Everson-Rose SA, Scherer PE, et al. Race-ethnic differences in adipokine levels: the study of women's health across the nation (SWAN). *Metabolism* (2012) **61**:1261–9. doi:10.1016/j.metabol.2012.02.005
51. McKeigue PM, Pierpoint T, Ferrie JE, Marmot MG. Relationship of glucose intolerance and hyperinsulinaemia to body fat pattern in south Asians and Europeans. *Diabetologia* (1992) **35**:785–91.
52. Rush EC, Freitas I, Plank LD. Body size, body composition and fat distribution: comparative analysis of European, Maori, Pacific Island and Asian Indian adults. *Br J Nutr* (2009) **102**:632–41. doi:10.1017/S0007114508207221
53. Taaffe DR, Cauley JA, Danielson M, Nevitt MC, Lang TF, Bauer DC, et al. Race and sex effects on the association between muscle strength, soft tissue, and bone mineral density in healthy elders: the health, aging, and body composition study. *J Bone Miner Res* (2001) **16**:1343–52. doi:10.1359/jbmr.2001.16.7.1343
54. Miljkovic I, Cauley JA, Petit MA, Ensrud KE, Strotmeyer E, Sheu Y, et al. Greater adipose tissue infiltration in skeletal muscle among older men of African ancestry. *J Clin Endocrinol Metab* (2009) **94**:2735–42. doi:10.1210/jc.2008-2541
55. Nam HS, Shin MH, Zmuda JM, Leung PC, Barrett-Connor E, Orwoll ES, et al. Race/ethnic differences in bone mineral densities in older men. *Osteoporos Int* (2010) **21**:2115–23. doi:10.1007/s00198-010-1188-3
56. Chantler S, Dickie K, Goedecke JH, Levitt NS, Lambert EV, Evans J, et al. Site-specific differences in bone mineral density in black and white premenopausal South African women. *Osteoporos Int* (2012) **23**:533–42. doi:10.1007/s00198-011-1570-9
57. Malan NT, Hamer M, Schutte AE, Huisman HW, Van Rooyen JM, Schutte R, et al. Low testosterone and hyperkinetic blood pressure responses in a cohort of South African men: the SABPA study. *Clin Exp Hypertens* (2013) **35**:228–35. doi:10.3109/10641963.2012.721839
58. Heo M, Faith MS, Pietrobelli A, Heymsfield SB. Percentage of body fat cut-offs by sex, age, and race-ethnicity in the US adult population from NHANES 1999–2004. *Am J Clin Nutr* (2012) **95**:594–602. doi:10.3945/ajcn.111.025171

**Conflict of Interest Statement:** The authors declare that the research was conducted in the absence of any commercial or financial relationships that could be construed as a potential conflict of interest.

*Received: 29 January 2015; paper pending published: 08 February 2015; accepted: 10 February 2015; published online: 17 March 2015.*

*Citation: Zengin A, Prentice A and Ward KA (2015) Ethnic differences in bone health. *Front. Endocrinol.* **6**:24. doi: 10.3389/fendo.2015.00024*

*This article was submitted to Bone Research, a section of the journal *Frontiers in Endocrinology*.*

*Copyright © 2015 Zengin, Prentice and Ward. This is an open-access article distributed under the terms of the Creative Commons Attribution License (CC BY). The use, distribution or reproduction in other forums is permitted, provided the original author(s) or licensor are credited and that the original publication in this journal is cited, in accordance with accepted academic practice. No use, distribution or reproduction is permitted which does not comply with these terms.*

# Romosozumab and blosozumab: alternative drugs of mechanical strain-related stimulus toward a cure for osteoporosis

Toshihiro Sugiyama\*, Tetsuya Torio, Tsuyoshi Miyajima, Yoon Taek Kim and Hiromi Oda

Department of Orthopaedic Surgery, Saitama Medical University, Saitama, Japan

**Keywords:** osteoporosis, mechanostat, sclerostin, romosozumab, blosozumab

## Treat-to-Target Strategy in Osteoporosis

In addition to other chronic diseases such as hypertension, hypercholesterolemia, and diabetes, a treat-to-target strategy was recently applied in rheumatoid arthritis and has now been discussed in osteoporosis. An important goal of osteoporosis therapy is normal risk of hip fracture associated with significant morbidity and mortality, but the anti-fracture efficacies of currently approved drugs are limited (1, 2). Although fundamental methods to effectively prevent osteoporotic fracture include pharmacological treatment of sarcopenia that results in improving bone fragility as well as reducing fall risk, the present article focuses on anti-sclerostin antibodies such as romosozumab and blosozumab, the investigational agents for osteoporosis, and provides new insights into their effects from natural homeostatic system in the skeleton.

## OPEN ACCESS

### Edited and reviewed by:

Jonathan H. Tobias,  
University of Bristol, UK

### \*Correspondence:

Toshihiro Sugiyama  
tsugiym@saitama-med.ac.jp

### Specialty section:

This article was submitted to Bone Research, a section of the journal Frontiers in Endocrinology

Received: 15 March 2015

Accepted: 06 April 2015

Published: 21 April 2015

### Citation:

Sugiyama T, Torio T, Miyajima T, Kim YT and Oda H (2015) Romosozumab and blosozumab: alternative drugs of mechanical strain-related stimulus toward a cure for osteoporosis. *Front. Endocrinol.* 6:54.  
doi: 10.3389/fendo.2015.00054

## Alternative Drugs of Mechanical Strain-Related Stimulus

The human skeleton normally responds to the change in local mechanical environment at each skeletal site to maintain resultant elastic deformation (strain) of bone; increased or decreased bone strain would induce bone gain or loss, respectively (3–5). This mechanical strain-related feedback control called the mechanostat (6, 7) plays a key role in the management of osteoporosis; increased bone strength by an osteoporosis drug results in decreased bone strain, indicating that the effect of osteoporosis therapy is limited by the mechanostat (Figure 1) (5). Approaches to reduce the limitation include pharmacologically enhancing skeletal response to mechanical stimulation (8), but this might not efficiently reduce the risk of fall-related hip fracture because the skeleton is adapted to the mechanical environment resulting from habitual physical activity but not to the unusual direction of mechanical force by falls. Consequently, an ideal strategy is to develop an alternative agent of mechanical strain-related stimulus (5).

One example would be investigational anti-sclerostin antibodies such as romosozumab and blosozumab; experimental evidence has established that the production of sclerostin secreted by osteocytes is increased by skeletal disuse and decreased by skeletal loading (9, 10). In addition, bone formation induced by intermittent treatment with parathyroid hormone is associated with the inhibition of sclerostin (11), suggesting that teriparatide could partly have a similar effect. There is, however, an obvious difference between the effects of anti-sclerostin antibodies and teriparatide, if injected daily (8), on bone remodeling; remodeling-based, coupled bone resorption and formation are significantly promoted by the latter, but not by the former.

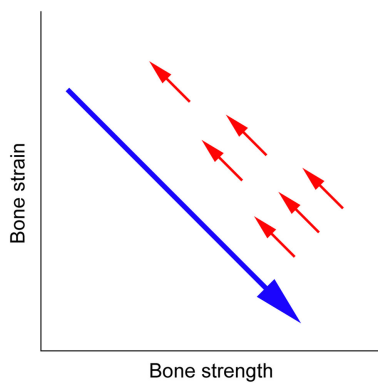


**FIGURE 1 | Mechanical strain-related feedback control of bone strength.** A long arrow indicates the effect of osteoporosis therapy that increases bone strength and thus decreases bone strain from physical activity, and short arrows indicate the negative feedback control of bone strength that returns bone strain to its pre-treatment level (5).

## Modeling-Based Effects of Anti-Sclerostin Antibodies

In contrast to bone remodeling, modeling-based bone formation and resorption are not coupled, and mechanical stimulation is a natural uncoupling factor that stimulates bone formation and inhibits bone resorption; experimental data in skeletally mature animals (12, 13) show that strong suppression of bone resorption by risedronate or denosumab does not impair modeling-based bone formation induced by artificial mechanical loading or habitual physical activity. In agreement with the above suggestion that investigational anti-sclerostin antibodies such as romosozumab and blosozumab are alternative drugs of mechanical strain-related stimulus, an experiment using male cynomolgus monkeys found a marked increase in modeling-based bone formation by romosozumab (14) and phase 2 clinical studies in postmenopausal women confirmed that both romosozumab and blosozumab treatments rapidly induced an increase in bone formation and a decrease in bone resorption (15, 16).

## Optimal Doses of Anti-Sclerostin Antibodies

In postmenopausal women with low areal bone mineral density (BMD), romosozumab and blosozumab treatments for 1 year increased areal BMD at the lumbar spine and hip dose-dependently; mean changes from baseline in areal BMD at the lumbar spine, total hip and femoral neck by romosozumab [placebo vs. highest dose (210 mg every 1 month)] were  $-0.1$  vs.  $11.3\%$ ,  $-0.7$  vs.  $4.1\%$ , and  $-1.1$  vs.  $3.7\%$ , respectively, while those by blosozumab [placebo vs. highest dose (270 mg every 2 weeks)] were  $-1.6$  vs.  $17.7\%$ ,  $-0.7$  vs.  $6.7\%$ , and  $-0.6$  vs.  $6.3\%$ , respectively (15, 16). Notably, however, areal BMD at the one-third radius was not changed by the highest dose of romosozumab ( $-0.9$  vs.  $-1.2\%$ , respectively) and non-significantly increased only by the highest dose of blosozumab ( $-1.4$  vs.  $0.9\%$ , respectively) (15, 16).

The effects of anti-sclerostin antibodies at the radius appear to reflect the fact that forearm is not exposed to high levels of mechanical strain under normal physical activity. Experimental evidence that the production of sclerostin secreted by osteocytes is increased by skeletal disuse and decreased by skeletal loading (9, 10) suggests that the levels of sclerostin expression in non-weight-bearing bones such as the radius could be higher than those in weight-bearing bones such as the lumbar spine and hip. Consequently, it would be possible to speculate that even highest doses of romosozumab and blosozumab selected in phase 2 clinical studies were not enough for the radius. Indeed, the strongest effects on areal BMD at the lumbar spine and hip were achieved with the highest dose of blosozumab and only this regimen resulted in a trend of increase in areal BMD at the radius (15, 16); further higher doses of blosozumab might increase areal BMD at the radius dose-dependently. Several lines of evidence to support this hypothesis include (i) patients with sclerosteosis due to deficiency of sclerostin have higher areal BMD at the radius as well as the lumbar spine and hip (17) and (ii) appropriate doses of anti-sclerostin antibodies effectively increase bone mass in animals with skeletal disuse or unloading (18, 19).

If the above logic is correct, the highest doses of romosozumab (210 mg every 1 month) and blosozumab (270 mg every 2 weeks) are unlikely to cause unwanted bony overgrowth at non-weight-bearing sites such as the face and skull in postmenopausal women with osteoporosis. In contrast, however, further higher doses of these drugs would be required to improve skeletal fragility in patients with reduced physical activity; one useful indicator to determine optimal doses of anti-sclerostin antibodies could be areal BMD at the radius.

## Limitation of Treatment with Anti-Sclerostin Antibodies

Both romosozumab and blosozumab treatments in postmenopausal women with low areal BMD showed that marked changes in circulating bone formation and resorption markers returned to the pre-treatment levels within a year despite the continued treatments (15, 16). The existence of other mechanotransduction pathways independent of sclerostin (20) indicates that treatment with an anti-sclerostin antibody cannot escape from the mechanostat-related limitation of osteoporosis therapy (5).

The relation between circulating sclerostin and bone mass would support this theory. Sclerostin-related high bone mass in patients with sclerosteosis or van Buchem disease and heterozygous carriers of these diseases is linked to lower levels of circulating sclerostin (21, 22), while circulating sclerostin and bone mass in normal women and men have a positive correlation (23–25). This discrepancy suggests that higher bone mass associated with other mechanotransduction pathways independent of sclerostin would cause lower mechanical strain in the skeleton and thus could result in compensatory higher sclerostin production according to the mechanostat, although the positive correlation between circulating sclerostin and bone mass is also influenced by the fact that higher bone mass results in more osteocytes, which are the main source of sclerostin (26).

## Withdrawal of Treatment with Anti-Sclerostin Antibodies

Results of 1-year post-treatment follow-up after 1-year treatment with blosozumab were recently reported in the phase 2 clinical trial of postmenopausal women with low areal BMD. Mean changes from baseline in areal BMD at the lumbar spine, total hip, and femoral neck by the highest dose (270 mg every 2 weeks) of blosozumab (1-year treatment vs. 1-year treatment plus 1-year follow-up without treatment) were 17.7 vs. 6.9%, 6.7 vs. 3.9%, and 6.3 vs. 5.3%, respectively (27).

The mechanostat indicates that bone strength returns to baseline after the withdrawal of treatment (5) and the speed of this reverse change depends on the drug (28–30). The above site-specific difference in the reduction of areal BMD could partly result from less mechanical loading at the lumbar spine, possibly associated with higher sclerostin production (9, 10). Treatment with an anti-sclerostin antibody can reinforce the fragile skeleton by non-site-specific bone apposition, while its discontinuation

would result in mechanical strain-related, site-specific bone loss. Local bone strain from normal physical activity is lower in the inner compartments, suggesting that bone loss caused by the mechanostat-related negative feedback is higher at the trabecular and endosteal surfaces. In contrast, newly formed bone at the periosteal surface through modeling-based apposition might not be resorbed because of a lack of efficient bone resorption in this region.

## Conclusion

Anti-sclerostin antibodies such as romosozumab and blosozumab are the alternative drugs of mechanical strain-related stimulus that can overcome the mechanostat-related limitation of osteoporosis therapy (Figure 1) (5). It is expected that these agents will make a treat-to-target strategy in osteoporosis possible in the near future. Further studies are desired to investigate their optimal doses, especially depending on the levels of habitual physical activity, as well as appropriate duration of the treatments.

## References

1. Crandall CJ, Newberry SJ, Diamant A, Lim YW, Gellad WF, Booth MJ, et al. Comparative effectiveness of pharmacologic treatments to prevent fractures: an updated systematic review. *Ann Intern Med* (2014) **161**:711–23. doi:10.7326/M14-0317
2. Kanis JA, McCloskey E, Branco J, Brandi ML, Dennison E, Devogelaer JP, et al. Goal-directed treatment of osteoporosis in Europe. *Osteoporos Int* (2014) **25**:2533–43. doi:10.1007/s00198-014-2787-1
3. Christen P, Ito K, Ellouz R, Boutroy S, Sornay-Rendu E, Chapurlat RD, et al. Bone remodelling in humans is load-driven but not lazy. *Nat Commun* (2014) **5**:4855. doi:10.1038/ncomms5855
4. Bhatia VA, Edwards WB, Johnson JE, Troy KL. Short-term bone formation is greatest within high strain regions of the human distal radius: a prospective pilot study. *J Biomech Eng* (2015) **137**:011001. doi:10.1115/1.4028847
5. Sugiyama T, Kim YT, Oda H. Osteoporosis therapy: a novel insight from natural homeostatic system in the skeleton. *Osteoporos Int* (2015) **26**:443–7. doi:10.1007/s00198-014-2923-y
6. Frost HM. Bone's mechanostat: a 2003 update. *Anat Rec A Discov Mol Cell Evol Biol* (2003) **275**:1081–101. doi:10.1002/ar.a.10119
7. Meakin LB, Price JS, Lanyon LE. The contribution of experimental in vivo models to understanding the mechanisms of adaptation to mechanical loading in bone. *Front Endocrinol (Lausanne)* (2014) **5**:154. doi:10.3389/fendo.2014.00154
8. Sugiyama T, Torio T, Sato T, Matsumoto M, Kim YT, Oda H. Improvement of skeletal fragility by teriparatide in adult osteoporosis patients: a novel mechanostat-based hypothesis for bone quality. *Front Endocrinol (Lausanne)* (2015) **6**:6. doi:10.3389/fendo.2015.00006
9. Robling AG, Turner CH. Mechanical signaling for bone modeling and remodeling. *Crit Rev Eukaryot Gene Expr* (2009) **19**:319–38. doi:10.1615/CritRevEukarGeneExpr.v19.i4.50
10. Moustafa A, Sugiyama T, Prasad J, Zaman G, Gross TS, Lanyon LE, et al. Mechanical loading-related changes in osteocyte sclerostin expression in mice are more closely associated with the subsequent osteogenic response than the peak strains engendered. *Osteoporos Int* (2012) **23**:1225–34. doi:10.1007/s00198-011-1656-4
11. Kramer I, Keller H, Leupin O, Kneissel M. Does osteocytic SOST suppression mediate PTH bone anabolism? *Trends Endocrinol Metab* (2010) **21**:237–44. doi:10.1016/j.tem.2009.12.002
12. Sugiyama T, Meakin LB, Galea GL, Jackson BF, Lanyon LE, Ebetino FH, et al. Risedronate does not reduce mechanical loading-related increases in cortical and trabecular bone mass in mice. *Bone* (2011) **49**:133–9. doi:10.1016/j.bone.2011.03.775
13. Ominsky MS, Libanati C, Niu QT, Boyce RW, Kostenuik PJ, Wagman RB, et al. Sustained modeling-based bone formation during adulthood in cynomolgus monkeys may contribute to continuous BMD gains with denosumab. *J Bone Miner Res* (2015). doi:10.1002/jbmr.2480
14. Ominsky MS, Niu QT, Li C, Li X, Ke HZ. Tissue-level mechanisms responsible for the increase in bone formation and bone volume by sclerostin antibody. *J Bone Miner Res* (2014) **29**:1424–30. doi:10.1002/jbmr.2152
15. McClung MR, Grauer A, Boonen S, Bolognese MA, Brown JP, Diez-Perez A, et al. Romosozumab in postmenopausal women with low bone mineral density. *N Engl J Med* (2014) **370**:412–20. doi:10.1056/NEJMoa1305224
16. Recker RR, Benson CT, Matsumoto T, Bolognese MA, Robins DA, Alam J, et al. A randomized, double-blind phase 2 clinical trial of blosozumab, a sclerostin antibody, in postmenopausal women with low bone mineral density. *J Bone Miner Res* (2015) **30**:216–24. doi:10.1002/jbmr.2351
17. Gardner JC, van Bezoijen RL, Mervis B, Hamdy NA, Lowik CW, Hamersma H, et al. Bone mineral density in sclerosteosis; affected individuals and gene carriers. *J Clin Endocrinol Metab* (2005) **90**:6392–5. doi:10.1210/jc.2005-1235
18. Tian XY, Jee WS, Li X, Paszty C, Ke HZ. Sclerostin antibody increases bone mass by stimulating bone formation and inhibiting bone resorption in a hindlimb-immobilization rat model. *Bone* (2011) **48**:197–201. doi:10.1016/j.bone.2010.09.009
19. Spatz JM, Ellman R, Cloutier AM, Louis L, van Vliet M, Suva LJ, et al. Sclerostin antibody inhibits skeletal deterioration due to reduced mechanical loading. *J Bone Miner Res* (2013) **28**:865–74. doi:10.1002/jbmr.1807
20. Morse A, McDonald M, Kelly N, Melville K, Schindeler A, Kramer I, et al. Mechanical load increases in bone formation via a sclerostin-independent pathway. *J Bone Miner Res* (2014) **29**:2456–67. doi:10.1002/jbmr.2278
21. van Lierop AH, Hamdy NA, Hamersma H, van Bezoijen RL, Power J, Loveridge N, et al. Patients with sclerosteosis and disease carriers: human models of the effect of sclerostin on bone turnover. *J Bone Miner Res* (2011) **26**:2804–11. doi:10.1002/jbmr.474
22. van Lierop AH, Hamdy NA, van Egmond ME, Bakker E, Dikkers FG, Papapoulos SE. Van Buchem disease: clinical, biochemical, and densitometric features of patients and disease carriers. *J Bone Miner Res* (2013) **28**:848–54. doi:10.1002/jbmr.1794
23. Modder UI, Hoey KA, Amin S, McCready LK, Achenbach SJ, Riggs BL, et al. Relation of age, gender, and bone mass to circulating sclerostin levels in women and men. *J Bone Miner Res* (2011) **26**:373–9. doi:10.1002/jbmr.217
24. Polyzos SA, Anastasilakis AD, Bratengeier C, Woloszczuk W, Papatheodorou A, Terpos E. Serum sclerostin levels positively correlate with lumbar spinal bone mineral density in postmenopausal women – the six-month effect of

- risedronate and teriparatide. *Osteoporos Int* (2012) **23**:1171–6. doi:10.1007/s00198-010-1525-6
25. Szulc P, Bertholon C, Borel O, Marchand F, Chapurlat R. Lower fracture risk in older men with higher sclerostin concentration: a prospective analysis from the MINOS study. *J Bone Miner Res* (2013) **28**:855–64. doi:10.1002/jbmr.1823
26. Gregson CL, Poole KE, McCloskey EV, Duncan EL, Rittweger J, Fraser WD, et al. Elevated circulating sclerostin concentrations in individuals with high bone mass, with and without LRP5 mutations. *J Clin Endocrinol Metab* (2014) **99**:2897–907. doi:10.1210/jc.2013-3958
27. Recknor CP, Recker RR, Benson CT, Robins DA, Chiang AY, Alam J, et al. The effect of discontinuing treatment with blosozumab: follow-up results of a phase 2 randomized clinical trial in postmenopausal women with low bone mineral density. *J Bone Miner Res* (2015). doi:10.1002/jbmr.2489
28. Boonen S, Ferrari S, Miller PD, Eriksen EF, Sambrook PN, Compston J, et al. Postmenopausal osteoporosis treatment with antiresorptives: effects of discontinuation or long-term continuation on bone turnover and fracture risk – a perspective. *J Bone Miner Res* (2012) **27**:963–74. doi:10.1002/jbmr.1570
29. Padhi D, Jang G, Stouch B, Fang L, Posvar E. Single-dose, placebo-controlled, randomized study of AMG 785, a sclerostin monoclonal antibody. *J Bone Miner Res* (2011) **26**:19–26. doi:10.1002/jbmr.173
30. McColm J, Hu L, Womack T, Tang CC, Chiang AY. Single- and multiple-dose randomized studies of blosozumab, a monoclonal antibody against sclerostin, in healthy postmenopausal women. *J Bone Miner Res* (2014) **29**:935–43. doi:10.1002/jbmr.2092

**Conflict of Interest Statement:** The authors declare that the research was conducted in the absence of any commercial or financial relationships that could be construed as a potential conflict of interest.

Copyright © 2015 Sugiyama, Torio, Miyajima, Kim and Oda. This is an open-access article distributed under the terms of the Creative Commons Attribution License (CC BY). The use, distribution or reproduction in other forums is permitted, provided the original author(s) or licensor are credited and that the original publication in this journal is cited, in accordance with accepted academic practice. No use, distribution or reproduction is permitted which does not comply with these terms.

## ADVANTAGES OF PUBLISHING IN FRONTIERS



### FAST PUBLICATION

Average 90 days  
from submission  
to publication



### COLLABORATIVE PEER-REVIEW

Designed to be rigorous –  
yet also collaborative, fair and  
constructive



### RESEARCH NETWORK

Our network  
increases readership  
for your article



### OPEN ACCESS

Articles are free to read,  
for greatest visibility



### TRANSPARENT

Editors and reviewers  
acknowledged by name  
on published articles



### GLOBAL SPREAD

Six million monthly  
page views worldwide



### COPYRIGHT TO AUTHORS

No limit to  
article distribution  
and re-use



### IMPACT METRICS

Advanced metrics  
track your  
article's impact



### SUPPORT

By our Swiss-based  
editorial team